THE APPLICATION OF ORTHOTROPIC PLATE THEORY TO DECKING SYSTEMS

Summary of

Thesis presented for the Degree
of Doctor of Philosophy of
the University of Glasgow.

by

Henry Kinloch, M.Sc., A.R.C.S.T.

January, 1966.

ProQuest LLC.
789 East Eisenhower Parkway
P.O. Box 1346
Ann Arbor, MI 48106 – 1346

The purpose of the work presented in this thesis was to examine the applicability of orthotropic plate theory to the behaviour of corrugated decking under lateral loading, and to pursue parallel to the theoretical work an appropriate experimental investigation.

A review of the relevant published literature is given in Chapter I. The development of orthotropic plate theory and its application to engineering problems is outlined and it is noted that much of the theoretical work of the past has been limited due to the difficulty of adequately defining the convergence of the assumed series solutions. Further, this difficulty has inhibited the development of solutions of a general nature defining all possible variations of the elastic stiffnesses for a given plate shape. It is further indicated that while there has been a great deal of interest shown in the experimental evaluation of the appropriate plate moduli and stiffnesses, little work has been carried out in applying the results of these tests to the behaviour of orthotropic plates under different loading and boundary conditions.

The theoretical work of Chapter II opens with a brief outline of the derivation of the governing equations for the elastic behaviour of an orthotropic plate. The orthotropic plate compatibility equation and consistent boundary conditions are then derived and the author's solution to the problem of the bending of an orthotropic plate under uniform transverse loading is given. A complete investigation of the two major modes of solution is given and the plate behaviour for various combinations of stiffness ratios presented. The chapter closes with an outline of a method devised by the author for the assessment of the anticlastic surface exhibited by an orthotropic strip when bent by a pure moment. This analysis is used to justify the experimental evaluation of the principal stiffness of a plate by a simple bend test and the use of the reciprocal relationships in orthotropic plates.

Chapter III describes the experimental techniques developed to measure the plate stiffnesses and also the apparatus built to test and measure the behaviour of decking specimens under a uniformly distributed load.

The results of the experimental deflection and strain investigations are compared with the theoretical values in Chapter IV and good agreement is shown to obtain.

The design aspects of light gauge metal decking are discussed in Chapter V and this section demonstrates the utility of the strut compression test in estimating that stress at which elastic buckling in a light gauge metal deck under uniform load is initiated. An experimental investigation undertaken to substantiate the above statement is detailed and the chapter closes with the substantiation of a simplified collapse load concept to provide the basis for design.

Chapter VI summarises the main findings of the theoretical and experimental work and Chapter VII contains a full bibliography and author index.

The thesis concludes with six appendices which enlarge on various aspects of the analysis and also present the detailed results of the experimental investigations.

THE APPLICATION OF ORTHOTROPIC PLATE THEORY TO DECKING SYSTEMS

Thesis presented for the Degree
of Doctor of Philosophy of
the University of Glasgow.

by

Henry Kinloch, M.Sc., A.R.C.S.T.

January, 1966.

I N D E X

C O N T E N T S

A B S T R A C T

The purpose of the work presented in this thesis was to examine the applicability of orthotropic plate theory to the behaviour of corrugated decking under lateral loading, and to pursue parallel to the theoretical work an appropriate experimental investigation.

A review of the relevant published literature is given in Chapter I. The development of orthotropic plate theory and its application to engineering problems is outlined and it is noted that much of the theoretical work of the past has been limited due to the difficulty of adequately defining the convergence of the assumed series solutions. Further, this difficulty has inhibited the development of solutions of a general nature defining all possible variations of the elastic stiffnesses for a given plate shape. It is further indicated that while there has been a great deal of interest shown in the experimental evaluation of the appropriate plate moduli and stiffnesses, little work has been carried out in applying the results of these tests to the behaviour of orthotropic plates under different loading and boundary conditions.

The theoretical work of Chapter II opens with a brief outline of the derivation of the governing equations for the elastic behaviour of an orthotropic plate. The orthotropic plate compatibility equation and consistent boundary conditions are then derived and the author's solution to the problem of the bending of an orthotropic plate under uniform transverse loading is given. A complete investigation of the two major modes of solution is given and the plate behaviour for various combinations of stiffness ratios presented. The chapter closes with an outline of a method devised by the author for the assessment of the anticlastic surface exhibited by an orthotropic strip when bent by a pure moment. This analysis is used to justify the experimental evaluation of the principal stiffness of a plate by a simple bend test and the use of the reciprocal relationships in orthotropic plates.

Chapter III describes the experimental techniques developed to measure the plate stiffnesses and also the apparatus built to test and measure the behaviour of decking specimens under a uniformly distributed load.

The results of the experimental deflection and strain investigations are compared with the/

the theoretical values in Chapter IV and good agreement is shown to obtain.

The design aspects of light gauge metal decking are discussed in Chapter V and this section demonstrates the utility of the strut compression test in estimating that stress at which elastic buckling in a light gauge metal deck under uniform lateral load is initiated. An experimental investigation undertaken to substantiate the above statement is detailed and the chapter closes with the substantiation of a simplified collapse load concept to provide the basis for design.

Chapter VI summarises the main findings of the theoretical and experimental work and Chapter VII contains a full bibliography and author index.

The thesis concludes with six appendices which enlarge on various aspects of the analysis and also present the detailed results of the experimental investigations.

NOTATION

x, y, z	Cartesian co-ordinates
α, β	angles
a, b	length and breadth in directions x and y respectively
a_{ij}, b_{ij}	elastic modulus and constant respectively
ν_{ij}	Poisson's Ratio relating an extensional strain in the direction "i" to the corresponding strain in the direction "j"
D_{11}, D_{22}	elastic flexural stiffnesses in the x and y directions respectively
D_{66}	elastic torsional stiffness

$$D_{12} = \nu_{12} . D_{22} = \nu_{21} . D_{11} \quad ; \quad D_{33} = D_{12} + 2D_{66}$$

$$R_1 = D_{11}/D_{22} \quad ; \quad R_2 = D_{66}/D_{22}$$

w	deflection in the direction z
q	applied loading
h	plate thickness
ρ	radius of curvature
σ_i, τ_{ij}	normal and shear stress respectively
ϵ, γ	extensional and shear strains respectively
M_x, M_y	longitudinal and transverse bending moment per unit length
M_{xy}	twisting moment per unit length
Q_x, Q_y	shear force per unit breadth and per unit length respectively

R_x	shear reaction per unit breadth
V	potential energy
Δ	value of a determinant
δ	variational term
Y_m	Lévy transform operator
ϕ, ψ	roots of the characteristic equation (uniform loading)
θ, γ	real and imaginary parts of a complex root (uniform loading)
M	applied moment
ς, ξ	roots of the characteristic equation (constant moment)
χ, λ	real and imaginary parts of a complex root (constant moment)
τ	wall thickness of a thin walled section
σ_c	critical longitudinal compressive stress which initiates local elastic buckling
σ_m	average compressive stress at maximum load carrying capacity
σ_y	yield or 0.1% proof stress
E, ν	Young's Modulus and Poisson's Ratio
C_L	local plate stress factor
b_e	effective width

The following constants also appear in the text and are defined when derived:

$$F, \quad f, \quad g, \quad M, \quad N, \quad K, \quad \bar{K}, \quad L, \quad R$$

CHAPTER I

CRITICAL REVIEW OF PUBLISHED LITERATURE

I.1. INTRODUCTION.

The theory of the behaviour of anisotropic bodies has been for some considerable time a fruitful field of research for those mathematicians who have applied their efforts to the mathematical theories of elasticity. Much work of a purely theoretical nature has been orientated towards finding a general solution to the governing equations of anisotropic elasticity without considering specific problems of anisotropic behaviour. The author has not reviewed this type of work in the belief that such attempts, while of considerable interest, do not make a significant contribution to the solution of practical problems. Nor has the author found it expedient to set out in this review a separate account of each aspect of anisotropic elasticity but has chosen to review relevant work in chronological order. This has the advantage of requiring a minimum of cross-referencing and enables a clearer picture of the development of particular lines of thought to be given.

Anisotropic plate theory has for many years been applied to the engineering investigation of various forms of stiffened plates. The problems investigated/

investigated have been principally those of the behaviour of rectangular plates under bending or shearing load actions, the principal axes of elasticity of such plates being at right angles to each other and parallel to the sides of the plate - the so-called "specially orthotropic" plate. The orthotropic nature of the plates has been obtained by various forms of stiffener attached to thin isotropic sheets or by altering the cross-section of a uniformly thick plate to give an appreciable difference in stiffness in the longitudinal and transverse directions. Alternatively, the orthotropic nature of the plate has been due to the composition of the material, for example, various forms of plywood and fibreglass constructions, or to the geometrical configuration of the plate cross-section as is the case in corrugated plates.

The section I.2 of this review has been written to provide a conspectus of previous work on orthotropic plate problems, bearing in mind the limitations of the present investigation, namely, that the plates considered are of corrugated cross-section, and that the analytical work has been carried out on the basis of the so-called "small deflection" plate equation.

It is appropriate at this point to set down the definition of some of the terms used in the following chapters.

The term "anisotropic" is used as referring to a body in which the principal planes of elasticity are inclined to each other at any general angle α . "Generally orthotropic" denotes a body in which the angle α between the principal planes of elasticity is 90^{o}. In "specially orthotropic" plates α is again 90^{o} and the principal planes of elasticity contain the major geometrical axes of the plate which is of rectangular form.

In this thesis the word "orthotropic" used by itself denotes "specially orthotropic".

Throughout many of the papers reviewed below, the terminology used has been random and subject only to each writer's particular taste. Consequently for this review the author has found it necessary to re-cast many of the quoted equations, etc., and will use throughout the following connotations for the various constants employed. Where it has been found impossible to follow this procedure, special mention is made in the text.

Rectangular plates are characterized by a Cartesian system of co-ordinates, the plate-length in the direction x being a the breadth in the direction y being b.

The quantity a_{ij} is termed the elastic MODULUS and relates an extensional stress in the direction j to an extensional strain in the direction i. Where the direction of the applied stress and the consequent strain are in the same direction (e.g. $i = j = 1$) the modulus a_{ij} is the reciprocal of the Young's modulus for the direction considered,

$$\text{e.g.} \quad a_{11} = \frac{1}{E_{11}} \quad ; \quad a_{22} = \frac{1}{E_{22}}$$

where the subscript 1 refers to the direction x, the direction y being referred to by the subscript 2.

The elastic CONSTANTS b_{ij} are those constants obtained by solving for the stress terms the general statement of Hooke's Law for an anisotropic body.

The elastic flexural and torsional STIFFNESSES D_{ij} are the values obtained by integrating the terms b_{ij} over a predetermined region. In this review all values of D_{ij} are those obtained by integrating the/

the appropriate expressions for b_{ij} over a plate thickness.

Section I.3 is a brief review of the problem of the incidence of anticlastic curvature in isotropic plates. The purpose of this section is to furnish the background to the work in section II.6. of this thesis which deals with the behaviour of orthotropic plates under pure bending.

I.2. ORTHOTROPIC PLATE THEORY.

The earliest recorded investigation of anisotropic theory is that of GEHRING (1860) whose work was primarily an extension of that of Navier and Cauchy on isotropic bodies. The practical application of this work to the solution of engineering problems was the contribution of HUBER (1922, 1929) who derived the orthotropic plate equation.

$$D_{11}\frac{\partial^4 w}{\partial x^4} + 2D_{33}\frac{\partial^4 w}{\partial x^2 \partial y^2} + D_{22}\frac{\partial^4 w}{\partial y^4} = q \qquad \text{(I.2.1)}$$

Subject to the limitation that $D_{33} = \sqrt{D_{11}.D_{22}}$ Huber applied equation (I.2.1) to the behaviour of concrete slabs and to that of rectangular plywood plates under a uniformly distributed load, the edges of the/

the plates being simply supported. Huber presented tables for the maximum central deflection given in the form

$$w_{max} = \frac{q b^4}{D_{22}} \cdot \phi \qquad \text{(I.2.2)}$$

where ϕ is a coefficient dependent on the plate aspect ratio and the ratio D_{11}/D_{22}.

Huber also scrutinized the case of the bending of an infinitely long rectangular orthotropic strip with simply supported edges subjected to a uniformly distributed transverse line load of finite length orientated across the strip and over part of the strip width b.

For this case, the applied load was considered to be expanded as a Fourier Series

$$q \cdot \sum_{n=1}^{\infty} a_n \cdot \sin \frac{n\pi y}{b} \qquad \text{(I.2.3)}$$

Huber then derived from equation (I.2.1) the following expression for the maximum deflection at the middle of the loaded part of the plate

$$w_{max} = \frac{q b^3}{\pi^4 D_{22}} \cdot \frac{0.939}{\sqrt{\frac{D_{33}}{2D_{22}}} + \frac{1}{2}\sqrt{\frac{D_{11}}{D_{22}}}} \qquad \text{(I.2.4)}$$

Also presented were expressions for the maximum bending moment in the x and y directions.

Huber dealt with the problem of the behaviour of a strip under the action of a concentrated force by considering such force action as the limiting case of a load having a finite resultant and distributed over an infinitely small region.

SEYDEL (1930, 1931) published work on the behaviour of corrugated plates under the action of shear loads applied at the edges of a plate in the plane of the plate. He considered an infinitely long narrow plate and used a method devised by SOUTHWELL and SKAN (1924) to solve equation (I.2.1) for the case when $q = -2\tau\left(\frac{\partial^2 w}{\partial x \partial y}\right)$ where τ is the intensity of the uniformly distributed shear load along the edges of the plate. The assumed deflected form was

$$w = e^{i\pi\frac{x}{b}} \sum C_r . e^{i\lambda_r (y/b)} \qquad \text{(I.2.5)}$$

where the constants C_r were obtained from the plate edge conditions, these being fixed and free longitudinal/

longitudinal edges.

Seydel considered the compressive component corresponding to the applied shear acting as the governing condition and applied the Euler concepts for eccentrically loaded columns to the behaviour of a sheet whose corrugated cross-section could be represented by a simple trigonometric wave form. He obtained expressions for the elastic stiffnesses etc. in terms of the wave height $f/2$, wave length $\ell/2$, the developed length of the sheet over one wave length $s/2$, and the plate thickness h as follows:

$$D_{11} = \frac{\ell}{s} \cdot \frac{Eh^3}{12(1-\nu^2)}$$

$$D_{22} = EI$$

$$D_{33} = \frac{s}{\ell} \cdot \frac{Gh^3}{6}$$

where I is the moment of inertia of the section of the corrugated sheet per unit length about the neutral axis.

KATO (1932) considered the case of an orthotropic plate clamped at its four edges or clamped on two opposite edges and supported on the other two/

two, subjected to a uniformly distributed load. He attempted a solution where the deflected form was represented by a Fourier double cosine series. Graphs were presented for the central deflection and bending moments along the central line of the plate under the action of the uniformly distributed transverse load and extended this to the case of transverse vibration. The solutions so obtained appear to yield satisfactory results over the middle half length of the plate, but deviate from the assumed conditions at the plate boundaries.

An interesting theoretical paper was published by HOLL (1936) on the analysis of thin rectangular isotropic plates simply supported on opposite edges. The paper studied many aspects of the behaviour of such plates, but of particular relevance to the work contained in this thesis is that related to the case of a rectangular isotropic plate simply supported on two opposite edges and free on the other two.

Proceeding from a Lévy form of solution Holl presented graphs of the variation of deflection, moments and shear forces throughout the plate under a/

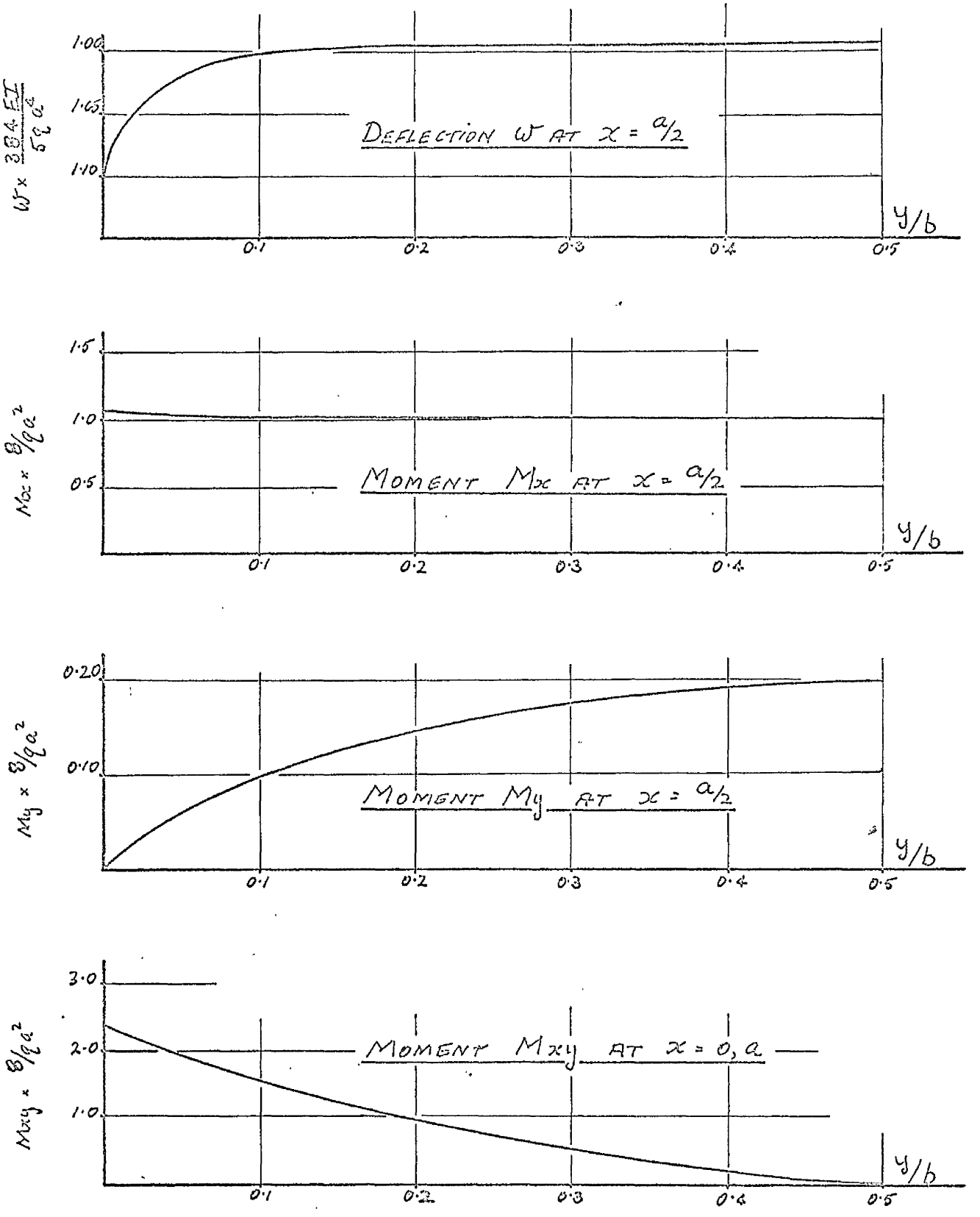

FIG.I.1. Properties of a Square Plate simply supported on edges x = 0, a, free on edges y = 0, b.

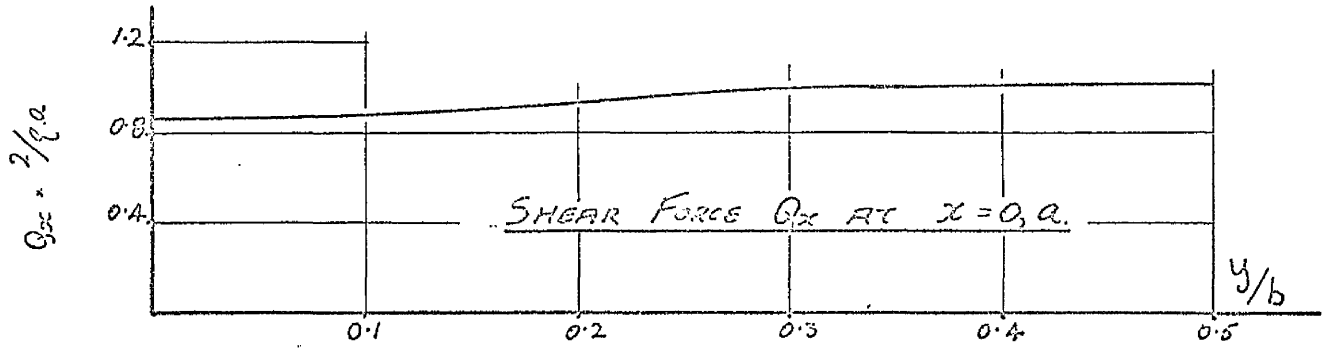

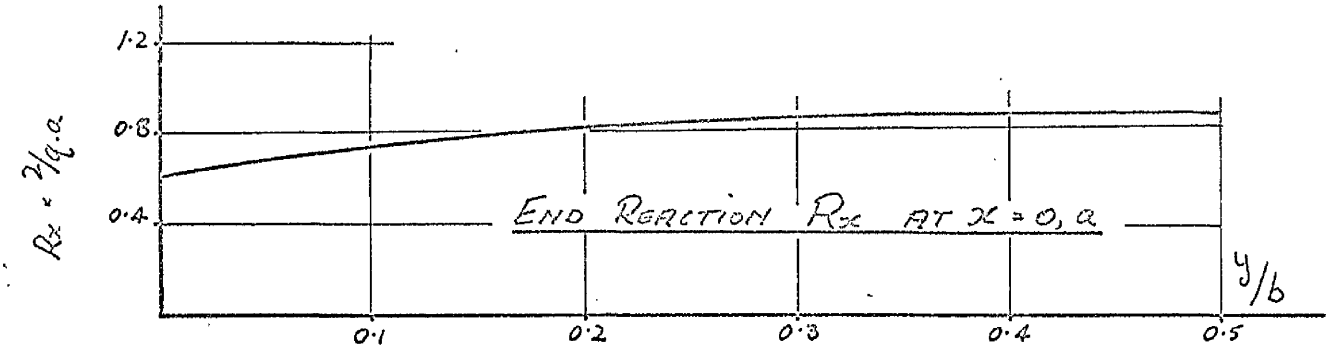

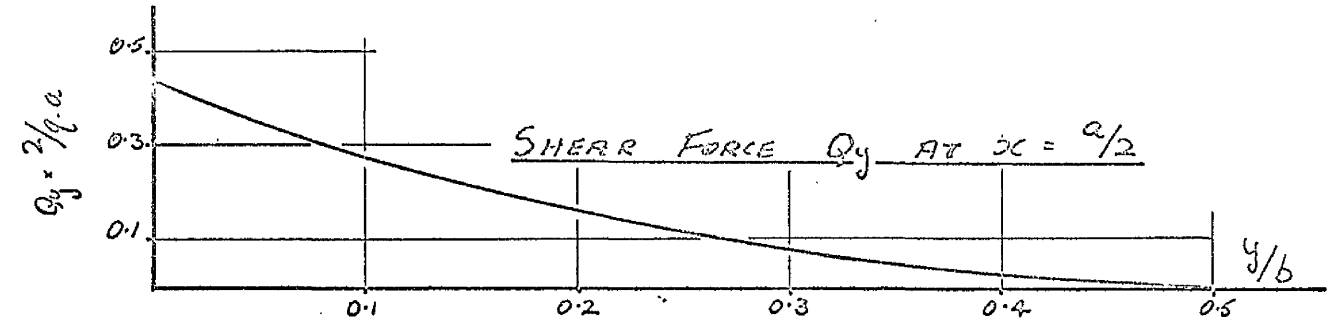

FIG. I.2 Properties of a square plate simply supported on edges x = 0,a, free on edges y = 0,b.

a uniform load of intensity q . The results were presented in the form of the conventional expressions for a thin beam under the same loading conditions multiplied by an appropriate coefficient.
Figs. I.1 and I.2 indicate the figures produced by Holl for a square isotropic plate with Poissson's ratio $\nu = 0.25$, the plate being free on the edges $y = o,b$ and simply supported on $x = o,a$.

The wider implications of Holl's work will be discussed in Chapter II, section II.5.

SCHADE (1940) discussed the problem of a rectangular grid of orthogonally intersecting beams simply supported along the edges of the grid. The construction was plated on one or both surfaces and supported a uniformly distributed transverse load over the whole surface. Schade proceeded from Huber's solution for the deflection w of an infinite strip subjected to a partial line load.

$$w = \sum C.e^{-\alpha x}\left(\cos\beta x + \frac{\alpha}{\beta}\sin\beta x\right)\sin\frac{n\pi y}{b} \qquad (I.2.6)$$

where C is a constant dependent on the load intensity and α and β are factors of the plate aspect ratio/

ratio and number of stiffening beams. This deflected form was modified by Schade introducing the interacting loads between the stiffening beams and the plate of which rigid transverse support is a special case, these loads arising from the intersection of the longitudinal and transverse beams.

He then proceeded to assume that there were an infinite number of negative transverse lineal loads equally spaced along the infinite strip. A panel between any two of these lineal loads can then be considered as a rectangular element of stiffened plating. On this basis he devised loading conditions and deflected forms which permitted the estimation of central deflection and the appropriate values of bending and shearing stresses.

The examination of flat plywood plates under uniform and concentrated loads was undertaken by MARCH (1942), the cases considered being all edges simply supported and clamped respectively. The deflected form was assumed to be sinusoidal and all the work related to the case when the roots of the characteristic equation obtained from (I.2.1) were real. March obtained solutions which exhibited significant/

significant correspondence to those previously deduced by Huber for the uniformly distributed load case and graphs showing the correspondence were presented. An approximate analysis was also put forward based on the behaviour of an infinite orthotropic strip subject to the above mentioned boundary conditions, correspondence to the earliest work of Huber again being evidenced.

THIELEMANN (1945) carried out a comprehensive examination of the anisotropy of various types of plywood, discussing the behaviour of these plates under the action of shearing forces, the plates being assumed to be infinitely long elastic strips. Following the method pioneered by Southwell and Skan for isotropic plates and utilised by Seydel, Thielemann assumed a deflected form similar to equation (I.2.5) and applied this to a strip whose edges were simply supported and clamped respectively. Thielemann also formulated an energy method of determining the buckling loads of plates under pure longitudinal compression, this method being based on the equation of the energy of deformation of the plate to the work done by the externally applied forces. This method was also used for the case of a plate loaded in pure shear, values of the actual loads being obtained for plates/

plates whose ratio of stiffnesses $D_{33}/D_{12} = 2.2$ the roots of the characteristic equation for this value being real. A final point about this paper is that a method devised by NADAI (1915, 1925) and developed by BERGSTRASSER (1927) for testing isotropic plates in bending and twisting was used to determine the elastic moduli of the various plywoods.

The vibration of rectangular wood and plywood plates were studied by HEARMON (1946). The expression for deflection of the governing differential equation was taken to be of a double sinusoidal form and a solution obtained by means of the method of Rayleigh-Ritz for the case of a rectangular orthotropic plate clamped on all four edges. The importance of this paper lies in the fact that together with the work of WARBURTON (1954) it is a source reference for a great deal of research on the vibration of rectangular orthotropic plates.

LEKHNITSKII (1950, 1957) in his two books on anisotropic media and anisotropic plates respectively has reviewed the field in a most comprehensive manner. The former volume established the basic equations and problems of anisotropic elasticity while the latter/

latter dealt with investigations on the deflection and stability of anisotropic plates. It is to the latter book that this review refers, and then only to such sections of it as are considered pertinent to the present investigation.

Lekhnitskii considered the calculation of the elastic stiffnesses D_{11} etc. for a corrugated plate subjected to loading applied in the plane of the plate, with the corrugated cross-section expressed as a simple trigonometric form. The technique of evaluation of these stiffnesses was identical to that carried out by Seydel, Lekhnitskii specifying that the plate could be considered uniform and orthotropic if the number of waves was sufficiently large, that is, the chord of the corrugation is small in comparison with the plate length.

To the author's knowledge Lekhnitskii was the first investigator to indicate the three possible modes of solution to equation (I.2.1) for the bending behaviour of orthotropic plates. Lekhnitskii began by examining the behaviour of uniform thin orthotropic plates under pure bending, pure twisting and the case/

case of bending to a cylindrical surface. A detailed examination of the bending of an orthotropic rectangular plate with four edges simply supported was undertaken, the expression for deflection being postulated as

$$w = \sum_{m=1}^{\infty} \sum_{n=1}^{\infty} F_{mn} \sin \frac{m\pi x}{a} \sin \frac{n\pi y}{b} \qquad \text{(I.2.7)}$$

A similar form for the applied loading q was also used. For the above case, a solution for the orthotropic plate analogous to the Navier solution for an isotropic plate was obtained. Due to the unwieldy nature of this solution, and indeed from the computational viewpoint of most double series solutions, Lekhnitskii reconstituted the plate problems in order that a method pioneered by Lévy (1899) for isotropic plates could be applied.

For the case of an infinitely long plate with the longitudinal edges simply supported, Lekhnitskii took the solution for deflection of equation (I.2.1) to be:

$$w = \sum X_n \sin \frac{n\pi y}{b} \qquad \text{(I.2.8)}$$

where X_n is a function of x only.

Substitution of this expression into equation (I.2.1) yielded a characteristic equation for which three modes of solution were possible, these being:

(1) The four roots of the equation were real and unequal.

(2) The four roots were real and equal.

(3) The four roots were complex.

Attention was confined to the first root condition and the following two sets of boundary conditions were considered in detail:

(1) A plate with four simply supported edges.

(2) A plate with two opposite edges simply supported and the other two edges clamped.

For these problems, the maximum deflection and bending moments were found at the plate centre, these being similar in form to the expressions obtained by Huber.

Lekhnitskii then formulated a method of solution for the problem of the bending of an orthotropic plate with two, three, or four simply supported edges under arbitrary load, utilising the theory of bending of an orthotropic strip. An infinite strip was/

was divided into a series of rectangles by straight lines perpendicular to the sides of the strip, each rectangle being equal in area to that of the original orthotropic plate under consideration. It is interesting to note that the method of solution and final results bear a striking resemblance to the results obtained by Schade. Lekhnitskii attributes much of this to Huber whose work predated that of Schade who appeared to have been unaware of much of Huber's work which appeared in publications of limited circulation.

This section of the book then proceeded to discuss the Ritz solution of the expression for the strain energy content of a rectangular orthotropic plate. The solution for deflection was expressed in the form of a double series solution and the energy expression minimized for the case of a rectangular orthotropic plate clamped on all four edges. The subsequent expressions obtained for the maximum central deflection were compared with those derived by the Lévy method when the limiting case of an isotropic plate was considered in each problem. The value of deflection ascertained by the Ritz method was found to/

to be 3.8% smaller than that found by the Lévy method.

ASHWELL (1952) carried out some interesting work on the stability of shallow corrugated plates where the mode of instability was assumed as similar to that of curved thin plates in bending. The work is reviewed in more detail in Section I.3.

HEARMON and ADAMS (1952) dealt with the determination of the elastic moduli for plywood plates by the series of bending and twisting tests suggested by Thielemann, derived from the work of Bergstrasser. The relationships relating the plate deflections to the plate moduli were determined from the general statement of Hooke's Law for anisotropic media, and these together with the above experimental work were used to ascertain the plate elastic moduli for several forms of plywood and isotropic metal plates. The degree of accuracy obtained was such that the maximum deviation from the mean for the plate moduli was about 3% for the metal plates, but fairly large discrepancies were evident in the case of some plywood specimens - up to the order of 30%. Despite the discrepancies noted, Hearmon and Adams concluded that for plywood/

plywood plates the basic assumptions of anisotropic elasticity hold for the behaviour of such plates when subjected to uniform bending and torsional moments.

Identical tests to those carried out by Hearmon and Adams were those of WITT, HOPPMANN and BUXBAUM (1953), the materials under consideration being three forms of bonded fibreglass. The results do not demonstrate a marked degree of anisotropy and the ratio E_{11}/E_{22}, the principal Young's moduli was not greater than 1.33.

A further point is that, in common with Hearmon and Adams, the results for the elastic moduli for the plates studied were not used to discuss the behaviour of those plates for loading conditions other than bending and twisting.

In a series of papers reporting work carried out at the Johns Hopkins University, Hoppmann and Huffington have examined several aspects of orthotropic plate behaviour.

HOPPMANN (1955) applied the tests of Hearmon and Adams to three forms of stiffened plate, a rectangular thin steel plate with longitudinal grooves/

grooves milled from one surface, a rectangular thin steel plate with brass stiffeners of circular cross-section silver soldered to one face and a circular duralumin plate with rectangular grooves milled in one face parallel to a diameter. The plate stiffnesses D_{11} etc. were determined and he discussed the accuracy of determination of the various moduli, particularly the validity of the assumption $a_{12} = a_{21}$

Substantially different values were obtained for these moduli, and Hoppmann in an interesting discussion arising out of the written comment on this paper justified his recourse to an averaging process for the value $a_{12} = a_{21}$ on the grounds that the plate deflections were not sensitive to this constant. The values of the elastic stiffnesses obtained from the tests were used to predict the central deflection of a circular test plate with a clamped edge under uniform pressure loading, the variance between experiment and theory being 8.5%, theory underestimating the value of deflection.

An attempt to evaluate the elastic constants by theoretical methods was presented by HUFFINGTON (1956), where the flexural and twisting stiffnesses D_{11} etc. were conceived as applying to a homogeneous orthotropic/

orthotropic plate which was equivalent to the actual plate-stiffener combination discussed. This combination was a thin isotropic plate with equally spaced stiffeners of rectangular cross-section disposed symmetrically about the middle plane of the plate, a limitation on the stiffener height being that it did not exceed the stiffener width. The determination of D_{11} was as follows:

The actual plate was considered as made up of a series of plates of width $2c$, thickness h, separated by beams of rectangular cross-section having width $2e$ and depth $2f+h$. The equivalent orthotropic plate was regarded as an infinite strip, simply supported on the boundaries and loaded by uniform pressure. The strain energy of bending and twisting for the equivalent and actual plates were evaluated and equated. From this equation a limiting value of D_{11} was found to be given by

$$D_{11} = D + \frac{EI_s}{S} \qquad \text{(I.2.9)}$$

where $D = Eh^3/12(1-\nu^2)$

I_s = Moment of Inertia of two stiffeners with respect to the middle plane of the plate.

$S = 2(c+e)$ = width of a repeating section.

This result for D_{11} is that which would be obtained by treating the stiffened plate as a wide flange beam.

The evaluation of D_{22} was carried out in an identical manner. Two values for D_{22} were postulated, the first or lower bound being $D_{22} = D$. This corresponds to neglect of the stiffeners when estimating transverse rigidity. The upper bound was given as

$$D_{22} = \frac{E \cdot [h(y)]^3}{12(1-\nu^2)} \qquad \text{(I.2.10)}$$

where $h(y)$ is the total thickness of the plate/stiffener combination. This upper bound corresponds to the situation where there are enough stiffeners present to provide approximate homogeneity.

The effective orthotropic shear modulus D_{66} was determined by comparison of the torsional rigidities of the actual and equivalent orthotropic plates. The value of D_{66} is given by

$$D_{66} = \frac{K_a' \cdot G}{4S} \qquad \text{(I.2.11)}$$

where G = the shear modulus of the isotropic plate material

K_a' = form factor dependent upon the cross-section of the actual stiffened plate.

D_{12} was determined from the equality of bending moments for the direction normal to the plate of curvature in the actual and equivalent plates. A limiting value of D_{12} was found to be given by

$$D_{12} = \nu . D \qquad \text{(I.2.12)}$$

and the limiting values of the two Poisson's Ratios to be:

$$\nu_{12} = \frac{D_{12}}{D_{22}} \quad ; \quad \nu_{21} = \frac{D_{12}}{D_{11}} \qquad \text{(I.2.13)}$$

In the conclusions to this paper Huffington stressed that the theory employed was essentially a plate theory and that the analysis was subject to the limitation that the ratio of stiffener rigidity to plate rigidity must not become such that beam action was predominant. He however suggested as a possible extension to the case when the ratio of stiffener height to stiffener width is greater than unity, that a reduced height of the order of stiffener width be employed.

HOPPMANN, HUFFINGTON and MAGNESS (1956) made a preliminary study of the natural frequencies of vibration of isotropic rectangular plates rendered/

rendered orthotropic by grooves machined on one or both surfaces of the plate. The plate moduli were determined in a manner identical to that used in previous work by Hoppmann (1955), the values of a_{12} and a_{21} quoted for each form of plate being different by a small amount, of the order of 10%.

HOPPMANN (1956) suggested an experimental method to determine the elastic constants of orthotropic plates when bending and stretching of the middle plane was significant. The plates were tested as previously - Hoppmann (1955) - and the appropriate moduli evaluated, these being proportional to the cube of the plate thickness. Tensile and shearing tests were then carried out to determine a further set of constants proportional to the plate thickness. While the results are of interest, it is to be noted that the figures indicated by the author give a change of value of a_{11}, a_{22} and a_{66} of the order of 0.0045, 6.0 and 0.006% respectively, and the values of a_{12} and a_{21} are radically different, a_{21} is quoted as -12.9 times the value of a_{12} .

A study of the free flexural vibrations of stiffened plate was reported by HOPPMANN and MAGNESS/

MAGNESS (1957). The analytical methods used in the paper to predict frequency of vibration took the form of presuming the deflection of the plate to be:

$$w = \sum \sum \sin \frac{m\pi x}{a} \cdot \sin \frac{n\pi y}{b} \cdot F(\tau) \qquad \text{(I.2.14)}$$

where $F(\tau)$ is a harmonic function of time. This solution was applied to the differential equation of free vibration of an orthotropic plate (this is identical in form to equation (I.2.1)) with $q = -\bar{\rho} h \cdot \partial^2 w / \partial \tau^2$ where $\bar{\rho} h$ = mass per unit area of the middle surface of the plate. This provided a frequency equation. The values of the plate constants used were those obtained in the author's earlier work - HOPPMANN (1956) - for the case when stretching of the middle plane is considered. The results, while they do exhibit some discrepancy from observed values of frequency, do demonstrate the utility of data obtained by simple bending and torsion tests.

Continuing their work on the vibrations of rectangular orthotropic plates, HUFFINGTON and HOPPMANN (1958) applied to the equation for flexural vibrations of an orthotropic plate a solution of the Lévy type. A variety of rectangular plate boundary/

boundary conditions were examined all conforming to two opposite edges simply supported and frequency equations for each case were derived. This paper does not set out a comparison with theory and experiment, but refers to the earlier work by the authors which has been reviewed above. Reference is, however, made in written discussion to experimental work on plates whose ratio of constants is E_{11}/E_{22} =3.17.

A postscript to this work was provided by HUFFINGTON (1961) who investigated the occurrence of nodal patterns in vibrating rectangular orthotropic plates. Although it is considered that a detailed account of this work is outwith the scope of this review, it is pertinent to note that a numerical example using elastic constants determined by the bending and twisting tests of Hoppmann (1955) was given, where:

$$\frac{D_{11}}{D_{33}} = 1.543 \qquad \frac{D_{33}}{D_{22}} = 4.810$$

demonstrating that the roots of the characteristic equation were still real.

CHANG (1958) discussed the solution to equation (I.2.1) for a rectangular orthotropic plate clamped on four edges under the action of uniformly/

uniformly distributed transverse loading. As with many previous investigators the expression for deflection was stated as a double sinusoidal series. This expression together with that for the strain energy of deformation was used to obtain equations for the edge reactions which were then equated to the known edge moments and deflections. Chang also examined the rate of convergence of the derived solutions. The general question of convergence is discussed in Appendix VIII.5.

Orthotropic rectangular plates with arbitrary boundary conditions were analysed by KACZKOWSKI (1959) where the plate was loaded by edge forces acting in the plane of the plate which was vibrating. The expression for deflection was taken as a double sinusoidal series and this was used to deduce expressions for the plate edge reactions.

Once again one has reservations regarding the mode of solution used in this publication, particularly with regard to evaluation of quantities such as edge moment near the corners of the plate due to the difficulty of obtaining convergence of the assumed series.

HOLMES (1959) considered the behaviour under transverse load, of a flat plate stiffened by beams of regular cross-section. The analysis was that of a flat plate and associated beams. Expressions for the stress components in the plate and in the beam were set up and the strains in the plate and the stiffening beams at their common surface were equated. Results were presented for longitudinal strain and central deflection, but the important point of lateral strain variation is not touched upon.

WILDE (1960) probed precisely the same problem as Kaczkowski only taking the expression for deflection as a cosine series. The expressions derived are of course similar, but the importance of Wilde's work is that he examines the convergence of this form of double series and shows that with $m = 12$ the coefficient for deflection represents an improvement in accuracy of $2\frac{1}{2}\%$ on that for $m = 2$, that is, the convergence of the series must be considered to be rather slow.

CHENG (1962) looked at the theory of bending of sandwich plates, the core of which was considered to be an orthotropic honeycomb structure. A sixth/

sixth order governing lineal differential equation for deflection was derived, this equation being analogous to the biharmonic equation in the theory of isotropic plates.

For the case of a simply supported, uniformly loaded rectangular plate the behaviour equation was found to be:

$$\left(1 - D_{22}\frac{\partial^2}{\partial x^2} - D_{11}\frac{\partial^2}{\partial y^2}\right)\Delta\Delta w = \frac{q}{D} \qquad \text{(I.2.15)}$$

D_{11} and D_{22} being the plate constants for the orthotropic core.

The general solution to (I.2.15) was taken as

$$w = \frac{qa^4}{D}\sum_{m=1,3}^{\infty}\left[\frac{4}{(m\pi)^5} + A_m \cosh\frac{m\pi y}{a} + B_m \frac{m\pi y}{a}\sinh\frac{m\pi y}{a}\right]\sin\frac{m\pi x}{a} \qquad \text{(I.2.16)}$$

where the plate is simply supported on all four edges.

By substitution into the boundary conditions, and solving for A_m and B_m an expression defining the plate deflection was obtained.

An important paper on new techniques for the solution of orthotropic plate problems was written by VINSON (1962). The principal method was to solve/

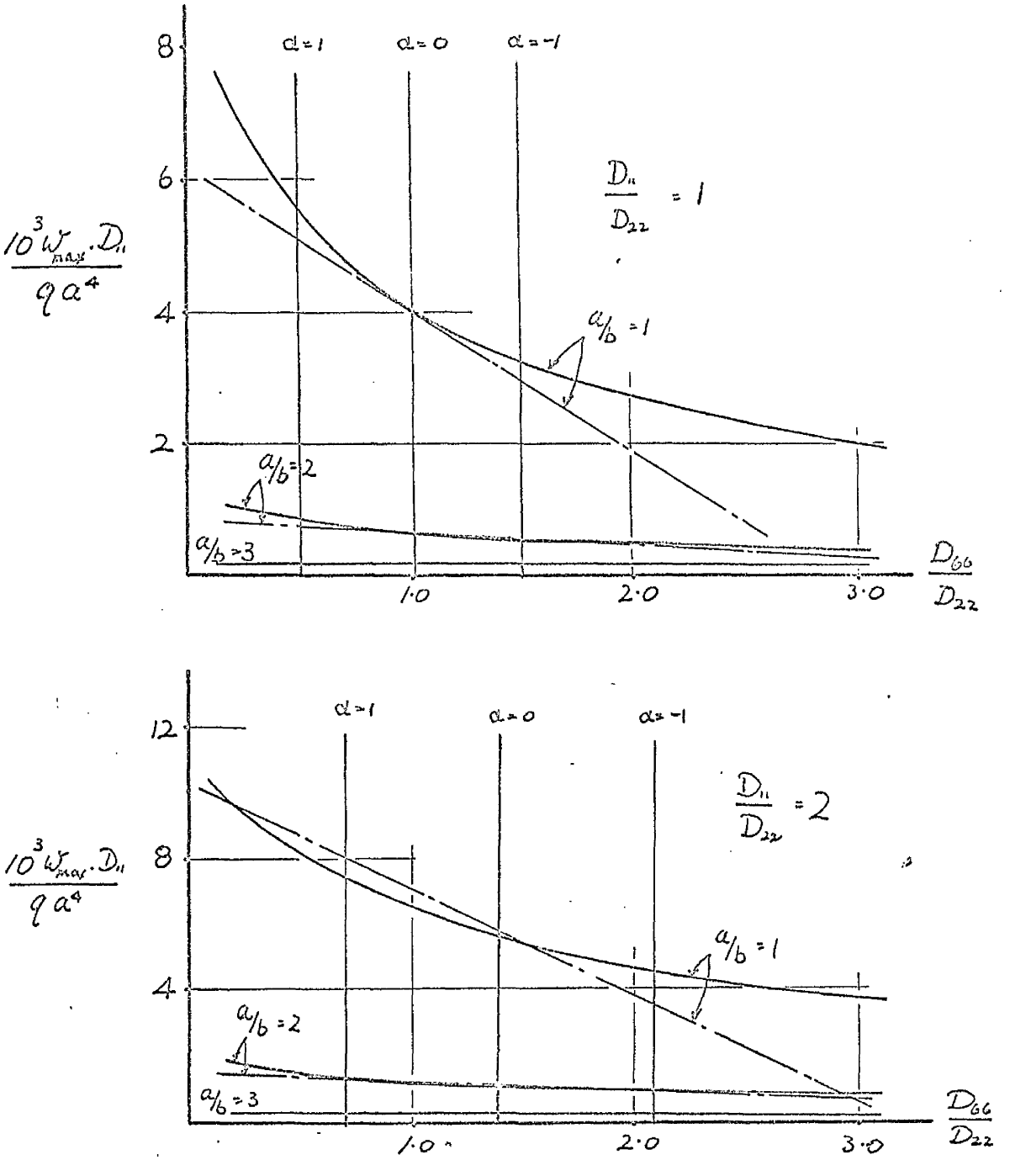

FIG.I.3 Comparison of perturbation solution with Levy solution.

solve the orthotropic plate equation (I.2.1) by a perturbation technique. The existence of a series solution to (I.2.1) of the form

$$w = \sum_{n=0}^{\infty} \phi_n(x, \bar{y})\alpha^n \qquad \text{(I.2.17)}$$

was examined where

$$\bar{y} = \left(\frac{D_{22}}{D_{11}}\right)^{-\frac{1}{4}} \cdot y \qquad \alpha = 2\left[1 - \frac{D_{66}/D_{11}}{(D_{22}/D_{11})^{\frac{1}{2}}}\right]$$

Vinson demonstrated the convergence of this solution for the case of a rectangular simply supported plate and stated that convergence to a satisfactory degree was obtained with the first two terms. A comparison of the derived solution with the exact value obtained by the Lévy method was made, and it was shown that for a rectangular orthotropic plate simply supported on all edges under a uniform lateral pressure for a range of values $-1 \leq \alpha \leq 0.9$ with $D_{11}/D_{22} = 1$ the value of the central deflection was within 10% of the exact value; Vinson's graphs demonstrating this correspondence are shown in Fig. I.3. Also demonstrated was the expected result that for a square plate the orthotropic effects are greatest and these diminish significantly as the length to width ratio/

ratio increases or decreases from unity.

This paper demonstrated the effectiveness of this form of approximate method in determining the deflection of an orthotropic plate but on examination the method suffers from the limitation that the ratio D_{11}/D_{22} must be close to unity, certainly within the range $0.5 \leq D_{11}/D_{22} \leq 2.0$ for maximum deflection values to be within 10% of the classical solution.

TSAI and SPRINGER (1963) published a modification of the twisting tests of Bergstrasser for the determination of the moduli of anisotropic plates. As this paper was based wholly on Bergstrasser's notation and techniques etc., one must confess to some difficulty in interpreting its purpose.

The use of MacLaurin's series to analyse an orthotropic plate was suggested by RAJAPPA and REDDY (1963) where the expression for deflection was taken as

$$w = C_1 + C_2 x^2 + C_3 y^2 + C_4 x^4 + C_5 x^2 y^2 + C_6 y^4$$

This method was based on first determining the deflection expression for the condition of zero/

zero deflection at the plate boundary and then modifying it by introducing moments to cancel those given by the original expression. In the light of the fact that the solution depends for its convergence on a particular set of boundary conditions this method would seem to be more applicable to the analysis of beam gridworks than to that of plates.

In an analysis for the bending of an infinite isotropic strip reinforced by equally spaced identical stiffeners on one side under uniform pressure YAMACKI (1963) solved the problem as a combined boundary value problem associated with the conventional plate and beam theories. The stiffened plate was treated as a series of plate segments separated by stiffeners, the deformation of each determined by applying ordinary plate and beam theories, taking into account the conditions of equilibrium and compatibility along the junction of the plate segment and stiffener. It can be seen, therefore, that the work is principally a continuation of that of Holmes. While there are obvious advantages to the method, namely easier computation than the orthotropic plate theory, it does seem in some ways to by-pass the problem of the/

the interaction of the two elements comprising the complete structure.

I.3. THE BENDING OF PLATES TO AN ANTICLASTIC SURFACE.

In section II.6 of this thesis, a theoretical examination of the bending of orthotropic plates under a uniform moment is examined. This is undertaken in order than an accurate determination of the elastic stiffnesses of the orthotropic plates considered in the experimental sections of Chapter III may be conducted. To the author's knowledge no such examination is available elsewhere, consequently the following short review is of the bending of isotropic plates to an anticlastic surface, the principles of which are utilized in the subsequent examination of the bending of orthotropic plates.

The essential reference to work on the anticlastic curvature of plates in bending is that of LAMB (1891) who examined the flexure of a flat elastic spring bent into a circle of radius ρ by moments on both ends. Lamb showed that the equation for w the deviation at any point of the middle surface from the/

the cylindrical surface of radius ρ is:

$$\frac{h^2\rho^2}{3}\cdot\frac{d^4w}{dx^4} + (1-\nu^2)(w+\epsilon_0\rho) = 0 \qquad \text{(I.3.1)}$$

where y is the longitudinal axis of the strip,

x the lateral

$2h$ = the strip thickness,

$2b$ = the strip breadth.

ϵ_0 = the extension of the medial plane in the x - direction

ν = Poisson's Ratio.

The solution of (I.3.1) was considered to be

$$(w+\epsilon_0\rho) = A_m \cos\alpha x \cosh\alpha x + B_m \sin\alpha x \sinh\alpha x \qquad \text{(I.3.2)}$$

where

$$\alpha = \sqrt[4]{\frac{3(1-\nu^2)}{4h^2\rho^2}} \qquad \text{(I.3.3)}$$

The boundary conditions formulated by Lamb were that on the edges $x = \pm b$

$$\frac{d^2w}{dx^2} - \frac{\nu}{\rho} = \frac{d^3w}{dx^3} = 0 \qquad \text{(I.3.4)}$$

Substitution of (I.3.2) into (I.3.4) gave values of the constants A_m and B_m which defined the deviation of the strip from the cylindrical form of radius of curvature ρ .

Lamb examined the implications of the solution, particularly its accuracy at the strip edges and reached the conclusion that at the edge the magnitude of the deviation from the cylindrical form was comparable with the strip thickness $2h$. A further point that emerged from the above analysis was that this deviation diminishes rapidly towards the centre of the plate, but that the sign of deviation fluctuates. Lamb concluded by noting that amplitudes of these fluctuations were so small that they were never likely to be the subject of observation.

SEARLE (1908) examined in some detail the distortion of the cross-section of rods and plates under uniform bending and he showed that if a thin plate or "blade" is bent by a uniform moment to a cylindrical form of radius of curvature ρ , the radius of curvature in the transverse direction is given by ν/ρ , ν being the Poisson's Ratio for the plate. material. Searle also demonstrated that an element/

element of the plate with a longitudinal force T acting on it, and a radius of curvature ρ experiences a resultant radial force of magnitude $2T \sin \alpha/2$ acting towards the centre of curvature, where α is the angle subtended by the ends of the filament at the centre of curvature. This force tends to reduce the anticlastic curvature developed and Searle estimated that such curvature will be eliminated when $b^2/\rho d \geq b$, b and d being the breadth and depth of the strip respectively.

An interesting experimental study to confirm the expressions deduced by Lamb and Searle was undertaken by ASHWELL and GREENWOOD (1950). The plates used were 15 in. broad, 0.125 in. thick, and supported on knife edges 4 feet apart, uniform moment being applied by weights at the end of a 2 feet overhang at each end. The authors concluded that on a qualitative basis the results for deflections obtained admirably demonstrated the distinction suggested by theory between the behaviour of plates having initial curvatures of opposite sign, and quantitatively the results were a satisfactory demonstration of the theories of Lamb and Searle.

ASHWELL (1950) reviewed and extended the work of Lamb and Searle, investigating fully the implications of the analysis for anticlastic curvature where the transverse effects were considered as analogous to the bending behaviour of a beam on an elastic foundation subjected to a non-uniformly distributed load. Ashwell confirmed Lamb's analysis regarding the fluctuations in sign of the deviation across the plate from the cylindrical form and confirmed that the critical ratio $b^2/\rho d$ defines the mode of distortion of the plate cross-section.

The stability of corrugated plates was also studied by ASHWELL (1952) using equation (I.3.1) to define the deflected form. The method used was essentially that of expressing the corrugated shape in as general a form as possible, this usually being an infinite trigonometric series, substituting this series into (I.3.1) and thereby obtaining an expression for the distorted cross-section of the plate in terms of the radius of curvature and the constant α derived by Lamb - equation (I.3.3).

The analysis showed that as the curvature is increased the corrugations become progressively flatter/

flatter, this effect being due to the same radial force as cause suppression of the anticlastic curvature of flat plates in pure bending. The limitations of the analysis are that the corrugated forms that can be tackled by this method would need to have a cross-section which could be expressed by a comparatively simple mathematical series and the overall height of the corrugations would be limited to a maximum of three times the plate thickness.

CONWAY and NICKOLA (1964) used the work of Lamb to obtain expressions for the stress variation across a flat sheet when bent by a constant moment to an anticlastic surface. The paper is of interest primarily for the experimental work which was carried out on thin steel and aluminium sheets, 14 and 24 in. long respectively. Measurement of longitudinal and lateral strains was effected by electrical resistance foil strain gauges and the measured values were used to deduce stresses which were compared to those obtained theoretically. The agreement obtained is very good, particularly when one reflects that the experimental values of Young's Modulus and Poisson's Ratio were only known to an accuracy of 2 - 3%. The only reservation that could be expressed is that the/

the moments were applied to the plates through a supporting bar to which the plates were fixed thereby inducing some restraint on the transverse edges of the plate.

I.4. SUMMARY AND COMMENTARY.

Any assessment of the theoretical work to date on orthotropic plates must be made with the recognition that the advent of computers and their widespread availability in the last decade or so has radically altered the mathematical outlook on the problems of elasticity and elastic behaviour. Thus, to criticise the work of one's precursors on their apparent unwillingness to undertake problems of wide applicability is to ignore the very nature of the computational tools available to them. The author hopes, therefore, that the following critical assessment will be regarded as criticising without castigating and disapproving without deprecating.

Early theoretical work concentrated almost exclusively on orthotropic plate problems where the characteristic behaviour equation for the considered plate loading produced wholly real roots when operated upon by the Lévy method. For orthotropic/

orthotropic plates supported on all four edges HUBER and LEKHNITSKII have exhausted all the possible solutions for real roots, the former using for most cases a Fourier series for the deflected form and such numerical work as was done was carried out using only the first term of the infinite series. LEKHNITSKII was to the author's knowledge the first to note the limitation of the Fourier series methods and re-formulated some of the plate problems for analysis by the Lévy method. As before, the cases considered revealed only real roots of the characteristic equation, although Lekhnitskii did set out the extension of the method to deal with complex roots. The author would therefore consider that for the problems of orthotropic plates under lateral load the basic work of Huber and Lekhnitskii indicates that the double series method, while of value, does not contribute to any appreciable degree to the solution of such problems, With this in mind, it follows that a great deal of the theoretical work subsequent to that of the above two analysts when applied to practical problems does not fulfil the promise of its stated intentions.

It is also noteworthy that the work of HOLL/

HOLL which would seem to the author to have indicated fruitful lines of thought on orthotropic applications of his methods has not been the spur to further investigations. To a lesser degree, the same could be said of the analysis carried out by SEYDEL, which posed many questions regarding the behaviour of corrugated plates. Indeed, the work of Holl in evaluating forces and moments throughout an isotropic plate with two edges free and that of Seydel in applying to corrugated plates under edge shear loading the orthotropic plate equation, seem to the author to be pioneering work which has been sadly ignored.

WILDE and VINSON are the only recent investigators to have considered the very relevant problems of the convergence of the form of the solution assumed, and as such these contributions are of particular value.

Some recent papers have been but restatements of the work of earlier theoreticians. However the paper by RAJAPPA and REDDY putting forward a method whereby the deflected form is considered as a MacLaurin's series is a welcome addition to the literature. The author believes that this work, while/

while valuable, has a greater applicability to the problems of linked beams and grillage networks which have been comprehensively tackled by TRENKS (1954), PFLUGER (1947) and HENDRY and JAEGER (1958).

To date all the experimental work to find the elastic stiffnesses of orthotropic plates has been based on the bending and twisting tests of NADAI and BERGSTRASSER, and with the exception of those performed by WITT et. al(1953), HOPPMANN (1955) and HOPPMANN et. al(1956) has been on various configurations of plywood or similar constructions.

One of the major results of this experimentation has been the initiation of an animated correspondence (Journal of Applied Mechanics, 1955) on the relative values of the moduli a_{12} and a_{21}. The implications of the assumption $a_{12} = a_{21}$ are discussed in Chapter II, but the author would like to record at this point his view that Hoppmann's concept is in all probability the correct one, namely, that the moduli a_{12} and a_{21} are in fact equal.

A considerable amount of work has been based on the evaluation of the elastic constants for an/

an orthotropic plate considered as a series of beams linked by a considerably weaker plate. While this is a justifiable premise in many cases, the author holds the view that any accurate analysis of the bending of orthotropic plates must take into account the overall behaviour of the structure which is to be considered as a plate. Furthermore, there has been a general reluctance to apply the constants evaluated either experimentally or theoretically for a plate to the behaviour of the plate under essentially different loading or boundary conditions. In this context, the work of MARCH (1942), HOPPMANN (1955) and HOPPMANN and MAGNESS (1957) is exceptional, although March himself has taken the values of the elastic stiffnesses for his wooden plates from the work of others and describes these values as "tentative". Hoppmann and Magness have used the values derived from bending tests to investigate the nodal patterns exhibited in vibrating orthotropic plates, the correspondence between theory and experiment being well demonstrated. In all the above papers the authors stress the value and difficulty of obtaining accurate experimental data.

As has been mentioned in the review, some authors have considered the behaviour of an orthotropic plate as being equivalent to a series of orthotropic strips or beams, without stating either the basis of this assumption or the range of stiffness ratios for which it is assumed to apply. The author accepts that in many cases the justification lies in the applied loading, e.g. longitudinal shear or traction give boundary conditions to which the infinite strip approach is particularly suited, but it is difficult to rationalize the strip approach for problems involving transverse loading in any form. One of the purposes of the theoretical section in this thesis is to investigate the validity of this approach.

In the light, therefore, of the above factors, the work set out in this thesis was orientated to investigate and discuss the following:

1. The analysis of the behaviour of orthotropic plates as integral structures and the application of a concept of linked beams.
2. The experimental evaluation of the orthotropic stiffness of corrugated plates and the use of these in orthotropic plate analysis.

3. The theoretical and experimental behaviour of corrugated decking under uniform loading, the decking being regarded as orthotropic constructions.
4. The development of a rational basis for the design of decking systems.

CHAPTER II

THEORETICAL ANALYSIS

II.1. THE ELASTIC MODULI AND CONSTANTS FOR GENERALLY ORTHOTROPIC PLATES.

To obtain relationships between the components of force and the components of deformation in an elastic body, it is necessary to choose some model which reflects the elastic properties of that body.

In the following analysis it will be assumed that the components of strain are linear functions of those of stress, that is, the material under discussion conforms to the generalised Hooke's Law. For the general case of a homogeneous anisotropic body, the equations which express Hooke's Law in Cartesian co-ordinates x, y, z have the form:

$$\begin{aligned}
\epsilon_x &= a_{11}\sigma_x + a_{12}\sigma_y + a_{13}\sigma_z + a_{14}\tau_{yz} + a_{15}\tau_{xz} + a_{16}\tau_{xy} \\
\epsilon_y &= a_{21}\sigma_x + a_{22}\sigma_y + \text{- - - - - - - -} \\
&\vdots \\
\gamma_{xy} &= a_{61}\sigma_x + a_{62}\sigma_y + a_{63}\sigma_z + a_{64}\tau_{yz} + a_{65}\tau_{xz} + a_{66}\tau_{xy}.
\end{aligned} \qquad \text{(II.1.1)}$$

Where the coefficients a_{ij} are referred to as the "elastic moduli" for the body material.

If the body under consideration is in the form of a plate where the lateral dimensions are much greater than the plate thickness, equation (II.1.1) can/

can be simplified to:

$$\epsilon_x = a_{11}\sigma_x + a_{12}\sigma_y + a_{16}\tau_{xy}$$

$$\epsilon_y = a_{21}\sigma_x + a_{22}\sigma_y + a_{26}\tau_{xy} \qquad \text{(II.1.2)}$$

$$\gamma_{xy} = a_{61}\sigma_x + a_{62}\sigma_y + a_{66}\tau_{xy}$$

Similarly the stresses σ_x etc. can be formulated as functions of the condition of strain as

$$\sigma_x = b_{11}\epsilon_x + b_{12}\epsilon_y + b_{16}\gamma_{xy}$$

$$\sigma_y = b_{21}\epsilon_x + b_{22}\epsilon_y + b_{26}\gamma_{xy} \qquad \text{(II.1.3)}$$

$$\tau_{xy} = b_{61}\epsilon_x + b_{62}\epsilon_y + b_{66}\gamma_{xy}$$

Where b_{ij} are referred to as the "elastic constants" for the plate material.

Assuming that the Maxwell reciprocal relationships hold, namely $a_{ij} = a_{ji}$, $b_{ij} = b_{ji}$ and applying the normal rules for the solution of equations to (II.1.2) and (II.1.3) the following identities relating a_{ij} and b_{ij} can be found

$$\Delta b_{11} = a_{22}.a_{66} - a_{26}^2$$

$$\Delta b_{21} = \Delta b_{12} = a_{16}.a_{26} - a_{12}.a_{66}$$

$$\Delta b_{22} = a_{11}.a_{66} - a_{16}^2$$

$$\Delta b_{66} = a_{11}.a_{22} - a_{12}^2 \qquad \text{(II.1.4)}$$

$$\Delta b_{16} = \Delta b_{61} = a_{12}.a_{26} - a_{22}.a_{16}$$

$$\Delta b_{26} = \Delta b_{62} = a_{12}.a_{16} - a_{11}.a_{26}$$

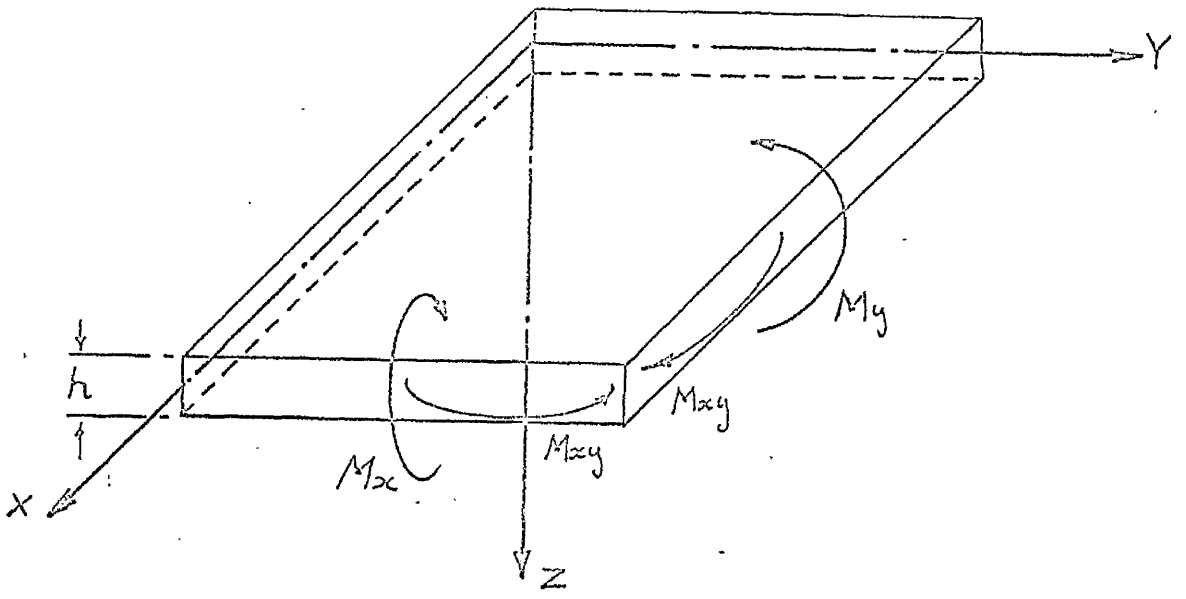

FIG.II.1 Moments in the cross-section of a plate element.

where:

$$\Delta = \begin{vmatrix} a_{11} & a_{12} & a_{16} \\ a_{21} & a_{22} & a_{26} \\ a_{61} & a_{62} & a_{66} \end{vmatrix}$$

As indicated above the six elastic moduli a_{11}, a_{22}, a_{12}, a_{16}, a_{26} and a_{66} fully characterize the elastic behaviour of a generally orthotropic plate.

II.2. THE BENDING OF GENERALLY ORTHOTROPIC PLATES.

The usual assumptions of the classical theory of bending are made, namely:

1. The plate is thin and may be considered to be in a state of plane stress.
2. The bending deflection of the plate is small compared to the plate thickness, i.e. the radius of curvature is large.

For an element of a generally orthotropic plate under a uniform lateral load q acted upon by moments M_x, M_y, M_{xy} as shown in Fig. II.1 the equilibrium condition can be stated as (TIMOSHENKO and WOINOWSKY - KRIEGER 1959):

$$\frac{\partial^2 M_x}{\partial x^2} + 2\frac{\partial^2 M_{xy}}{\partial x\, \partial y} + \frac{\partial^2 M_y}{\partial y^2} = q \qquad \text{(II.2.1)}$$

where:

$$M_x = \int_{-\frac{h}{2}}^{\frac{h}{2}} \sigma_x \cdot z \cdot dz \quad ; \quad M_y = \int_{-\frac{h}{2}}^{\frac{h}{2}} \sigma_y \cdot z \cdot dz$$

$$M_{xy} = \int_{-\frac{h}{2}}^{\frac{h}{2}} \tau_{xy} \cdot z \cdot dz. \qquad \text{(II.2.2)}$$

Assuming a linear strain distribution over the plate thickness then for a point in the plate distance z from the neutral surface the displacements due to the curvature of the plate are:

$$\epsilon_x = -z \frac{\partial^2 w}{\partial x^2} \quad ; \quad \epsilon_y = -z \frac{\partial^2 w}{\partial y^2}$$

$$\gamma_{xy} = -2z \frac{\partial^2 w}{\partial x \partial y} \qquad \text{(II.2.3)}$$

where w is the bending deflection of the plate.

On substituting the expressions for the stresses and strains from equations (II.1.2) and (II.2.3) respectively into equation (II.2.2) and then putting the resulting expressions for M_x etc. into equation (II.2.1) the following equation is obtained:

$$D_{11}\frac{\partial^4 w}{\partial x^4} + 4D_{16}\frac{\partial^4 w}{\partial x^3 \partial y} + 2D_{33}\frac{\partial^4 w}{\partial x^2 \partial y^2} + 4D_{26}\frac{\partial^4 w}{\partial x \partial y^3} + D_{22}\frac{\partial^4 w}{\partial y^4} = q \qquad \text{(II.2.4)}$$

where:

$$D_{11} = \frac{h^3}{12} \cdot b_{11} \quad ; \quad D_{16} = \frac{h^3}{12} \cdot b_{16} \quad ; \quad D_{22} = \frac{h^3}{12} \cdot b_{22}$$

$$D_{26} = \frac{h^3}{12} \cdot b_{26} \quad ; \quad D_{33} = \frac{h^3}{12}(b_{12} + 2b_{66}) = D_{12} + 2D_{66}$$

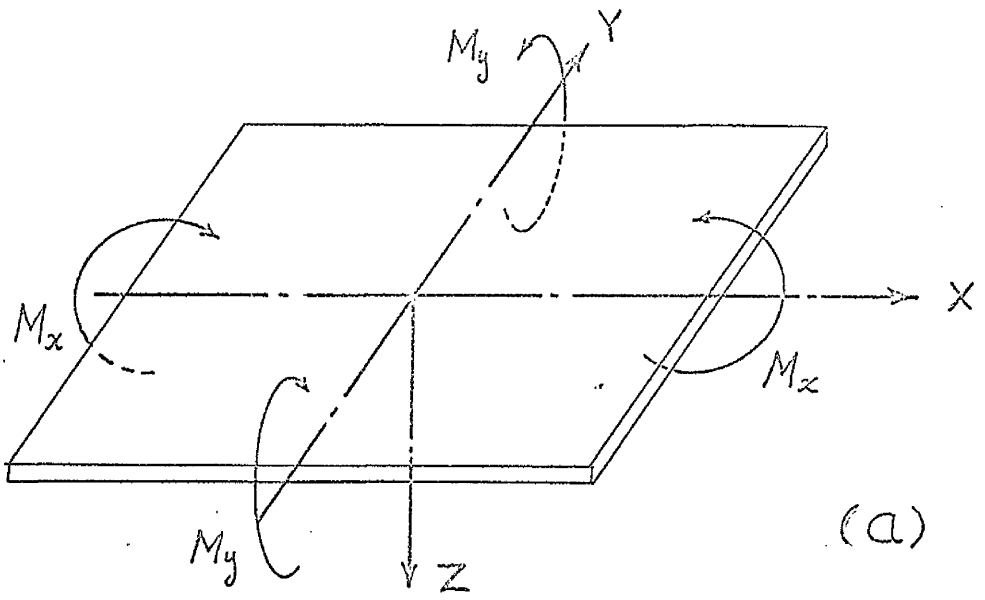

Condition of pure longitudinal stress.

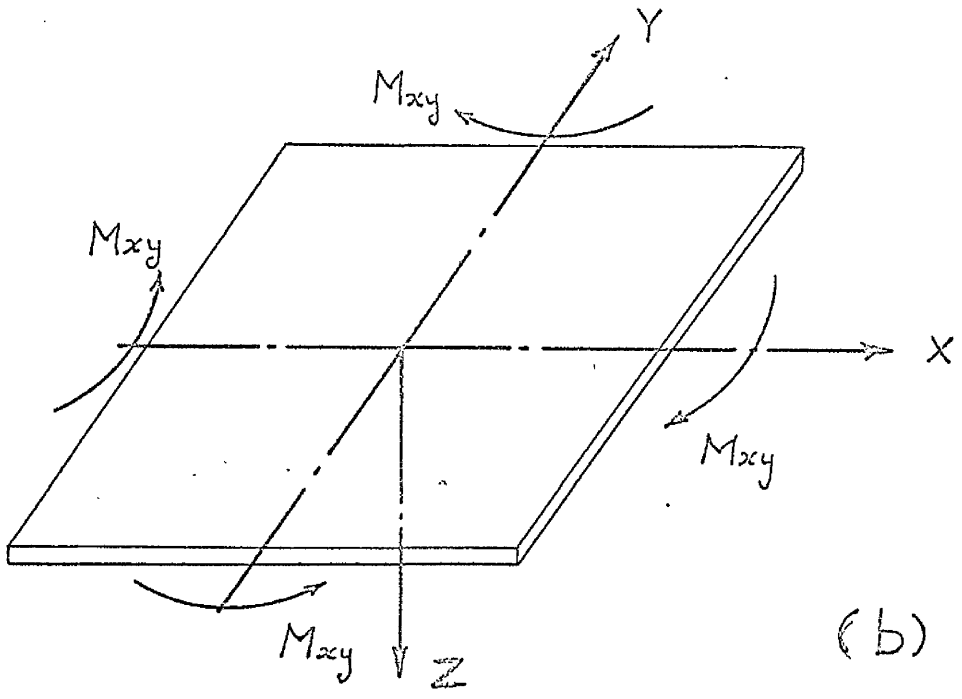

Condition of pure shear stress.

FIG.II.2

This equation (II.2.4) is the deflection equation for a generally orthotropic plate subject to a uniform loading of intensity q . The constants D_{11} etc. which contain the six elastic moduli will be referred to as the "elastic stiffnesses" of the plate.

II.3. THE DETERMINATION OF THE ELASTIC MODULI OF GENERALLY ORTHOTROPIC PLATES.

It has been shown that the elastic behaviour of the generally orthotropic plate can be characterized by six elastic moduli. This section sets out the theoretical background to the experimental evaluation of these moduli.

Nadai has referred to the fact that to determine the elastic moduli of isotropic plates two conditions of stresses are particularly suitable, those of pure longitudinal stress and shearing stress - Figs. II.2(a) and (b).

To determine a relationship between the stresses produced by the plate loading and the plate deflection equate the displacements ϵ_x, ϵ_y and γ_{xy} as given by equations (II.1.2) and (II.2.3) where/

where $z = h/2$.

$$\frac{\partial^2 w}{\partial x^2} = -\frac{2}{h}\left(a_{11}\sigma_x + a_{12}\sigma_y + a_{16}\tau_{xy}\right)$$

$$\frac{\partial^2 w}{\partial y^2} = -\frac{2}{h}\left(a_{21}\sigma_x + a_{22}\sigma_y + a_{26}\tau_{xy}\right) \qquad \text{(II.3.1)}$$

$$\frac{\partial^2 w}{\partial x \partial y} = -\frac{2}{h}\left(a_{16}\sigma_x + a_{26}\sigma_y + a_{66}\tau_{xy}\right)$$

Thielemann has shown that a general form for the deflection w which satisfies equation (II.3.1) is given by :

$$\begin{aligned} w = & -\frac{\sigma_x}{h}\left(a_{11}x^2 + a_{21}y^2 + a_{16}xy\right) \\ & -\frac{\sigma_y}{h}\left(a_{12}x^2 + a_{22}y^2 + a_{26}xy\right) \\ & -\frac{\tau_{xy}}{h}\left(a_{16}x^2 + a_{26}y^2 + a_{66}xy\right) \\ & + C_1 x + C_2 y + C_3 \end{aligned} \qquad \text{(II.3.2)}$$

The term $C_1x + C_2y + C_3$ determines the position of the plate in space and for the present discussion has a value of zero, the origin of the system being taken as the origin of the plate.

Lekhnitskii has demonstrated that the moduli a_{ij} can be considered as the reciprocal of the respective Young's Modulus or Modulus of Rigidity for the direction ij

direction $i\,j$

$$a_{11} = \frac{1}{E_{11}} \quad ; \quad a_{22} = \frac{1}{E_{22}}$$

$$a_{12} = \frac{-\nu_{12}}{E_{11}} = \frac{-\nu_{21}}{E_{22}} \qquad \text{(II.3.3)}$$

$$a_{16} = \frac{-\nu_{16}}{E_{11}} \quad ; \quad a_{26} = \frac{-\nu_{26}}{E_{22}} \quad ; \quad a_{66} = \frac{1}{G_{66}}$$

Where ν_{ij} is the Poisson's Ratio relating a stress in the direction i to a strain in the direction j

The above analysis indicates that by careful selection of a series of bending and twisting tests the moduli a_{ij} can be obtained for an orthotropic plate and that such values together with equations (II.1.7) will yield the values of the elastic stiffnesses in the orthotropic plate equation.

These tests and their application to troughed decking are described in Chapter III.

II.4. VERIFICATION OF THE SPECIALLY ORTHOTROPIC PLATE COMPATIBILITY EQUATION AND CONSISTENT BOUNDARY CONDITIONS.

It can be shown from the general statement of Hooke's Law for an orthotropic plate that the expression for the potential energy of bending is given/

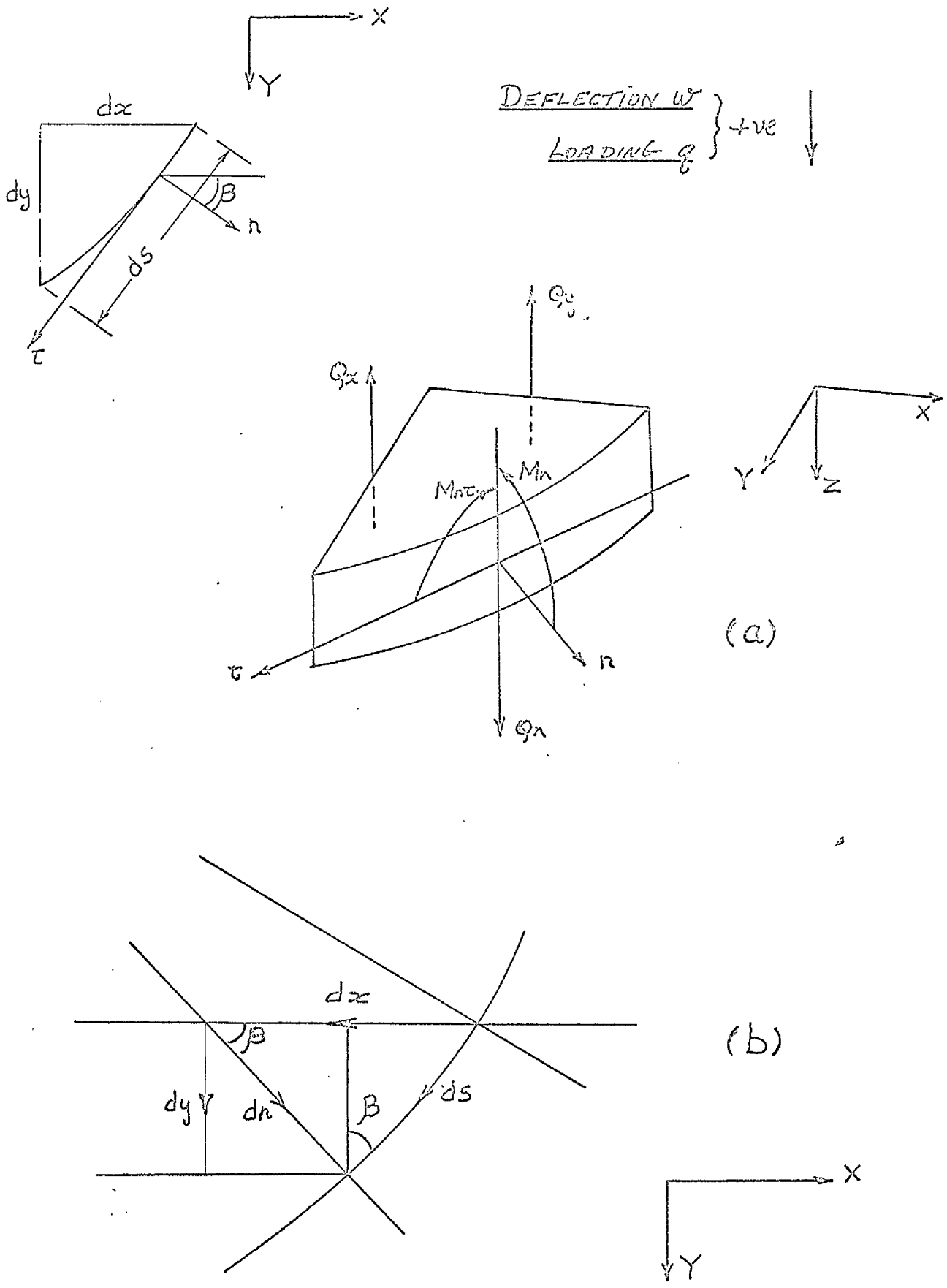
X
Y
dx
dy
β
n
ds
τ
DEFLECTION w
LOADING q
+ve
Qy
Qx
Mnτ
Mn
Z
(a)
Qn
dx
β
dy
dn
β
ds
(b)

FIG. II.3

given by

$$V = \frac{1}{2}\iint \left[D_{11}\left(\frac{\partial^2 w}{\partial x^2}\right)^2 + 2D_{12}\frac{\partial^2 w}{\partial x^2}\cdot\frac{\partial^2 w}{\partial y^2} + D_{22}\left(\frac{\partial^2 w}{\partial y^2}\right)^2 + 4D_{66}\left(\frac{\partial^2 w}{\partial x\,\partial y}\right)^2 \right] dx\,dy \qquad \text{(II.4.1)}$$

Applying the principle of virtual displacements, it is assumed that a small variation δw of the plate deflection w is produced. During this assumed virtual displacement the change in strain energy of the plate must be equal to the work done by the external forces. If the direction of the bending moments M_n and M_{nt} and shear forces Q_n acting on the plate subjected to a uniform lateral load of intensity q distributed over the plate surface are as indicated in Fig. II.3(a) then the expression for the work done during this virtual displacement is given by

$$\delta V = \iint q.\delta w\,dx\,dy - \int M_n \frac{\partial \delta w}{\partial n}.ds + \int \left(Q_n + \frac{\partial M_{nt}}{\partial s}\right)\delta w.ds \qquad \text{(II.4.2)}$$

The first integral represents the work of the lateral load during the displacement δw. The second, extended along the boundary of the plate represents the work done by the bending moments due to the rotation $\partial \delta w/\partial n$ of the edge of the plate, while the third integral represents the work of the transverse/

transverse shear forces applied along the edge of the plate.

The calculation of the variation δV of the strain energy of the plate will be presented here in detail for the first term of equation (II.4.1), that for the other terms being presented in Appendix VIII.1.

Therefore:

$$\delta \iint D_{11}\left(\frac{\partial^2 w}{\partial x^2}\right)^2 dx\,dy = 2D_{11}\iint \frac{\partial^2 w}{\partial x^2}\cdot\frac{\partial^2 \delta w}{\partial x^2}\cdot dx\,dy$$

$$= 2D_{11}\iint\left[\frac{\partial}{\partial x}\left(\frac{\partial^2 w}{\partial x^2}\cdot\frac{\partial \delta w}{\partial x}\right) - \frac{\partial^3 w}{\partial x^3}\cdot\frac{\partial \delta w}{\partial x}\right] dx\,dy$$

$$= 2D_{11}\iint\left[\frac{\partial}{\partial x}\left(\frac{\partial^2 w}{\partial x^2}\cdot\frac{\partial \delta w}{\partial x}\right) - \frac{\partial}{\partial x}\left(\frac{\partial^3 w}{\partial x^3}\cdot\delta w\right) + \frac{\partial^4 w}{\partial x^4}\cdot\delta w\right] dx\,dy$$

In a Cartesian system of co-ordinates for any function P of x

$$\iint \frac{\partial P}{\partial x}\,dx\,dy = \int P\cdot\cos\beta\cdot ds$$

$$\iint \frac{\partial P}{\partial y}\,dx\,dy = \int P\sin\beta\, ds$$

where the simple integrals are extended along the boundary, β being the angle between the outer normal and the x-axis as shown in Fig. II.3(a)

$$\therefore \delta \iint D_{11}\left(\frac{\partial^2 w}{\partial x^2}\right)^2 dx\,dy = 2D_{11}\iint \frac{\partial^4 w}{\partial x^4}\cdot\delta w\cdot dx\,dy$$

$$+ 2D_{11}\int\left(\frac{\partial^2 w}{\partial x^2}\cdot\frac{\partial \delta w}{\partial x} - \frac{\partial^3 w}{\partial x^3}\cdot\delta w\right)\cos\beta\, ds$$

Advancing along the boundary in the direction shown in Fig. II.3(b)

$$\therefore \frac{\partial \delta w}{\partial x} = \frac{\partial \delta w}{\partial n} \cdot \frac{dn}{dx} + \frac{\partial \delta w}{\partial s} \cdot \frac{ds}{dx} = \frac{\partial \delta w}{\partial n} \cdot \cos\beta - \frac{\partial \delta w}{\partial s} \cdot \sin\beta$$

$$\therefore \delta \iint D_{11} \left(\frac{\partial^2 w}{\partial x^2}\right)^2 dx\,dy = 2D_{11} \iint \frac{\partial^4 w}{\partial x^4} \cdot \delta w \cdot dx\,dy + 2D_{11} \int \frac{\partial^2 w}{\partial x^2} \left(\frac{\partial \delta w}{\partial n} \cos\beta - \frac{\partial \delta w}{\partial s} \sin\beta\right) \cos\beta$$

$$- 2D_{11} \int \frac{\partial^3 w}{\partial x^3} \cdot \delta w \cdot \cos\beta \, ds$$

Integrating by parts the second of the bracketed terms of the R.H.S. of the above equation

$$-2D_{11} \int \frac{\partial^2 w}{\partial x^2} \cdot \sin\beta \cos\beta \frac{\partial \delta w}{\partial n} \cdot ds$$

$$= -2D_{11} \left[\left(\frac{\partial^2 w}{\partial x^2} \cdot \sin\beta \cos\beta \, \delta w \right) - \int \delta w \frac{\partial}{\partial s} \left(\frac{\partial^2 w}{\partial x^2} \cdot \sin\beta \cos\beta \right) ds \right]$$

As the integral is over the closed boundary of the plate, the first term on the R.H.S. of the above equation is zero.

Therefore the variation of the first term of equation (II.4.1) is found to be

$$\delta \iint D_{11} \left(\frac{\partial^2 w}{\partial x^2}\right)^2 dx\,dy$$

$$= 2D_{11} \iint \frac{\partial^4 w}{\partial x^4} \cdot \delta w \, dx\,dy + 2D_{11} \iint \frac{\partial^2 w}{\partial x^2} \cos^2\beta \frac{\partial \delta w}{\partial n} \cdot ds \qquad \text{(II.4.3)}$$

$$+ 2D_{11} \iint \left[\frac{\partial}{\partial s} \left(\frac{\partial^2 w}{\partial x^2} \cdot \sin\beta \cos\beta \right) - \frac{\partial^3 w}{\partial x^3} \cdot \cos\beta \right] \delta w \cdot ds$$

A similar procedure can be carried out for the variations of each of the other terms of equation/

equation (II.4.1) to obtain

$$\delta D_{22} \iint \frac{\partial^2 w}{\partial y^2}\, dx\, dy$$

$$= 2D_{22} \iint \frac{\partial^4 w}{\partial y^4}\, \delta w\, dx\, dy + 2D_{22} \int \frac{\partial^2 w}{\partial y^2} \cdot \sin^2\beta\, \frac{\partial \delta w}{\partial n} \cdot ds$$

$$- 2D_{22} \iint \left[\frac{\partial}{\partial s}\left(\frac{\partial^2 w}{\partial y^2} \sin\beta \cos\beta \right) + \frac{\partial^3 w}{\partial y^3} \cdot \sin\beta \right] \delta w \cdot ds$$

$$\delta 2 D_{12} \iint \left(\frac{\partial^2 w}{\partial x^2}\right)\left(\frac{\partial^2 w}{\partial y^2}\right) dx\, dy$$

$$= 4 D_{12} \iint \frac{\partial^4 w}{\partial x^2 \partial y^2}\, dx\, dy - 2D_{12} \int \left(\frac{\partial^3 w}{\partial x \partial y^2} \cos\beta + \frac{\partial^3 w}{\partial x^2 \partial y} \cdot \sin\beta \right) \delta w \cdot ds$$

$$+ 2D_{12} \int \frac{\partial}{\partial s}\left[\frac{\partial^2 w}{\partial y^2} - \frac{\partial^2 w}{\partial x^2} \right] \sin\beta \cdot \cos\beta\, \delta w \cdot ds$$

$$+ 2D_{12} \int \left(\frac{\partial^2 w}{\partial y^2} \cos^2\beta + \frac{\partial^2 w}{\partial x^2} \sin^2\beta \right) \frac{\partial \delta w}{\partial n} \cdot ds$$

$$\delta 4 D_{66} \iint \left(\frac{\partial^2 w}{\partial x \partial y} \right)^2 dx\, dy$$

$$= 8 D_{66} \iint \frac{\partial^4 w}{\partial x^2 \partial y^2} \cdot \delta w\, dx\, dy + 8 D_{66} \int \frac{\partial^2 w}{\partial x \partial y} \sin\beta \cos\beta\, \frac{\partial \delta w}{\partial n} \cdot ds$$

$$+ 4 D_{66} \int \frac{\partial}{\partial s}\left[\frac{\partial^2 w}{\partial x \partial y} (\sin^2\beta - \cos^2\beta) \right] \delta w \cdot ds$$

$$+ 4 D_{66} \iint \left[\frac{\partial^3 w}{\partial x \partial y^2} \cdot \cos\beta + \frac{\partial^3 w}{\partial x^2 \partial y} \cdot \sin\beta \right] \delta w \cdot ds$$

The variation of the strain energy is therefore given by the sum of all the above derived/

derived relationships

$$\delta V = \left[D_{11} \iint \frac{\partial^4 w}{\partial x^4} + D_{22} \iint \frac{\partial^4 w}{\partial y^4} + 2D_{12} \iint \frac{\partial^4 w}{\partial x^2 \partial y^2} + 4D_{66} \iint \frac{\partial^4 w}{\partial x^2 \partial y^2} \right] \delta w \, dx \, dy$$

$$+ \left[D_{11} \int \frac{\partial^2 w}{\partial x^2} \cos^2\beta + D_{22} \int \frac{\partial^2 w}{\partial y^2} \sin^2\beta \right.$$

$$\left. + D_{12} \int \left(\frac{\partial^2 w}{\partial y^2} \cos^2\beta + \frac{\partial^2 w}{\partial x^2} \sin^2\beta \right) + 4D_{66} \int \frac{\partial^2 w}{\partial x \partial y} \sin\beta \cos\beta \right] \frac{\partial \delta w}{\partial n} \, ds$$

$$+ \left\{ D_{11} \int \left[\frac{\partial}{\partial s} \left(\frac{\partial^2 w}{\partial x^2} \sin\beta \cos\beta \right) - \frac{\partial^3 w}{\partial x^3} \cos\beta \right] - D_{22} \int \left[\frac{\partial}{\partial s} \left(\frac{\partial^2 w}{\partial y^2} \sin\beta \cos\beta \right) + \frac{\partial^3 w}{\partial y^3} \sin\beta \right] \right.$$

$$+ D_{12} \int \left[\frac{\partial}{\partial s} \left(\frac{\partial^2 w}{\partial y^2} - \frac{\partial^2 w}{\partial x^2} \right) \sin\beta \cos\beta - D_{12} \int \left(\frac{\partial^3 w}{\partial x \partial y^2} \cos\beta + \frac{\partial^3 w}{\partial x^2 \partial y} \sin\beta \right) \right.$$

$$\left. \left. + 2D_{66} \int \frac{\partial}{\partial s} \left[\frac{\partial^2 w}{\partial x \partial y} \left(\sin^2\beta - \cos^2\beta \right) \right] - \left[\frac{\partial^3 w}{\partial x \partial y^2} \cos\beta + \frac{\partial^3 w}{\partial x^2 \partial y} \sin\beta \right] \right\} \delta w \, ds$$

Substituting this expression for δV into equation (II.4.2) and equating appropriate series of terms to zero the following three equations are obtained

$$\iint \left[D_{11} \frac{\partial^4 w}{\partial x^4} + D_{22} \frac{\partial^4 w}{\partial y^4} + 2\left(D_{12} + 2D_{66} \right) \frac{\partial^4 w}{\partial x^2 \partial y^2} - q \right] \delta w \, dx \, dy = 0 \qquad \text{(II.4.4)}$$

$$\int \left[D_{11} \frac{\partial^2 w}{\partial x^2} \cos^2\beta + D_{22} \frac{\partial^2 w}{\partial y^2} \sin^2\beta + D_{12} \left(\frac{\partial^2 w}{\partial y^2} \cos^2\beta + \frac{\partial^2 w}{\partial x^2} \sin^2\beta \right) \right.$$

$$\left. + 4D_{66} \left(\frac{\partial^2 w}{\partial x \partial y} \sin\beta \cos\beta \right) + M_n \right] \frac{\partial \delta w}{\partial n} \, ds = 0 \qquad \text{(II.4.5)}$$

$$\iint \Big\{ D_{11}\Big[\frac{\partial}{\partial s}\Big(\frac{\partial^2 w}{\partial x^2}\cdot \sin\beta\cos\beta\Big) - \frac{\partial^3 w}{\partial x^3}\cdot\cos\beta\Big] - D_{22}\Big[\frac{\partial}{\partial s}\Big(\frac{\partial^2 w}{\partial y^2}\sin\beta\cos\beta\Big) + \frac{\partial^3 w}{\partial y^3}\cdot\sin\beta\Big]$$

$$+ D_{12}\Big[\frac{\partial}{\partial s}\Big(\frac{\partial^2 w}{\partial y^2} - \frac{\partial^2 w}{\partial x^2}\Big)\Big]\sin\beta\cos\beta - D_{12}\Big(\frac{\partial^3 w}{\partial x\partial y^2}\cos\beta + \frac{\partial^3 w}{\partial x^2\partial y}\cdot\sin\beta\Big) \qquad \text{(II.4.6)}$$

$$+ 2D_{66}\Big[\frac{\partial}{\partial s}\Big(\frac{\partial^2 w}{\partial x\partial y}\{\sin^2\beta - \cos^2\beta\}\Big) - \Big(\frac{\partial^3 w}{\partial x\partial y^2}\cos\beta + \frac{\partial^3 w}{\partial x^2\partial y}\sin\beta\Big) - \Big(q_n + \frac{\partial M_{n\tau}}{\partial s}\Big)\Big]\Big\}\delta w\,.\,ds = 0$$

Equation (II.4.4) will be satisfied only if for every point in the middle plane of the plate

$$D_{11}\frac{\partial^4 w}{\partial x^4} + 2\big(D_{12} + 2D_{66}\big)\frac{\partial^4 w}{\partial x^2\partial y^2} + D_{22}\frac{\partial^4 w}{\partial y^4} = q \qquad \text{(II.4.7)}$$

This is the compatibility or deflection equation for an orthotropic plate.

In the case of a simply supported edge

$\delta w = 0$ and $M_n = 0$

i.e. equation (II.4.6) is satisfied if $\delta w = 0$

Equation (II.4.5) is satisfied if

$$D_{11}\frac{\partial^2 w}{\partial x^2}\cdot\cos^2\beta + D_{22}\frac{\partial^2 w}{\partial y^2}\cdot\sin^2\beta + D_{12}\Big(\frac{\partial^2 w}{\partial y^2}\cdot\cos^2\beta + \frac{\partial^2 w}{\partial x^2}\cdot\sin^2\beta\Big) + 4D_{66}\Big(\frac{\partial^2 w}{\partial x\partial y}\cdot\sin\beta\cos\beta\Big) = 0$$

In the particular case of a simply supported rectilinear edge parallel to the y-axis, $\beta = 0^\circ$.

$$\therefore M_x = -\Big(D_{11}\frac{\partial^2 w}{\partial x^2} + D_{12}\frac{\partial^2 w}{\partial y^2}\Big) = 0 \qquad \text{(II.4.8)}$$

For a free edge δw and $\frac{\partial(\delta w)}{\partial n}$ are entirely arbitrary. Also $M_n = 0$ and $Q_n + \frac{\partial M_{ns}}{\partial s} = 0$

Therefore from equations (II.4.5) and (II.4.6)

$$D_{11}\frac{\partial^2 w}{\partial x^2}\cos^2\beta + D_{22}\frac{\partial^2 w}{\partial y^2}\sin^2\beta + D_{12}\left(\frac{\partial^2 w}{\partial y^2}\cos^2\beta + \frac{\partial^2 w}{\partial x^2}\sin^2\beta\right) + 4D_{66}\left(\frac{\partial^2 w}{\partial x \partial y}\cdot \sin\beta\cos\beta\right) = 0 \qquad \text{(II.4.9)}$$

and

$$\left\{ \begin{aligned} & D_{11}\left[\frac{\partial}{\partial s}\left(\frac{\partial^2 w}{\partial x^2}\sin\beta\cos\beta\right) - \frac{\partial^3 w}{\partial x^3}\cos\beta\right] - D_{22}\left[\frac{\partial}{\partial s}\left(\frac{\partial^2 w}{\partial y^2}\sin\beta\cos\beta\right) + \frac{\partial^3 w}{\partial y^3}\sin\beta\right] \\ & + D_{12}\left[\frac{\partial}{\partial s}\left\{\frac{\partial^2 w}{\partial y^2} - \frac{\partial^2 w}{\partial x^2}\right)\sin\beta\cos\beta - \frac{\partial^3 w}{\partial x \partial y^2}\cos\beta + \frac{\partial^3 w}{\partial y \partial x^2}\sin\beta\right] \\ & + 2D_{66}\left[\frac{\partial}{\partial s}\left(\frac{\partial^2 w}{\partial x \partial y}\left\{\sin^2\beta - \cos^2\beta\right\}\right) - \frac{\partial^3 w}{\partial x \partial y^2}\cos\beta - \frac{\partial^3 w}{\partial x^2 \partial y}\cdot\sin\beta\right] \end{aligned} \right\} = 0 \qquad \text{(II.4.10)}$$

For a free rectilinear edge parallel to the x-axis, $\beta = 90^\circ$, (II.4.9) yields

$$M_y = -\left(D_{22}\frac{\partial^2 w}{\partial y^2} + D_{12}\frac{\partial^2 w}{\partial x^2}\right) = 0 \qquad \text{(II.4.11)}$$

and (II.4.10) gives

$$Q_y + \frac{\partial M_{xy}}{\partial x} = -\left(D_{22}\frac{\partial^3 w}{\partial y^3} + D_{12}\frac{\partial^3 w}{\partial x^2 \partial y} + 4D_{66}\frac{\partial^3 w}{\partial x^2 \partial y}\right) = 0 \qquad \text{(II.4.12)}$$

II.5. THE SOLUTION OF THE OTRHOTROPIC PLATE EQUATION.

It has been shown in the previous section that/

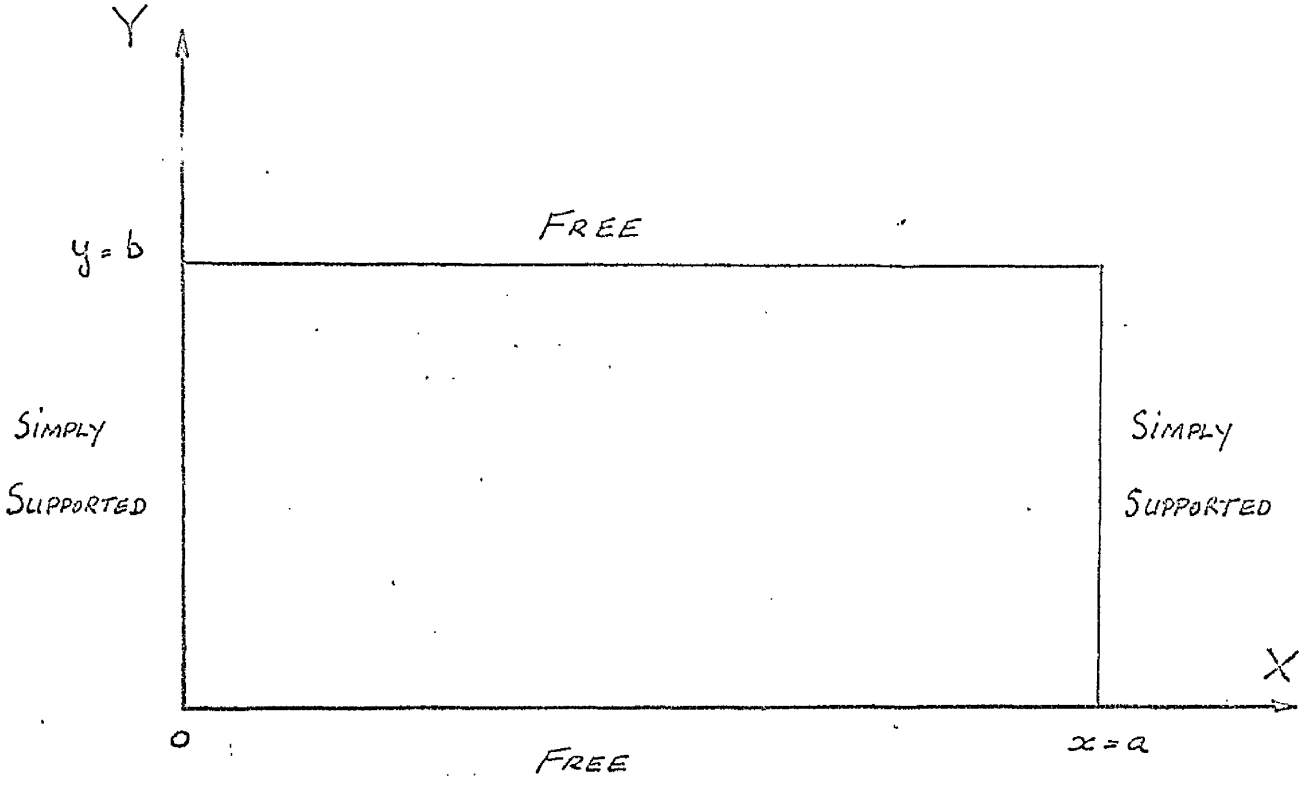

FIG.II.4 Boundary conditions of orthotropic plate.

that for an orthotropic plate, the deflection equation can be written as:

$$D_{11}\frac{\partial^4 w}{\partial x^4} + 2D_{33}\frac{\partial^4 w}{\partial x^2 \partial y} + D_{22}\frac{\partial^4 w}{\partial y^4} = q \qquad \text{(II.5.1)}$$

where

$$D_{33} = D_{12} + 2D_{66}$$

This section considers the solution of equation (II.5.1) for the case of a uniformly loaded orthotropic plate which has two opposite edges simply supported and the other two edges free, the origin of co-ordinates being taken as a corner of the plate as shown in Fig. II.4.

A solution of equation (II.5.1) can be obtained by the following substitution

$$w = w_1 + w_2 \qquad \text{(II.5.2)}$$

where w_1 is a solution satisfying the equation

$$D_{11}\frac{\partial^4 w_1}{\partial x^4} = q$$

Expressing w_1 as a trigonometric series representing the deflected form of a uniformly loaded strip parallel to the x-axis, simply supported over a length a

$$w_1 = \frac{4qa^4}{\pi^5 D_{11}} \sum \frac{1}{m^5} \cdot \sin\frac{m\pi x}{a} \qquad \text{(II.5.3)}$$

The expression w_2 must satisfy

$$D_{11}\frac{\partial^4 w_2}{\partial x^4} + 2D_{33}\frac{\partial^4 w_2}{\partial x^2 \partial y^2} + D_{22}\frac{\partial^4 w_2}{\partial y^4} = 0 \qquad \text{(II.5.4)}$$

Adopting a Lévy form of solution for w_2

$$w_2 = \sum_{m=1,3\ldots}^{\infty} Y_m \sin\frac{m\pi x}{a} \qquad \text{(II.5.5)}$$

where Y_m is a function of y only.

This expression (II.5.5) effects a separation of variables for plates having two opposite edges simply supported.

Substitute (II.5.5) into (II.5.4) to obtain

$$\frac{d^4 Y_m}{dy^4} - 2\frac{D_{33}}{D_{22}}\left(\frac{m\pi}{a}\right)^2\frac{d^2 Y_m}{dy^2} + \frac{D_{11}}{D_{22}}\left(\frac{m\pi}{a}\right)^4 Y_m = 0 \qquad \text{(II.5.6)}$$

The four characteristic roots of this equation are $\pm\phi$, $\pm\psi$ where

$$\phi = \frac{m\pi}{a}\cdot\frac{1}{\sqrt{D_{22}}}\cdot\left\{D_{33} + \sqrt{D_{33}^2 - D_{11}D_{22}}\right\}^{\frac{1}{2}}$$

$$\psi = \frac{m\pi}{a}\cdot\frac{1}{\sqrt{D_{22}}}\cdot\left\{D_{33} - \sqrt{D_{33}^2 - D_{11}D_{22}}\right\}^{\frac{1}{2}} \qquad \text{(II.5.7)}$$

From inspection of these roots, there are three possible cases consistent with the actual values of D_{11} etc.

1. $D_{33}^2 > D_{11}.D_{22}$ - all roots real.

For this case, the form of Ym is given by

$$Y_m = A_m \cosh \phi y + B_m \sinh \phi y + C_m \cosh \psi y + D_m \sinh \psi y.$$

2. $D_{33}^2 = D_{11} D_{22}$ - equal pairs of roots. $\phi = \psi$

$$Y_m = (A_m + B_m y) \cosh \phi y + (C_m + D_m y) \sinh \phi y$$

3. $D_{33}^2 < D_{11}.D_{22}$ - all roots complex.

$$\phi = \theta \pm i\zeta \quad ; \quad \psi = -\theta \pm i\zeta$$

$$Y_m = (A_m \cos \zeta y + B_m \sin \zeta y) \cosh \theta y + (C_m \cos \zeta y + D_m \sin \zeta y) \sinh \theta y.$$

It is readily seen that for any investigation into the behaviour of orthortopic plates, cases 1 and 3 above must be fully examined; case 2, that of equal pairs of roots can be considered as a special case of 1 and 3 and is not discussed separately.

1. <u>All Roots Real</u>.

The deflection w is given by $w = w_1 + w_2$

$$\therefore w = \frac{q a^4}{D_{11}} \sum_{m=1,3,\ldots}^{\infty} \left[\frac{4}{(m\pi)^5} + A_m \cosh \phi y + B_m \sinh \phi y + C_m \cosh \psi y + D_m \sinh \psi y \right] \sin \frac{m\pi x}{a} \qquad \text{(II.5.8)}$$

which satisfies the boundary conditions on $x = 0$ and $x = a$.

From equations (II.4.11) and (II.4.12) the/

the boundary conditions on $y = 0$ and $y = b$ to be satisfied are:

$$D_{12}\frac{\partial^2 w}{\partial x^2} + D_{22}\frac{\partial^2 w}{\partial y^2} = 0$$

$$D_{22}\frac{\partial^3 w}{\partial y^3} + D_{12}\frac{\partial^3 w}{\partial x^2 \partial y} + 4D_{66}\frac{\partial^3 w}{\partial x^2 \partial y} = 0 \qquad \text{(II.5.9)}$$

Application of equation (II.5.8) to equations (II.5.9) gives the following group of simultaneous equations:

$$\gamma A_m + \delta C_m = F$$

$$\phi B_m(\gamma - R) + \psi D_m(\delta - R) = 0$$

$$\gamma A_m \cosh\phi b + \gamma B_m \sinh\phi b + \delta C_m \cosh\psi b + \delta D_m \sinh\psi b = F \qquad \text{(II.5.10)}$$

$$\phi A_m(\gamma - R)\sinh\phi b + \phi B_m(\gamma - R)\cosh\phi b + \psi C_m(\delta - R)\sinh\psi b + \psi D_m(\delta - R)\cosh\psi b = 0$$

where:

$$\gamma = D_{22}\phi^2 - D_{12}\left(\frac{m\pi}{a}\right)^2$$

$$\delta = D_{22}\psi^2 - D_{12}\left(\frac{m\pi}{a}\right)^2$$

$$F = \frac{4D_{12}}{(m\pi)^3 a^2} \quad ; \quad R = 4D_{66}\left(\frac{m\pi}{a}\right)^2$$

Solution of the group of equations (II.5.10) as indicated in Appendix VII.2 leads to the following expressions for A_m etc.

$$A_m = \frac{F\psi\delta}{\mathcal{K}}\left[\psi\gamma^2\sinh\phi b\sinh\psi b + \phi\delta^2(1 + \cosh\phi b - \cosh\psi b - \cosh\phi b\cosh\psi b)\right] \qquad \text{(II.5.11)}$$

$$B_m = \frac{F\psi\delta}{\mathcal{K}}\left[\phi\delta^2\sinh\phi b(\cosh\psi b - 1) - \psi\gamma^2\sinh\psi b(\cosh\phi b - 1)\right]$$

$$C_m = \frac{F}{\delta\mathcal{H}}\left[\phi^2\delta^4 \sinh\phi b \sinh\psi b + \phi\delta^2\psi\gamma^2(1 - \cosh\phi b + \cosh\psi b - \cosh\phi b \cosh\psi b)\right]$$

$$D_m = \frac{F\phi\delta}{\mathcal{H}}\left[\psi\gamma^2 \sinh\psi b\,(\cosh\phi b - 1) - \phi\delta^2(\cosh\psi b - 1)\sinh\phi b\right] \qquad \text{(II.5.11)}$$

where

$$\mathcal{H} = (\phi^2\delta^4 + \psi^2\gamma^4)\sinh\phi b \sinh\psi b - 2\phi\delta^2\psi\gamma^2(\cosh\phi b \cosh\psi b - 1)$$

3. <u>All Roots Complex</u>.

The deflection $w = w_1 + w_2$ is given by

$$w = \frac{qa^4}{D_{11}} \sum_{m=1,3\ldots}^{\infty}\left[\frac{4}{(m\pi)^5} + (A_m \cos\zeta y + B_m \sin\zeta y)\cosh\theta y + (C_m \cos\zeta y + D_m \sin\zeta y)\sinh\theta y\right]\sin\frac{m\pi x}{a} \qquad \text{(II.5.12)}$$

Application of this equation (II.5.12) to the boundary conditions (II.5.9) gives the following group of equations:

$$A_m f + D_m g = F$$

$$B_m\zeta(f - R + 2D_{22}\theta^2) + C_m\theta(f - R - 2D_{22}\zeta^2) = 0$$

$$\begin{aligned}
&A_m(f\cosh\theta b\cos\zeta b - g\sinh\theta b\sin\zeta b)\\
&+B_m(f\cosh\theta b\sin\zeta b + g\sinh\theta b\cos\zeta b)\\
&+C_m(f\sinh\theta b\cos\zeta b - g\cosh\theta b\sin\zeta b)\\
&+D_m(f\sinh\theta b\sin\zeta b + g\cosh\theta b\cos\zeta b) = F
\end{aligned} \qquad \text{(II.5.13)}$$

$$\begin{aligned}
&A_m\{(f-R)(\theta\sinh\theta b\cos\zeta b - \zeta\cosh\theta b\sin\zeta b) - g(\zeta\sinh\theta b\cos\zeta b + \theta\cosh\theta b\sin\zeta b)\}\\
&+B_m\{(f-R)(\zeta\cosh\theta b\cos\zeta b + \theta\sinh\theta b\sin\zeta b) - g(\zeta\sinh\theta b\sin\zeta b - \theta\cosh\theta b\cos\zeta b)\}\\
&+C_m\{(f-R)(\theta\cosh\theta b\cos\zeta b - \zeta\sinh\theta b\sin\zeta b) - g(\zeta\sinh\theta b\cos\zeta b + \theta\sinh\theta b\sin\zeta b)\}\\
&+D_m\{(f-R)(\zeta\sinh\theta b\cos\zeta b + \theta\cosh\theta b\sin\zeta b) - g(\zeta\sinh\theta b\sin\zeta b - \theta\sinh\theta b\cos\zeta b)\}\\
&= 0
\end{aligned}$$

where:

$$f = D_{22}(\theta^2 - \zeta^2) - D_{12}\left(\frac{m\pi}{a}\right)^2$$

$$g = 2\theta\zeta D_{22}$$

$$F = \frac{4D_{12}}{(m\pi)^3 a^2} \quad ; \quad R = 4D_{66}\left(\frac{m\pi}{a}\right)^2$$

Solution of the above group of equations as indicated in Appendix VIII.2 leads to the following expressions for the plate constants:

$$D_m = \frac{F}{K}\left\{ \begin{array}{l} f(M^2+N^2)\dfrac{\tanh\theta b \tan\zeta b}{\cosh\theta b \cos\zeta b}\left\{\dfrac{1}{\cosh\theta b \cos\zeta b} - 1 + \left(\dfrac{g}{f}\right)\tanh\theta b \tan\zeta b\right\} \\ -(M\tanh\theta b - N\tan\zeta b)\{(fN-gM)\tanh\theta b - (fM+gN)\tan\zeta b\} \end{array} \right\}$$

$$C_m = FN\left\{ \begin{array}{l} \dfrac{1}{L}\left\{\dfrac{1}{\cosh\theta b \cos\zeta b} - 1 + \left(\dfrac{g}{f}\right)\tanh\theta b \tan\zeta b\right\} \\ + \dfrac{1}{K}\left\{ \begin{array}{l} \left(\frac{1}{f}\right)\tanh\theta b \tan\zeta b (f^2+g^2)(M\tanh\theta b - N\tan\zeta b) \\ -\dfrac{(M^2+N^2)(f^2+g^2)\tanh^2\theta b \tan^2\zeta b\left\{\dfrac{1}{\cosh\theta b\cos\zeta b} - 1 + \left(\dfrac{g}{f}\right)\tanh\theta b \tan\zeta b\right\}}{\cosh\theta b \cos\zeta b[(fN-gM)\tanh\theta b - (gN+fM)\tan\zeta b]} \end{array} \right. \end{array} \right\} \quad \text{-(II.5.14)}$$

$$A_m = \left(\frac{F}{f}\right) - g\left(\frac{D_m}{f}\right)$$

$$B_m = -C_m\left(\frac{M}{N}\right)$$

where:

$$M = \theta(f - R - 2D_{22}\zeta^2) \quad ; \quad N = \zeta(f - R + 2D_{22}\theta^2)$$

$$L = (fN-gM)\tanh\theta b - (fM+gN)\tan\zeta b$$

$$K = (fN-gM)^2\tanh^2\theta b - (fM+gN)^2\tan^2\zeta b + (M^2+N^2)(f^2+g^2)\frac{\tanh^2\theta b \tan^2\zeta b}{\cosh\theta b \cos\zeta b}$$

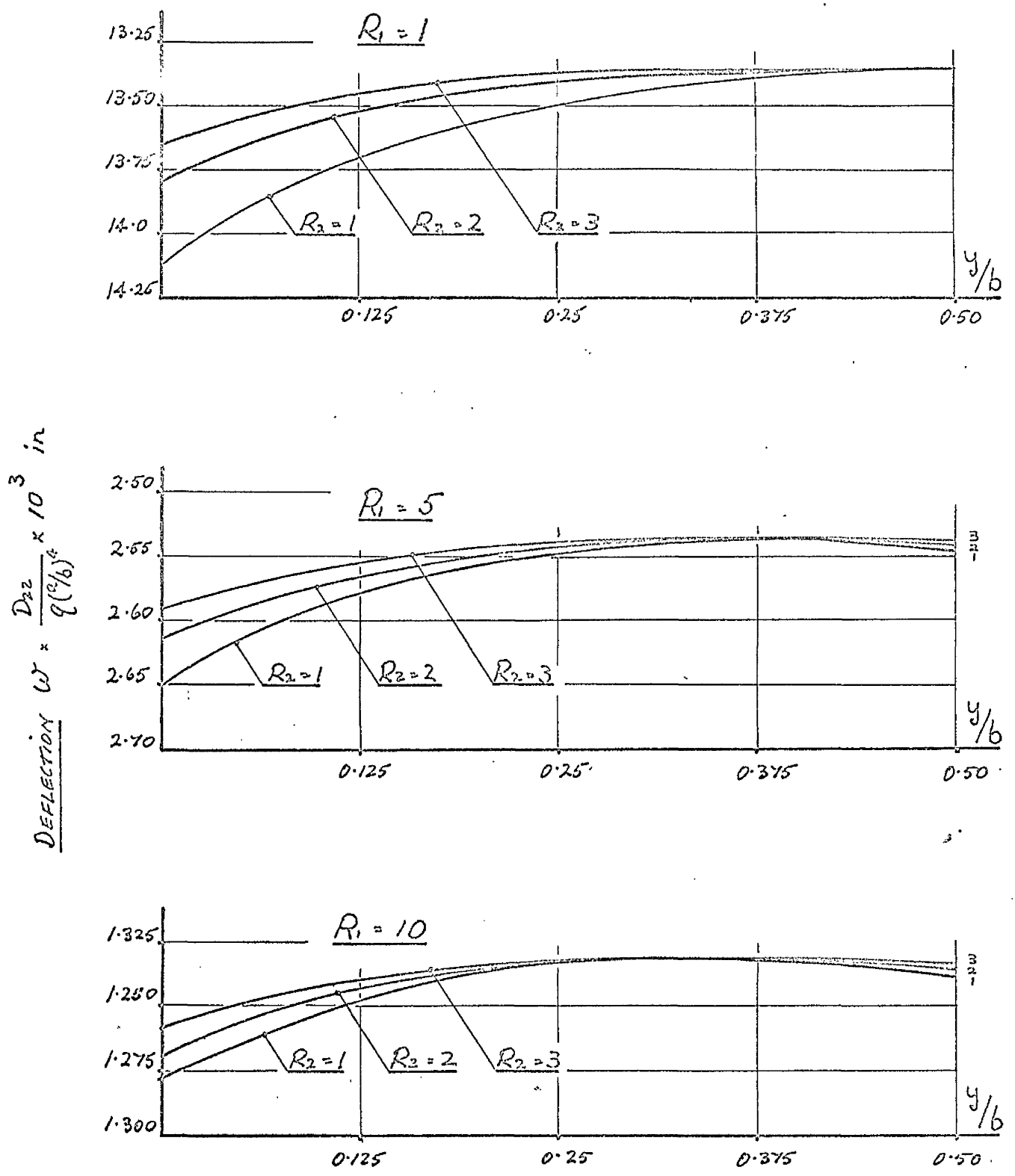

FIG.II.5 Deflected form at plate centre x = a/2.

D_{22} = 300 a/b = 4/3

It is seen from the above that the deflection of an orthotropic plate can be defined for the given boundary conditions for any variation of elastic stiffnesses and aspect ratio a/b. This in turn gives a means of determining the distribution of moments and shears throughout the plate for any variation of these parameters.

In the following discussion the values quoted are those obtained using the first three terms ($m = 1, 3, 5$) of the sum to infinity for each quantity. The convergence of the infinite series for these quantities is discussed in Appendix VIII.5 together with the relevant sections of the computational procedure. Also the designation R_1 is given to the ratio D_{11}/D_{22} and R_2 to the ratio D_{66}/D_{22}, while all the theoretical graphs plotted for variations of these two ratios have been calculated for a value of D_{22} of 300, this being the quantity $Eh^3/12(1-\nu^2)$ for a steel plate 0.048 in. thick with a Young's Modulus E of 30×10^6 lbf/in^2 and a Poisson's Ratio ν of 0.28.

The Deflected Surface: Fig. II.5 displays /

displays the variation in the deflected cross-section of an orthotropic plate as the parameters R_1 and R_2 are varied. It is seen that as for the isotropic plate investigated by HOLL the deflection surface across the plate is saddle shaped with a marked edge effect.

As the ratio R_1 is increased the value of the deflection across the plate diminishes. It is also of interest to note that as R_1 is increased the point of minimum deflection does not remain in the centre but moves across the plate. This effect was theoretically noted by HUBER for the case of an orthotropic plate simply supported on all edges and experimentally by MARCH for the same boundary conditions. An attempt by March to correlate theory and experiment must, however, be treated with some caution, as March himself described the values of the elastic moduli for his plates as "tentative".

As would be intuitively expected, for a given value of R_1 an increase in R_2, the ratio defining the torsional stiffness of the plate, reduces the variation of deflection across the plate causing the central portion to remain relatively flat.

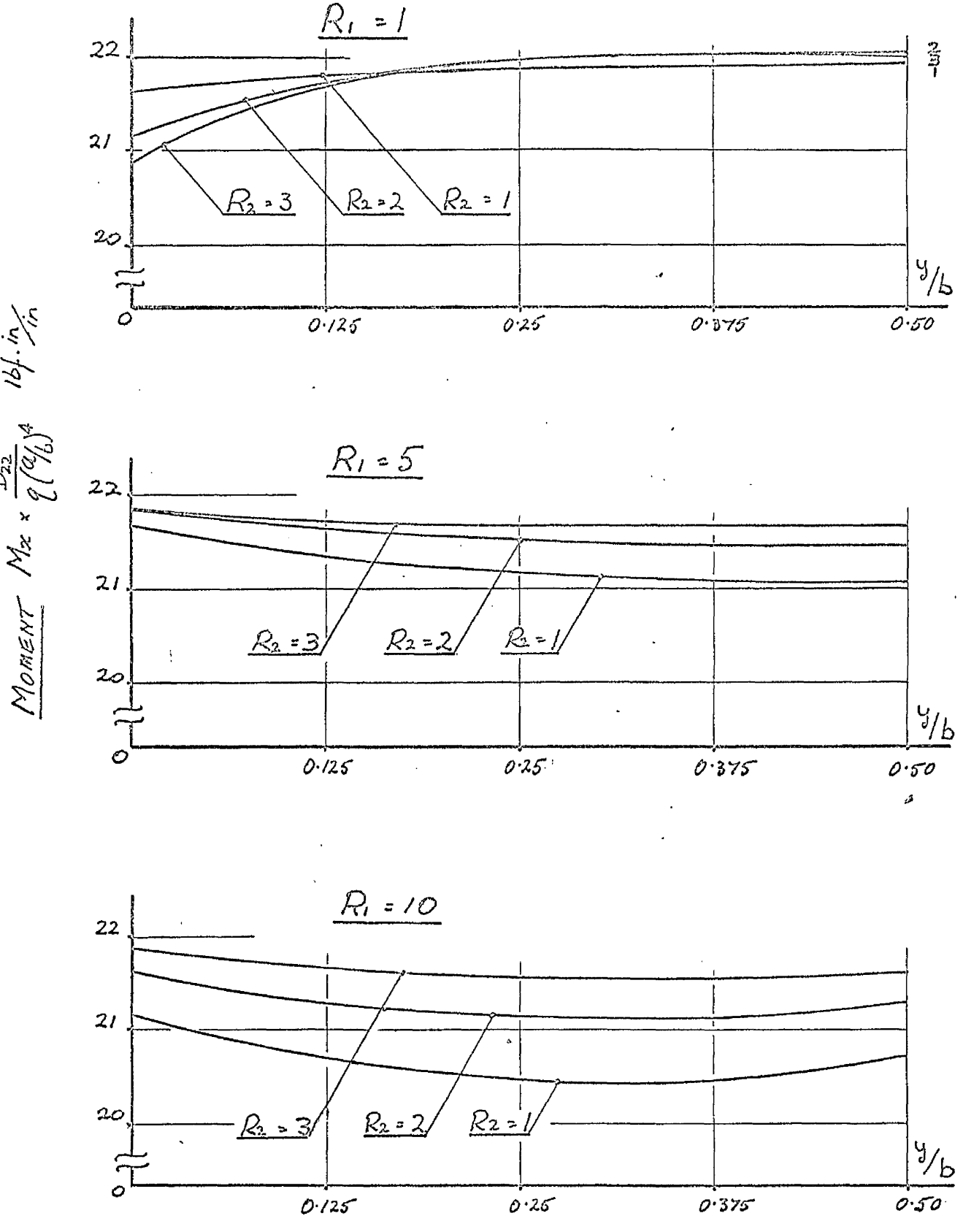

FIG.II.6 Moment intensity M_x at plate centre x = a/2

D_{22} = 300 a/b = 4/3

Due to the transform applied to reconstitute the orthotropic plate equation as an ordinary differential equation, the theoretical deflected form along the length of the plate is assumed to be a sine wave. This is borne out by the experimental work on steel and aluminium plates described in the following chapter.

The Bending Moments: the bending moments M_x acting on planes parallel to the y-axis are given by:

$$M_x = -\left(D_{11}\frac{\partial^2 w}{\partial x^2} + D_{12}\frac{\partial^2 w}{\partial y^2}\right) \qquad \text{(II.5.15)}$$

where the deflection w is given for the case of real or complex roots by the appropriate equations (II.5.8) and (II.5.12).

The variation of this moment across an orthotropic plate at the centre ($x = a/2$) is given in Fig. II.6. For the ratios R_1 and R_2 equal to unity the maximum value of this moment is at the plate centre and has a value of $21.933\ q(a/b)^4/D_{22}$ which for 0.048 in. thick steel reduces to $1.037\ q(a/b)^2/8$ a value which agrees exactly with that obtained by HOLL for an isotropic plate of the same physical dimensions. Examination of the expression for M_x indicates that this is due to the domination of the/

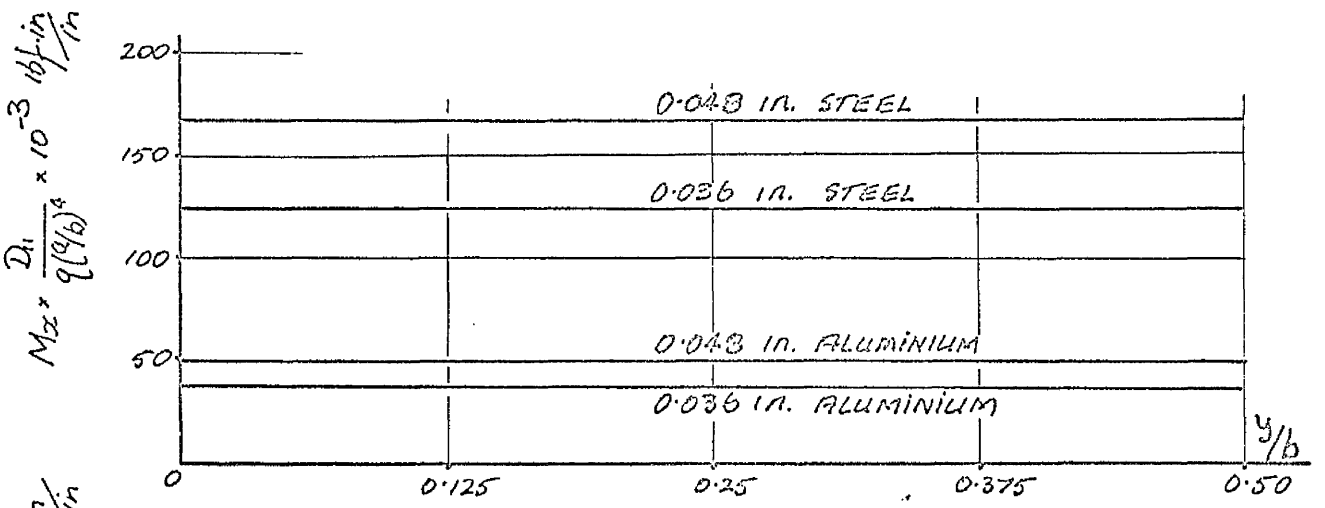

DISTRIBUTIONS OF M_x AND M_y AT $x = a/2$

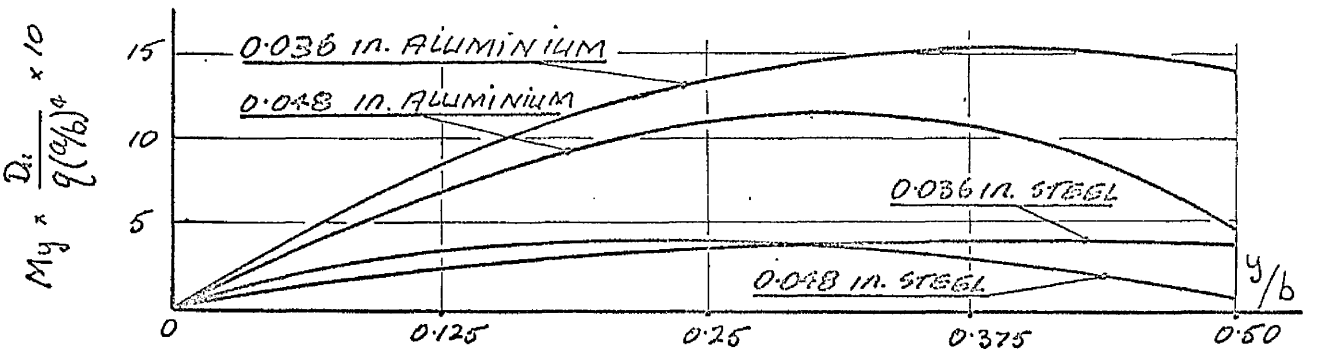

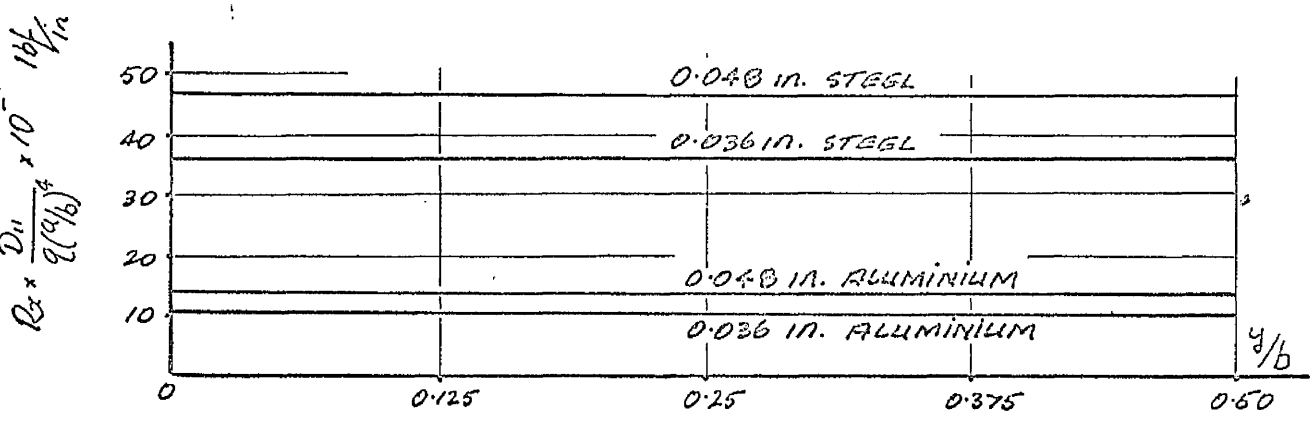

DISTRIBUTIONS OF R_x AND Q_x AT $x = 0, a$.

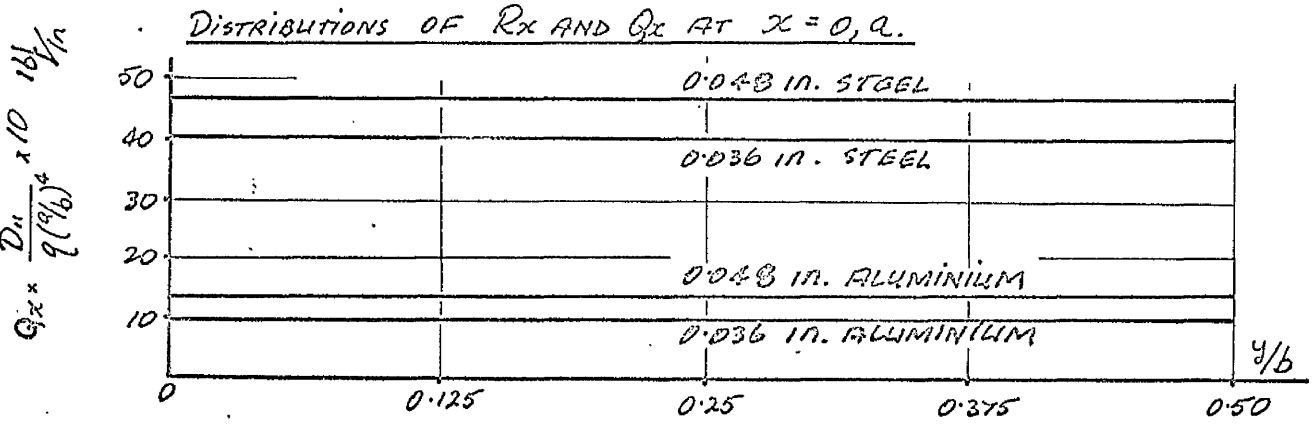

FIG.II.7 Moments and shears in actual plates

the term $D_{11}(\partial^2 w/\partial x^2)$.

The value of M_x is relatively insensitive to increase in the ratio R_1, but the shape of the distribution across the plate alters such that the position of maximum M_x is at the plate edges, although the difference in the M_x values between neighbouring points across the plate decreases. This concentration of moment intensity at the edges of the plate is, however, very small, and it is the author's opinion that this is more an indication of the increasing importance of the term $D_{12}(\partial^2 w/\partial y^2)$ in the expression for M_x than a description of an actual phenomenon. Fig. II.7 gives the values of the expression for M_x applied to the actual plates described in Chapter III. This shows that M_x is a constant of value 16.814 $\times$ $\times (q(a/b)^4/D_{11}) \times 10^4$ for 0.0468 in. thick steel which on insertion of the appropriate values of D_{11} and (a/b) becomes 0.999851 $q(a/b)^2/8$ this being the value derived if one considers the orthotropic plate as a series of strips or beams.

In his work on isotropic plates HOLL showed that for a given plate as Poisson's Ratio increased, the value of M_x at the free edge also increased./

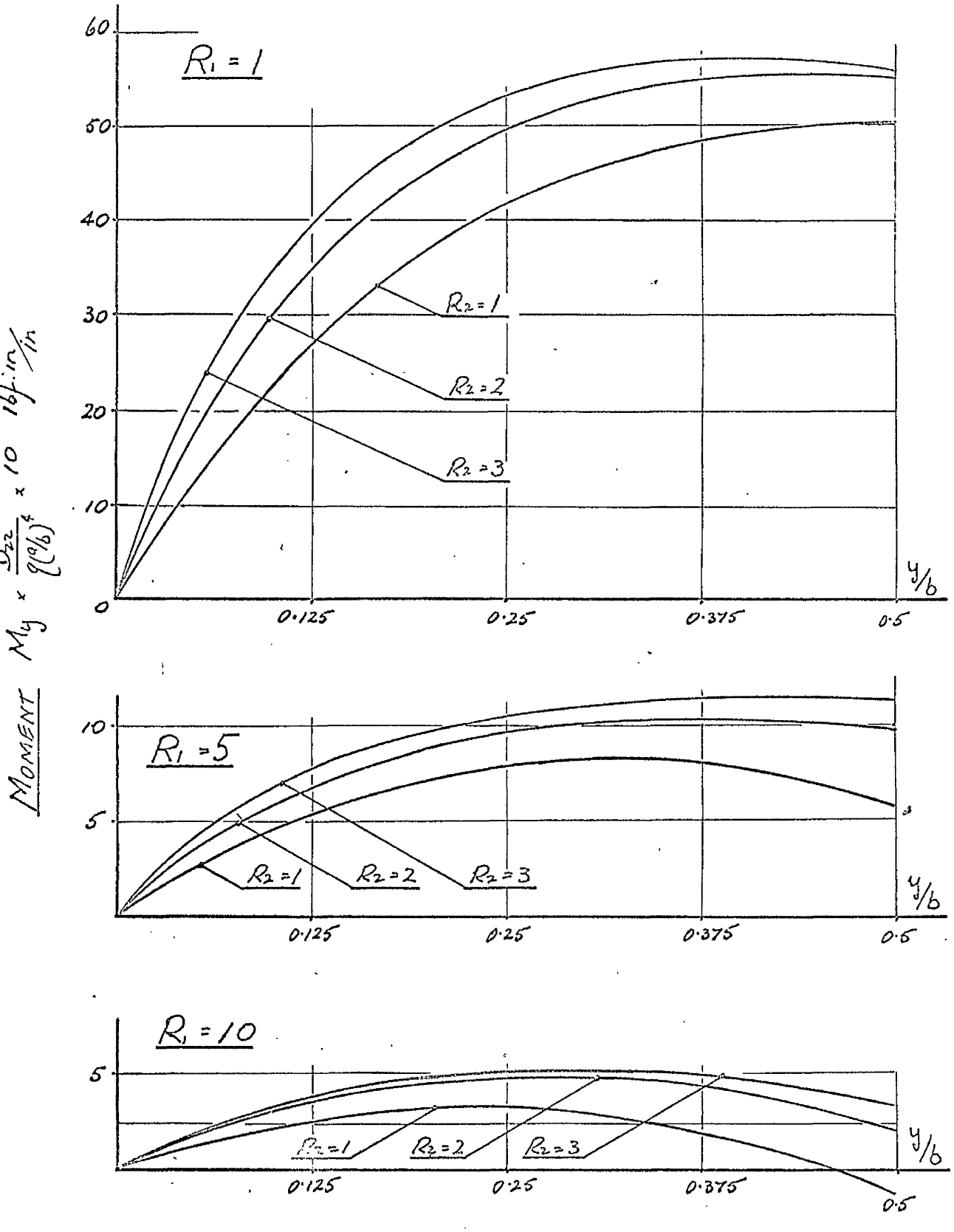

FIG.II.8 Moment intensity M_y at plate centre x = a/2

D_{22} = 300 a/b = 4/3

increased. This result is substantiated to some degree by the curves of Fig. II.6 which show that for any given value of R_1 increase in R_2 gives a larger value of M_x at the plate edges. This difference is, however, small, and for values of $R_1 \neq 1$ variation of R_2 does not alter the distribution of M_x to any appreciable degree.

The bending moment M_y acts on planes parallel to the x-axis and is defined as:

$$M_y = -\left(D_{12}\frac{\partial^2 w}{\partial x^2} + D_{22}\frac{\partial^2 w}{\partial y^2}\right) \qquad \text{(II.5.16)}$$

The theoretical valuation of this moment across an orthotropic plate at the plate centre is given in Fig. II.8. As expected, the value of M_y at the plate edge is zero while the intensity at any section decreases with increasing R_1 and for any given value of R_1 increases with increasing value of R_2. This latter effect is readily explained by the increasing effect of the term $D_{12}\,\partial^2 w/\partial x^2$ in the expression for M_y.

For R_1 and R_2 equal to unity the shape of the distribution agrees with that for the isotropic plate but for any other values of R_1 and R_2 the/

the shape of the distribution alters. It is interesting to note that at a value of $R_1 = 10$ and $R_2 = 1$ the distribution of M_y has a small negative value at the plate centre which coincides with the minimum value of central deflection in Fig. II.5 and an apparently inconsistent value of the shear force Q_y acting on planes parallel to the x-axis given in Fig. II.10. Examination of these values leads one to the conclusion that they are consistent within themselves and that the development of a negative value of M_y is rational.

For the actual plates described in Chapter III, the theoretical distributions of M_y shown in Fig. II.7 exhibit greater convexity for low values of the ratio R_2. The actual numerical values of the intensity M_y are small and are positive. The longitudinal distribution of this moment M_y is sinusoidal and therefore vanishes at the supported edges of the plate.

The End Reactions: the support reactions at the simply supported ends are given by:

$$R_x = Q_x + \frac{\partial M_{xy}}{\partial y} = -\left[D_{11}\frac{\partial^3 w}{\partial x^3} + (D_{12} + 4D_{66})\frac{\partial^3 w}{\partial x\, \partial y^2}\right] \qquad \text{(II.5.17)}$$

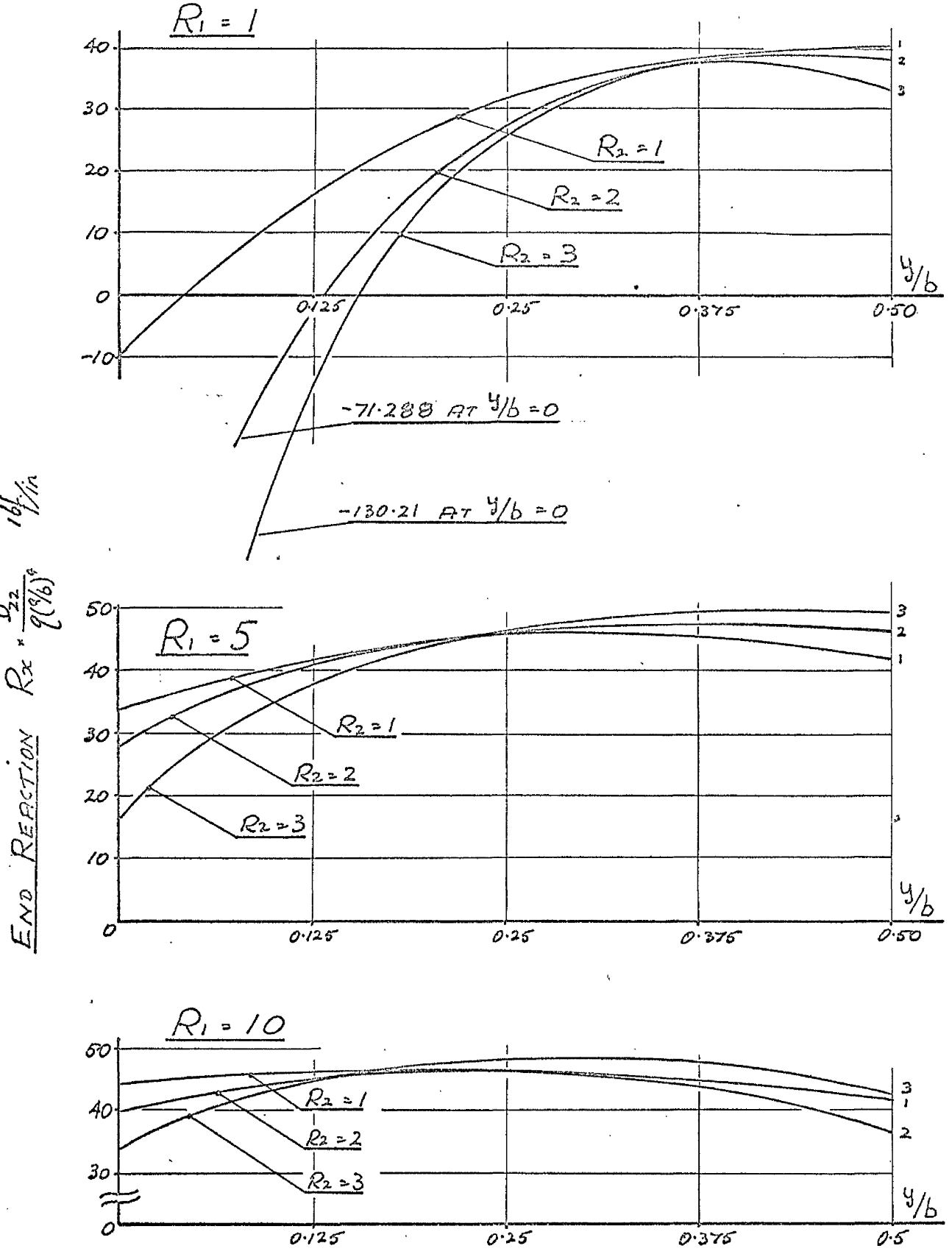

FIG.II.9 End reaction R_x at x = 0 and x = a

D_{22} = 300 a/b = 4/3

The distribution of this reaction is given in Fig. II.9 and is of considerable interest from the theoretical viewpoint. The curves indicate that for low values of R_1 the variation at the corners of the plate is negative, i.e. downwards, a result which would seem surprising were it not for the fact that in the case of an isotropic plate simply supported on all four edges under the action of a uniformly distributed load the corners do tend to lift. For an isotropic plate with two free edges the end reaction R_x is of course positive, but increase in the ratio R_2 for a value of $R_1 = 1$ gives a markedly negative value of corner reaction. This is explained by the increasing effect of the term $4D_{66}\left(\partial^3 w / \partial x \partial y^2\right)$ in the expression for R_x, which is twice the rate of variation of the shear moment M_{xy}.

For the actual plates the variation of R_x is shown in Fig. II.7 and is indicated as a uniform reaction. This is what would be anticipated from the curves of Fig. II.9 which demonstrate that as the ratio R_1 is increased the end reaction tends to a uniform value with the greatest variation from this uniform state corresponding to the highest value of/

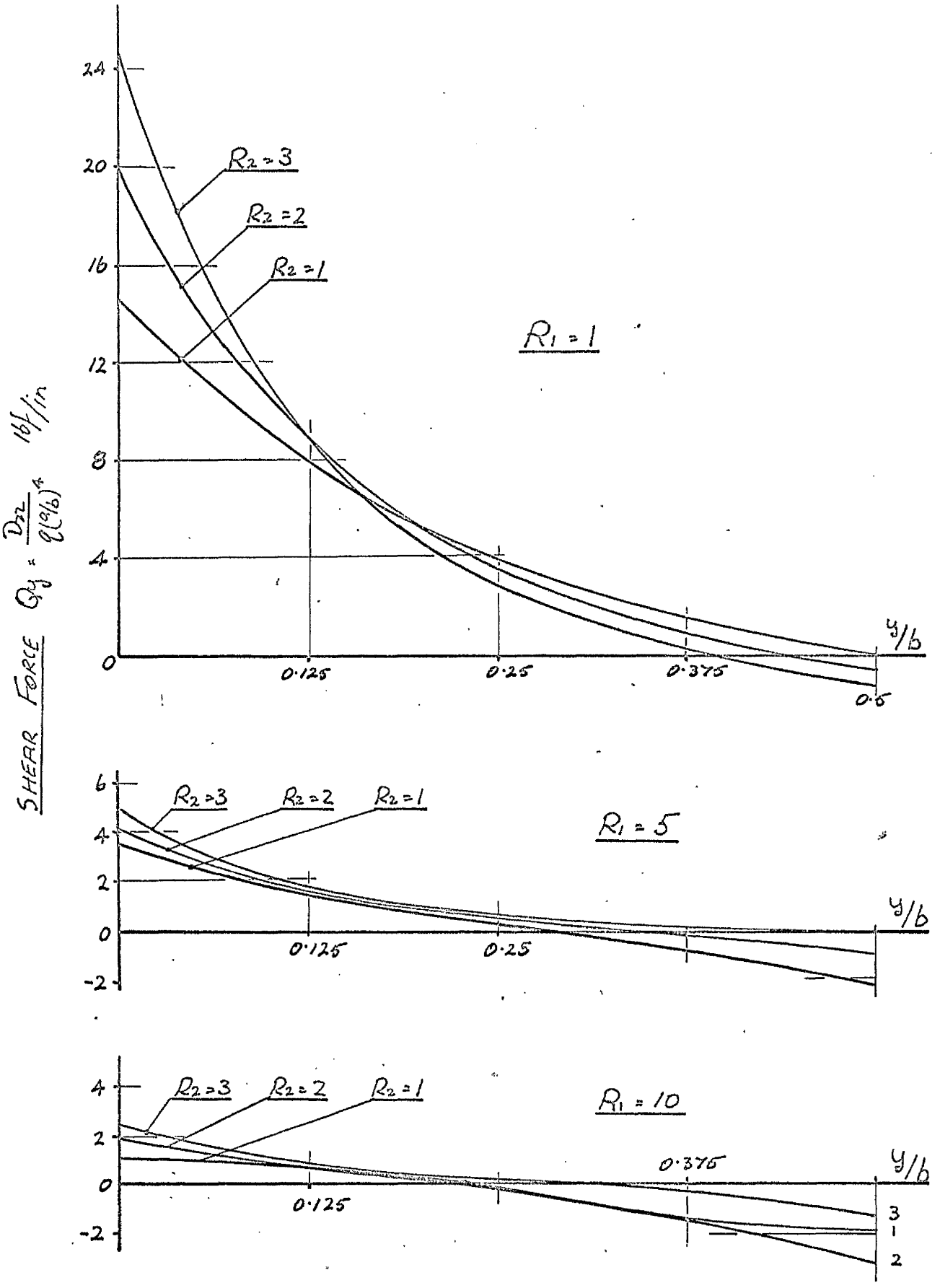

FIG.II.10 Shear force Q_y at x = a/2

D_{22} = 300 a/b = 4/3

of R_2 for a given value of R_1. For the first three terms of the infinite series for R_x the value for the 0.048 in. thick steel plate is given as $0.93297\, q^{(a/b)/2}$ where $q^{(a/b)/2}$ is that value that would be obtained considering the plate as a series of beams or strips.

The Shear Forces and Torsional Moment: the shear force Q_y acting on planes parallel to the x-axis differs from the expression for the edge reaction by the quantity $2 D_{22} (\partial^3 w / \partial x^2 \partial y)$ which is the rate of change of shear moment M_{xy} along the plate free edge.

$$Q_y = -\left[D_{22} \frac{\partial^3 w}{\partial y^3} + (D_{12} + 2D_{66}) \frac{\partial^3 w}{\partial x^2 \partial y} \right] \qquad \text{(II.5.18)}$$

Thus the shear force Q_y is not zero on the free edges but in fact, as is shown in Fig. II.10 is a maximum along these edges for a value of the ratio $R_1 = 1$.

The change in shape of the curves for Q_y as R_1 increases can be explained by the diminishing effect of the term $D_{22}(\partial^3 w / \partial y^3)$ and the resultant domination of the expression $(D_{12} + 2D_{66})\, \partial^3 w / \partial x^2 \partial y$ which is dependent on the ratio R_2. This is the principal reason for the resemblance between the graphs of shear force and those of shear moment/

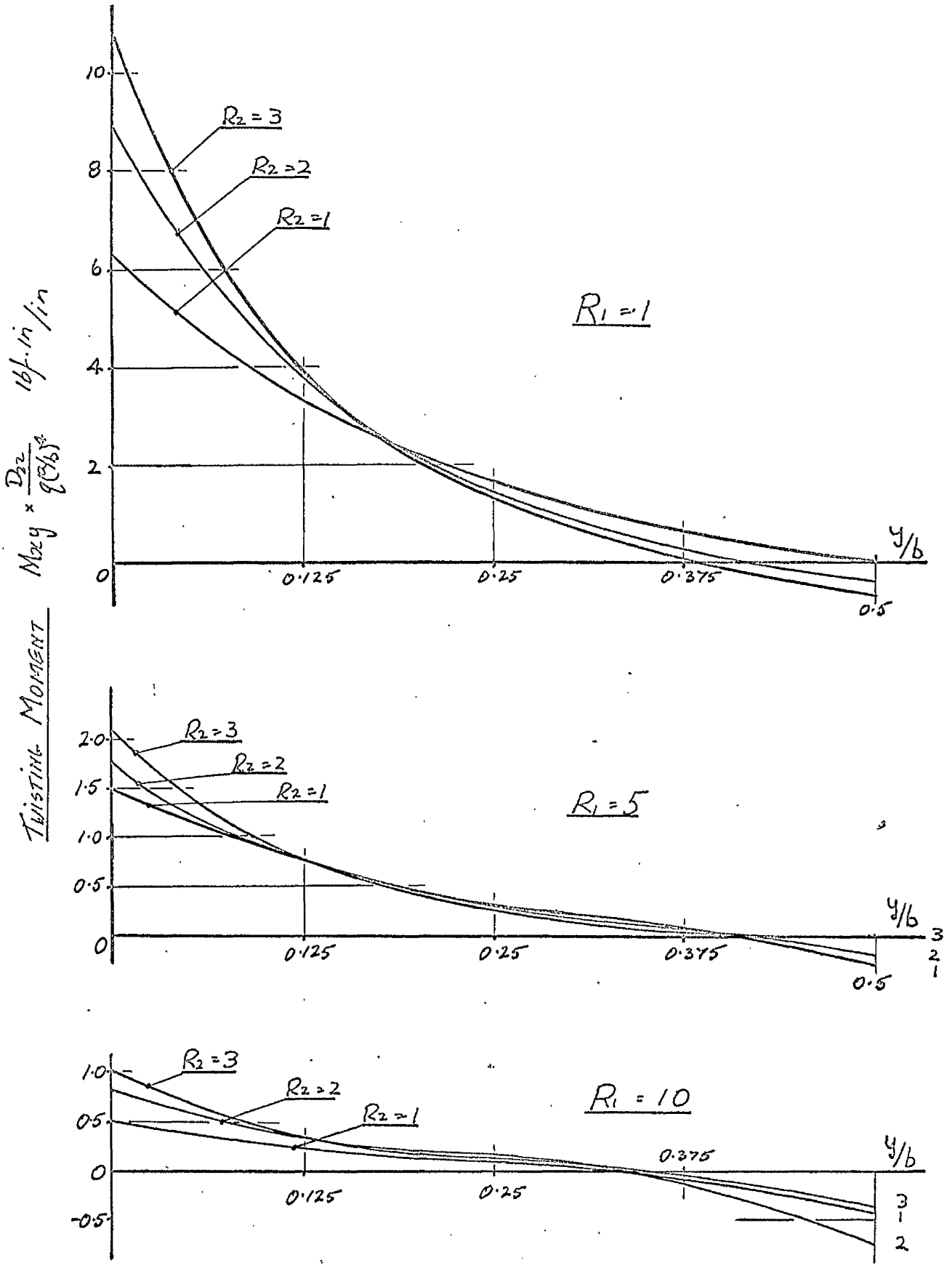

FIG.II.11 Twisting moment M_{xy} at x = 0 and x = a

D_{22} = 300 a/b = 4/3

II.1(a) SHEAR FORCE Q_y AT $x = a/2$

PLATE	y/b					
	0	0.1	0.2	0.3	0.4	0.5
0.048" steel	-34.31×10^{-11}	-91.92×10^{-17}	-24.63×10^{-22}	-65.98×10^{-28}	-17.68×10^{-33}	-47.36×10^{-39}
0.036" steel	-29.94×10^{-11}	-80.20×10^{-17}	-21.49×10^{-22}	-57.57×10^{-28}	-15.42×10^{-33}	-41.32×10^{-39}
0.048" alum.	-14.87×10^{-10}	-39.85×10^{-16}	-10.85×10^{-21}	-28.61×10^{-27}	-76.64×10^{-33}	-20.53×10^{-38}
0.036" alum.	-13.61×10^{-10}	-36.47×10^{-16}	-97.71×10^{-22}	-26.18×10^{-27}	-70.18×10^{-33}	-18.79×10^{-38}

II.1(b) TWISTING MOMENT M_{xy} AT $x = 0, a$

PLATE	y/b					
	0	0.1	0.2	0.3	0.4	0.5
0.048" steel	57.78×10^{-6}	20.76×10^{-13}	77.24×10^{-21}	28.74×10^{-28}	10.69×10^{-35}	39.80×10^{-43}
0.036" steel	49.76×10^{-6}	18.52×10^{-13}	68.90×10^{-21}	25.64×10^{-28}	95.41×10^{-36}	35.50×10^{-43}
0.048" alum.	20.07×10^{-5}	74.68×10^{-13}	27.79×10^{-20}	10.34×10^{-27}	38.48×10^{-35}	14.32×10^{-42}
0.036" alum.	80.35×10^{-6}	29.90×10^{-13}	11.13×10^{-20}	41.40×10^{-28}	15.41×10^{-35}	57.33×10^{-43}

TABLE II.1 - Variation of Q_y and M_{xy} for actual plates.

moment M_{xy} - Fig. II.11 as the rate of change with y of Q_y reflects the value of $\partial M_{xy}/\partial y$ at any section. The graphs for the distribution of M_{xy} have been drawn to indicate the variation of this torsional couple at the support, as at the centre of the plate the value of this couple is zero, this being due to the cosine distribution of the series for M_{xy}.

For the plates used in the experimental investigation the variation of Q_y and M_{xy} are shown in Tables II.1(a) and II.1(b). It is to be noted that these quantities throughout the plate are small and can be stated to be negligible compared to the values of M_x, R_x and Q_y with the exception of the values of M_{xy} at the plate corners where a finite corner load of magnitude $2M_{xy}$ is produced. Thus the summation of $(R_x + 4M_{xy})$ along a supported edge of the plate gives one half of the total static load on the plate.

The shear force Q_x acting on planes parallel to the y-axis differs from the end reaction R_x by a quantity $2D_{66}\,\partial^3 w/\partial x\,\partial y^2$ but the dominant term in the expression for Q_x is $D_{11}\,\partial^3 w/\partial x^3$.

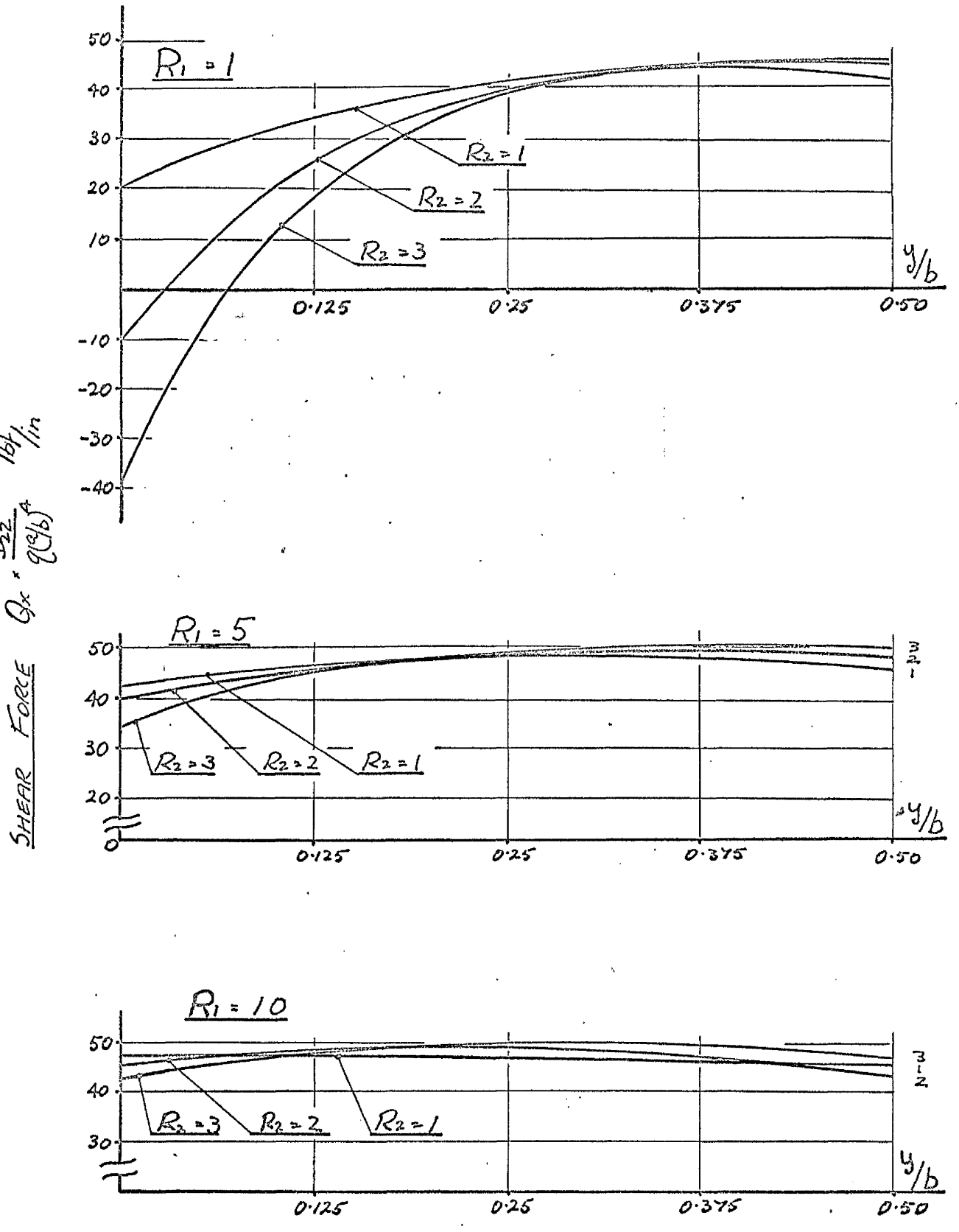

FIG.II.12 Shear force Q_x at x = 0 and z = a

D_{22} = 300 a/b = 4/3

$$Q_x = -\left[D_{11} \frac{\partial^3 w}{\partial x^3} + (D_{12} + 2D_{66}) \frac{\partial^3 w}{\partial x \partial y^2} \right] \qquad \text{(II.5.19)}$$

Thus as R_1 increases the value of Q_x will be closer to that of R_x . This can readily be seen from the graphs of Fig. II.12 which show the distribution of Q_x becoming more uniform as the ratio R_1 increases.

For the actual plates the values of Q_x are identical to those for R_x to the fourth significant digit indicating that the variation of the shear moment M_{xy} with the plate length x is negligible.

II.6. THE BENDING OF AN ORTHOTROPIC STRIP TO AN ANTICLASTIC SURFACE.

In Section VIII.3 of this thesis a complete analysis of the bending of an orthotropic strip to an anticlastic surface is given. This analysis has been carried out to demonstrate the utility of a pure bending test on an orthotropic strip to determine the value of the elastic modulus a_{11} . A brief outline of this analysis is given.

The compatibility equation for an orthotropic strip bent by a constant moment M is:

$$D_{11} \frac{\partial^4 w}{\partial x^4} + 2(D_{12} + 2D_{66}) \frac{\partial^4 w}{\partial x^2 \partial y^2} + D_{22} \frac{\partial^4 w}{\partial y^4} + \frac{E_{11} h w}{\rho^2} = 0 \qquad \text{(II.6.1)}$$

where w is the distortion of any point on the bent plate from the principal values of curvature ρ and E_{11} is the Young's Modulus in the direction of the length a .

Applying the transform:

$$w = \sum_{m=1,3..}^{\infty} Y_m \sin \frac{m\pi x}{a}$$

to the equation (II.6.1) yields the ordinary differential equation

$$\frac{d^4 Y_m}{dy^4} - 2\frac{D_{33}}{D_{22}}\left(\frac{m\pi}{a}\right)^2 \frac{d^2 Y_m}{dy^2} + \frac{D_{11}}{D_{22}}\left(\frac{m\pi}{a}\right)^4 \left[1 + \frac{96\,H(1-\nu_{12}.\nu_{21})}{(m\pi)^4}\right] Y_m = 0 \quad \text{(II.6.2)}$$

where H is a coefficient defining the central deflection of the strip in terms of the plate thickness h .

Proceeding as outlined in Appendix VIII.3 the roots of the equation (II.6.2) are determined for the cases when all the roots of the equation are real and complex respectively.

The solution of (II.6.2) for real roots can be stated as

$$w = \sum_{m=1,3,..}^{\infty} \left[A_m \cosh \xi_1 y + B_m \sinh \xi_1 y + C_m \cos \xi_2 y + D_m \sinh \xi_2 y \right] \sin \frac{m\pi x}{a} \quad \text{(II.6.3)}$$

and for complex roots as

$$w = \sum_{m=1,3,\ldots}^{\infty} \left[(A_m \cos \lambda y + B_m \sin \lambda y) \cosh \chi y + (C_m \cos \lambda y + D_m \sin \lambda y) \sinh \chi y \right] \sin \frac{m\pi x}{a} \qquad \text{(II.6.4)}$$

The constants A_m etc. are obtained from the appropriate boundary conditions and the shape of the distorted cross-section obtained as indicated and discussed in Appendix VIII.3. Thus the distortion from a cylindrical form of radius ρ due to anticlastic effects can be estimated.

It is also demonstrated in Appendix VIII.3 that these effects can be considered negligible for the plates described in Chapter III and the value of a_{11} determined from the bending of a strip to cylindrical surface of radius ρ is accurate to within the limits of experimental error.

A further use of this analysis is to examine the validity of the assumption $a_{12} = a_{21}$ for the range of plates discussed in Chapter III. As shown in Appendix VIII.3 this assumption reduces to an examination of the validity of the relationship

$$\nu_{21} = \nu_{12} \cdot \frac{D_{22}}{D_{11}} \qquad \text{(II.6.5)}$$

where ν_{12} is the Poisson's Ratio relating an extensional strain in the x-direction to the corresponding strain in the y-direction and ν_{21} is that relating an extensional strain in the y-direction to the consequent strain in the x-direction.

As is demonstrated in Appendix VIII.3 the distortions given by (II.6.3) and (II.6.4) can be computed for relationships other than (II.6.5) and it is shown that for the range of experimental plates considered the relationship (II.6.4) must hold. That is, as stated in the Critical Review, the author believes that the statement made by HOPPMANN (1955) regarding the applicability and validity of the relationship $a_{12} = a_{21}$ to be correct and in fact the only viable condition for orthotropic plates.

CHAPTER III

EXPERIMENTAL INVESTIGATION

The experimental work presented in this Chapter covers:

1. Evaluation of the orthotropic plate moduli and corresponding stiffnesses for decking units of light gauge metal.

2. Tests of full scale corrugated deck units under pressure loading. These tests included complete deflection and strain gauge examinations of decking behaviour.

III.1. THE TEST SPECIMENS AND DETERMINATION OF THE ELASTIC MODULI.

The test specimens were formed from sheet material of galvanized steel and aluminium alloy which was nominally 0.036 and 0.048 in. thick. The effect of the galvanizing on the behaviour of the steel sheets was considered to be negligible. A thickness survey of the specimens revealed a variation not greater than 0.05% for either material.

The steel specimens used were particularized by B.S. 3083 and, the aluminium alloy NS3H by B.S. 1470.

For each test two samples were cut from the/

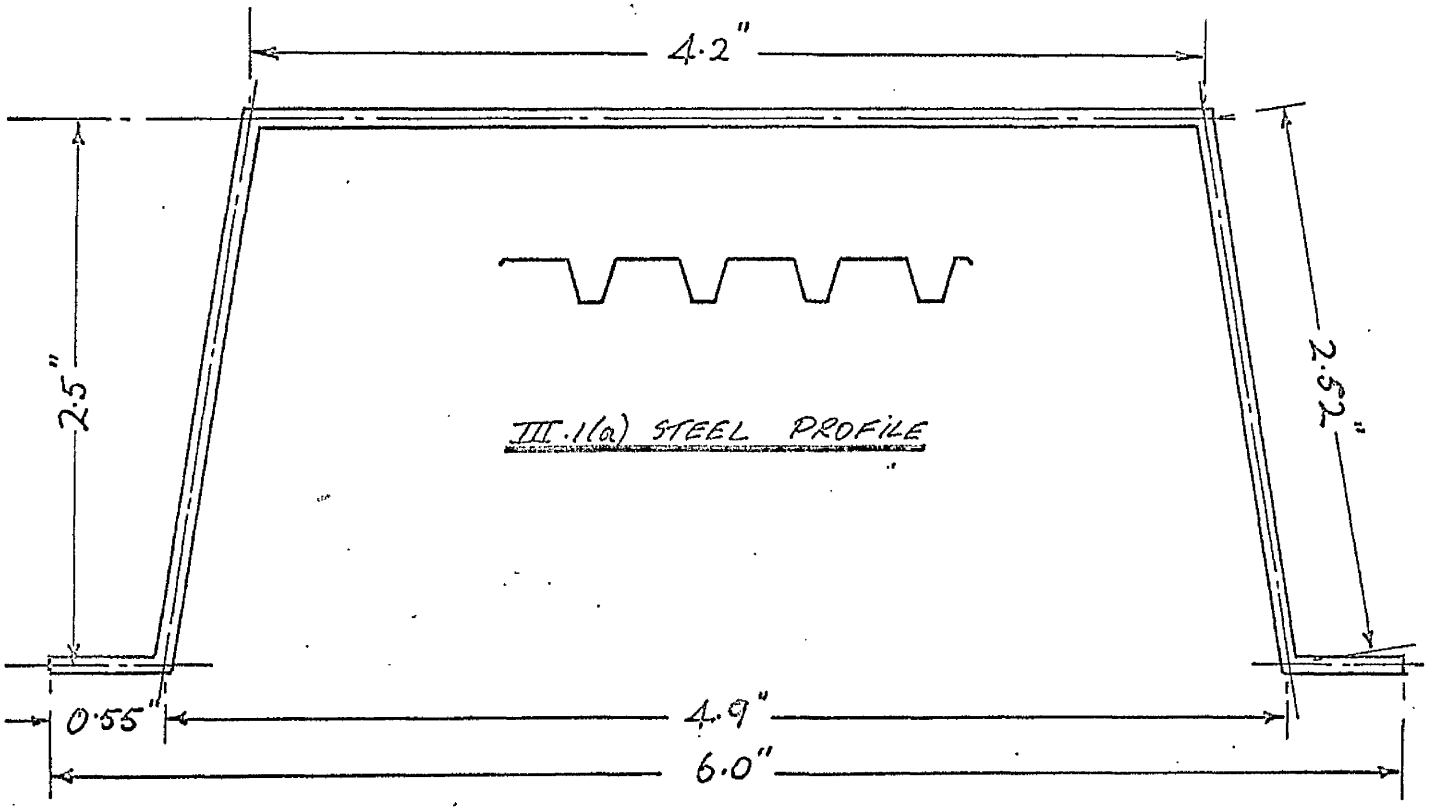

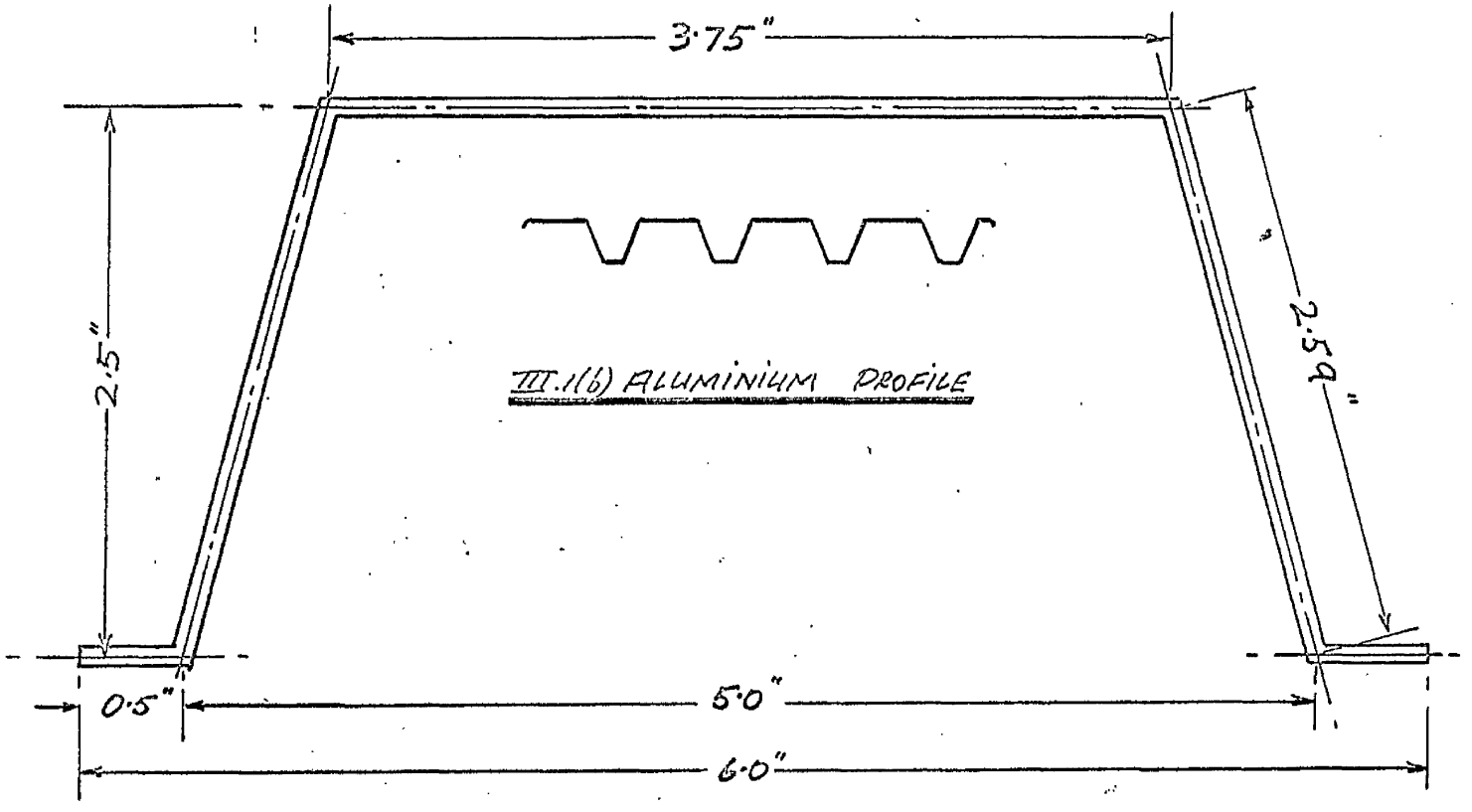

FIG.III.1 Section Profiles.

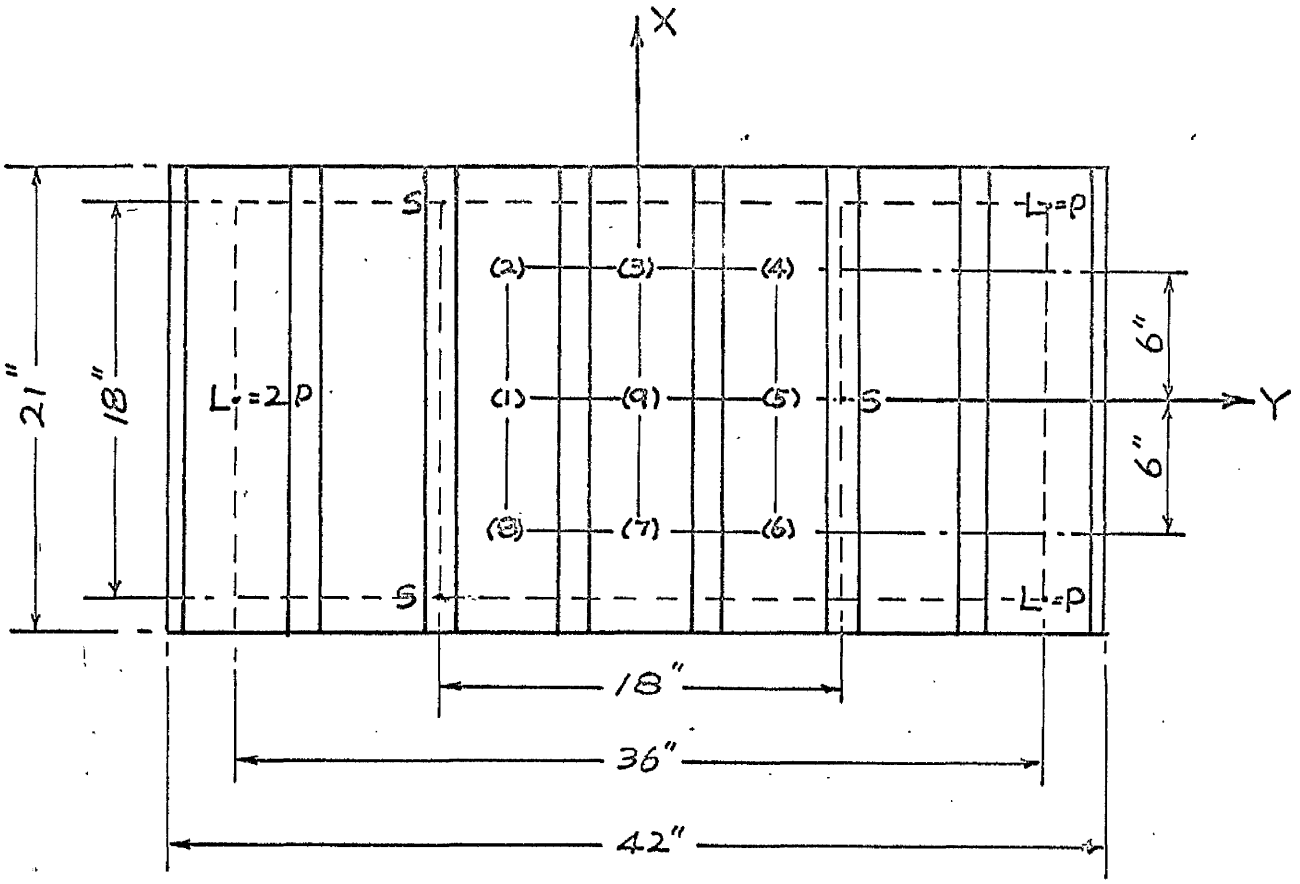

S - SUPPORT POINTS L - LOAD POINTS

FIG.III.2 Co-ordinate system for the determination of a_{22}

the large scale unit and tensile tests were carried out to determine Young's Modulus and Poisson's Ratio, some seventy tests in all being undertaken - see Appendix VIII.6. The average values of Poisson's Ratio which were subsequently used in the theoretical work were:

Aluminium Alloy: Poisson's Ratio $\nu = 0.33$

Steel: Poisson's Ratio $\nu = 0.28$

The actual troughed decking was cold formed from sheets of 0.036 and 0.048 in. thick steel and aluminium, each individual trough having the profile shown in Fig. III.1(a) and Fig. III.1(b) for steel and aluminium respectively.

The determination of a_{zz} : for the evaluation of a_{zz} the rectangular plate having the co-ordinate system shown in Fig. III.2 was used. The pattern of points (1) to (9) was marked on the flange of the sheet and on a specially prepared part of the floor surface perpendicularly below. The deflection of the plates was measured by micrometer stick and the increments of loading were such as to provide adequate magnitudes of deflection. The test consisted of applying increments of load up to/

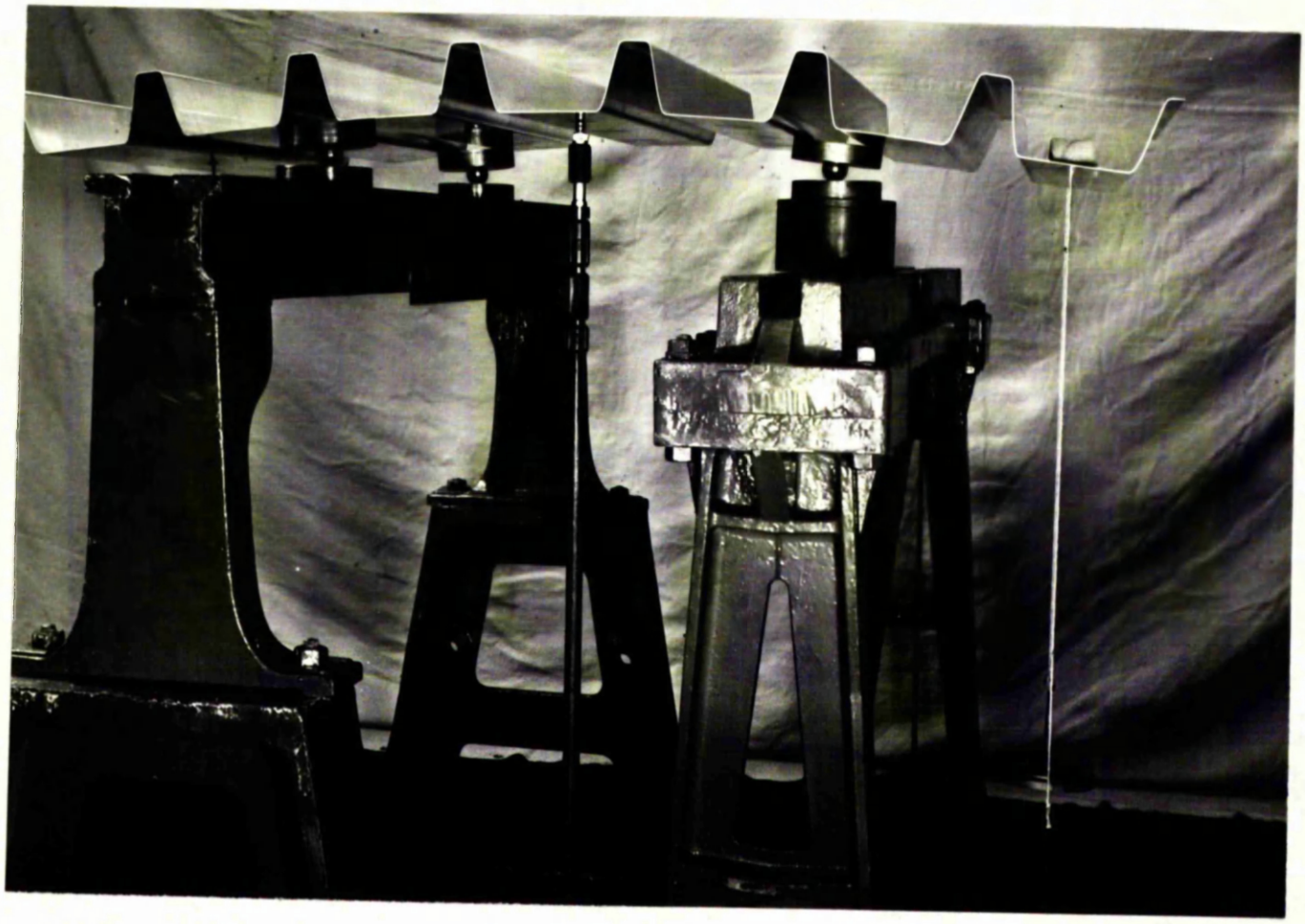

FIG. III.3 Bending Test for a_{22}

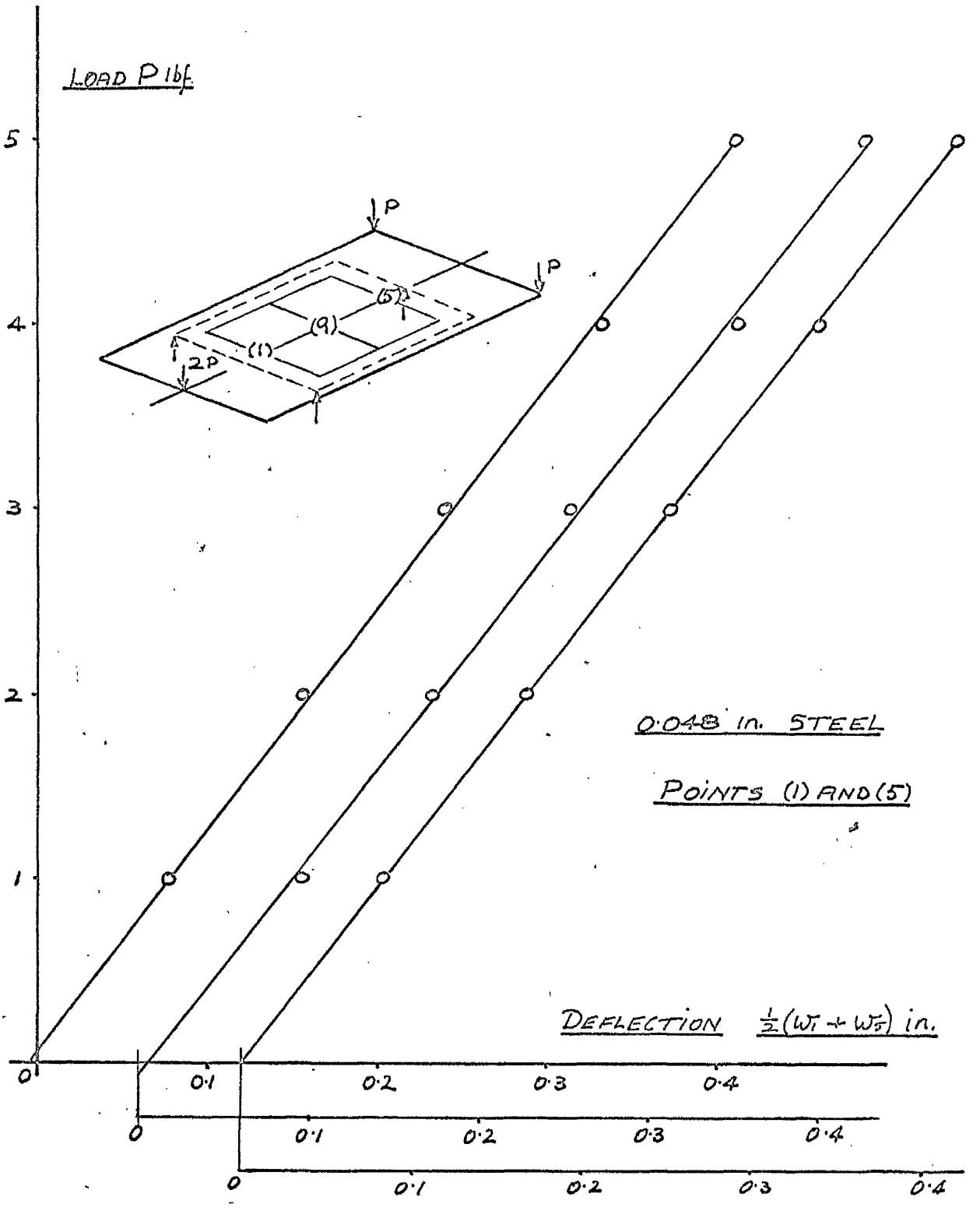

FIG.III.4 Bending tests for a_{22}

Deflections relative to that of (9)

N.B. Shift of origin to facilitate graphing of similar tests.

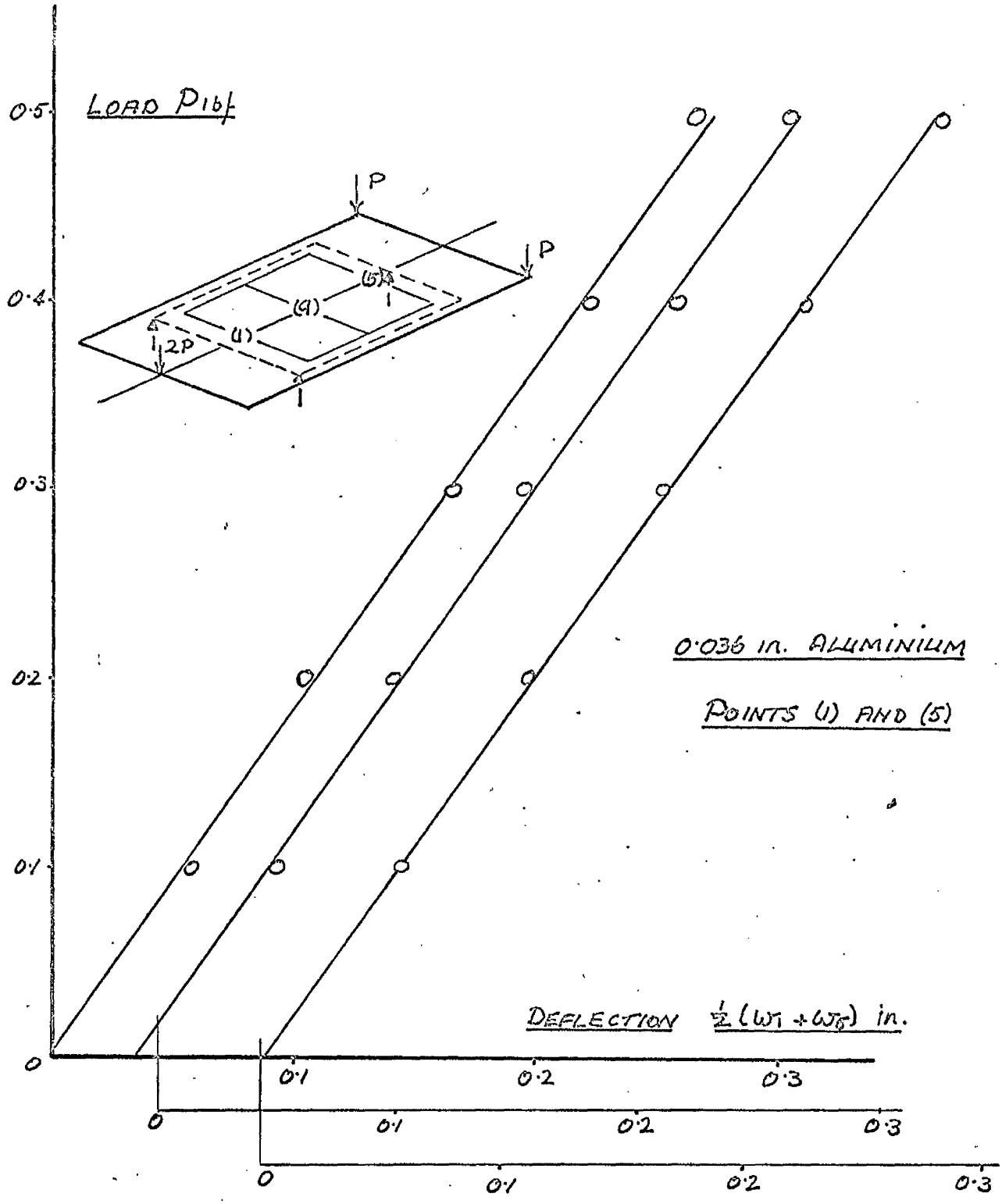

FIG.III.5 Bending tests for a_{22}

Deflections relative to that of (9)

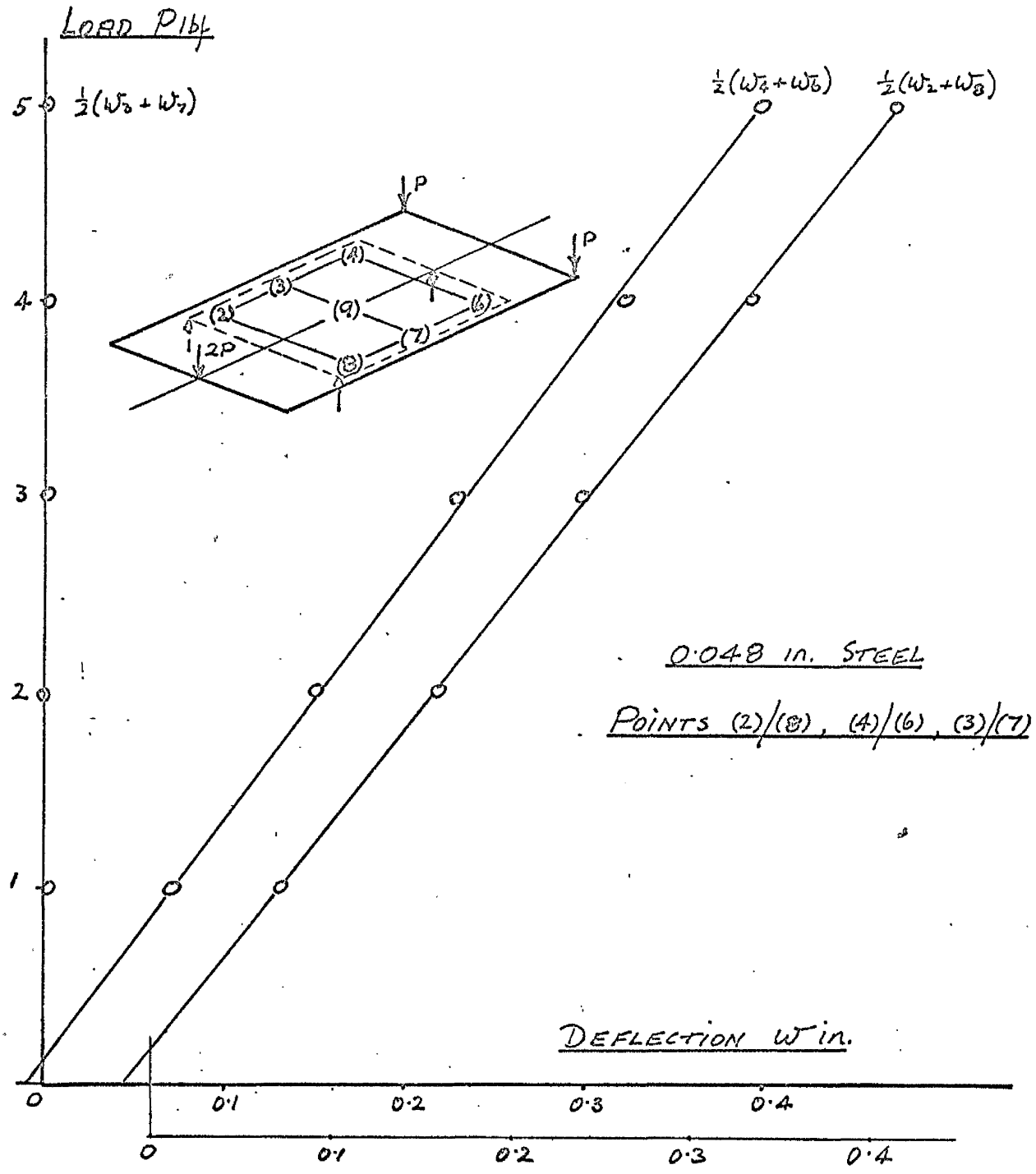

FIG.III.6 Bending tests for a_{22}
Deflections relative to that of (9)

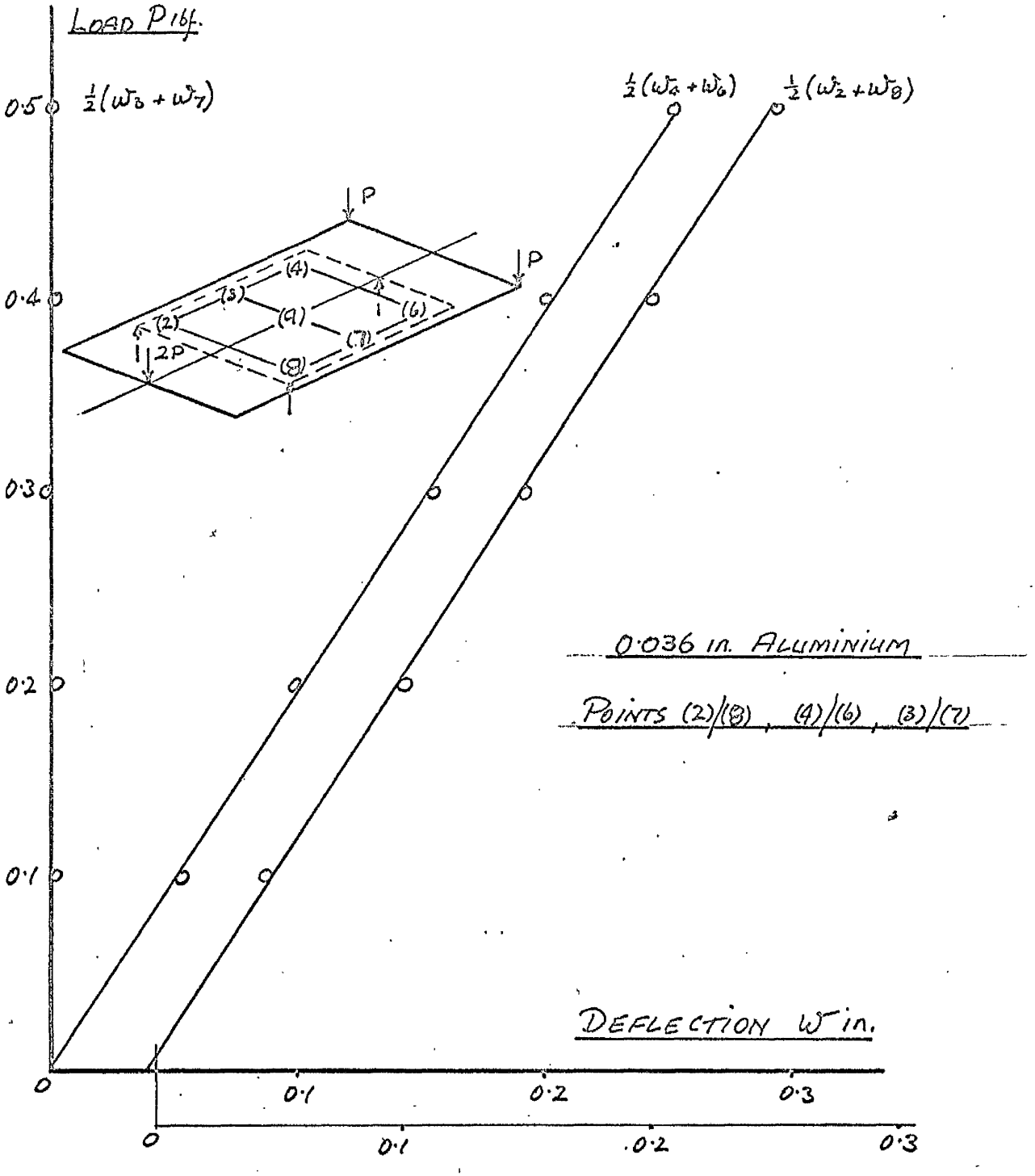

FIG.III.7 Bending tests for a_{22}

Deflections relative to that of (9)

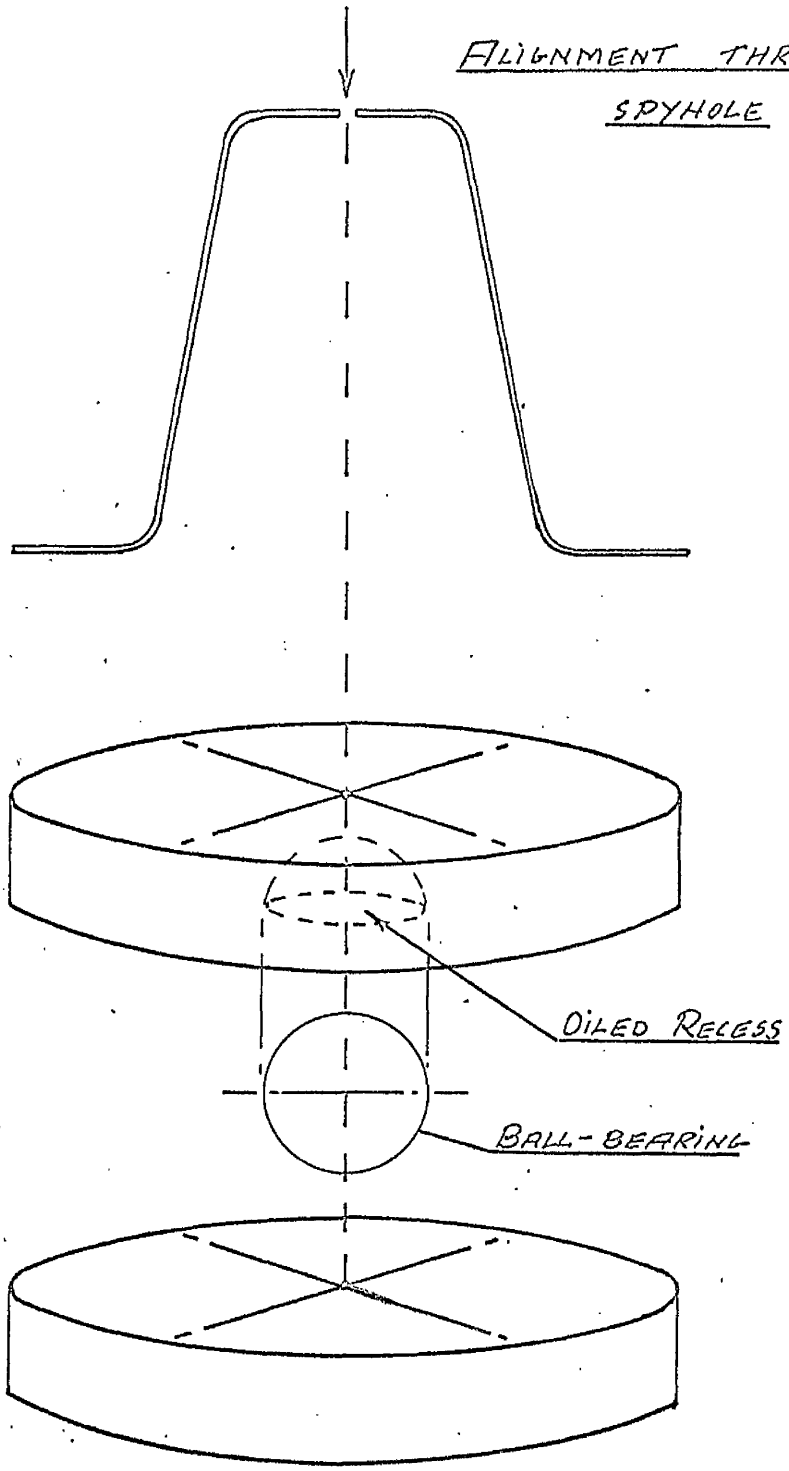

FIG.III.8 Diagrammatic view of Alignment Device.

to a predetermined value, measuring the deflections of the points (1) to (9). The loading was then decreased in steps to zero, the deflections of points (1) to (9) again being measured. Fig. III.3 shows a typical plate under test and Figs. III.4. and III.5 give typical sets of results for 0.048 in. thick steel and 0.036 in. thick aluminium respectively, a full range of results being given in Appendix VIII.6. The slopes of the line through the experimental points in all cases was determined by computation via the method of least squares and these were subsequently used as shown in Chapter IV to evaluate the modulus a_{22} . The symmetry characteristics of the plate behaviour are demonstrated in Figs. III.6 and III.7, which give the deflections of points other than those used to evaluate a_{22} .

Three tests were undertaken for each plate, and a careful examination of the results made. Particular care was exercised in lining up the plate under test and Fig. III.8 shows the arrangement for ascertaining that the plate was correctly positioned over each ball bearing support. A small spyhole facilitated the positioning of the support points - Fig. III,2, over the top bearing plate whose underside/

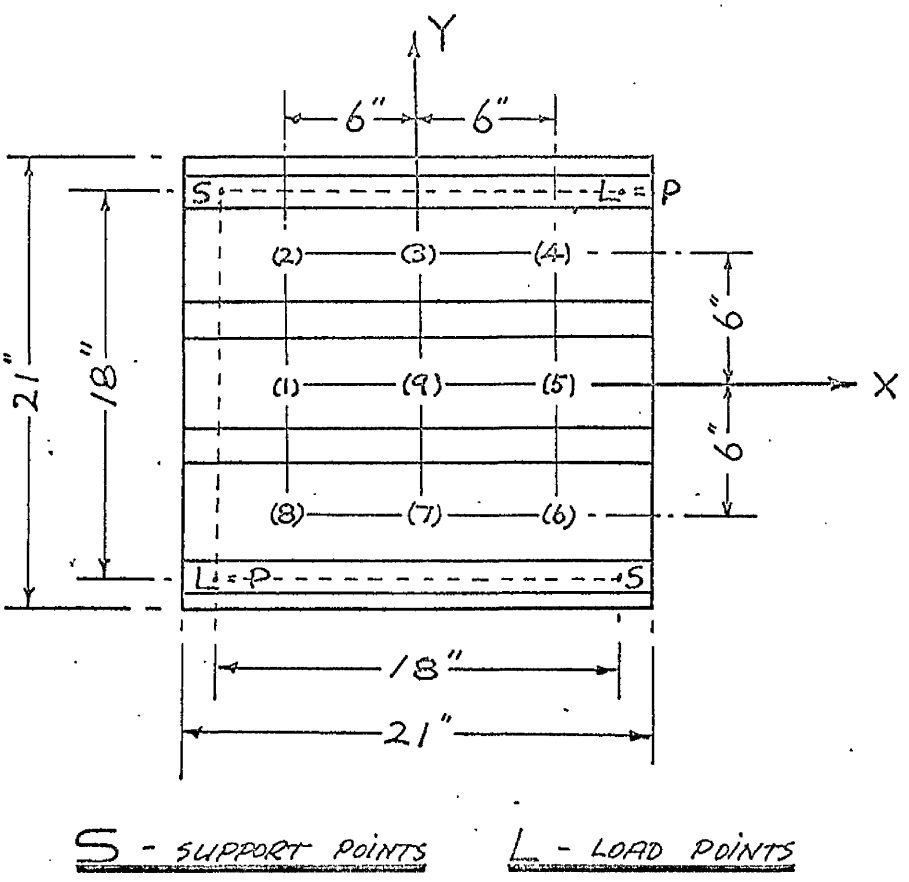

FIG.III.9 Co-ordinate system for determination of a_{66}

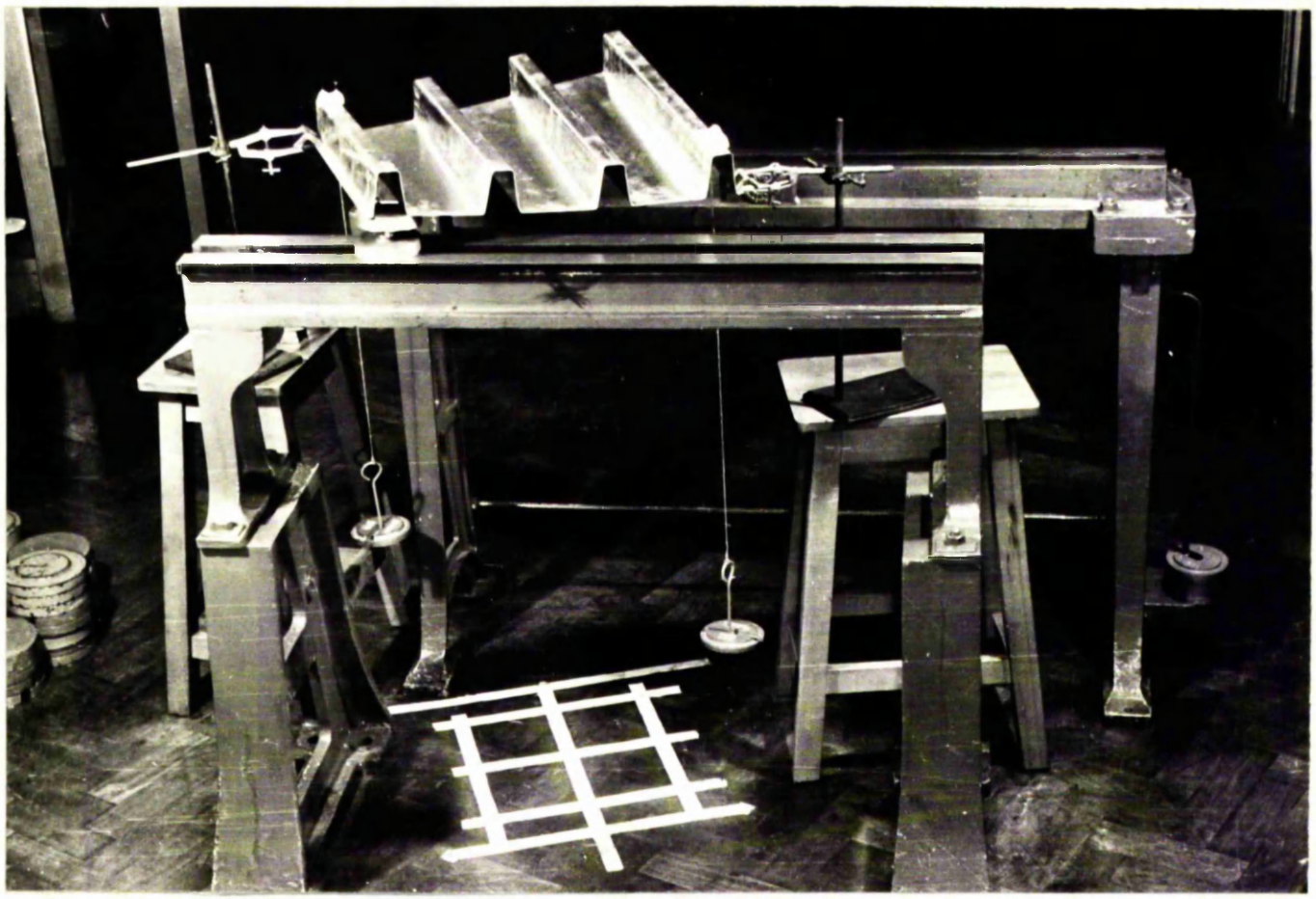

FIG. III.10 Twisting Test for a_{66}

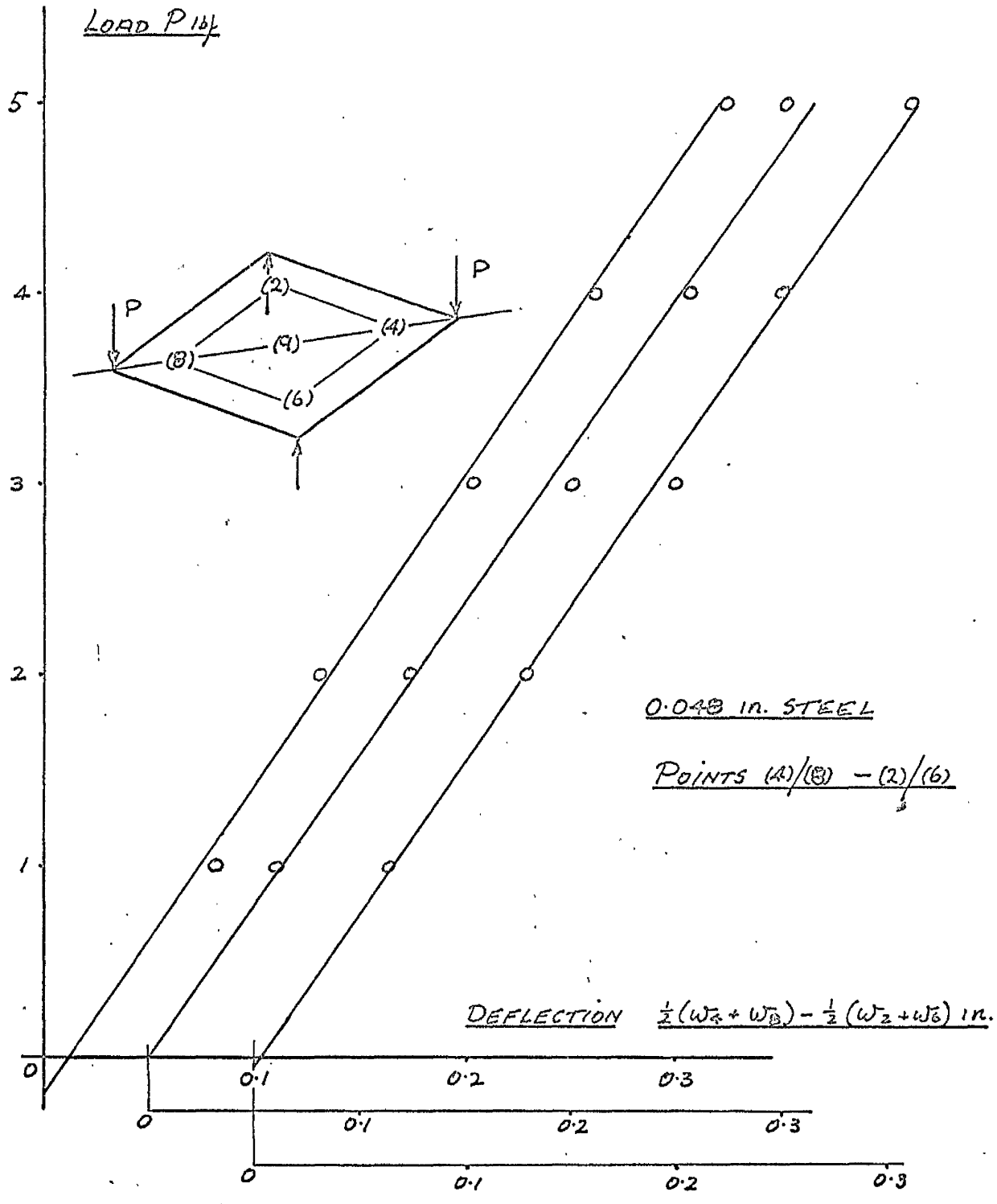

FIG.III.11 Twisting tests for a66

Deflections relative to that of (9)

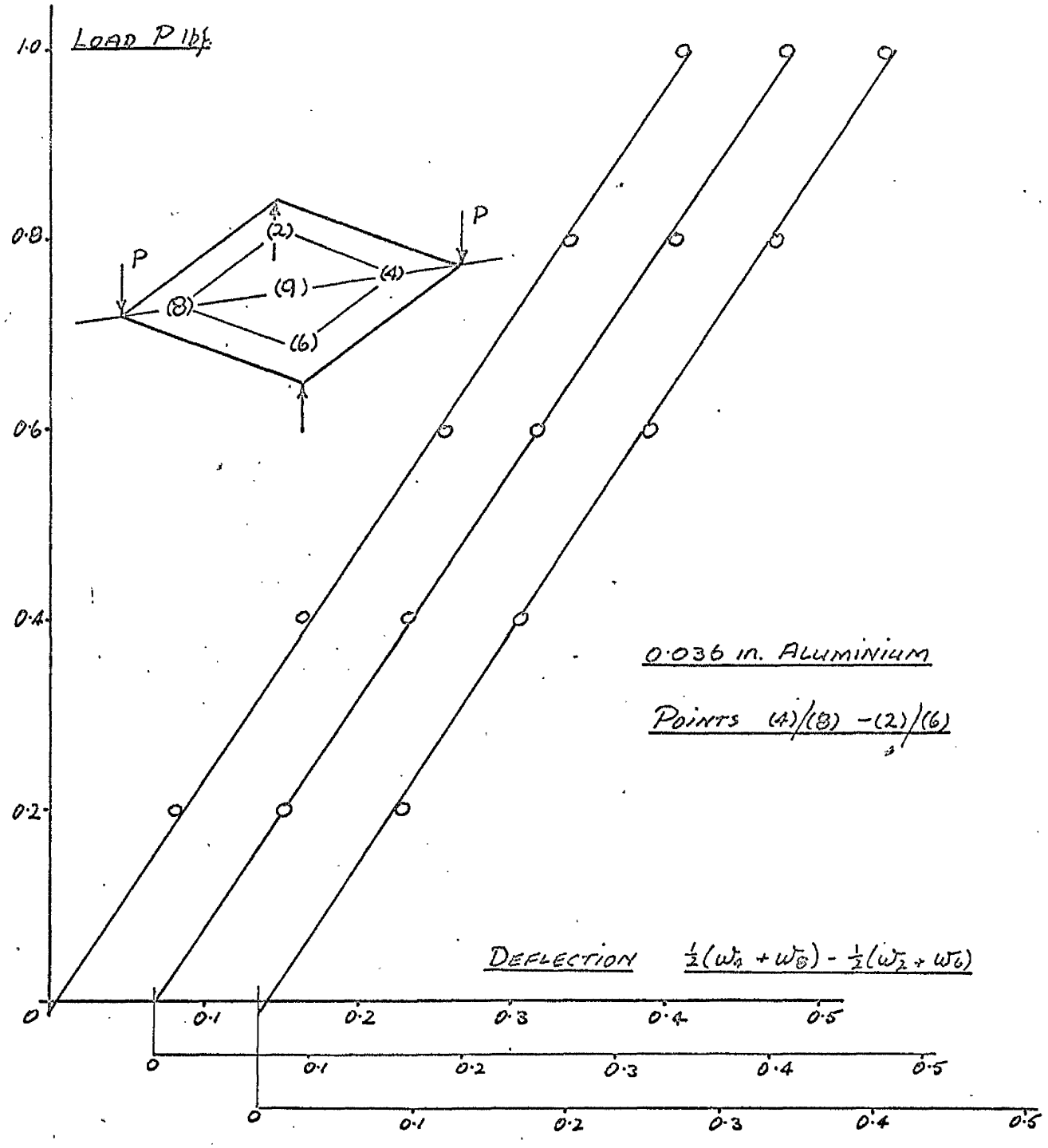

FIG.III.12 Twisting tests for a_{66}

Deflections relative to that of (9)

underside contained an oiled recess in which the ball bearing could rotate. The bottom support plate had marked on it the position through which the point support given by the ball bearing had to act, and adjustment was made using a Cartesian system of axes marked on this plate. Both the bearing plates were made of 5/8 in. thick steel whose surfaces had been machined smooth and the bottom plate was fixed by adhesive to a solid steel frame.

The determination of a_{66} : for this test a square plate with the dimensions shown in Fig. III.9 was used. The plate was supported on two ball bearing supports at opposite corners while the twisting load was applied at the other two corners. Fig. III.10 shows a plate undergoing a twisting test for which the testing technique and the pattern marked on the plate and floor were identical to those used in the bend test for a_{22} , measurement of deflection again being by means of a micrometer stick. A typical set of results for 0.048 in. thick steel is given in Fig. III.11 and for 0.036 in. thick aluminium in Fig. III.12, the appropriate analysis from the slope of these graphs being pursued in Chapter IV. The symmetrical nature of the test results is indicated/

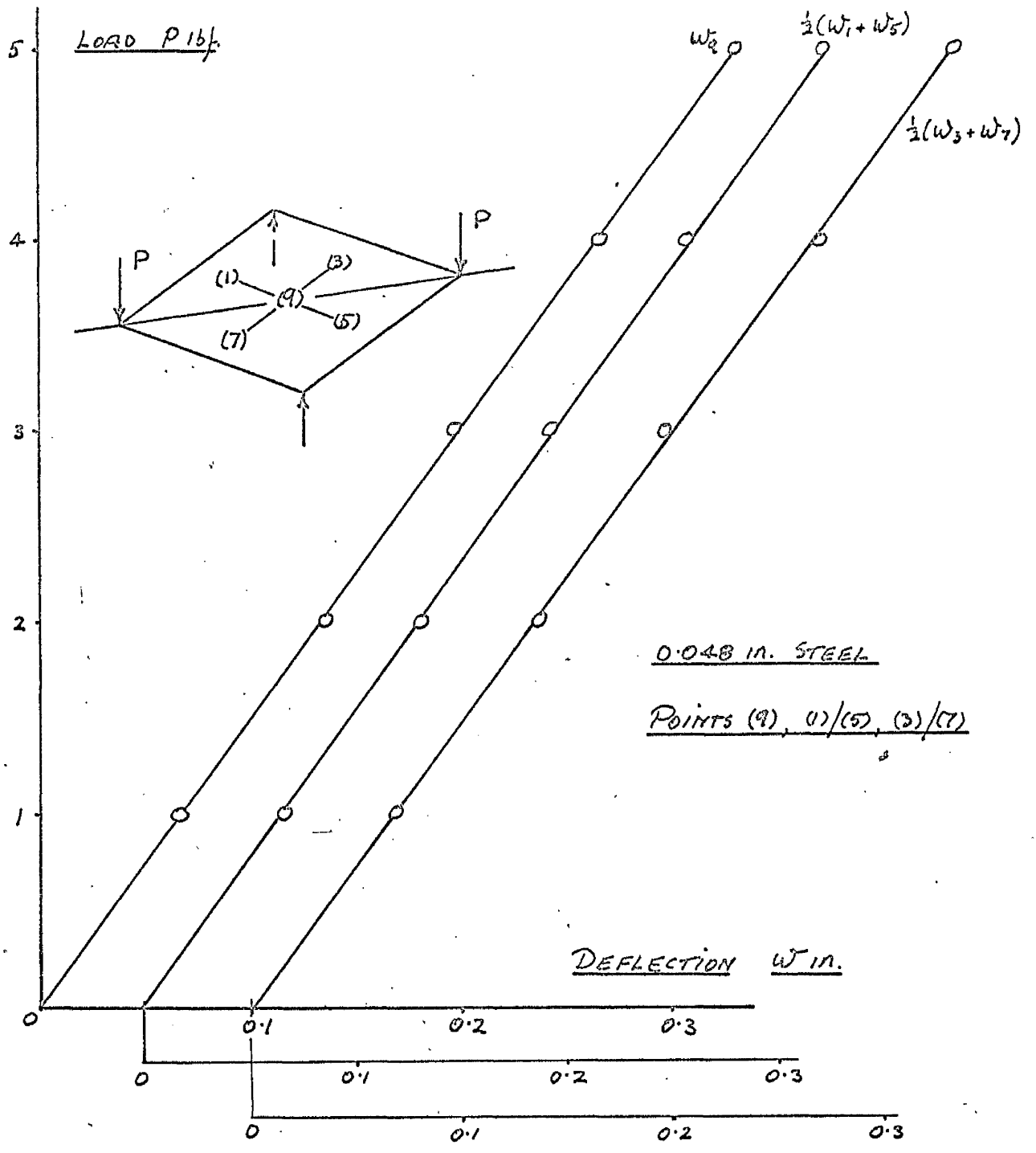

FIG.III.13 Twisting tests for a_{66}

Actual deflections.

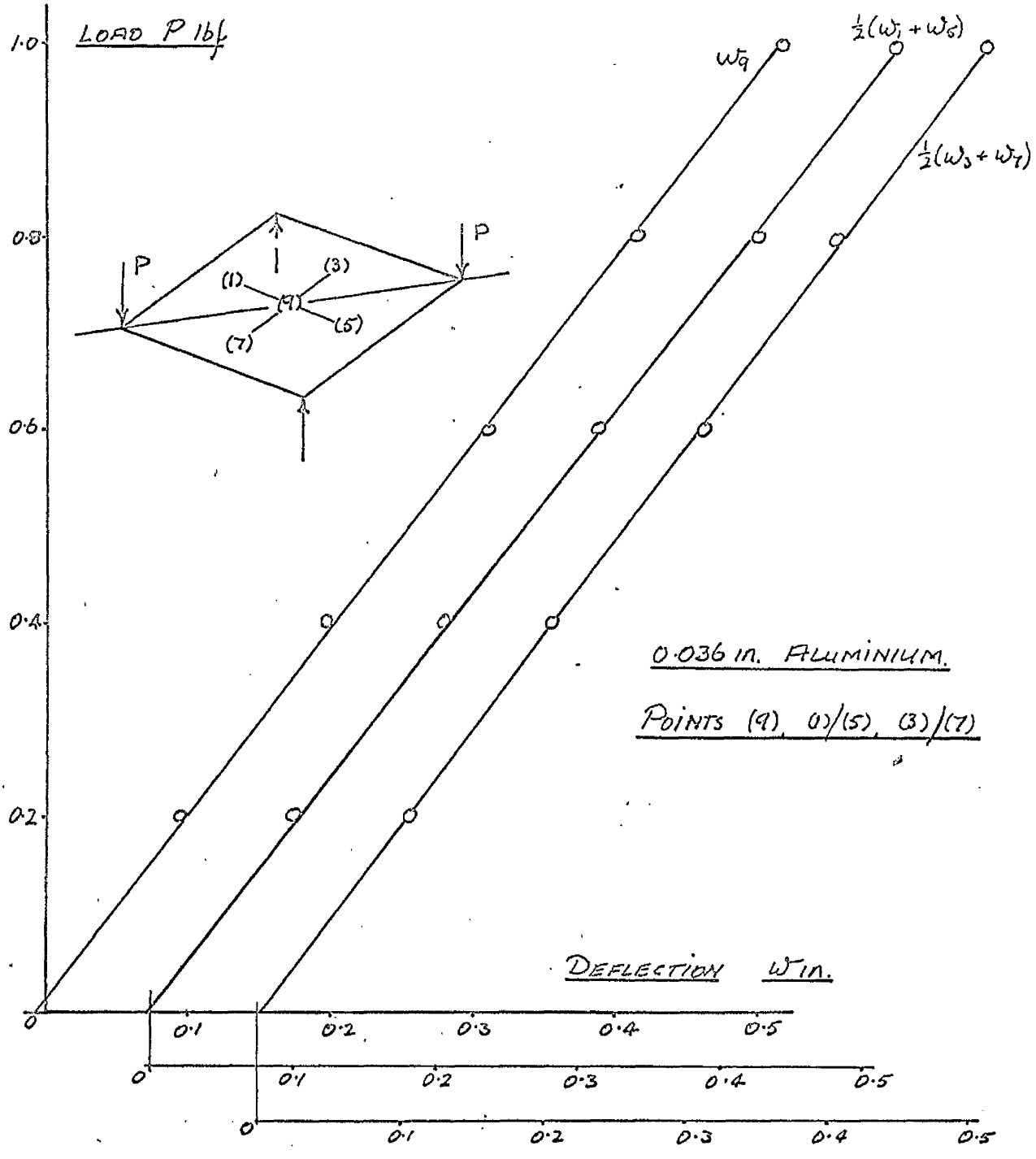

FIG.III.14 Twisting tests for a_{66}

Actual deflections.

FIG. III.15 Bending Test for a_{11}

indicated by Figs. III.13 and III.14.

As for the determination of a_{22} great care was taken when the load was changed and this was facilitated by clamping the plate in the deflected position, increasing the load and then releasing the clamps. As before, three tests were carried out on each plate, deflection readings being taken for increasing and decreasing load. The full results of the tests are presented in Appendix VIII.6.

The determination of a_{11} : two methods were available for the determination of a_{11} . The first of these was to pursue an identical technique to that used for the determination of a_{22} . A preliminary test demonstrated this method to be experimentally unreliable as the rigidity of the plate in the direction of the corrugations was such that the degree of bending obtained in this direction was too small for consistent measurement.

To obviate this difficulty it was decided to test a single trough under pure bending and pursue a separate analysis to determine a_{11} from this test. A typical test is shown in Fig. III.15. Under load, the deflected form of the trough was mapped using the/

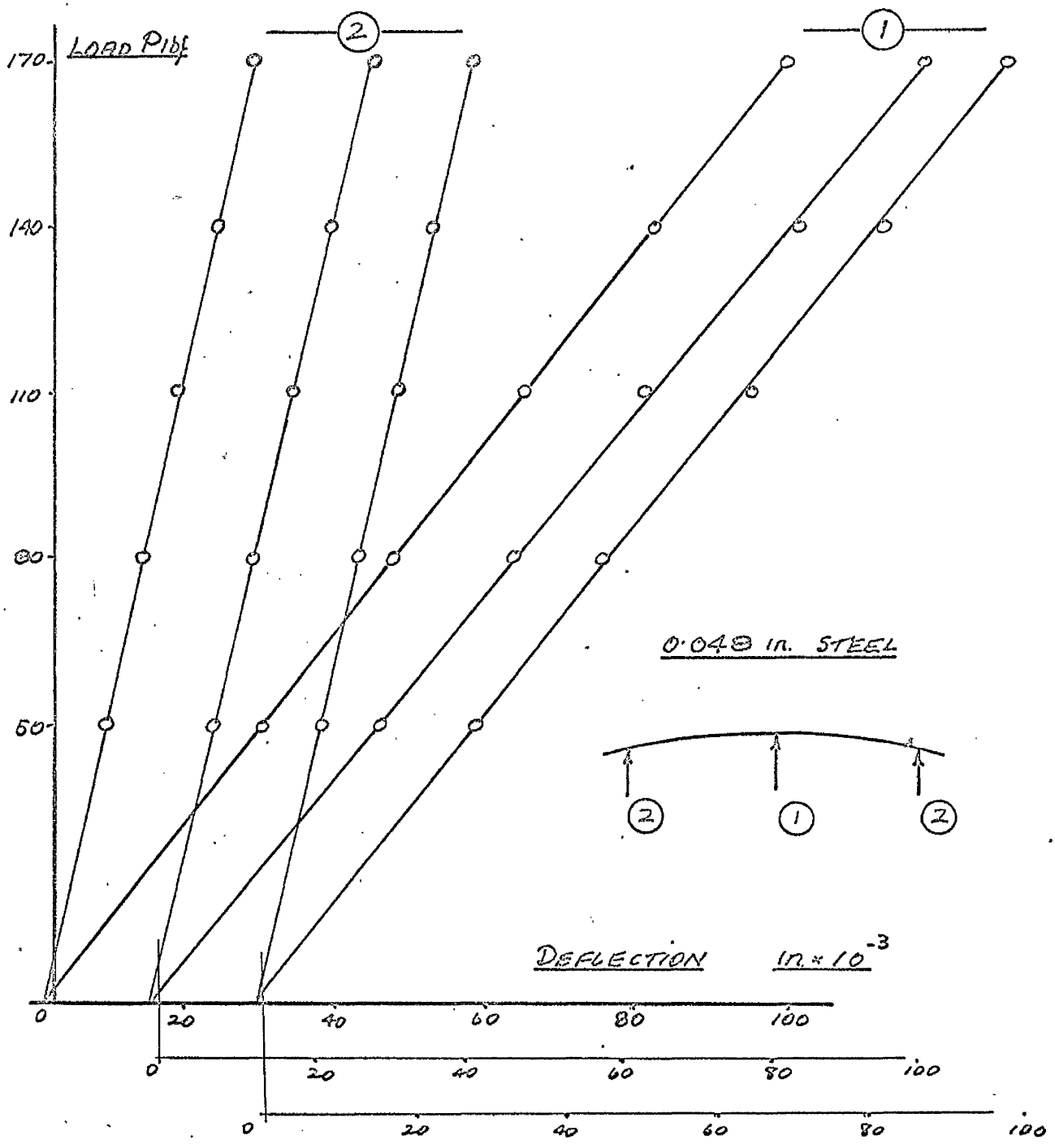

FIG.III.16 Bending tests for a_{11}

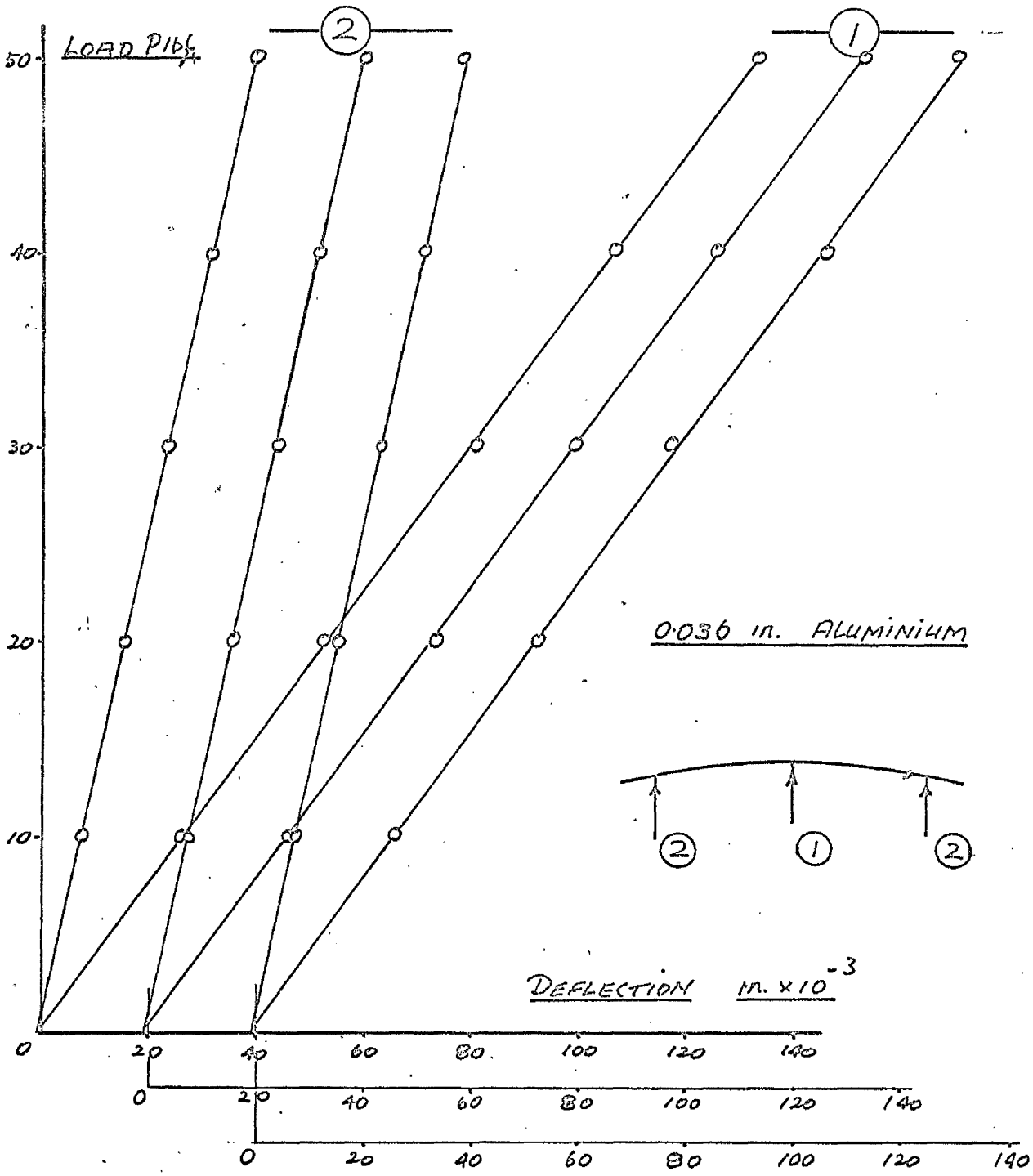

FIG.III.17 Bending tests for a_{11}

the three dial gauges shown in Fig. III.15, the trough being restrained in its original profile by the brackets equally spaced along the trough. To assess whether cross-section distortions occurred, as originally anticipated, the test was repeated with the brackets removed. No difference in behaviour was observed. Even at large deflections there was no evidence to suggest that the trough was in any way splaying. Three tests were carried out for each material and profile. The analysis of these is considered in Chapter IV and a full range of results is given in Appendix VIII.6. Typical sets of results for 0.048 in. thick steel and 0.036 in. thick aluminium are given in Figs. III.16 and III.17.

III.2. DECKING UNDER LATERAL LOAD.

The test apparatus: before building a full scale test apparatus for the examination of the behaviour of cold formed decking units under uniform lateral loading some preliminary tests were performed on single sheets 9 feet long and 2 feet wide, each consisting of four corrugations of the profiles shown in Fig. III.1. The sheets were bolted to fixed end supports, the two longitudinal edges being free and/

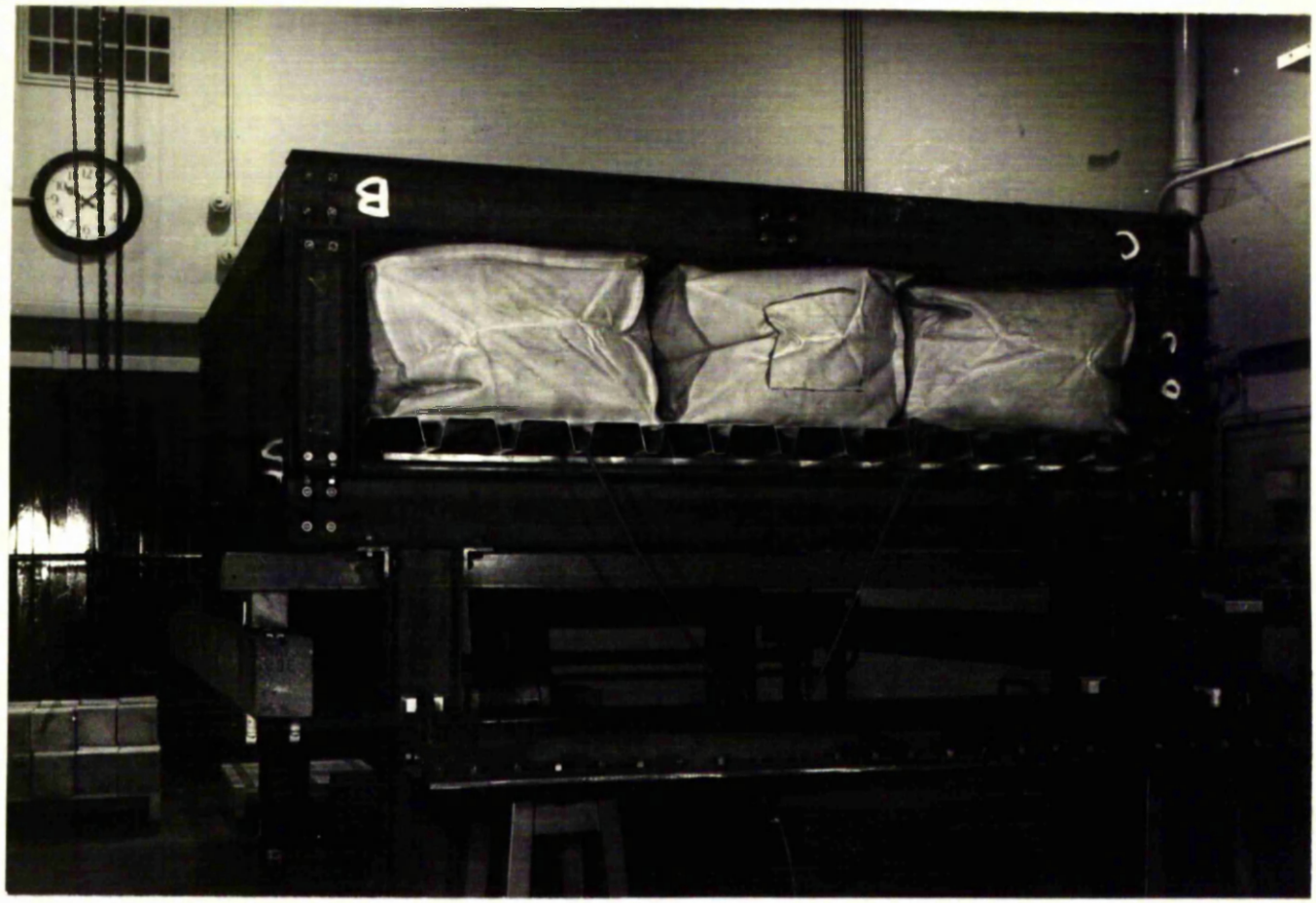

FIG. III.18 Loading Frame and Specimen

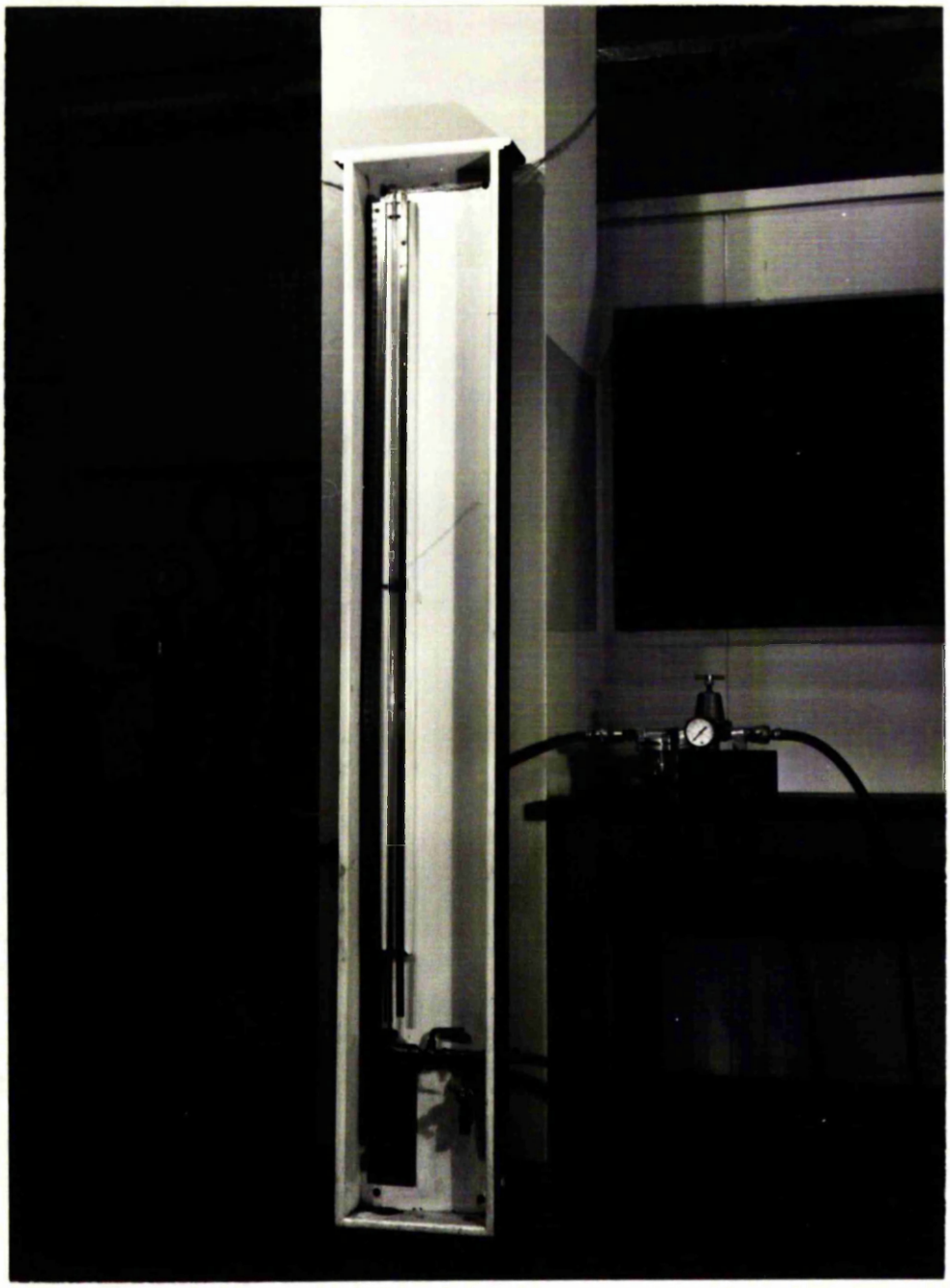

FIG. III.19 Water Manometer and Inlet Valve

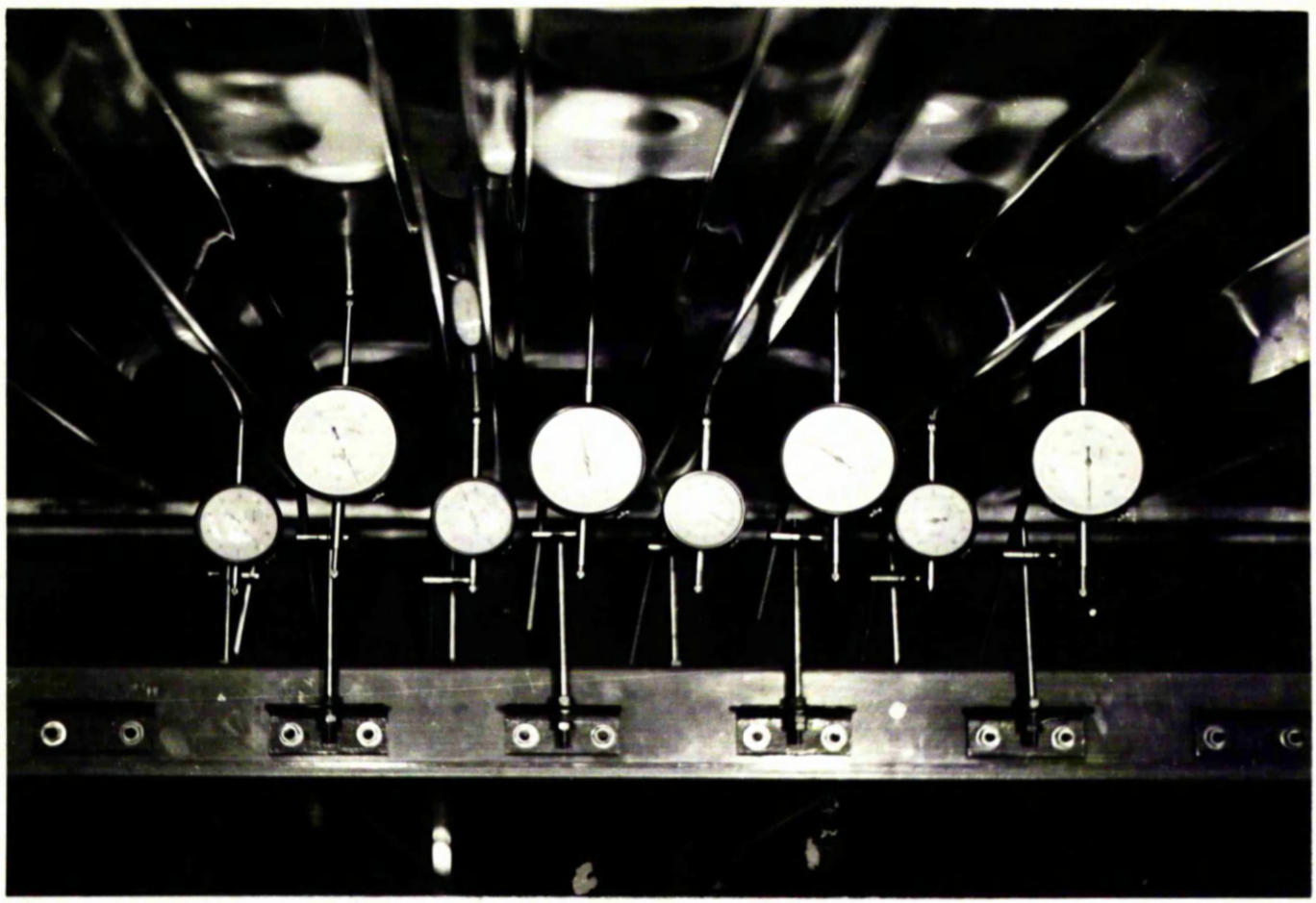

FIG. III.20 Dial Gauges on Travelling Beam.

and dead loading in the form of 25 and 56 lbf weights was uniformly distributed over the plate surface. It was found that at a very low value of load intensity the plates exhibited local buckling at the supports after which the behaviour was as though the plates were simply supported.

Thus when the design of an apparatus to test multi-breadth sheet was under consideration, it was decided to make the loading arrangements such that the composite sheet was simply supported on two ends and completely free along the two spanwise edges. Fig. III.18 shows the structure built to subject a deck to uniform lateral loading. Each deck was made up of three linked parallel corrugated plates, 9 feet long by 2 feet wide. Pressure was applied to the decking under test by means of three air vessels with flexible walls, each of which was connected to an inlet reservoir, the two outside vessels also being connected to a water manometer - Fig. III.19. The supported span of the multi-breadth decking tested was 8 feet and deflections over this span were measured by means of dial gauges mounted on a travelling beam as shown in Fig. III.20. The runway for the beam consisted of V-rails set into solid/

solid wooden beams which ran the length of the test rig.

An air compressor with a delivery pressure of 200 lbf/in^2 was used to pressurize the vessels and control was effected by means of a Schrader air control valve on the delivery side positioned near the water manometer for ease of accurate control.

The end supports of the composite deck were mild steel flats bolted on to the decking at a span of 8 feet. These flats rested on a 1 in. diameter steel rod welded to the test frame, thus ensuring that the deck unit was free to rotate about the end supports.

Test procedure: three single deck units 9 feet long by 2 feet wide were arranged parallel with edges overlapping. The mild steel flats were then laid across the decking at a span of 8 feet and holes marked through on to the smaller (tension) flange. The sheets were then screwed to the flats by means of 2 B.A. set screws, rubber and steel washers. When the three single sheets had been fitted together to form a deck, lines were scribed on to the underside/

underside of the sheet. These lines which were to mark the position of the required deflection readings were at 1 foot from the line of each support and at the quarter and centre points of the larger (compression) flange.

The composite unit was then turned over to bring the compression flange uppermost, a layer of heavy felt placed on top and the three air vessels laid on, these running longitudinally along the line of the troughs. The complete assembly was then lifted and placed into the frame, the inlet tubes connected to the inlet reservoir and the outlet to a common line to the water manometer, the vessels partially blown up to a position resembling that shown in Fig. III.18 and then the last cover plate was put into place.

A traverse was then made with the dial gauges mounted on the travelling beam, zero readings noted and then the pressure successively increased in suitable increments. The pressure reading at which waving in the compression flange was initiated was noted and the structure was loaded to collapse.

Two complete tests were performed for each/

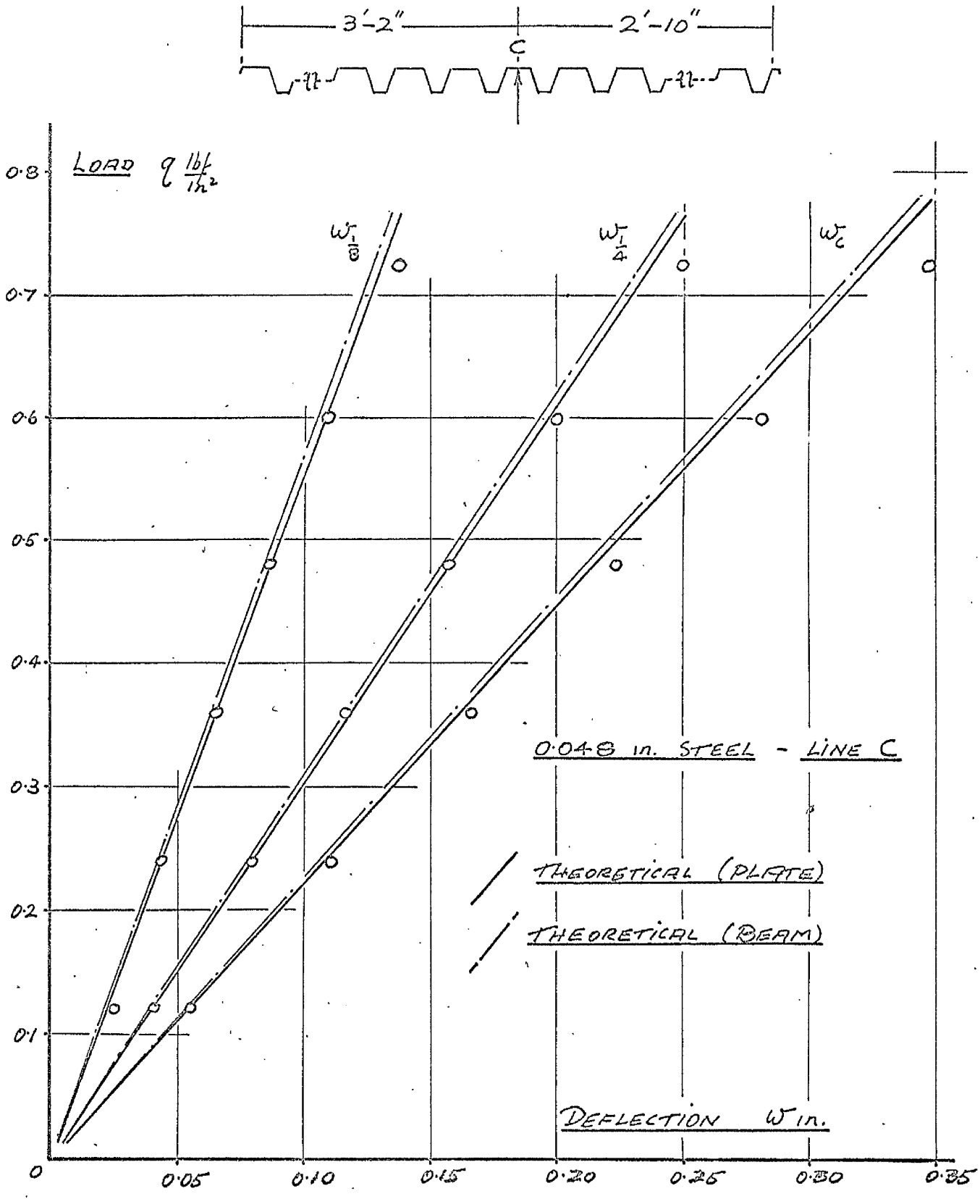

FIG.III.21 $\frac{1}{8}$, $\frac{1}{4}$ and centre line deflections of full scale decking tests.

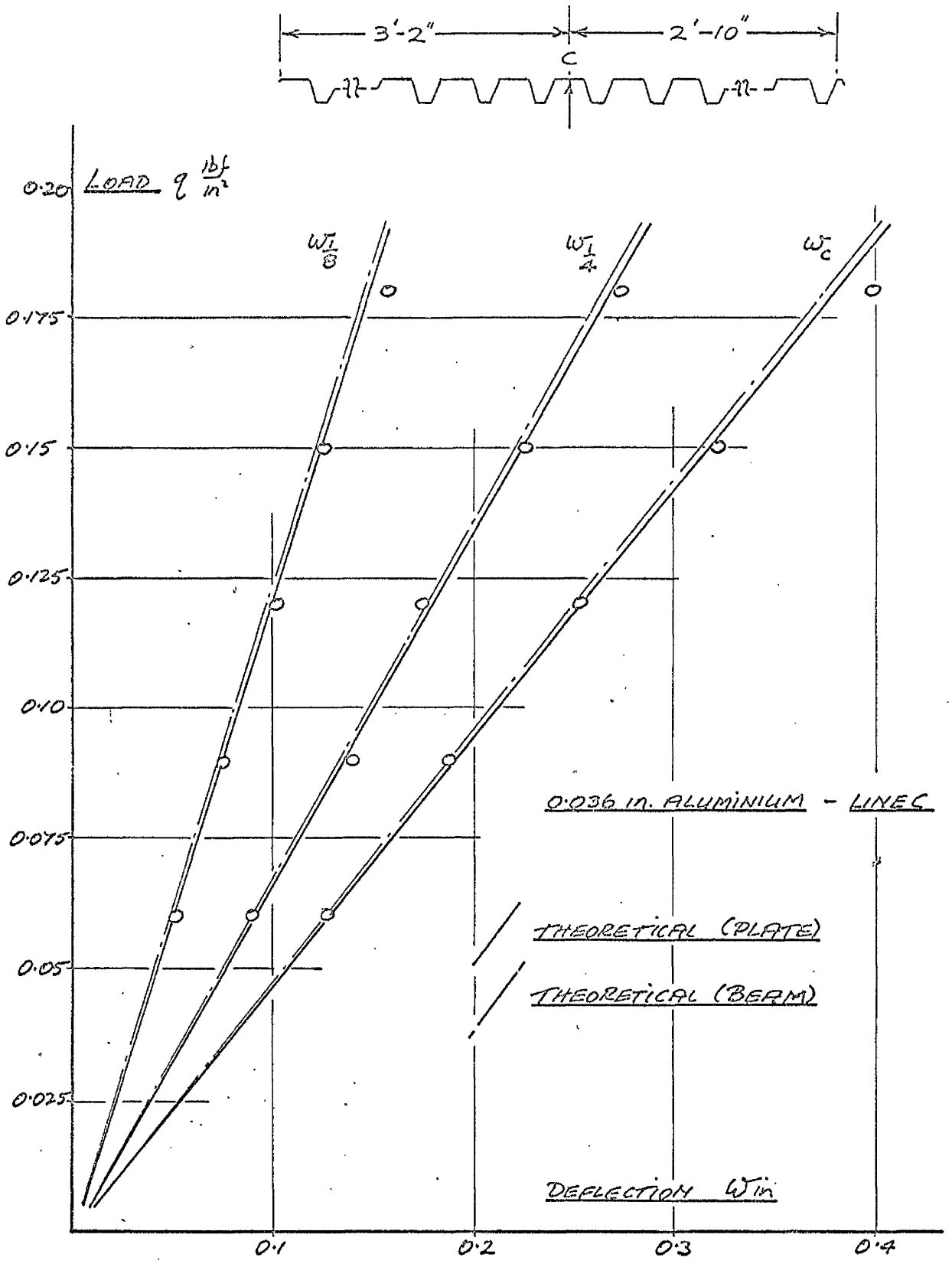

FIG.III.22 $\frac{1}{8}$, $\frac{1}{4}$ and centre line deflections of full scale decking tests.

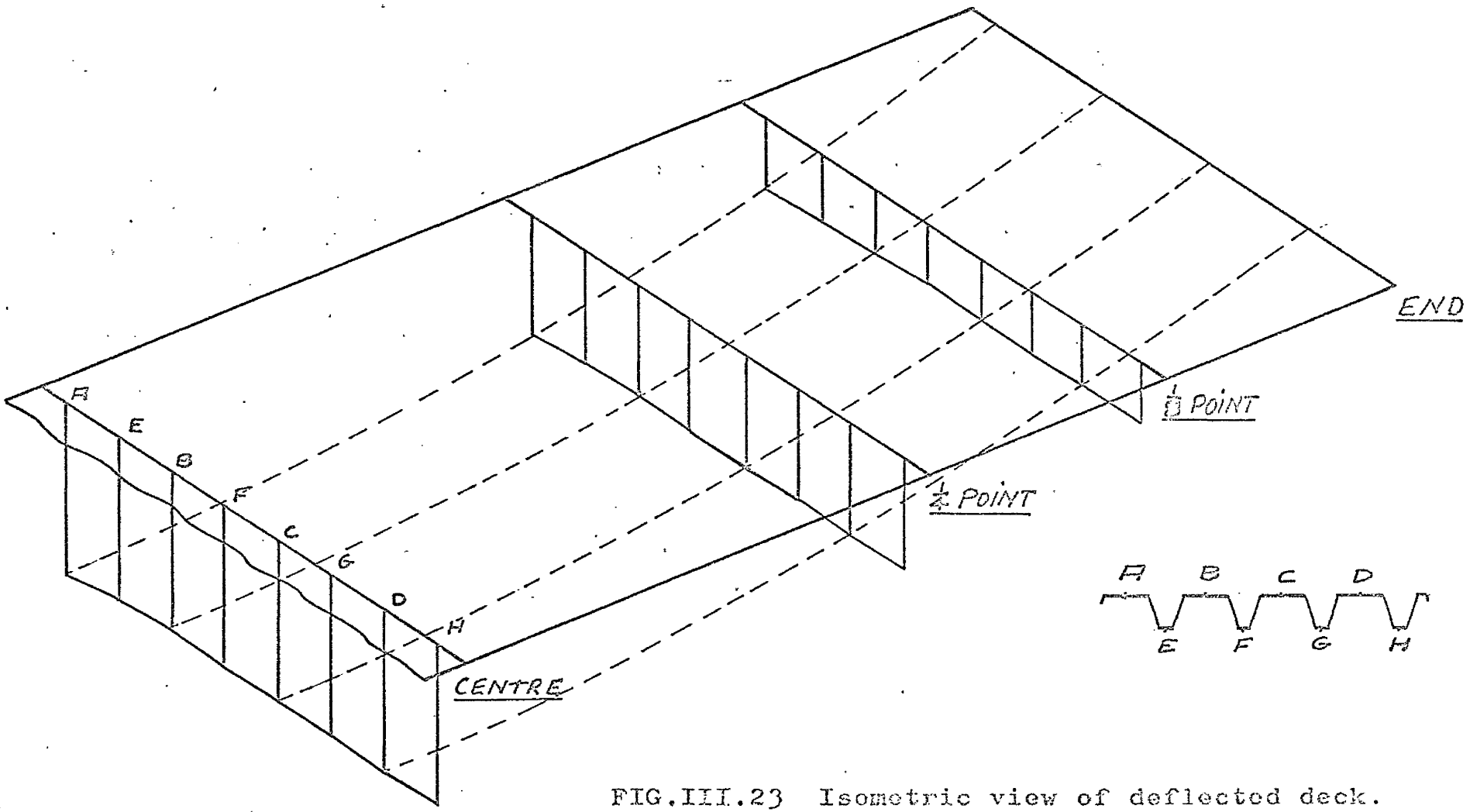

FIG.III.23 Isometric view of deflected deck.
0.048 in. steel - half deck - 0.5 lbf/in^2
DEFLECTION SCALE 1 in. = $\frac{1}{2}$ in. defl.

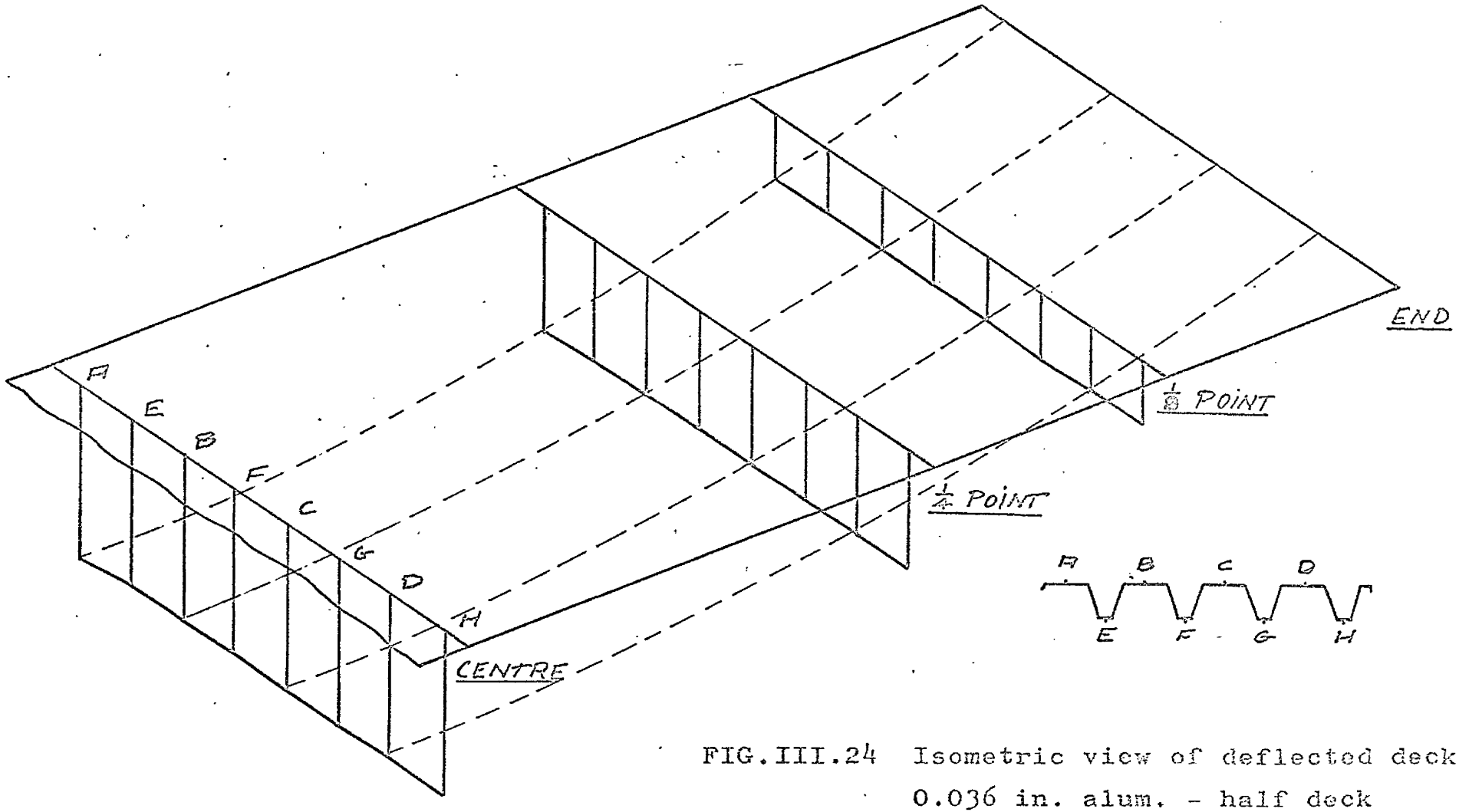

FIG.III.24 Isometric view of deflected deck
0.036 in. alum. - half deck
0.15 lbf/in^2.
DEFLECTION SCALE 1 in. = $\frac{1}{2}$ in. defl

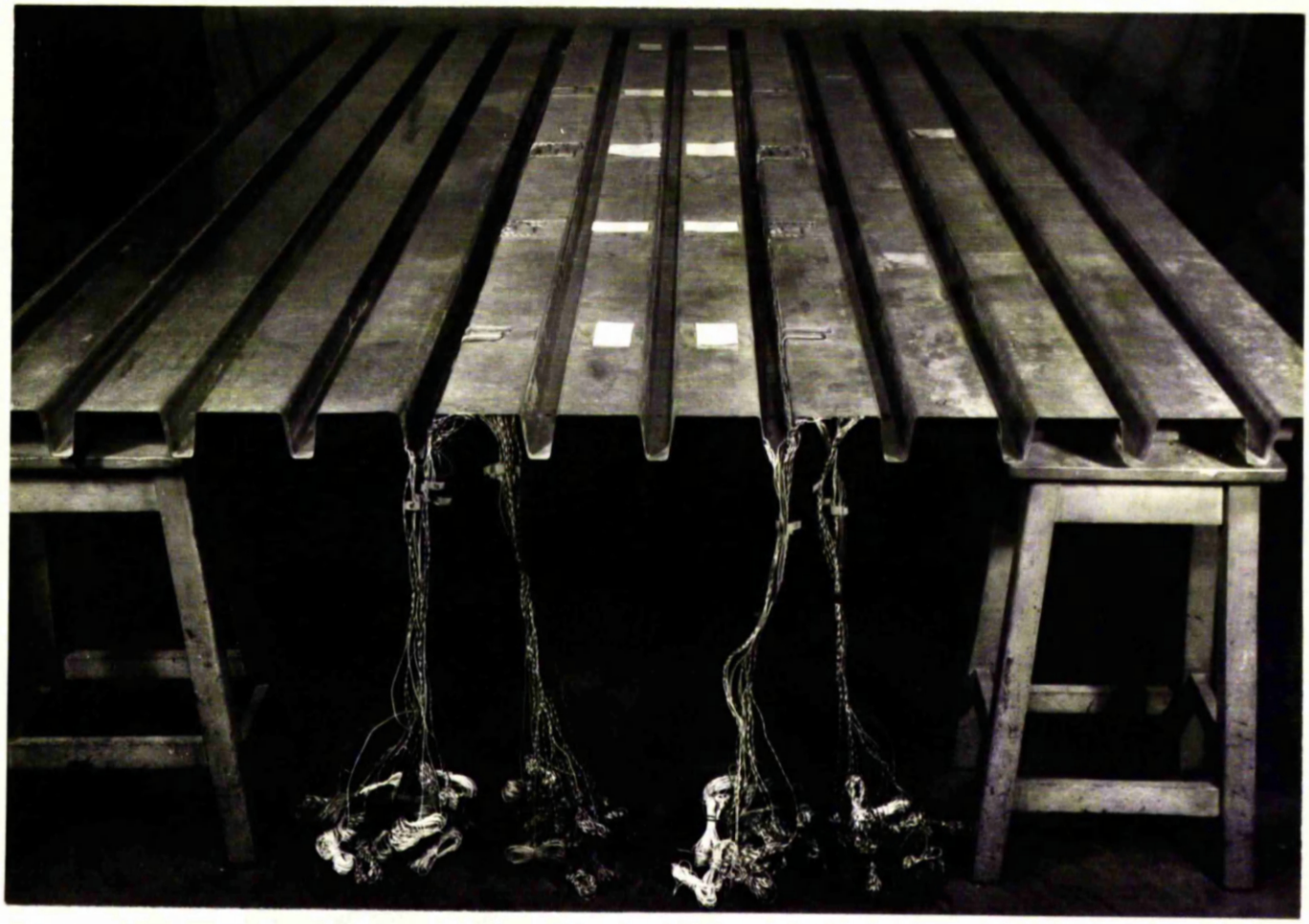

FIG. III.25 Strain Gauge Wiring

0.048 in. thick steel.

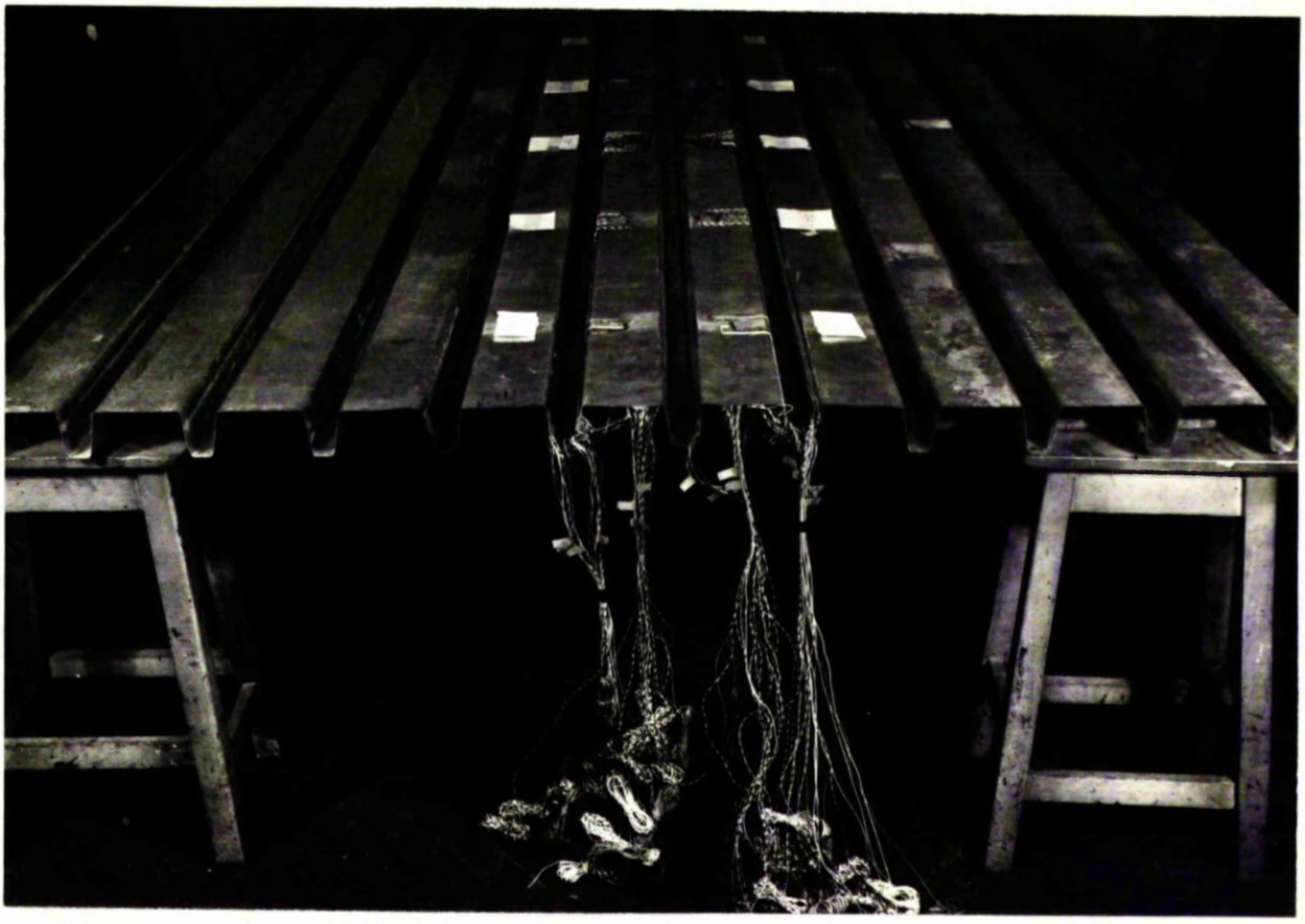

FIG. III.26 Strain Gauge Wiring

0.036 in. thick steel.

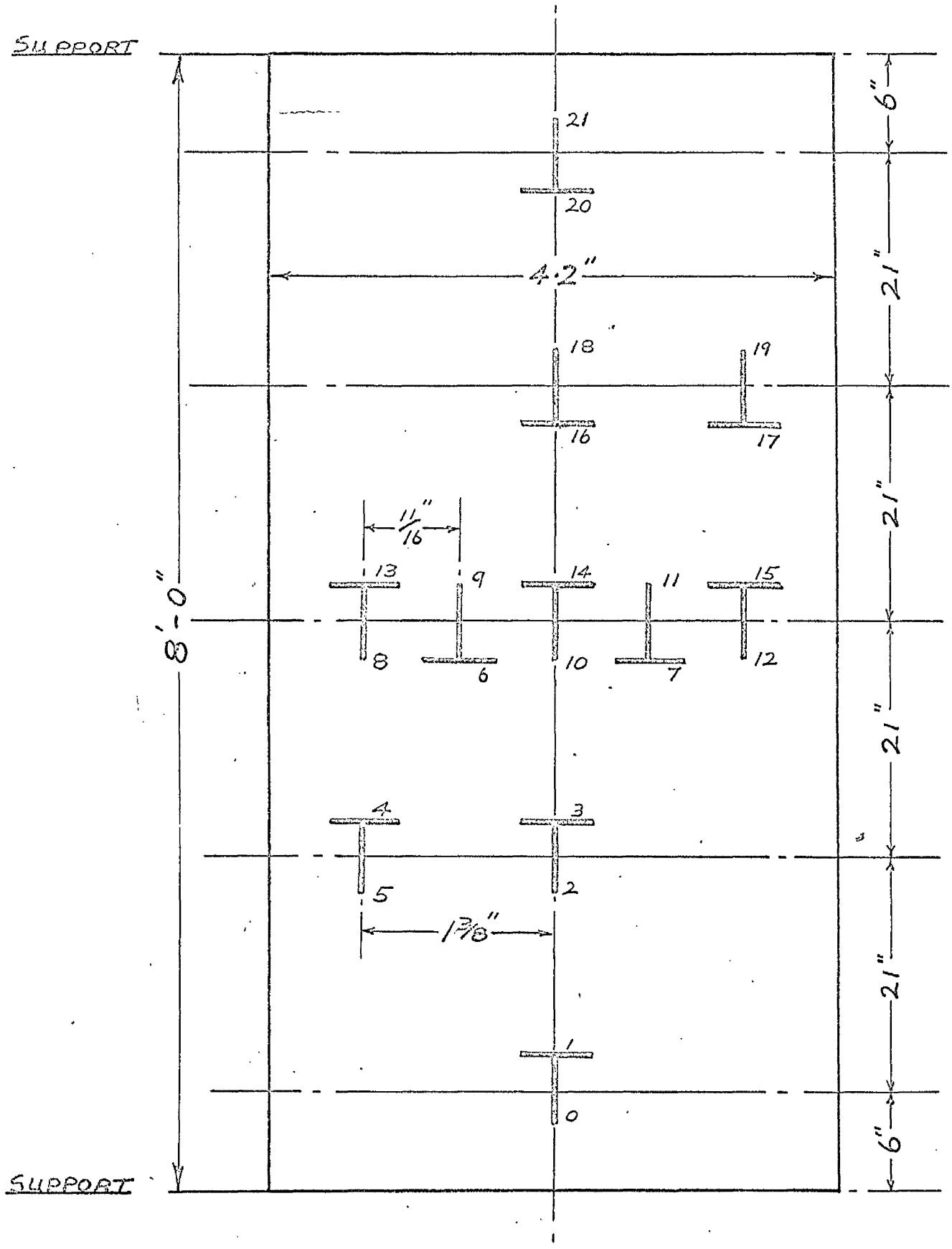

FIG.III.27 Diagrammatic sketch of strain gauge layout on a steel decking trough.

1/2 in. gauges

each material, thickness and profile, eight tests in all. Typical sets of results for 0.048 in. thick steel and 0.036 in. thick aluminium are shown in Fig. III.21 and III.22, a full range of results being given in Appendix VIII.6. An isometric view of the cylindrical surface to which each plate deformed is given in Figs. III.23 and III.24.

To supplement and complete the above investigation, a complete strain gauge examination was carried out for each type of deck. Four decks were strain gauged using $\frac{1}{2}$-inch linear 70 ohm foil strain gauges attached to both surfaces of the larger (compression) flange.

To avoid unnecessary duplication of the labour involved in fixing some 88 gauges per channel the decks were gauged as shown in Fig. III.25 and Fig. III.26 for 0.048in. thick and 0.036 in. thick steel respectively, that is, one deck was used to obtain the strain variation on the two outside troughs of a sheet, the other used for the two inner troughs. A map of the strain gauge layout on the top side of single trough is given in Fig. III.27. An identical and corresponding pattern was used on the/

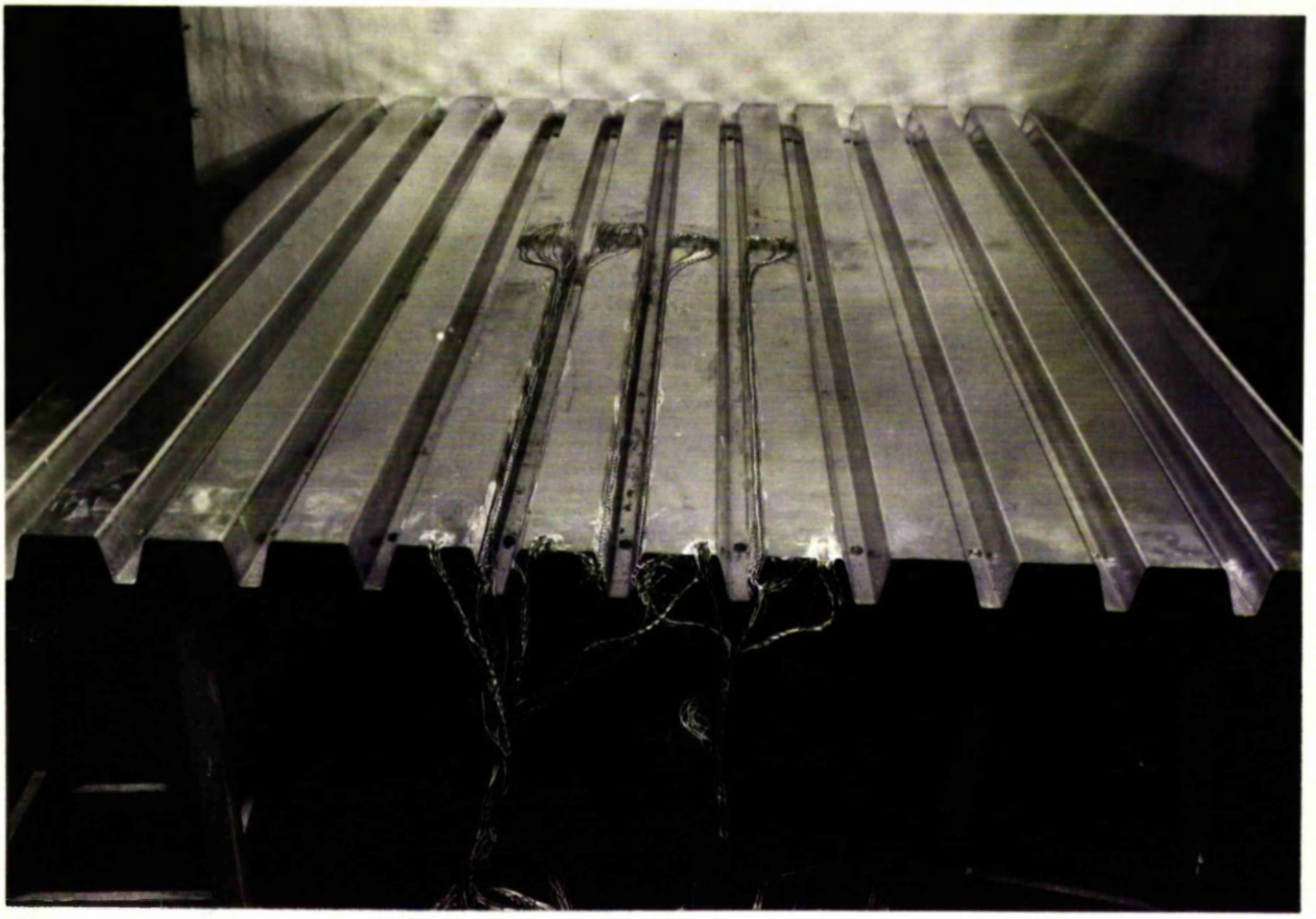

FIG. III.28 Strain Gauge Wiring

Aluminium Decking.

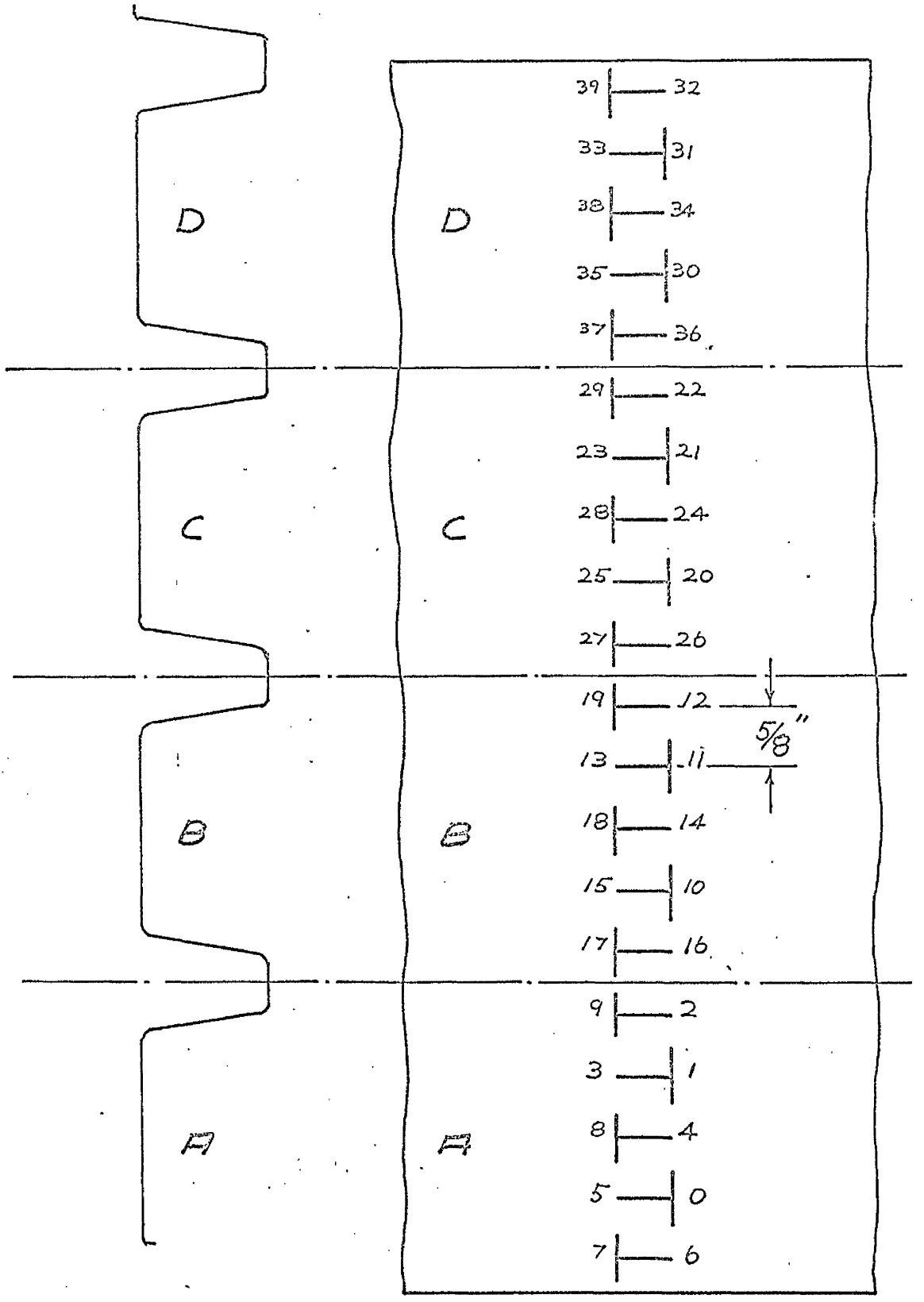

FIG.III.29 Diagrammatic sketch of strain gauge layout on the aluminium decking.

1/2 in. gauges.

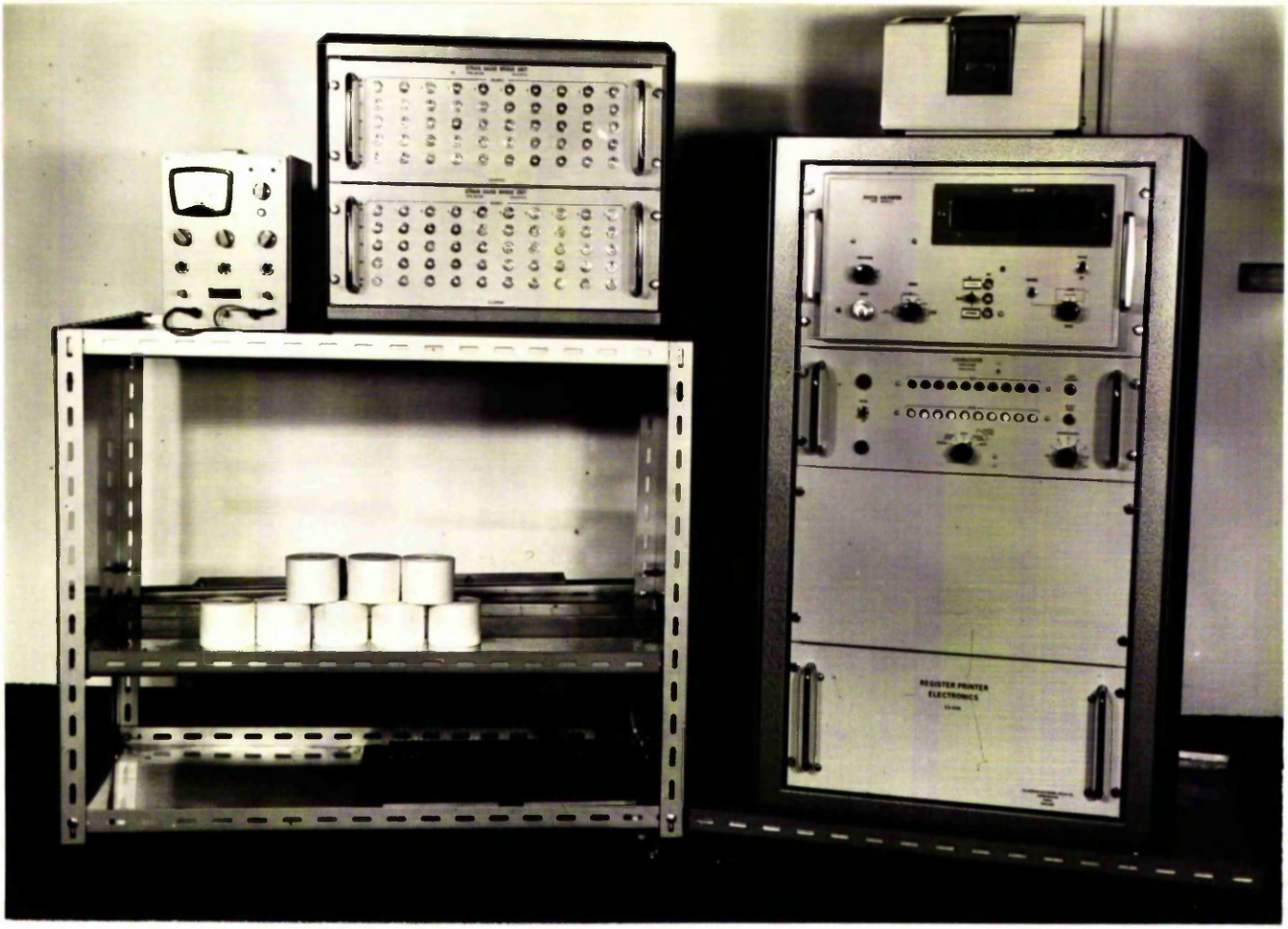

FIG. III.30 Solartron Data Logging Equipment

the underside and the two gauges covering each point wired in series to read direct effects only.

The aluminium alloy decks were used to examine the lateral strain variation across a plate. Fig. III.28 shows an aluminium plate with the strain gauges in position and Fig. III.29 indicates the gauge layout on each trough. Once again the plate was gauged on both sides to obtain direct effects only.

The tests on the strain gauged plates were carried out using a test procedure similar to that adopted for the determination of the deflection distribution. The strain readings were recorded using "Solartron Data Logging Equipment". This equipment which measured voltage changes corresponding to strains on a digital voltmeter and printed out the readings at rates up to 10 channels per second, is shown in Fig III.30. All the strains were measured at each increment of loading in the elastic range, the maximum load being a load just less than that required to initiate yield in the compression flange, and then unloaded in decrements to zero. Two complete tests were performed for each material thickness and profile, making eight tests in all, and/

and in an average test some 700 strain readings were noted.

Figs. III.31, III.32, III.33 and III.34 indicate typical results for the longitudinal strain ϵ_x and the lateral strain ϵ_y for 0.048 in. thick steel and 0.036 in. thick aluminium respectively. A full range of results is given in Appendix VIII.6.

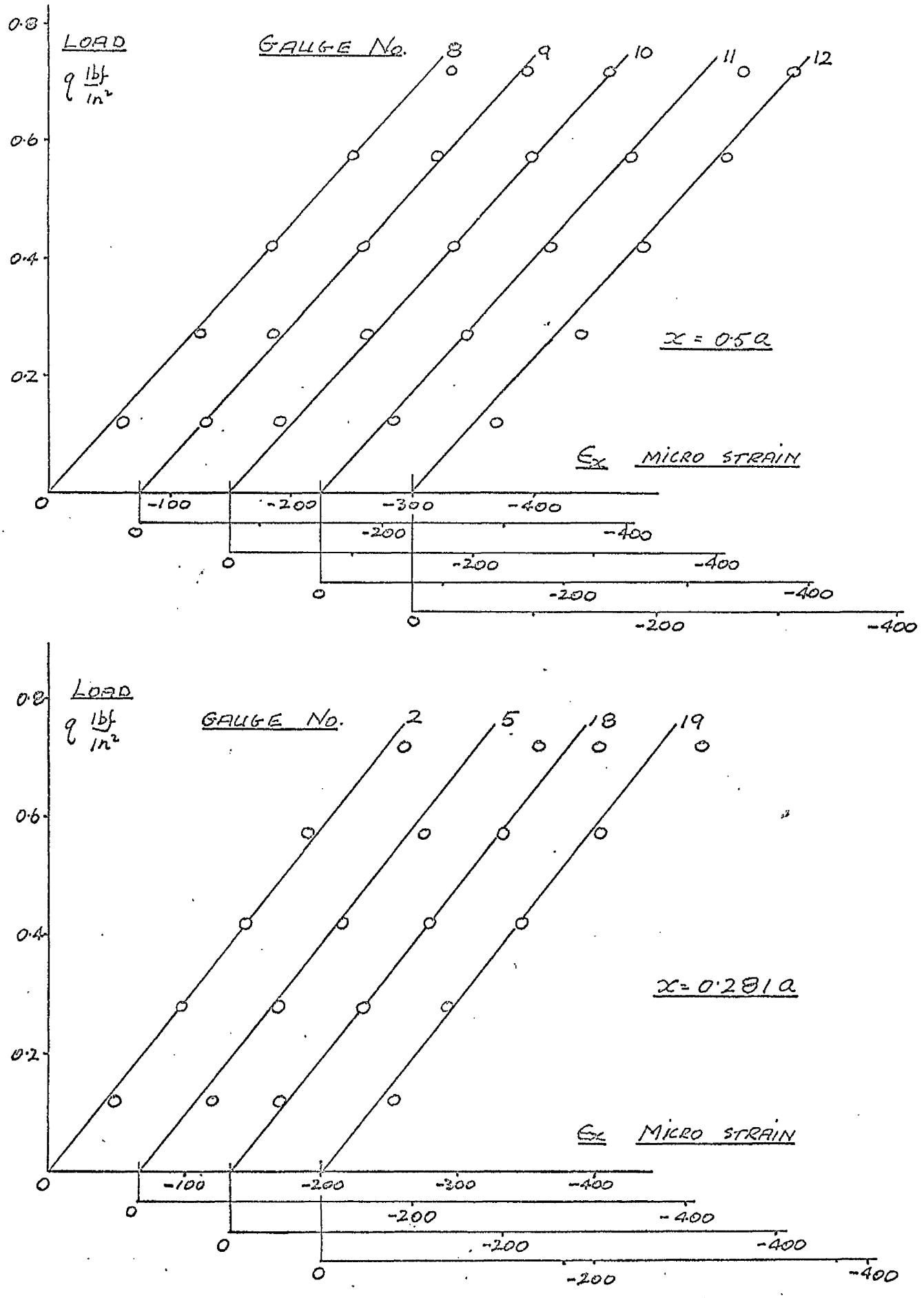

FIG.III.31 Longitudinal strain ε_x for 0.048 in. steel deck . Beam theory indicates strains 99.97% of those from the plate theory indicated.

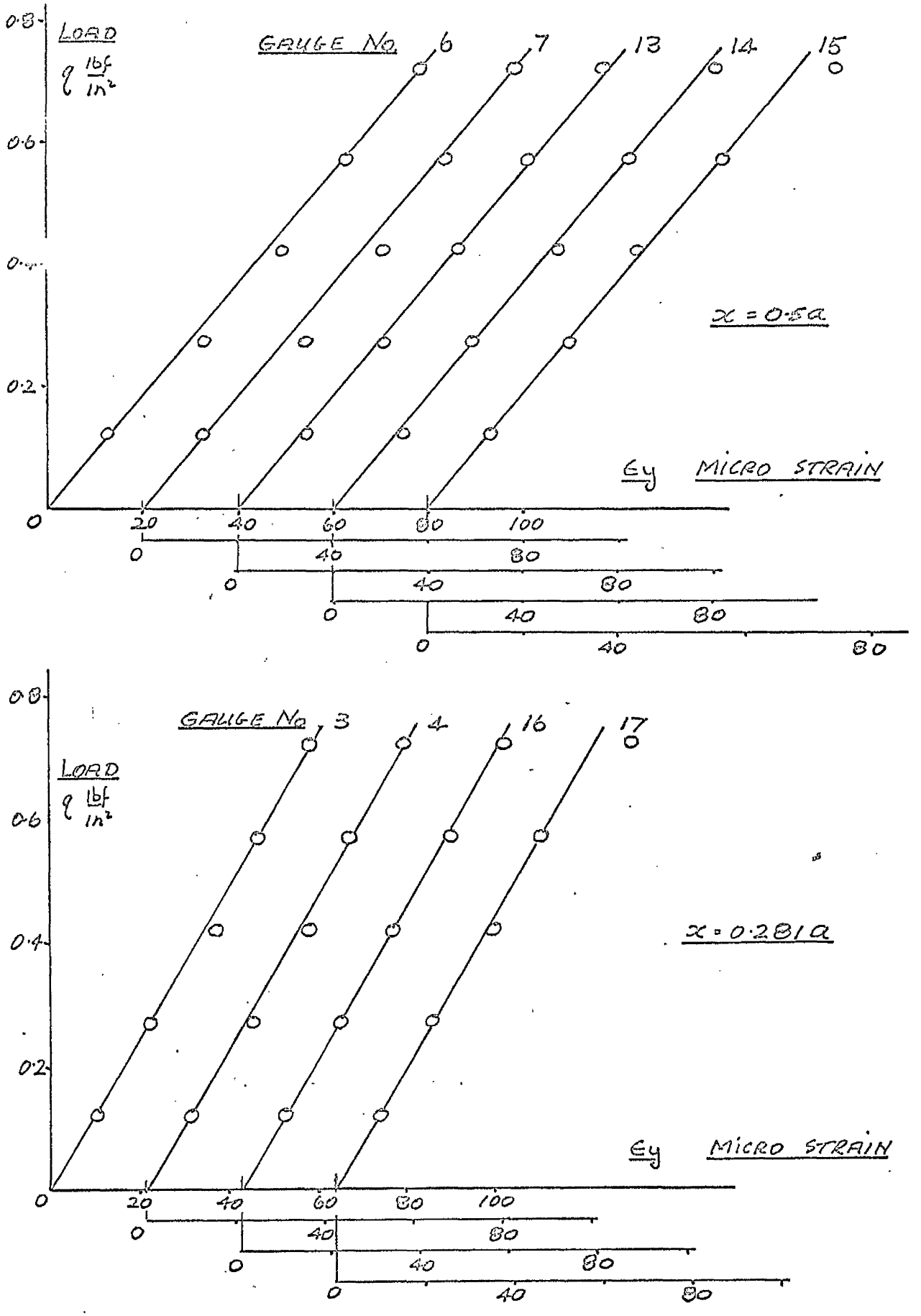

FIG.III.32 Lateral strain ϵ_y for 0.048 in. steel deck.

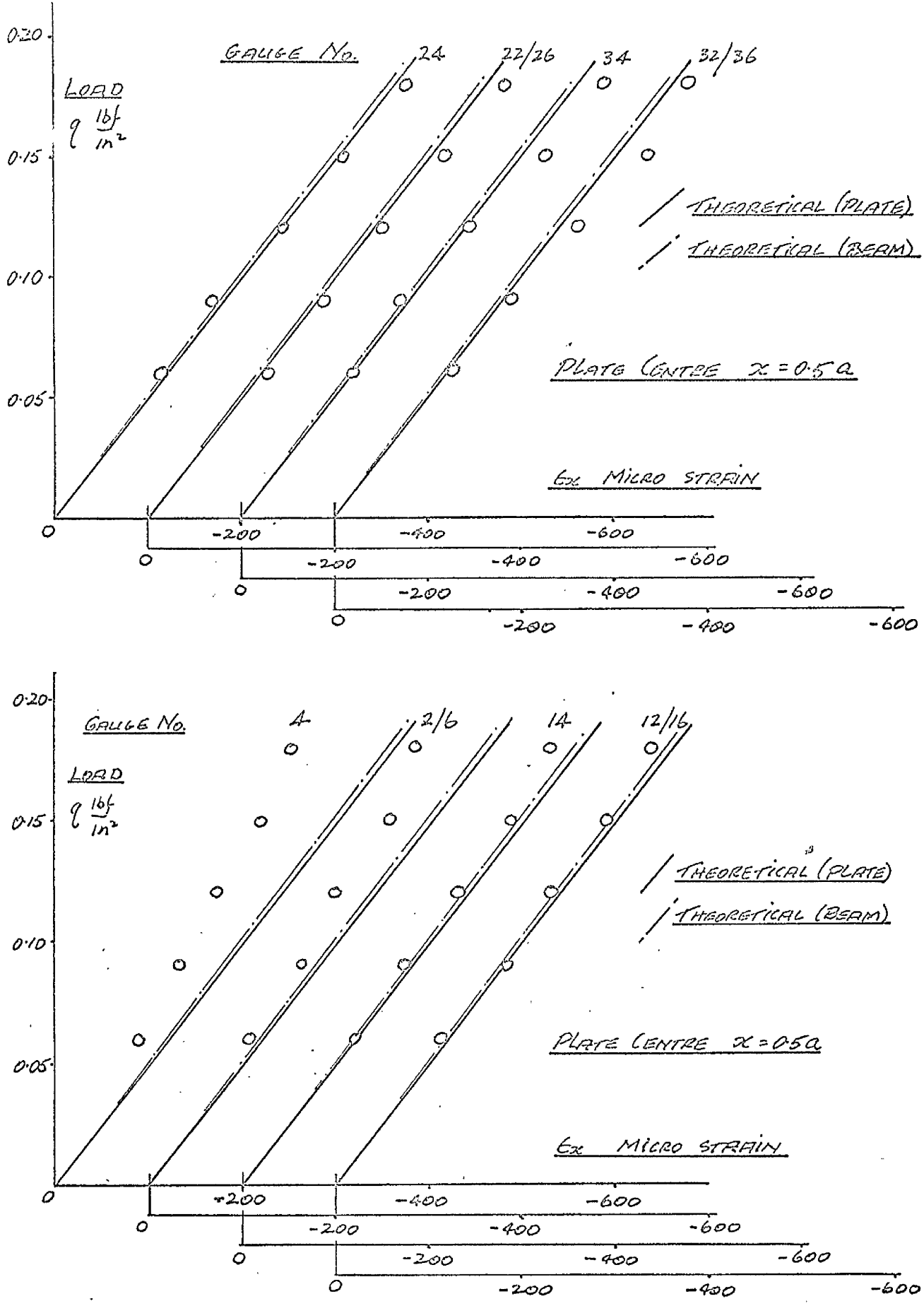

FIG.III.33 Longitudinal strains ϵ_x for 0.036 in. aluminium deck.

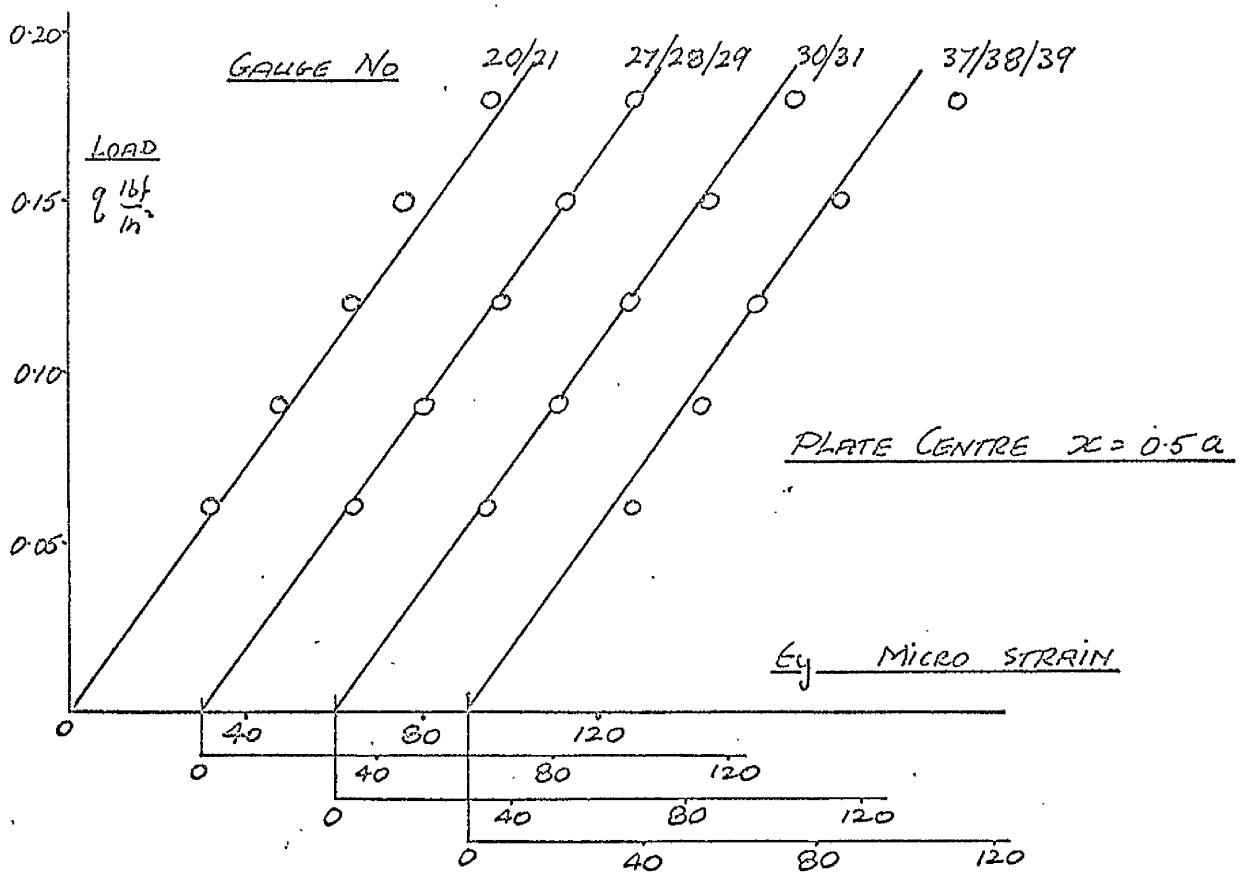

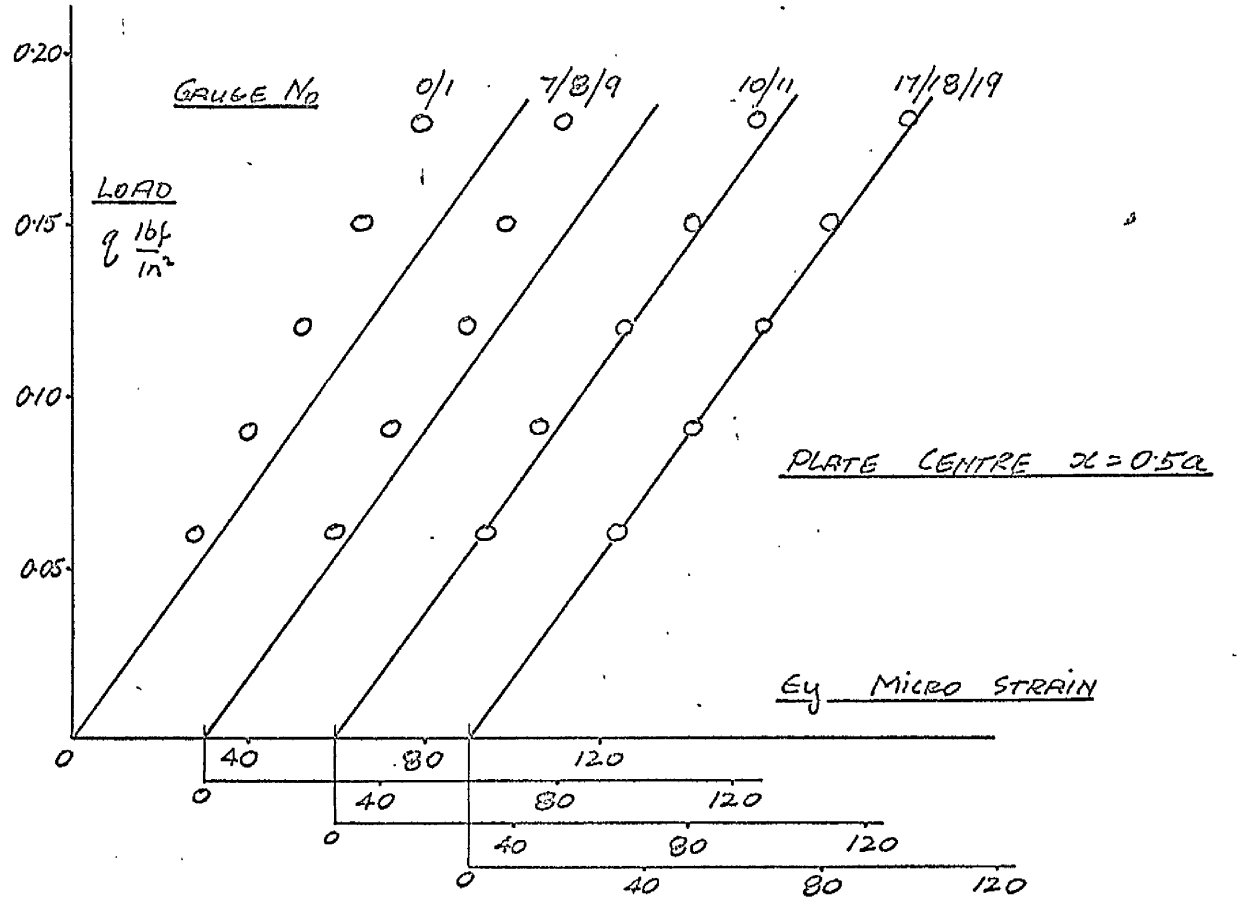

FIG.III.34 Lateral strains ϵ_y for 0.036 in. aluminium deck.

CHAPTER IV

DISCUSSION OF RESULTS

IV.1. THE DETERMINATION OF THE ELASTIC MODULI.

In the bending tests used to determine the elastic moduli a_{22} and a_{66} the deflections relative to that of the central point (9) of all the points (1) to (8) for any given load were read. Appendix VIII.6, however, presents only those actually used to derive the values of the moduli, other deflection readings used to demonstrate symmetry being excluded as they are wholly repetitious. Each of the graphs Fig. VIII.8 to Fig. VIII.13 shows the experimentally measured values as points and the solid line represents that calculated from the experimental points by the method of least squares.

The calculation of a_{22} is carried out in detail in Appendix VIII.4 and the method can be summarised as follows for a 0.048 in. thick steel plate, the behaviour of which in this test is typified by Fig. III.4.

From equation (II.3.2) and considering the loading arrangement described in Chapter III the modulus a_{22} is given by

$$a_{22} = \frac{7.w.h^3}{36.P.y^2} \quad in^2/lbf$$

Constant / Plate	a_{11} in^2/lbf.	a_{22} in^2/lbf.	a_{66} in^2/lbf.
0.048" steel	$0.41827 \times 10^{-6} I_{//}$	$455.61 \times 10^{-6} h^3$	$337.24 \times 10^{-6} h^3$
0.036" steel	$0.54136 \times 10^{-6} I_{//}$	$1292.0 \times 10^{-6} h^3$	$635.24 \times 10^{-6} h^3$
0.048" alum.	$1.4055 \times 10^{-6} I_{//}$	$1077.0 \times 10^{-6} h^3$	$1182.7 \times 10^{-6} h^3$
0.036" alum.	$1.8854 \times 10^{-6} I_{//}$	$3003.1 \times 10^{-6} h^3$	$2233.5 \times 10^{-6} h^3$

TABLE IV.1 - The Plate Moduli

where w is the average deflection of the points (1) and (5) for increasing values of load P.

From Fig. III.4 the average value of is 11.855 lbf/in. and from Fig. III.2 $y = 6$ in.

$$\therefore \underline{a_{22} = 455.61 \times 10^{-6} h^3 \text{ in}^2/\text{lbf}}$$

A complete range of values is given in Table IV.1.

As a general statement it can be said that the stiffer the plate the more consistent is the test for a_{22}. The bending tests for the aluminium plates were in fact performed many times to obtain consistency, this being necessitated by the difficulty experienced in keeping the plates stable on the ball bearings. However, it can be concluded that the test was satisfactory and did give results which repeated to within 2% of the mean.

In the twisting tests for a_{66} the main difficulty lay in making sure that the specimen was at all times level. As for the test for a_{22} the deflections of points other than those actually used to derive the modulus were examined to check that the measured values of deflections were consistent and/

and obtained when the plate was in a stable position.

The calculation of a_{66} is carried out in detail in Appendix VIII.4 but 0.048 in. thick steel can be summarised as:

The co-ordinate system used is that given in Fig. III.9 where the points (2), (4), (6) and (8) have the co-ordinates (-x, y), (x, y), (x, -y) and (-x, -y) respectively.

From equation (II.3.2)

$$a_{66} = \frac{7.\,w.\,h^3}{36.\,P.\,xy}$$

where w is the mean of the deflections of the points (2), (4), (6) and (8) with respect to (9) for an increment of loading P .

From Fig. III.11 for 0.048 in. thick steel $\left(\frac{P}{w}\right)$ = 16.016 lbf/in.

$$\therefore \underline{a_{66} = 337.24 \times 10^{-6} h^3} \text{ in}^2/\text{lbf}$$

A complete range of values is given in Table IV.1.

In this series of tests, the maximum variation from the mean was again of the order of 2%.

The use of ball bearings to simulate point/

point support in both the above tests proved highly satisfactory as did the use of the micrometer stick to measure deflections from a fixed datum on the floor.

For the determination of a_{11} the tests involved the mapping of the deflected form of a single trough bending under constant moment. The value of deflection was read at selected points along the trough length firstly to obtain a contour and secondly to permit the determination of relative deflections and so minimize the effect of any movement at the supports. In Appendix VIII.4 the calculation of the modulus a_{11} is carried out in full, assuming that the anticlastic deformation is negligible. That this is tenable is shown in Appendix VIII.3 where the magnitude of the distortion to an anticlastic surface of an orthotropic plate bent by a constant moment is demonstrated to be negligible for the stiffness values of the plates considered in this thesis. In consequence the constants are evaluated from the values of deflection along the central line of a beam. This can be summarised as follows, a complete analysis being given in Appendix VIII.4.

Considering a beam bending under a pure moment/

moment M.

$$E_{\parallel} I_{\parallel} = \frac{M d^2}{2w}$$

and $M = P.x$

where w is the deflection relative to the centre of the beam of two points on the centre line of the beam a distance $2d$ apart. P is the load applied and is considered to be acting at a distance x from the supports - Fig. III.15.

From Fig. III.16 for 0.048 in. thick steel the average value of (P/w) is (1/0.42162) lbf/in. and d = 24 in.

Therefore from equation (II.3.3):

$$a_{\parallel} = 1/E_{\parallel} = \underline{0.41827 \times 10^{-7} I_{\parallel}} \text{ in}^2/\text{lbf}.$$

A full range of results is given in Table IV.1. As before, the maximum variation from the mean of a series of tests was of the order of 2%.

It is appropriate at this point to state the relevant effects that were noted during the performance of the tests for $a_{\parallel}$. As has already been stated, the single troughs when bent with the brackets removed exhibited no splaying at any section along the test length. Nor was there any difference/

difference between the deflected form on the compression flange of the trough and that along the trough lip. At all points throughout the loading range the deflected form was that of a shallow circular arc and attempts to detect a variation of deflection across the trough revealed a complete absence of any such effect. This substantiates the assumption that $a_{12} = a_{21}$. A full discussion on the background relevant to this assumption is given in Appendix VIII.3.

IV.2. THE BEHAVIOUR OF DECKING.

The testing and examination of the behaviour under lateral loading of large scale decking units of the dimensions used in the tests described in Chapter III constitute many problems, not the least of which is the simulation of a uniformly distributed load. The method described in Chapter III provides an excellent method of testing and control. With the use of a high pressure air source, an air control valve, a small degree of constant leakage from the system and a water manometer fitted on the low pressure side of the system the loading can be kept constant to $\pm$ 1/16 in. of head of water which corresponds to a pressure fluctuation of $\pm$ 0.00225 lbf/in^2 .

The deflection readings were taken with one and two inch travel dial gauges calibrated to read in divisions of 0.0005 in. In the graphs of Fig. III.21 and Fig. III.22 the points shown represent the average value of several tests, this averaging process being carried out to eliminate local fluctuations in the level of the travelling beam. Great care was taken to ensure that there was no movement of the travelling beam during the reading of the dial gauges, the averaging process being used to take care of small discrepancies. The solid and broken lines represent the theoretical deflected forms computed from equation (II.5.12) the constants etc. having been calculated from equations (II.5.14). The solid line represents the theoretical deflected form computed on the basis of a continuous plate, i.e. the aspect ratio $(a/b) = 4/3$ while the broken line represents that computed on the consideration of the plate as a series of linked beams each with aspect ratio $(a/b) = 16$. The difference between the two theories in all cases is not more than 4%, i.e. for the stiffness ratios and loading conditions obtaining the decks may be reasonably considered on the basis of a linked beam concept. Good agreement is shown, the/

the deviation at the top of the loading range being due to the initiation of elastic buckling.

Deflection readings were taken from all the troughs across the total width of 6 feet and for all the complete troughs there was no detectable difference in the deflected form, which agrees with the theoretical prediction of uniform deflection across the plate. Figs. III.23 and III.24 indicate the cylindrical surface to which the plates deform, the values shown being a complete justification of the sine transform for the longitudinal deflected form.

Typical results of the strain investigations are given in Figs. III.31 to Fig. III.34.

For the variation of $\epsilon_x = z \frac{\partial^2 w}{\partial x^2}$ the strain in the longitudinal direction, the agreement between the experimental and theoretical is good. However, as the loading approaches that corresponding to the limit stress of the material there is a tendency for the experimental values of ϵ_x to be greater than those predicted theoretically from the second derivative with respect to x of equation (II.5.12). Figs. III.31 and II.32 show the strain values for two sections/

sections along a typical trough of the steel decks. It is to be noted that a comparison of corresponding strain values in troughs forming the one deck do not show a significant variation in the values of ϵ_x and ϵ_y . It can be concluded from this that the overlapping arrangements in the steel decks provided an adequate support and in effect provided a support for the compression flange equivalent to that of a continuous section. Further, the results again demonstrate the validity of the linked beam approach.

This was not the case for the aluminium decking, however, and Figs. III.33 show the variation of the longitudinal strain ϵ_x in the 0.036 in. thick aluminium alloy decks. For the troughs C and D (Fig. III.29) the values of ϵ_x agree with those theoretically predicted, the theoretical prediction on the basis of a plate as against that of a beam being some 3.0% higher. For the troughs A and B indicated by the gauges 4, 2/6 and 14, 12/16 respectively the longitudinal strain drops to a value averaging 91% and 73% of the theoretical prediction. This can be attributed solely to the overlapping support condition at the end of the flange A, which, it appears/

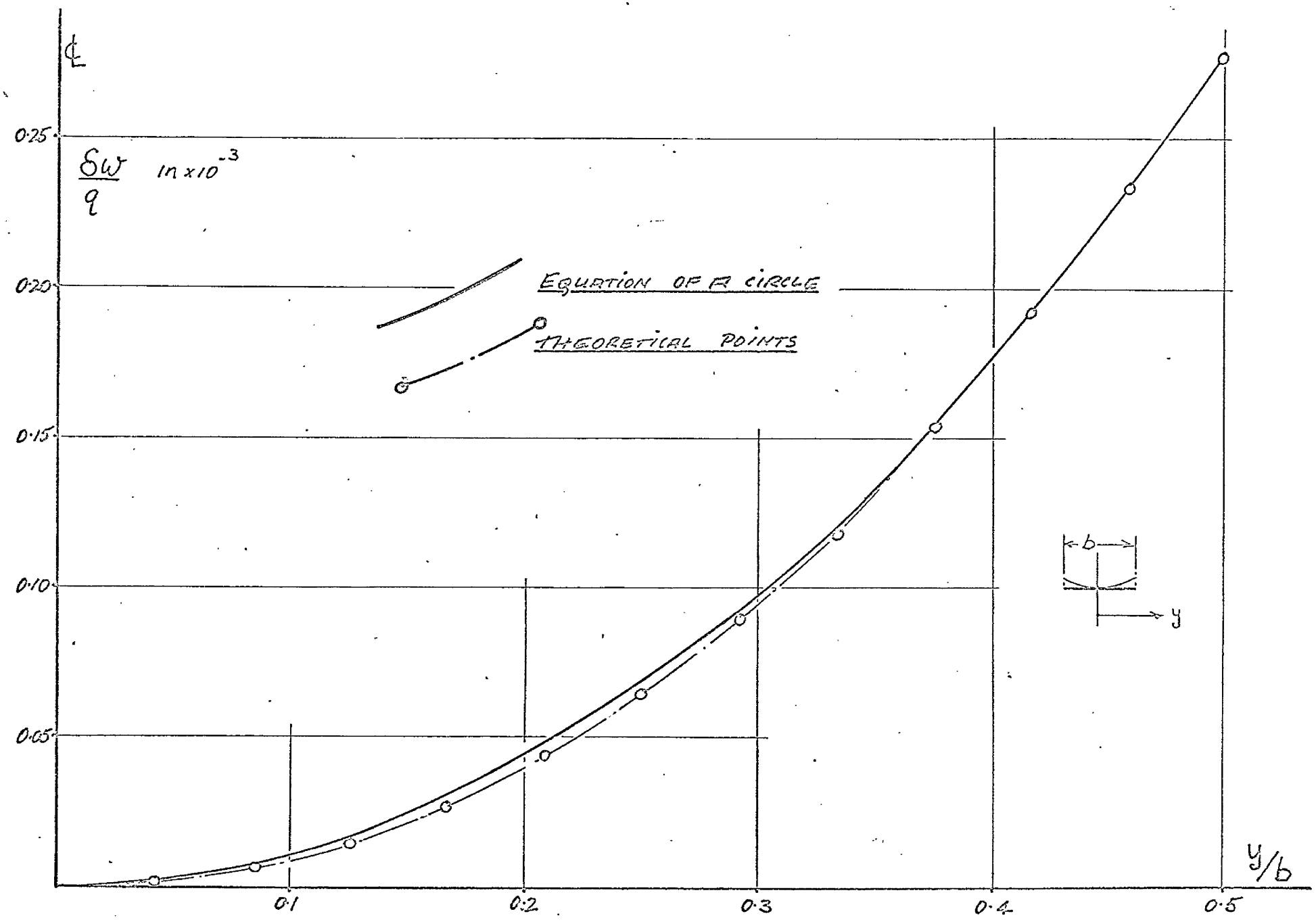

FIG.IV.1 Theoretical transverse deflected form for a single trough of 0·048 in. steel deck compared with the equation of a circle.

appears, did not give the required continuity to the plate.

As explained in Appendix VIII.5, the theoretical evaluation of the lateral strain set a number of problems which did mean laborious computational work for which the Ferranti Sirius computer was not suitable. In order to carry out the calculation of the transverse strain in a quick and effective manner, the following technique was used.

Considering each plate as a series of beams (i.e. $(a/b) = 16$) the deflected form across the trough was computed. On plotting the values obtained, it was found that they gave to a remarkable accuracy the form of a circular arc. This arc is plotted in Fig. IV.1 for 0.048 in. thick steel and in Appendix VIII.6 for each of the four types of deck considered.

For all points across a beam, therefore, the theoretical deflection δw relative to the central point of the trough was known and thus the radius of curvature of the corresponding circular arc calculated. Using the customary assumption that $1/\rho = \partial^2 w/\partial y^2$ in the transverse direction, the transverse strain can be predicted.

This was the method used to compute the theoretical strain distribution indicated by the solid lines in Figs. III.32 and III.34.

Figs. III.32 give the lateral strain distribution for a trough of 0.048 in. thick steel decking at two sections along the plate length a . The first point about the experimental values is that they indicate that the values of lateral strain across a typical trough is almost constant for a given value of loading and that the variation is linear. This is in complete agreement with the deflected for, of a circular arc obtained theoretically. Such variation as does obtain is consistent with Fig. IV.1 namely, the strain values away from the compression flange centre correspond with greater accuracy to those obtained from the circular arc concept. This effect is small and can only be observed over a large number of readings.

Figs. III.34 display the variation of the lateral strain ϵ_y for the 0.036 in. thick aluminium decks. As with the readings of longitudinal strain ϵ_x there is a lower value in the flange A, in this case gauges 0 and 1 gave values of ϵ_y which were/

were 65% of the theoretical for 0.048 in. thick aluminium. An interesting point is that the strain readings ϵ_y on the flange B were not diminished to quite the same extent as those of ϵ_x the reason probably being that the edges of the flange B provide more adequate support for lateral variation than for longitudinal variation whatever the support conditions of the flange A.

A basic assumption of the theoretical treatment is that of the linearity of the orthotropic plate material. It is notable that the specimens of orthotropic plate manufactured from cold formed aluminium sheet - a material which is non linear in the elastic range - do in fact exhibit this linearity in both the tests for the determination of the elastic moduli and those investigating the plate behaviour under lateral loading.

CHAPTER V

DESIGN CONSIDERATIONS

The preceding chapters of this thesis have been concerned with the determination of the elastic behaviour of decking under uniform lateral loading utilising orthotropic plate analysis. This analysis has shown that decks with the stiffness ratios of the order considered may, for the above stated loading conditions, be considered as a series of linked beams. Thus, when the problem of designing such decks is faced, a beam analysis can be considered to be appropriate. The purpose of this chapter is to demonstrate that the effective width concept as laid out Addendum No. 1 (1961) to B.S. 449, 1959, "The Use of Structural Steel in Building" is appropriate to the prediction of the uniform transverse loading for deck units manufactured from cold formed light gauge metal.

The compression flange of a thin walled beam bent in a plane perpendicular to the flange can be considered as subjected to a uniform compressirve stress and behaves in substantially the same manner as the plate element of a uniformly compressed strut. Such an element may fail due to local buckling at a stress below the yield or proof stress of the material.

V.1. THE MAXIMUM STRENGTH OF COMPRESSED PLATES IN LOCAL BUCKLING.

The critical longitudinal compressive stress which initiates local elastic buckling in concentrically loaded flat plates, or struts of thin walled section consisting of flat plate elements is given by

$$\sigma_c = \frac{\bar{K}\pi^2 E}{12(1-\nu^2)}\left(\frac{t}{b}\right)^2 \qquad (V.1.1)$$

in which E is the Young's Modulus, ν is the Poisson's Ratio, b is the width of the plate, t is the wall thickness and $\bar{K}$ is a numerical constant depending primarily on the longitudinal edge support conditions of the plate element.

Values of $\bar{K}$ have been obtained by a number of investigators - STOWELL, HEIMERL, LIBOVE and LUNDQUIST (1952), CHILVER (1951, 1953 (a)) and HARVEY (1953) - for a variety of edge support conditions.

Initial elastic buckling does not imply complete collapse, and it has been shown - CHILVER (1953 (b)) - that the average compressive stress at maximum load carrying capacity, σ_m , may be considerably greater than σ_c . The relevant/

relevant parameters are (σ_m/σ_y) and (σ_c/σ_y) where σ_y is the yield or proof stress of the material.

CHILVER (1953 (b)) has demonstrated that it is convenient to define σ_m in the form

$$\frac{\sigma_m}{\sigma_y} = F\sqrt{\left(\frac{\sigma_y}{\sigma_c}\right)} \qquad (V.1.2)$$

The coefficient F is determined by experiment and values for both steel and aluminium alloy have been obtained by Harvey and Chilver from tests on struts of these materials. The values of F define the average strength in compression and a conservative value of F for both steel and aluminium alloy was given by KENEDI, CHILVER, GRIFFIN and SHEARER SMITH (1960) as

$$\frac{\sigma_m}{\sigma_y} = 0.66\left(\frac{\sigma_c}{\sigma_y}\right)^{\frac{1}{3}} \qquad (V.1.3)$$

The plate components considered herein are the compression flanges of the decking units described in Chapter III and it is considered that in this case each plate component is adequately supported along the longitudinal edges. A value of $\bar{K} = 4$ is taken corresponding to a plate simply supported along both edges. σ_m can now be obtained from equations (V.1.1) and (V.1.3) by incorporating the/

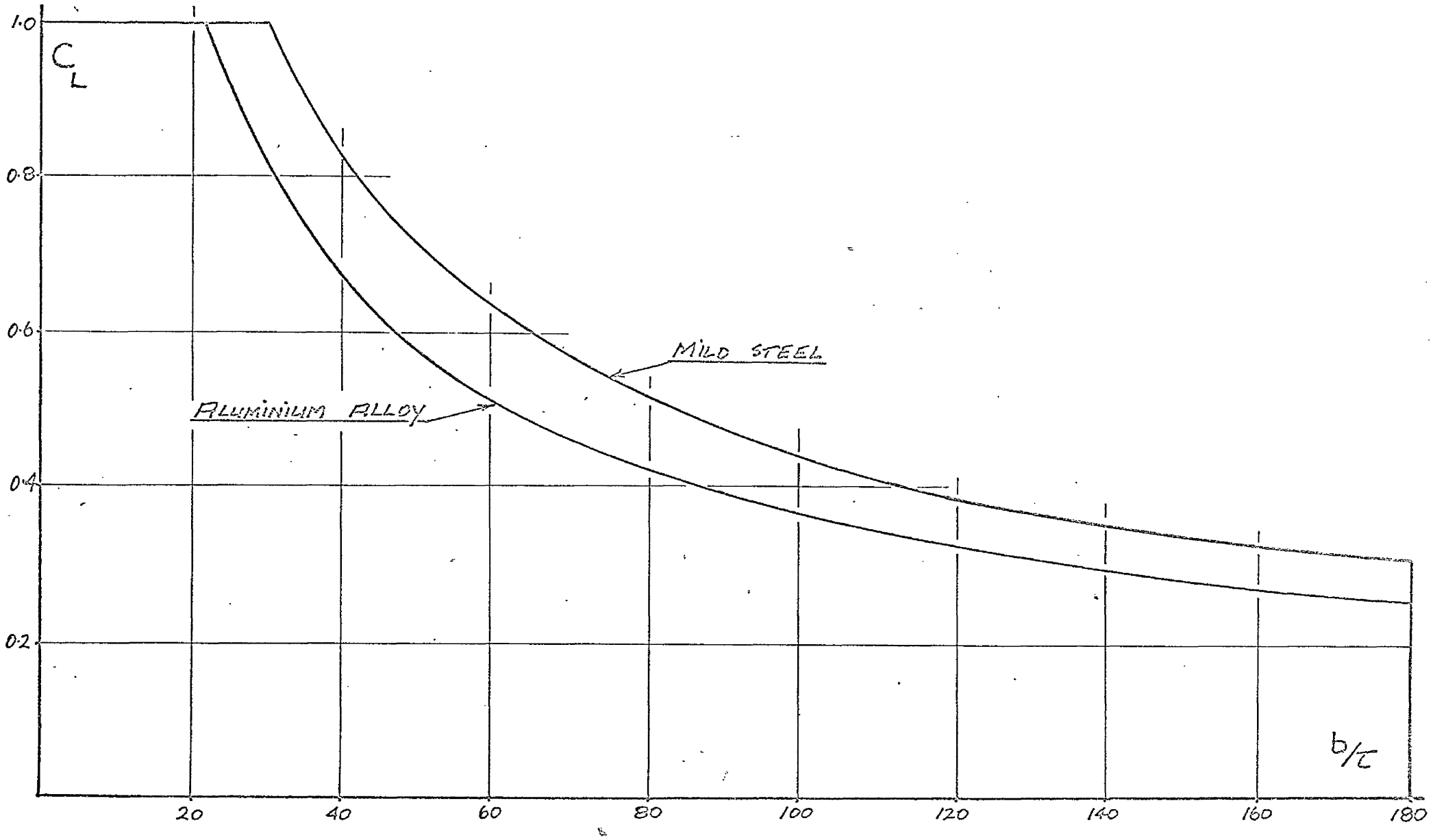

FIG.V.1 Local Plate Stress Factor C_L for steel and aluminium decking.

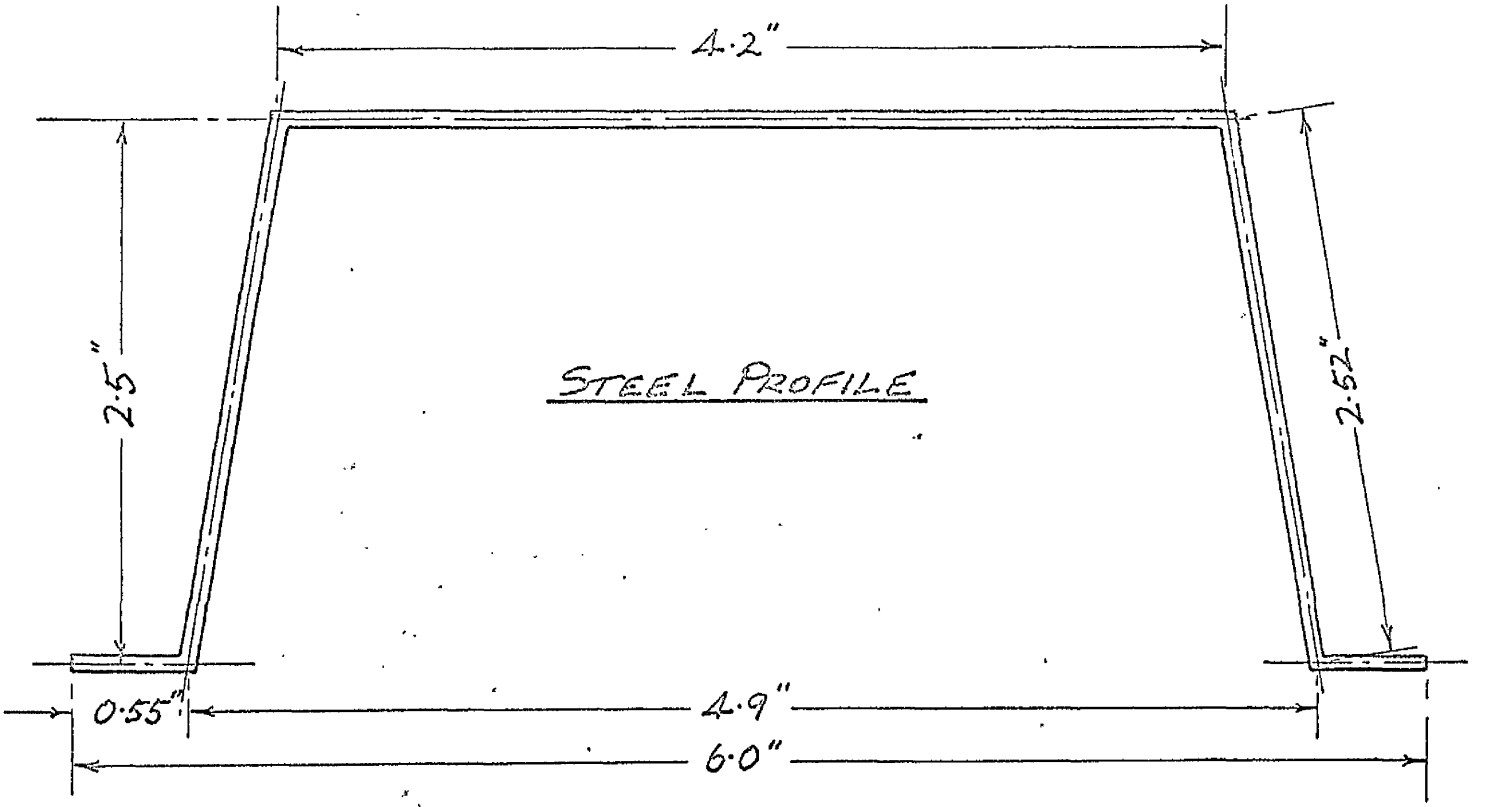

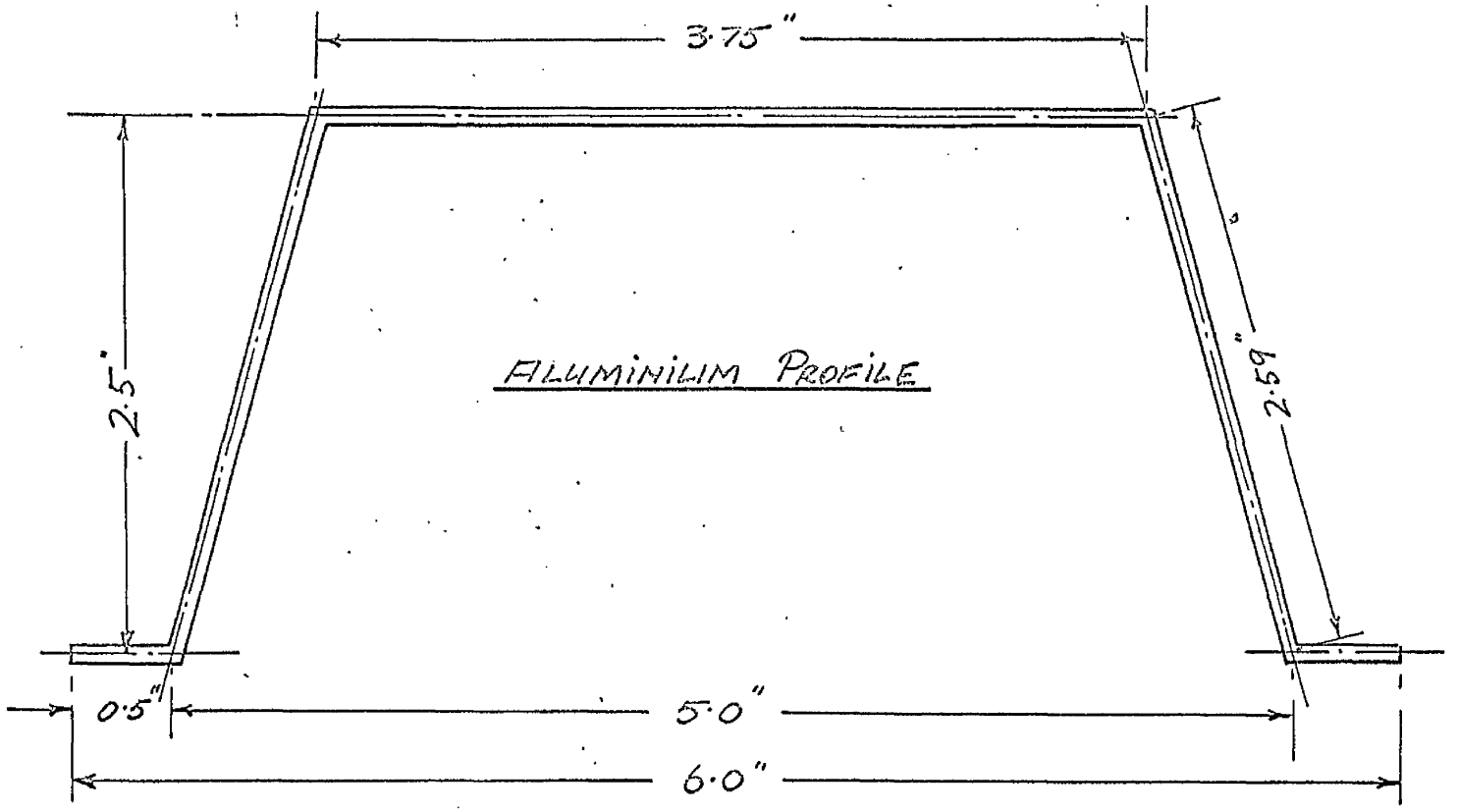

FIG.V.2 Strut cross-sections.

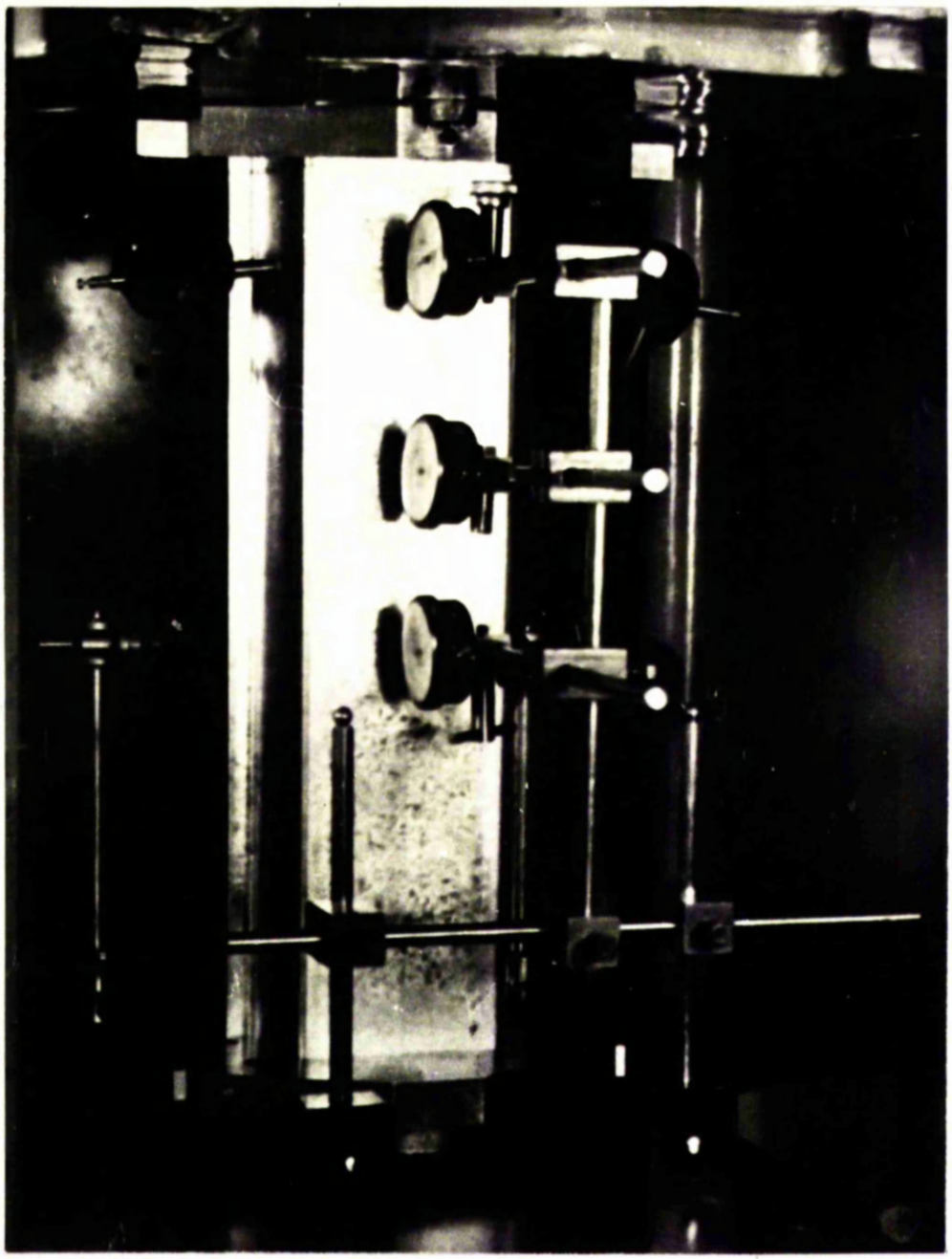

FIG. V.3 Dial Gauges measuring Flange Deflection

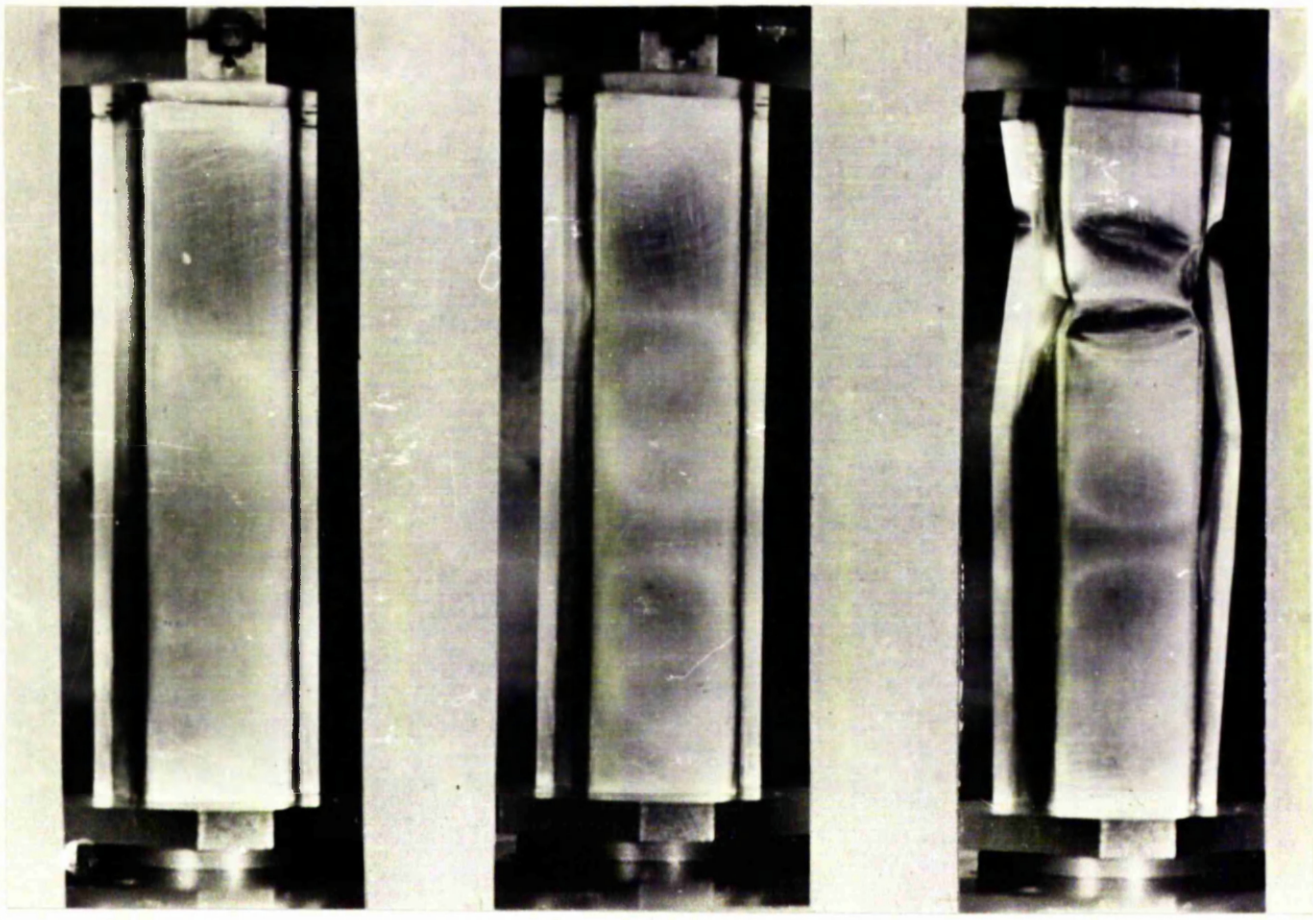

(a) (b) (c)

FIG. V.4 0.048 in. thick steel specimen under a load of:

(a) 1 tonf.

(b) 5 tonf.

(c) Collapse at 6.6 tonf.

the appropriate material constants. The σ_m values can be written in the form of "local plate stress factors" C_L where $C_L = (\sigma_m/\sigma_y)$ and these are shown in Fig. V.1.

V.2. THE EXPERIMENTAL EVALUATION OF THE CRITICAL LOAD.

A series of strut tests were carried out to investigate the validity of equation (V.1.3) for the compression flange width to thickness ratios of typical deck sections. The cross-sections of the struts tested are shown in Fig. V.2, and to ensure local buckling the overall length was limited to 18 in. Specimen thicknesses were 0.036 in. and 0.048 in. and the materials were those described in Chapter III for the large scale decking tests.

The ends of the strut were simply supported and lateral deflections of the flange were recorded using dial gauges as shown in Fig. V.3. The behaviour of a typical specimen as the load increased is shown in Fig. V.4.

An experimental critical load was obtained from a plot of compressive load against lateral/

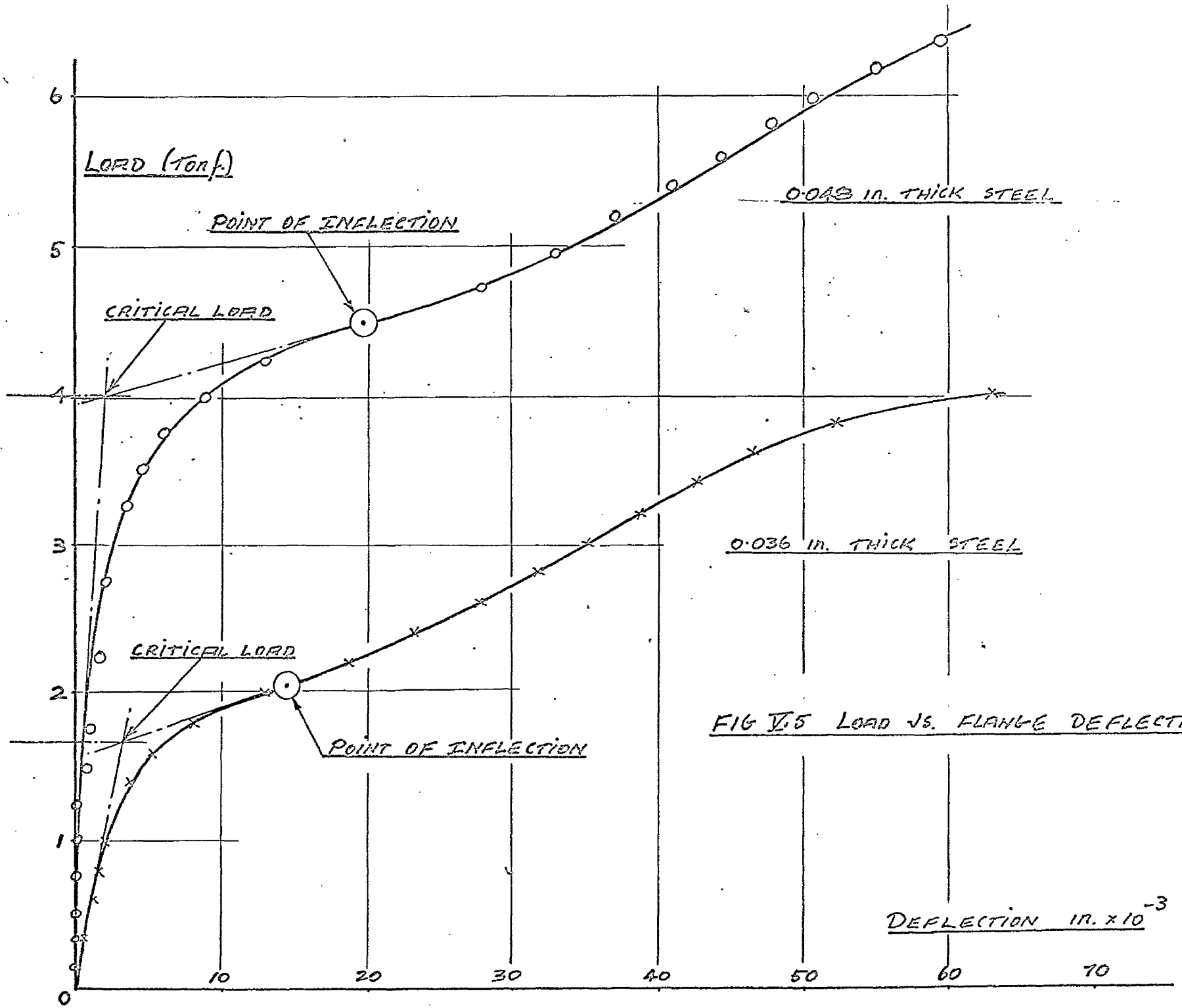

FIG V.5 LOAD VS. FLANGE DEFLECTION

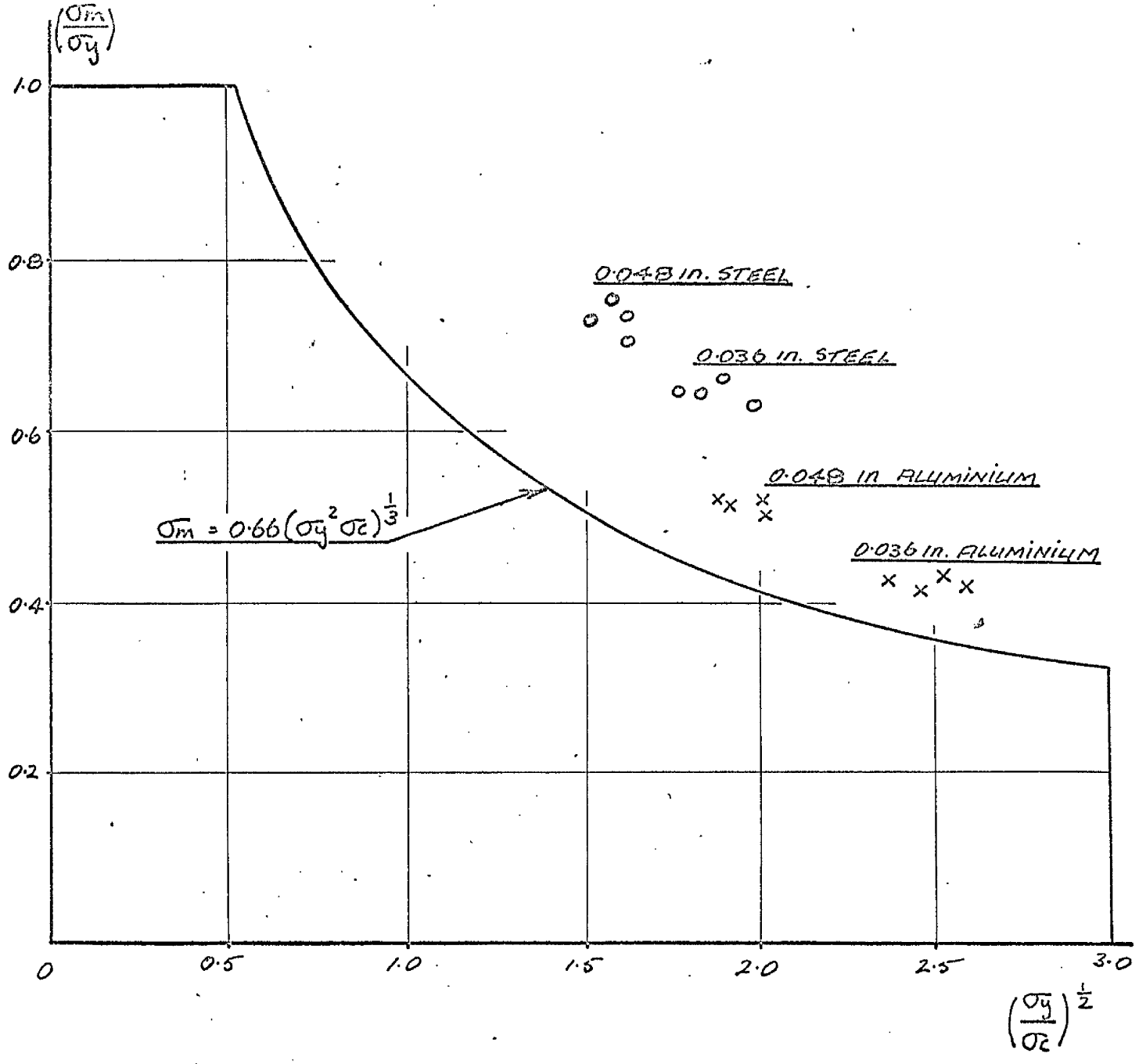

FIG.V.6 Compression tests on mild steel and aluminium alloy struts.

lateral deflection of the flange plate. A typical plot is shown in Fig. V.5 for two of the steel specimens. The critical load was taken at the point of intersection of a tangent to the curve through the point of inflection and a straight line through the pre-critical part of the curve. A full range of results is given in Appendix VIII.6, Figs. VIII.28 to VIII.35.

The σ_m values were derived from the experimental maximum load carried by the specimen. The values of σ_y the yield stress and 0.1% proof stress for steel and aluminium alloy respectively were determined by cutting specimens from the failed component and using electrical resistance strain gauges to determine the values of E , ν and σ_y . For the specimens used for the series of tests, there was some variation in the values obtained for the material characteristics and wherever necessary the individual values obtained from each tensile test were used in the analysis of experimental work.

The experimental results are compared with equation (V.1.3) in Fig. V.6. This shows that equation V.1.3 gives a conservative estimate of σ_m /

for the steel and aluminium alloy struts tested.

V.3. THE PREDICTION OF THE COLLAPSE LOAD FOR DECKING.

The critical compressive stress which initiates elastic buckling is that given by σ_c in equation (V.1.1). When the compressive stress reaches a certain average value of $\sigma_m > \sigma_c$ the compression flange ceases to take any further load. This, however, does not imply collapse of the beam which will not take place until the tension flange reaches the yield stress σ_y the whole beam failing in a manner similar to the concept of "plastic" failure. On this simplified basis the limitation of the compression flange stress to σ_m is equivalent to assuming that certain regions of the compression flange have become "ineffective" and that the operative effective width b_e is given by

$$b_e = \left(\frac{\sigma_m}{\sigma_y}\right) b \quad = C_L . b \qquad (V.3.1)$$

Failure of the beam as a whole is then assumed to take place in a "plastic" manner, the stress distribution at failure on the reduced section being of the fully plastic type.

Material	Experimental Collapse Loads lbf/in^2.	Theoretical Collapse Loads lbf/in^2.	Theoretical Buckling Loads lbf/in^2.
0.036 in. alum.	0.625	0.745	0.199
0.036 in. alum.	0.660	0.745	0.199
0.048 in. alum.	1.09	1.02	0.471
0.048 in. alum.	1.11	1.02	0.471
0.036 in. steel	1.13	1.25	0.465
0.036 in. steel	1.19	1.25	0.465
0.048 in. steel	1.72	1.78	1.11
0.048 in. steel	1.82	1.78	1.11

TABLE V.1 - Experimental and Theoretical Loads

σ_y for steel taken as the yield stress.

σ_y for aluminium taken as the 0.1% proof stress.

As has been mentioned in Chapter III, the deflection tests of the full scale decking units were taken to collapse of the deck. Considering the deck as a series of single troughs and using the methods outlined in the above analysis the loads to initiate elastic buckling and to cause collapse can be calculated as indicated in Appendix VIII.6 and the theoretical collapse loads are included in Table V.1. As can be seen from these, very good agreement was obtained between the theoretical and experimental collapse loads. This indicates that the concepts put forward form a rational basis for the design assessment of the ultimate load carrying capacity of corrugated decking.

CHAPTER VI

SUMMARY AND CONCLUSIONS

VI.1. THE ORTHOTROPIC PLATE EQUATION.

From a survey of the literature on orthotropic plate behaviour it is clear that previous theoretical work on engineering problems concentrated on those cases where the roots of the characteristic equation were real. Alternatively, the problems studied were such that a radical assumption could be made from the physical nature of the structure or plate system under consideration. This assumption usually took the form of considering the plate system to be that of a series of connected plate strips or beams. Furthermore, much work must be considered to be of very restricted applicability owing to the nature of the assumed deflected forms.

In the present work the effect of the variation of the stiffness ratios D_{11}/D_{22} and D_{66}/D_{22} has been clearly demonstrated and the distribution of deflection, moment intensity and shear force intensity throughout orthotropic plates under given loading and boundary conditions indicated. An important point that has been confirmed is that for the purpose of the consideration of an orthotropic plate as a series of beams, no theoretical prediction/

prediction of a change-over range can be deduced from orthotropic plate theory. However, it is noted that the distribution of the end reaction R_x and the moment intensities M_x and M_y throughout a plate indicate that for the determination of deflections and strains in the plate $D_{11}/D_{22} = 10$ provides a boundary line. For plates whose ratio of stiffnesses $D_{11}/D_{22} < 10$, any calculations carried out would need to be on the basis of plate behaviour. For plates therefore where $D_{11}/D_{22} > 10$ the behaviour of the complete plate may be readily estimated by the calculation of that of a typical beam or strip.

With regard to the computation of quantities such as the longitudinal distribution of deflection, the longitudinal strain ϵ_x and the longitudinal variation of moment intensity, sufficient accuracy for engineering purposes can be obtained by considering only the first term $(m = 1)$ of the appropriate infinite series - this applies for all values of the ratio D_{11}/D_{22}. For the lateral variation of deflection etc. the use of the Lévy Method and consequent transform means that while qualitatively the theoretical distributions are correct, an accurate/

accurate quantitative assessment can only be made by considering at least the first two terms ($m = 1, 3$) of the theoretical series. This is particularly true of the series for the lateral strain ϵ_y as the problem of "front end cancellation" which is explained in Appendis VIII.5 is met, and means refined and laborious computation. This does not in any way detract from the method as the convergence after two terms is good, while that after three terms ($m = 1, 3, 5$) is more than adequate for engineering purposes.

VI.2. THE APPLICATION OF ORTHOTROPIC PLATE THEORY TO DECKING.

One of the basic assumptions of the theoretical treatment delineated in this thesis is the "small deflection" limitation. Consequently any examination of orthotropic plates which derive their orthotropy from their corrugated form poses the problem of a definition of this limitation. For the decking units considered, the overall depth of which was $2\frac{1}{2}$ in. and the unformed sheet thickness a maximum of 0.048 in., it is manifest that a simple criterion of behaviour defined in terms of a plate thickness, real or equivalent, raises as many problems as it answers. From the experimental work and the/

the correspondence between it and the theoretical, the limitation to the theory emerges as that value of transverse loading which initiates a stress equal to that to initiate local elastic buckling in the compression flange of the formed corrugated deck. This limiting stress defines the range of applicability of orthotropic plate theory to the form of decking considered, the behaviour of decks made from both steel and aluminium alloy being linear up to this stress value.

From the correspondence between theory and experiment, in particular that between the values of lateral strain ϵ_y , it can be concluded that the determination of the plate constants by simple bending and twisting tests is satisfactory as this strain ϵ_y is particularly sensitive to variations in the constants D_{22} and D_{66} . Also, as demonstrated in Appendix VIII.3, the relationship $\nu_{21} = \nu_{12}(D_{22}/D_{11})$ does hold for corrugated decking, where ν_{12} is the value of the Poisson's Ratio for the unformed plate material. The determination of the modulus a_{11} and subsequently the stiffness D_{11} by the bending of a strip of material has been justified for the stiffness/

stiffness ratios involved and the analysis carried out in Appendix VIII.3 shows the utility of this form of test.

VI.3. THE DESIGN OF DECKING.

The design method put forward is based on the assessment of the behaviour of a typical beam. The vindication of this assumption has been stated in VI.1 for the stiffness ratios considered herein, and the excellent agreement between the theoretical and experimental collapse loads confirm the "effective width" concept as a rational basis for design.

CHAPTER VII

BIBLIOGRAPHY AND AUTHOR INDEX

B I B L I O G R A P H Y

ASHWELL, D.G. The Anticlastic Curvature of Rectangular Plates and Beams. Jo. Roy. Aero. Soc., Nov. 1950, p.708.

ASHWELL, D.G. and GREENWOOD, E.D. The Pure Bending of Rectangular Plates. Engineering, Vol. 170 (1950), p.51.

ASHWELL, D.G. The Stability in Bending of Slightly Corrugated Plates. Jo. Roy. Aero. Soc., Oct. 1952, p.782.

BERGSTRASSER, M. Bestimmen der bieden elastichen Konstanten von platten korpern. Zeitschrift fur techn. Physik, 1927, p. 355.

CHANG, F-V. Bending of the Clamped Edge Anisotropic Rectangular Plate. Scientica Sinica, July 1958, 7, p.716.

CHENG, S. On the Theory of Bending of Sandwich Plates. Procs. 4th U.S. Nat. Cong. Applied Mechanics, 1962, Vol. 1, p. 511.

CHILVER, A.H. Behaviour of Thin-walled Structural Members in Compression. Engineering, Vol. 172 (1951), p. 281.

CHILVER, A.H. (a) A Generalised Approach to the Local Instability of Certain Thin-walled Struts. Aeron. Itty 1953, p. 245.

(b) Maximum Strength of the Thin-walled Channel Strut. Civil Eng. Pub. Wks. Review, Vol. 48 (1953), p. 1143.

CONWAY, H.D. and NICKOLA, W.E. Anticlastic Action of Flat Sheets in Bending. Proc. Soc. Exp. Stress Analysis, Vol. 22 (1964), No. 1, p. 115.

GEHRING, F. Doctoral Thesis, Berlin, 1860.

HARVEY, J.M. Structural Strength of Thin-walled Channel Sections. Engineering, Vol. 175, (1953), p. 241.

HEARMON, R.F.S. The Fundamental Frequency of Vibration of Rectangular Wood and Plywood Plates. Proc. Phys. Soc. London, Vol. 58 (1946), p. 78.

HEARMON, R.F.S. and ADAMS, E.H. The Bending and Twisting of Anisotropic Plates. Brit. Jo. App. Phys., Vol.3 (1952), No. 5, p. 150.

HENDRY, A.W. and JAEGER, L.G. The Analysis of Grid Frameworks and Related Structures. Chatto and Windus, 1958.

HOLL, D.L. Analysis of Thin Rectangular Plates Supported on Opposite Edges. Bulletin No. 129, Iowa Experiments Station, 1936.

HOLMES, M. Stiffened Plating under Transverse Load. Quart. Jo. Mech. Appl. Maths., Vol. 12 (1959), p. 443.

HOPPMANN II, W.H. Bending of Orthogonally Stiffened Plates. Jo. App. Mechs., Vol. 22 (1955), p. 267.

HOPPMANN II, W.H. Elastic Compliances of Orthogonally Stiffened Plates. Proc. Soc. Exp. Stress Analysis, Vol. 14 (1956), No. 1, p. 137.

HOPPMANN II, W.H., HUFFINGTON Jr., N.J. and MAGNESS, L.S. A Study of Orthogonally Stiffened Plates. Jo. App. Mechs., Vol. 23 (1956), p. 343.

HOPPMANN II, W.H. and MAGNESS, L.S. Nodal Patterns of the Free Flexural Vibrations of Stiffened Plates. Jo. App. Mechs., Vol. 24 (1957), p. 526.

HUBER, M.T. Teorya Plyt. Lvov, 1922.

HUBER, M.T. Probleme der Statik Technisch Wichtiger Orthotroper Platten. Warsaw, 1929.

HUFFINGTON Jr., N.J. The Determination of the Rigidity Properties of Orthogonally Stiffened Plates. Jo. App. Mechs., Vol 23 (1956), p. 15.

HUFFINGTON Jr., N.J. and HOPPMANN II, W.H. On the Transverse Vibration of Rectangular Orthotropic Plates. Jo. App. Mechs., Vol. 25 (1958), p. 389.

HUFFINGTON Jr. N.J. On the Occurrence of Nodal Patterns of Non-parallel Form in Rectangular Orthotropic Plates. Jo. App. Mechs., Vol. 28 (1961), p. 459.

JOURNAL OF APPLIED MECHANICS. The discussions on the work of Hoppmann et.al can be found in the following: Jo. App. Mechs., Vol. 22 (1955), p. 607. Trans. A.S.M.E. Series E - Jo. App. Mechs., Vol. 26 (1959), p. 308.

KACZKOWSKI, Z. Orthotropic Rectangular Plates with Arbitrary Boundary Conditions. IXth Congres International de Mecanique Appliques Vol. VI, p. 430.

KATO, H. On the Bending and Vibration of Rectangular Plates. Jo. Soc. Nav. Archs. (Japan), Vol. 50 (1932), p. 209.

KENEDI, R.M., CHILVER, A.H., GRIFFIN, E. and SHEARER SMITH, W. Cold Formed Sections in Britain: Research and its Application to Design. International Association for Bridge and Structural Engineering Publications: Twentieth Volume, 1960, p. 137.

LAMB, H. On the Flexure of a Flat Elastic Spring. Phil. Mag. Vol. 31 (1891), p. 182.

LEKHNITSKII, S.G. (a) Teoriya Uprugosti Anizotropnogo Tela. Moscow - Leningrad 1950.
(b) Anizotropnȳe Plastinki. Moscow - Leningrad 1957.
Translations of the above are:
(a) Theory of Elasticity of an Anisotropic Elastic body. Holden Day Inc., San Francisco, 1963.

(b) Anisotropic Plates: Contributions to the Metallurgy of Steel, No. 50. American Iron and Steel Institute, New York, 1956. This is a translation of the 1st Edition (1950) of Anizotropnȳe Plastinki.

LÉVY, M. Sur L'equilibre d'une plaque rectangulaire Comptes Rendus, Vol. 129 (1899), p.535.

MARCH, H.W. Flat Plates of Plywood Under Uniform or Concentrated Loads. U.S. Dept., of Agric., Forest Products Lab. Rep. No. 1312 (1942).

NADAI, A. Forschungsarb. Vols. 170, 171, Berlin, 1917.

NADAI, A. Elastiche Platten. Berlin, 1925.

PFLUGER, A. Ingr - Arch, Vol. 16 (1947), p. 111.

RAJAPPA, N.R. and REDDY, D.V. Analysis of an Orthotropic Plate by MacLaurin's Series. Jo. Roy. Aero. Soc., Vol. 67, p. 126.

SCHADE, H.A. The Orthogonally Stiffened Plate under Uniform Lateral Load. Trans. A.S.M.E. - Jo. App. Mechs., Vol. 62 (1940), p. A-143.

SEARLE, G.F.C. Experimental Elasticity Cambridge Physical Series, Cambridge, 1908, p. 40.

SEYDEL, E. Contribution to the Question of Buckling of Reinforced Plates under Shear Load. Luftfahrtforschung, Vol. 8 (1930), p. 71.

SEYDEL, E. Shear Tests on Corrugated Sheets. Report from Deutschen Versuchanstalt fur Luftfahrt, E.V. Berlin - Adelshof, 1931.

SOUTHWELL, R.V. and SKAN, S.W. On the Stability under Shear of a Flat Elastic Strip. Procs. Roy. Soc., Vol. 105, Series A. 1924, p. 583.

STOWELL, E., HEIMERL, G.J., LIBOVE, C. and LUNDQUIST, E.E. Buckling Stresses for Flat Plates and Sections. Trans. A.S.C.E., Vol. 117, (1952), p. 545.

THIELEMANN, W. Contribution to the Problem of the Bulging of Orthotropic Plates, particularly Plywood Sheets. F.G.H. Report No. 150/19, 1945.

TIMOSHENKO, S.P. and WOINOWSKY - KRIEGER, S. Theory of Plates and Shells. McGraw Hill, 1959.

TRENKS, K. Bauingenieur, Vol. 29 (1954), p. 372.

TSAI, S.W. and SPRINGER, G.S. The Determination of the Moduli of Anisotropic Plates. Trans. A.S.M.E. Series E - Jo. App. Mechs. Vol. 30 (1963), p. 467.

VINSON, J.R. New Techniques of Solution for Problems in the Theory of Orthotropic Plates. Procs. 4th U.S. Nat. Congr. App. Mechs., Vol. II, p. 817.

WARBURTON, G.B. The Vibration of Rectangular Plates. Proc. I.Mech.E., Vol. 168 (1954), No. 12, p. 371.

WILDE, P. Rectangular Anisotropic Plate with Clamped Edges. Archiwum Mechaniki Stosowanej., Vol. 12 (1960), No. 2, p. 241.

WITT, R.K., HOPPMANN II, W.H. and BUXBAUM, R.S. Determination of Elastic Constants of Orthotropic Materials with Special reference to Laminates. Bulletin A.S.T.M., Dec. 1953.

YAMACKI, N. Bending of Stiffened Plates under Uniform Normal Pressure. Report Inst. High Speed Mechs., Tohoku Univ., Rep. No. 137, 1962/63, p. 115.

A U T H O R I N D E X

CHAPTER VIII

APPENDICES.

VIII.1. THE PLATE COMPATIBILITY EQUATION.

The expression for the potential energy of bending of an orthotropic plate is given in equation (II.4.1) as:

$$V = \frac{1}{2}\iint\left[D_{11}\left(\frac{\partial^2 w}{\partial x^2}\right)^2 + 2D_{12}\frac{\partial^2 w}{\partial x^2}\cdot\frac{\partial^2 w}{\partial y^2} + D_{22}\left(\frac{\partial^2 w}{\partial y^2}\right)^2 + 4D_{66}\left(\frac{\partial^2 w}{\partial x \partial y}\right)^2\right]dx\,dy \quad \text{(VIII.1.1)}$$

In section II.4 the variation of the first term $D_{11}\left(\frac{\partial^2 w}{\partial x^2}\right)^2$ is set out, the variations of the remaining terms are as follows:

$$\delta\iint 2D_{12}\left(\frac{\partial^2 w}{\partial x^2}\right)\left(\frac{\partial^2 w}{\partial y^2}\right)dx\,dy$$

$$= 2D_{12}\iint\left[\frac{\partial^2 w}{\partial y^2}\left(\frac{\partial^2 \delta w}{\partial x^2}\right) + \frac{\partial^2 w}{\partial x^2}\left(\frac{\partial^2 \delta w}{\partial y^2}\right)\right]dx\,dy$$

$$= 2D_{12}\iint\left[\frac{\partial}{\partial x}\left(\frac{\partial^2 w}{\partial y^2}\right)\left(\frac{\partial \delta w}{\partial x}\right) - \frac{\partial^3 w}{\partial x \partial y^2}\cdot\frac{\partial \delta w}{\partial x} + \frac{\partial}{\partial y}\left(\frac{\partial^2 w}{\partial x^2}\right)\left(\frac{\partial \delta w}{\partial y}\right) - \frac{\partial^3 w}{\partial x^2 \partial y}\cdot\frac{\partial \delta w}{\partial y}\right]dx\,dy$$

$$= 2D_{12}\iint\left[\frac{\partial}{\partial x}\left(\frac{\partial^2 w}{\partial y^2}\right)\left(\frac{\partial \delta w}{\partial x}\right) - \frac{\partial}{\partial x}\left(\frac{\partial^3 w}{\partial x \partial y^2}\cdot\delta w\right) + \frac{\partial^4 w}{\partial x^2 \partial y^2}\cdot\delta w\right.$$

$$\left. + \frac{\partial}{\partial y}\left(\frac{\partial^2 w}{\partial x^2}\right)\left(\frac{\partial \delta w}{\partial y}\right) - \frac{\partial}{\partial y}\left(\frac{\partial^3 w}{\partial x^2 \partial y}\cdot\delta w\right) + \frac{\partial^4 w}{\partial x^2 \partial y^2}\cdot\delta w\right]dx\,dy$$

using the relationships

$$\iint \frac{\partial P}{\partial x}\cdot dx\,dy = \int P\cos\beta\, ds \quad \text{(VIII.1.2)}$$

$$\iint \frac{\partial P}{\partial y}\,dx\,dy = \int P\sin\beta\, ds$$

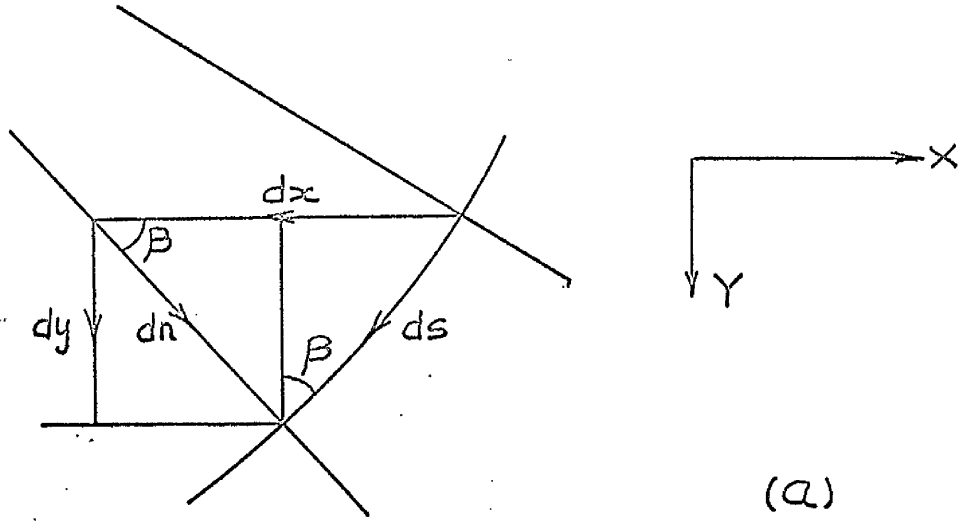

(a)

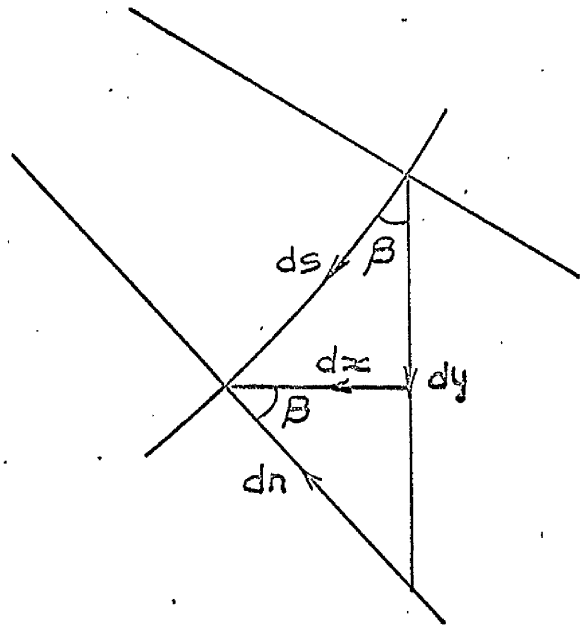

(b)

FIG.VIII.1

$$\therefore \delta \cdot 2D_{12} \iint \frac{\partial^2 w}{\partial x^2} \cdot \frac{\partial^2 w}{\partial y^2} \cdot dx\, dy$$

$$= 2D_{12} \iint 2\frac{\partial^4 w}{\partial x^2 \partial y^2} \cdot dx\, dy + 2D_{12} \int \left[\frac{\partial^2 w}{\partial y^2} \cdot \frac{\partial \delta w}{\partial x} - \frac{\partial^3 w}{\partial x \partial y^2} \cdot \delta w \right] \cos\beta\, ds \qquad \text{(VIII.1.3)}$$

$$+ 2D_{12} \int \left[\frac{\partial^2 w}{\partial x^2} \cdot \frac{\partial \delta w}{\partial y} - \frac{\partial^3 w}{\partial x^2 \partial y} \cdot \delta w \right] \sin\beta\, ds$$

examine the term: $2D_{12} \int \left[\frac{\partial^2 w}{\partial y^2} \cdot \frac{\partial \delta w}{\partial x} \right] \cos\beta\, ds$

Transform in the x-direction as indicated in Fig. VIII.1(a)

$$\frac{\partial \delta w}{\partial x} = \frac{\partial \delta w}{\partial n} \cdot \cos\beta - \frac{\partial \delta w}{\partial s} \cdot \sin\beta \qquad \text{(VIII.1.4)}$$

$$\therefore 2D_{12} \int \left[\frac{\partial^2 w}{\partial y^2} \cdot \frac{\partial \delta w}{\partial x} \right] \cos\beta\, ds$$

$$= 2D_{12} \int \frac{\partial^2 w}{\partial y^2} \cdot \cos^2\beta \cdot \frac{\partial \delta w}{\partial n} \cdot ds - 2D_{12} \int \frac{\partial^2 w}{\partial y^2} \cdot \cos\beta \cdot \sin\beta \frac{\partial \delta w}{\partial s} \cdot ds \qquad \text{(VIII.1.5)}$$

$$= 2D_{12} \int \frac{\partial^2 w}{\partial y^2} \cdot \cos^2\beta \frac{\partial \delta w}{\partial n} \cdot ds + 2D_{12} \int \frac{\partial}{\partial s} \left(\frac{\partial^2 w}{\partial y^2} \cdot \sin\beta \cos\beta \right) \delta w\, ds - 2D_{12} \left| \frac{\partial^2 w}{\partial y^2} \sin\beta \cos\beta\, \delta w \right|$$

As the integration is over the closed boundary of the plate the last term of the above is zero.

Examine the term: $2D_{12} \int \left[\frac{\partial^2 w}{\partial x^2} \cdot \frac{\partial \delta w}{\partial y} \right] \sin\beta\, ds$

Transform in the y-direction as indicated in Fig. VIII.1(b)

$$\frac{\partial \delta w}{\partial y} = \frac{\partial \delta w}{\partial n} \cdot \sin\beta + \frac{\partial \delta w}{\partial s} \cdot \cos\beta \qquad \text{(VIII.1.6)}$$

$$\therefore\ 2D_{12}\iint\left[\frac{\partial^2 w}{\partial x^2}\cdot\frac{\partial\delta w}{\partial y}\right]\sin\beta\,ds$$

$$= 2D_{12}\int\frac{\partial^2 w}{\partial x^2}\cdot\sin^2\beta\cdot\frac{\partial\delta w}{\partial n}\cdot ds + 2D_{12}\int\frac{\partial^2 w}{\partial x^2}\cdot\sin\beta\cos\beta\,\frac{\partial\delta w}{\partial s}\cdot ds \qquad \text{(VIII.1.7)}$$

$$= 2D_{12}\int\frac{\partial^2 w}{\partial x^2}\cdot\sin^2\beta\,\frac{\partial\delta w}{\partial n}\cdot ds - 2D_{12}\int\frac{\partial}{\partial s}\left(\frac{\partial^2 w}{\partial x^2}\cdot\sin\beta\cos\beta\right)\delta w\,ds$$

$$+ 2D_{12}\left|\frac{\partial^2 w}{\partial x^2}\sin\beta\cos\beta\,\delta w\right|$$

The last term of (VIII.1.7) is zero as the integration is over the closed boundary of the plate.

∴ Inserting equations (VIII.1.5) and (VIII.1.7) into equation (VIII.1.3) the variation is obtained as:

$$\delta.2D_{12}\iint\frac{\partial^2 w}{\partial x^2}\cdot\frac{\partial^2 w}{\partial y^2}\cdot dx\,dy$$

$$= 4D_{12}\iint\frac{\partial^4 w}{\partial x^2\partial y^2}\cdot dx\,dy - 2D_{12}\iint\left[\frac{\partial^3 w}{\partial x\,\partial y^2}\cdot\cos\beta + \frac{\partial^3 w}{\partial x^2\partial y}\cdot\sin\beta\right]ds.\delta w \qquad \text{(VIII.1.8)}$$

$$+ 2D_{12}\int\frac{\partial}{\partial s}\left[\frac{\partial^2 w}{\partial y^2} - \frac{\partial^2 w}{\partial x^2}\right]\sin\beta\cos\beta\,\delta w\cdot ds$$

$$+ 2D_{12}\iint\left[\frac{\partial^2 w}{\partial y^2}\cdot\cos^2\beta + \frac{\partial^2 w}{\partial x^2}\cdot\sin^2\beta\right]\frac{\partial.\delta w}{\partial n}\cdot ds$$

The variation of the third term in equation (VIII.1.1) is found as follows:

$$\delta\iint D_{22}\left(\frac{\partial^2 w}{\partial y^2}\right)^2 dx\,dy$$

$$= 2D_{22}\iint\frac{\partial^2 w}{\partial y^2}\cdot\frac{\partial^2\delta w}{\partial y^2}\cdot dx\,dy$$

$$= 2D_{22}\iint\left[\frac{\partial}{\partial y}\left(\frac{\partial^2 w}{\partial y^2}\cdot\frac{\partial \delta w}{\partial y}\right) - \frac{\partial^3 w}{\partial y^3}\cdot\frac{\partial \delta w}{\partial y}\right] dx\,dy$$

$$= 2D_{22}\iint\left[\frac{\partial}{\partial y}\left(\frac{\partial^2 w}{\partial y^2}\cdot\frac{\partial \delta w}{\partial y}\right) - \frac{\partial}{\partial y}\left(\frac{\partial^3 w}{\partial y^3}\cdot\delta w\right) + \frac{\partial^4 w}{\partial y^4}\cdot\delta w\right] dx\,dy$$

Using the relationships (VIII.1.2)

$$\delta\iint D_{22}\left(\frac{\partial^2 w}{\partial y^2}\right)^2 dx\,dy$$

$$= 2D_{22}\iint\frac{\partial^4 w}{\partial y^4}\cdot\delta w\cdot dx\,dy + 2D_{22}\int\left(\frac{\partial^2 w}{\partial y^2}\cdot\frac{\partial \delta w}{\partial y} - \frac{\partial^3 w}{\partial y^3}\cdot\delta w\right)\sin\beta\,ds$$

Transforming in the y-direction as indicated in equation (VIII.1.6)

$$\therefore \delta\iint D_{22}\left(\frac{\partial^2 w}{\partial y^2}\right)^2 dx\,dy$$

$$= 2D_{22}\iint\frac{\partial^4 w}{\partial y^4}\cdot\delta w\cdot dx\,dy \quad - 2D_{22}\int\frac{\partial^3 w}{\partial y^3}\cdot\delta w\cdot\sin\beta\,ds$$

$$+ 2D_{22}\int\frac{\partial^2 w}{\partial y^2}\left(\frac{\partial \delta w}{\partial n}\cdot\sin\beta + \frac{\partial \delta w}{\partial s}\cdot\cos\beta\right)\sin\beta\,ds$$

where: $2D_{22}\int\frac{\partial^3 w}{\partial y^2}\cdot\frac{\partial \delta w}{\partial s}\cdot\cos\beta\sin\beta\,ds$

$$= 2D_{22}\left|\frac{\partial^2 w}{\partial y^2}\cdot\sin\beta\cos\beta\,\delta w\right| - 2D_{22}\int\frac{\partial}{\partial s}\left(\frac{\partial^2 w}{\partial y^2}\cdot\sin\beta\cos\beta\right)\delta w\cdot ds$$

The first term of the above is zero as the integration is over the closed boundary of the plate.

$$\therefore \delta \iint D_{22}\left(\frac{\partial^2 w}{\partial y^2}\right) dx\,dy$$

$$= 2D_{22}\iint \frac{\partial^4 w}{\partial y^4}\cdot \delta w\cdot dx\,dy + 2D_{22}\int \frac{\partial^2 w}{\partial y^2}\cdot \sin^2\beta \cdot \frac{\partial \delta w}{\partial n}\cdot ds$$

$$- 2D_{22}\iint\left[\frac{\partial}{\partial s}\left(\frac{\partial^2 w}{\partial y^2}\cdot \sin\beta\cos\beta\right) + \frac{\partial^3 w}{\partial y^3}\cdot \sin\beta\right]\delta w\cdot ds \qquad \text{(VIII.1.9)}$$

The variation of the fourth term in equation (VIII.1.1) is found as follows:

$$\delta \iint 4D_{66}\left(\frac{\partial^2 w}{\partial x\,\partial y}\right)^2 dx\,dy$$

$$= 2\times 4D_{66}\iint\left(\frac{\partial^2 w}{\partial x\,\partial y}\right)\cdot\left(\frac{\partial^2 \delta w}{\partial x\,\partial y}\right) dx\,dy$$

$$= 4D_{66}\iint\left[\frac{\partial}{\partial x}\left(\frac{\partial^2 w}{\partial x\,\partial y}\right)\cdot\left(\frac{\partial \delta w}{\partial y}\right) - \left(\frac{\partial^3 w}{\partial x^2\,\partial y}\right)\left(\frac{\partial \delta w}{\partial y}\right)\right] dx\,dy \qquad \text{(VIII.1.10a)}$$

$$+ 4D_{66}\iint\left[\frac{\partial}{\partial y}\left(\frac{\partial^2 w}{\partial x\,\partial y}\right)\left(\frac{\partial \delta w}{\partial x}\right) - \left(\frac{\partial^3 w}{\partial x\,\partial y^2}\right)\left(\frac{\partial \delta w}{\partial x}\right)\right] dx\,dy \qquad \text{(VIII.1.10b)}$$

Examine the term (VIII.1.10a) which can be expressed as:

$$4D_{66}\iint\left[\frac{\partial}{\partial x}\left(\frac{\partial^2 w}{\partial x\,\partial y}\right)\left(\frac{\partial \delta w}{\partial y}\right) - \frac{\partial}{\partial y}\left(\frac{\partial^3 w}{\partial x^2\,\partial y}\cdot \delta w\right) + \left(\frac{\partial^4 w}{\partial x^2\,\partial y^2}\right)\delta w\right] dx\,dy$$

which on transforming via the relationships (VIII.1.2) becomes

$$4D_{66}\iint \frac{\partial^4 w}{\partial x^2 \partial y^2}\cdot \delta w \cdot dx\,dy \;+\; 4D_{66}\int \left(\frac{\partial^2 w}{\partial x\,\partial y}\right)\left(\frac{\partial \delta w}{\partial y}\right)\cos\beta\, ds \;-\; 4D_{66}\int \frac{\partial^3 w}{\partial x^2 \partial y}\cdot \delta w \cdot \sin\beta \cdot ds \qquad \text{(VIII.1.11)}$$

Considering the second term of (VIII.1.11) and transforming in the y-direction as in Fig. VIII.1(b).

$$\therefore\; 4D_{66}\int \left(\frac{\partial^2 w}{\partial x\,\partial y}\right)\left(\frac{\partial \delta w}{\partial y}\right)\cos\beta\, ds$$

$$= 4D_{66}\int \frac{\partial^2 w}{\partial x\,\partial y}\left[\frac{\partial \delta w}{\partial n}\cdot \sin\beta + \frac{\partial \delta w}{\partial s}\cdot \cos\beta\right]\cos\beta\, ds$$

$$= 4D_{66}\int \frac{\partial^2 w}{\partial x\,\partial y}\cdot \sin\beta\cos\beta \cdot \frac{\partial \delta w}{\partial n}\cdot ds \;+\; 4D_{66}\left|\frac{\partial^2 w}{\partial x\,\partial y}\cdot \cos^2\beta \cdot \delta w\right|$$

$$- 4D_{66}\int \frac{\partial}{\partial s}\left(\frac{\partial^2 w}{\partial x\,\partial y}\cdot \cos^2\beta\right)\delta w \cdot ds.$$

where the term $4D_{66}\left|\frac{\partial^2 w}{\partial x\,\partial y}\cdot \cos^2\beta \cdot \delta w\right|$ is zero as the integration is around the closed boundary of the plate.

Therefore (VIII.1.10a) can be expressed as:

$$4D_{66}\iint \frac{\partial^4 w}{\partial x^2 \partial y^2}\cdot \delta w \cdot dx\,dy \;-\; 4D_{66}\int \frac{\partial^3 w}{\partial x^2 \partial y}\cdot \delta w \cdot \sin\beta\, ds \qquad \text{(VIII.1.12)}$$

$$+ 4D_{66}\int \frac{\partial^2 w}{\partial x\,\partial y}\cdot \sin\beta\cos\beta\,\frac{\partial \delta w}{\partial n}\cdot ds \;-\; 4D_{66}\int \frac{\partial}{\partial s}\left(\frac{\partial^2 w}{\partial x\,\partial y}\cdot \cos^2\beta\right)\delta w \cdot ds$$

In a similar manner (VIII.1.10b) can be shown to be:

$$4D_{66}\iint \frac{\partial^4 w}{\partial x^2 \partial y^2}\,.\,\delta w\,.\,dx\,dy \;-\; 4D_{66}\int \frac{\partial^3 w}{\partial x\,\partial y^2}\,.\,\delta w\,.\cos\beta\,ds$$

$$+4D_{66}\int \frac{\partial^2 w}{\partial x \partial y}\,.\sin\beta\cos\beta\,\frac{\partial \delta w}{\partial n}\,.\,ds \;+\; 4D_{66}\int \frac{\partial}{\partial s}\left(\frac{\partial^2 w}{\partial x \partial y}\,.\sin^2\beta\right)\delta w\,.\,ds \qquad \text{(VIII.1.13)}$$

Adding equations (VIII.1.12) and (VIII.1.13) gives the variation of the fourth term to be:

$$\delta\iint 4D_{66}\left(\frac{\partial^2 w}{\partial x \partial y}\right)^2 dx\,dy$$

$$= 4D_{66}\left\{ 2\iint \frac{\partial^4 w}{\partial x^2 \partial y^2}\,.\,\delta w\,.\,dx\,dy \right.$$

$$+ 2\int \frac{\partial^2 w}{\partial x \partial y}\,.\sin\beta\cos\beta\,\frac{\partial \delta w}{\partial n}\,.\,ds \qquad \text{(VIII.1.14)}$$

$$+ \int \frac{\partial}{\partial s}\left[\frac{\partial^2 w}{\partial x \partial y}\left(\sin^2\beta - \cos^2\beta\right)\right]\delta w\,.\,ds$$

$$\left. - \iint\left[\frac{\partial^3 w}{\partial x\,\partial y^2}\,.\cos\beta + \frac{\partial^3 w}{\partial x^2 \partial y}\,.\sin\beta\right]\delta w\,.\,ds \right\}$$

Thus the equations (VIII.1.8), (VIII.1.9) and (VIII.1.14) together with equation (II.4.3) give the variation of the potential energy of bending of an orthotropic plate, the plate compatibility equation being derived as indicated in Section II.4

VIII.2. SOLUTION OF THE PLATE EQUATION.

The orthotropic plate equation for a rectangular plate under a uniformly distributed load can be stated in Cartesian co-ordinates as:

$$D_{11}\frac{\partial^4 w}{\partial x^4} + 2D_{33}\frac{\partial^4 w}{\partial x^2 \partial y^2} + D_{22}\frac{\partial^4 w}{\partial y^4} = q \qquad \text{(VIII.2.1)}$$

As shown in Chapter II the solution of (VIII.2.1) for the deflection w can be considered in the form:

$$w = w_1 + w_2 \qquad \text{(VIII.2.2)}$$

where:

$$w_1 = \frac{4qa^4}{\pi^5 D_{11}} \sum_{m=1,3,..}^{\infty} \frac{1}{m^5} \cdot \sin\frac{m\pi x}{a}$$

$$w_2 = \sum_{m=1,3...}^{\infty} Y_m \sin\frac{m\pi x}{a}$$

and the characteristic equation obtained for w_2 namely

$$\frac{d^4 Y_m}{dy^4} - 2\frac{D_{33}}{D_{22}}\left(\frac{m\pi}{a}\right)^2 \frac{d^2 Y_m}{dy^2} + \frac{D_{11}}{D_{22}}\left(\frac{m\pi}{a}\right)^4 Y_m = 0 \qquad \text{(VIII.2.3)}$$

The roots of this equation are:

$$\phi = \pm \frac{m\pi}{a}\frac{1}{\sqrt{D_{22}}}\left\{D_{33} + \sqrt{D_{33}^2 - D_{11}D_{22}}\right\}^{\frac{1}{2}}$$

$$\psi = \pm \frac{m\pi}{a}\frac{1}{\sqrt{D_{22}}}\left\{D_{33} - \sqrt{D_{33}^2 - D_{11}D_{22}}\right\}^{\frac{1}{2}} \qquad \text{(VIII.2.4)}$$

There are two possible cases consistent with the actual values of D_{11} etc. to be considered.

1. All Roots Real: $D_{33}^2 > D_{11} D_{22}$

The form of Y_m is given by:

$$Y_m = A_m \cosh \phi y + B_m \sinh \phi y + C_m \cosh \psi y + D_m \sinh \psi y$$

and the deflected form w in equation (VIII.2.1) is given by:

$$w = \frac{qa^4}{D_{11}} \sum_{m=1,3,\ldots}^{\infty} \left[\frac{4}{(m\pi)^5} + A_m \cosh \phi y + B_m \sinh \phi y + C_m \cosh \psi y + D_m \sinh \psi y \right] \sin \frac{m\pi x}{a} \quad \text{(VIII.2.5)}$$

From the equations (II.4.11) and (II.4.12) the boundary conditions on the free edges $y = 0$ and $y = b$ are

$$D_{12} \frac{\partial^2 w}{\partial x^2} + D_{22} \frac{\partial^2 w}{\partial y^2} = 0$$

$$D_{22} \frac{\partial^3 w}{\partial y^3} + D_{12} \frac{\partial^3 w}{\partial x^2 \partial y} + 4 D_{66} \frac{\partial^3 w}{\partial x^2 \partial y} = 0 \quad \text{(VIII.2.6)}$$

Therefore performing the appropriate differentiation on equation (VIII.2.5) the following conditions are obtained.

(a) On $y = 0$

$$D_{12} \frac{\partial^2 w}{\partial x^2} + D_{22} \frac{\partial^2 w}{\partial y^2} = 0$$

$$\therefore -D_{12}\left(\frac{m\pi}{a}\right)^2\left[\frac{4}{(m\pi)^5}+A_m+C_m\right]+D_{22}\left[\phi^2 A_m+\psi^2 C_m\right]=0$$

$$\therefore A_m\left[D_{22}\phi^2-D_{12}\left(\frac{m\pi}{a}\right)^2\right]+C_m\left[D_{22}\psi^2-D_{12}\left(\frac{m\pi}{a}\right)^2\right]$$

$$=\frac{4D_{12}}{(m\pi)^3 a^2}$$

$$\therefore \underline{A_m\gamma+C_m\cdot\delta=F} \qquad \text{(VIII.2.7)}$$

$$(b\,D_{22}\frac{\partial^3 w}{\partial y^3}+(D_{12}+4D_{66})\frac{\partial^3 w}{\partial x^2\partial y}$$

$$D_{22}\frac{\partial^3 w}{\partial y^3}+(D_{12}+4D_{66})\frac{\partial^3 w}{\partial x^2\partial y}=0$$

$$\therefore D_{22}(\phi^3 B_m+\psi^3 D_m)-(D_{12}+4D_{66})(\phi B_m+\psi D_m)\left(\frac{m\pi}{a}\right)^2=0$$

$$\therefore \phi B_m\left[D_{22}\phi^2-D_{12}\left(\frac{m\pi}{a}\right)^2-4D_{66}\left(\frac{m\pi}{a}\right)^2\right]+\psi D_m\left[D_{22}\psi^2-D_{12}\left(\frac{m\pi}{a}\right)^2-4D_{66}\left(\frac{m\pi}{a}\right)^2\right]$$

$$=0$$

$$\therefore \underline{\phi B_m(\gamma-R)+\psi D_m(\delta-R)=0} \qquad \text{(VIII.2.8)}$$

where $R=4D_{66}(m\pi/a)^2$

(c) On $y=b$ $\quad D_{12}\frac{\partial^2 w}{\partial x^2}+D_{22}\frac{\partial^2 w}{\partial y^2}=0$

$$\therefore -D_{12}\left(\frac{m\pi}{a}\right)^2\left[\frac{4}{(m\pi)^5}+A_m\cosh\phi b+B_m\sinh\phi b+C_m\cosh\psi b+D_m\sinh\psi b\right]\sin\frac{m\pi x}{a}$$

$$+D_{22}\left[\phi^2 A_m\cosh\phi b+\phi^2 B_m\sinh\phi b+\psi^2 C_m\cosh\psi b+\psi^2 D_m\sinh\psi b\right]\sin\frac{m\pi x}{a}=0$$

$$\therefore A_m\left[D_{22}\phi^2-D_{12}\left(\frac{m\pi}{a}\right)^2\right]\cosh\phi b+B_m\left[D_{22}\phi^2-D_{12}\left(\frac{m\pi}{a}\right)^2\right]\sinh\phi b$$

$$+C_m\left[D_{22}\psi^2-D_{12}\left(\frac{m\pi}{a}\right)^2\right]\cosh\psi b+D_m\left[D_{22}\psi^2-D_{12}\left(\frac{m\pi}{a}\right)^2\right]\sinh\psi b=4D_{12}/(m\pi)^3 a^2$$

$$\therefore \underline{A_m\gamma\cosh\phi b+B_m\gamma\sinh\phi b+C_m\cdot\delta\cosh\psi b+D_m\cdot\delta\sinh\psi b=F} \qquad \text{(VIII.2.9)}$$

(d) On $y=b$

$$D_{22}\frac{\partial^3 w}{\partial y^3}+(D_{12}+4D_{66})\frac{\partial^3 w}{\partial x^2\partial y}=0$$

$$\therefore D_{22}\left[\phi^3 A_m \sinh\phi b + \phi^3 B_m \cosh\phi b + \psi^3 C_m \sinh\psi b + \psi^3 D_m \cosh\psi b\right]$$

$$-(D_{12}+4D_{66})\left(\frac{m\pi}{a}\right)^2\left[\phi A_m \sinh\phi b + \phi B_m \cosh\phi b + \psi C_m \sinh\psi b + \psi D_m \cosh\psi b\right] = 0$$

$$\therefore \phi A_m\left[D_{22}\phi^2 - (D_{12}+4D_{66})\left(\frac{m\pi}{a}\right)^2\right]\sinh\phi b + \phi B_m\left[D_{22}\phi^2 - (D_{12}+4D_{66})\left(\frac{m\pi}{a}\right)^2\right]\cosh\phi b$$

$$+\psi C_m\left[D_{22}\psi^2 - (D_{12}+4D_{66})\left(\frac{m\pi}{a}\right)^2\right]\sinh\psi b + \psi B_m\left[D_{22}\psi^2 - (D_{12}+4D_{66})\left(\frac{m\pi}{a}\right)^2\right]\cosh\psi b = 0$$

$$\therefore \underline{\phi A_m(\gamma-R)\sinh\phi b + \phi B_m(\gamma-R)\cosh\phi b}$$

$$\underline{+\psi C_m(\delta-R)\sinh\psi b + \psi D_m(\delta-R)\cosh\psi b = 0} \qquad \text{(VIII.2.10)}$$

From (VIII.2.7) and (VIII.2.8)

$$C_m = \frac{F - A_m\cdot\gamma}{\delta} \qquad \text{and} \qquad D_m = -\frac{\phi B_m(\gamma-R)}{\psi(\delta-R)}$$

Substitute for C_m and D_m into (VIII.1.9)

$$\therefore A_m\gamma\cosh\phi b + B_m\gamma\sinh\phi b$$

$$+\left(\frac{F-A_m\gamma}{\delta}\right)\delta\cosh\psi b - \frac{\phi B_m(\gamma-R)}{\psi(\delta-R)}\cdot\delta\sinh\psi b = F \qquad \text{(VIII.2.11)}$$

Now examine the identity: $\dfrac{\gamma-R}{\delta-R} = \dfrac{\delta}{\gamma}$

$$\text{i.e. } \underline{R-(\gamma+\delta) = 0}$$

$$D_{22}(\phi^2+\psi^2) = \left(\frac{m\pi}{a}\right)^2 \cdot 2 \cdot D_{33}$$

$$= \left(\frac{m\pi}{a}\right)^2 \cdot 2\,(D_{12}+2D_{66})$$

$$\therefore \gamma+\delta = 4D_{66}\left(\frac{m\pi}{a}\right)^2 = R$$

i.e. <u>the identity is correct</u>.

Substitute (δ/γ) for $(\gamma-R)/(\delta-R)$ in equation (VIII.1.11)

$$\therefore A_m \gamma \cosh\phi b + B_m \gamma \sinh\phi b - A_m \gamma \cosh\psi b - \phi \frac{B_m \delta^2 \sinh\psi b}{\psi \gamma} = F(1-\cosh\psi b)$$

Hence

$$A_m = \frac{\psi\gamma F(1-\cosh\psi b) - B_m(\psi\gamma^2\sinh\phi b - \phi\delta^2\sinh\psi b)}{\psi\gamma^2(\cosh\phi b - \cosh\psi b)} \qquad \text{(VIII.2.12)}$$

Substitute into equation (VIII.2.10) C_m from equation (VIII.2.7), D_m from equation (VIII.2.8) and A_m from equation (VIII.2.12) to obtain:

$$(\phi\delta^2\sinh\phi b - \psi\gamma^2\sinh\psi b)\{\psi\gamma F(1-\cosh\psi b) - B_m(\psi\gamma^2\sinh\phi b - \phi\delta^2\sinh\psi b)\}$$

$$+\phi\delta^2\psi\gamma^2 B_m(\cosh\phi b - \cosh\psi b)^2 + F\psi\gamma\sinh\psi b(\cosh\phi b - \cosh\psi b)\psi\gamma^2 = 0$$

from which B_m is found as

$$B_m = \frac{F\psi\gamma\{\phi\delta^2\sinh\phi b(\cosh\psi b - 1) - \psi\gamma^2\sinh\psi b(\cosh\phi b - 1)\}}{(\phi^2\delta^4 + \psi^2\gamma^4)\sinh\phi b\sinh\psi b - 2\phi\delta^2\psi\gamma^2(\cosh\phi b\cosh\psi b - 1)}$$

Substitution for B_m into (VIII.2.12), (VIII.2.7) and (VIII.2.8) gives the following expressions for the constants A_m etc.

$$A_m = \frac{F\psi\gamma\{\psi\gamma^2\sinh\phi b\sinh\psi b + \phi\delta^2(1+\cosh\phi b - \cosh\psi b - \cosh\psi b\cosh\phi b)\}}{(\phi^2\delta^4 + \psi^2\gamma^4)\sinh\phi b\sinh\psi b - 2\phi\delta^2\psi\gamma^2(\cosh\phi b\cosh\psi b - 1)}$$

$$C_m = \frac{F\{\phi^2\delta^4 \sinh\phi b \sinh\psi b + \phi\delta^2\psi^2 (1-\cosh\phi b+\cosh\psi b - \cosh\psi b \cosh\phi b)\}}{\delta\{(\phi^2\delta^4+\psi^2\psi^4)\sinh\phi b \sinh\psi b - 2\phi\delta^2\psi^2(\cosh\phi b \cosh\psi b - 1)\}}$$

(VIII.2.13)

$$D_m = \frac{F\phi\delta\{\psi^2 \sinh\psi b(\cosh\phi b-1) - \phi\delta^2\sinh\phi b(\cosh\psi b-1)\}}{\{(\phi^2\delta^4+\psi^2\psi^4)\sinh\phi b \sinh\psi b - 2\phi\delta^2\psi^2(\cosh\phi b\cosh\psi b-1)\}}$$

Thus for the case when $D_{33}^2 > D_{11}D_{22}$ the deflected form defined by equation (VIII.2.5) can be computed for a series of uniform loads q .

2. All Roots Complex $D_{33}^2 < D_{11}D_{22}$

The form of Y_m is given by:

$$Y_m = \sum_{m=1,3,\ldots}^{\infty} (A_m \cos\gamma y + B_m \sin\gamma y)\cosh\theta y + (C_m \cos\gamma y + D_m \sin\gamma y)\sinh\theta y$$

where

$$\theta = \left(\frac{m\pi}{a}\right)\sqrt{\frac{D_{33}}{D_{22}}} \qquad \gamma = \left(\frac{m\pi}{a}\right)\frac{\sqrt[4]{D_{11}D_{22}-D_{33}^2}}{\sqrt{D_{22}}}$$

The deflected form w in equation (VIII.2.1) is given by:

$$w = \frac{qa^4}{D_{11}}\sum\left[\frac{4}{(m\pi)^5} + (A_m \cos\gamma y + B_m \sin\gamma y)\cosh\theta y + (C_m \cos\gamma y + D_m \sin\gamma y)\sinh\theta y\right]\sin\frac{m\pi x}{a}$$

(VIII.2.14)

Using the boundary conditions given by equations (VIII.2.6) the following are obtained:

(a) On $y = 0$

$$D_{12}\frac{\partial^2 w}{\partial x^2} + D_{22}\frac{\partial^2 w}{\partial y^2} = 0$$

$$\therefore -D_{12}\left(\frac{m\pi}{a}\right)^2\left[\frac{4}{(m\pi)^5} + A_m\right] + D_{22}\left[(\theta^2-\zeta^2)A_m + 2\theta\zeta D_m\right] = 0$$

$$\therefore A_m\left[D_{22}(\theta^2-\zeta^2) - D_{12}\left(\frac{m\pi}{a}\right)^2\right] + D_m \cdot 2\theta\zeta \cdot D_{22} = \frac{4D_{12}}{(m\pi)^3 \cdot a^2}$$

$$\therefore \underline{A_m \cdot f + D_m \cdot g = F} \qquad \text{(VIII.2.15)}$$

(b) On $y = 0$, $D_{22}\frac{\partial^3 w}{\partial y^3} + (D_{12} + 4D_{66})\frac{\partial^3 w}{\partial x^2 \partial y} = 0$

$$\therefore D_{22}\left[(\theta^2-\zeta^2)(B_m\cdot\zeta + C_m\cdot\theta) + 2\theta\zeta(B_m\cdot\theta - C_m\cdot\zeta)\right]$$

$$- (D_{12} + 4D_{66})\left[B_m\cdot\zeta + C_m\cdot\theta\right]\left(\frac{m\pi}{a}\right)^2 = 0$$

$$\therefore B_m\cdot\zeta\left[D_{22}(\theta^2-\zeta^2) - (D_{12}+4D_{66})\left(\frac{m\pi}{a}\right)^2 + 2D_{22}\theta^2\right]$$

$$+ C_m\cdot\theta\left[D_{22}(\theta^2-\zeta^2) - (D_{12}+4D_{66})\left(\frac{m\pi}{a}\right)^2 - 2D_{22}\cdot\zeta^2\right] = 0$$

$$\therefore \underline{B_m\cdot\zeta\left[f - R + 2D_{22}\cdot\theta^2\right] + C_m\cdot\theta\left[f - R - 2D_{22}\zeta^2\right] = 0} \qquad \text{(VIII.2.16)}$$

(c) On $y = b$, $D_{12}\frac{\partial^2 w}{\partial x^2} + D_{22}\frac{\partial^2 w}{\partial y^2} = 0$

$$\therefore D_{22}\left\{(\theta^2-\zeta^2)\left[A_m\cosh\theta b\cos\zeta b + B_m\cosh\theta b\sin\zeta b + C_m\sinh\theta b\cos\zeta b + D_m\sinh\theta b\sin\zeta b\right]\right.$$

$$\left. + 2\theta\zeta\left[B_m\sinh\theta b\cos\zeta b - A_m\sinh\theta b\sin\zeta b + D_m\cosh\theta b\cos\zeta b - C_m\cosh\theta b\sin\zeta b\right]\right\}$$

$$- D_{12}\left(\frac{m\pi}{a}\right)^2\left[\frac{4}{(m\pi)^5} + A_m\cosh\theta b\cos\zeta b + B_m\cosh\theta b\sin\zeta b + C_m\sinh\theta b\cos\zeta b + D_m\sinh\theta b\sin\zeta b\right]$$

$$\therefore A_m[f\cosh\theta b\cos\zeta b - g\sinh\theta b\sin\zeta b] + B_m[f\cosh\theta b\sin\zeta b + g\sinh\theta b\cos\zeta b]$$

$$+ C_m[f\sinh\theta b\cos\zeta b - g\cosh\theta b\sin\zeta b]$$

$$+ D_m[f\sinh\theta b\sin\zeta b + g\cosh\theta b\cos\zeta b] = F \qquad \text{(VIII.2.17)}$$

(d) On $y = b$ $\quad D_{22}\frac{\partial^3 w}{\partial y^3} + (D_{12} + 4D_{66})\frac{\partial^3 w}{\partial x^2 \partial y} = 0$

$$\therefore D_{22}\Big\{(\theta^2-\zeta^2)\big[A_m(-\zeta\cosh\theta b\sin\zeta b + \theta\sinh\theta b\cos\zeta b) + B_m(\zeta\cosh\theta b\cos\zeta b + \theta\sinh\theta b\sin\zeta b)$$

$$+ C_m(-\zeta\sinh\theta b\sin\zeta b + \theta\cosh\theta b\cos\zeta b) + D_m(\zeta\sinh\theta b\cos\zeta b + \theta\cosh\theta b\sin\zeta b)\big]$$

$$+ 2\theta\zeta\big[A_m(-\zeta\sinh\theta b\cos\zeta b - \theta\cosh\theta b\sin\zeta b) + B_m(-\zeta\sinh\theta b\sin\zeta b + \theta\cosh\theta b\cos\zeta b)$$

$$+ C_m(-\zeta\cosh\theta b\cos\zeta b - \theta\sinh\theta b\sin\zeta b) + D_m(-\zeta\cosh\theta b\sin\zeta b + \theta\sinh\theta b\cos\zeta b)\big]\Big\}$$

$$-(D_{12}+4D_{66})\left(\frac{m\pi}{a}\right)^2\big[A_m(\theta\sinh\theta b\cos\zeta b - \zeta\cosh\theta b\sin\zeta b) + B_m(\theta\sinh\theta b\sin\zeta b + \zeta\cosh\theta b\cos\zeta b)$$

$$+ C_m(\theta\cosh\theta b\cos\zeta b - \zeta\sinh\theta b\sin\zeta b) + D_m(\theta\cosh\theta b\sin\zeta b + \zeta\sinh\theta b\cos\zeta b)\big]$$

$$\therefore A_m[(f-R)(\theta\sinh\theta b\cos\zeta b - \zeta\cosh\theta b\sin\zeta b) - g(\zeta\sinh\theta b\cos\zeta b + \theta\cosh\theta b\sin\zeta b)]$$

$$+ B_m[(f-R)(\zeta\cosh\theta b\cos\zeta b + \theta\sinh\theta b\sin\zeta b) - g(\zeta\sinh\theta b\sin\zeta b - \theta\cosh\theta b\cos\zeta b)]$$

$$+ C_m[(f-R)(\theta\cosh\theta b\cos\zeta b - \zeta\sinh\theta b\sin\zeta b) - g(\zeta\cosh\theta b\cos\zeta b + \theta\sinh\theta b\sin\zeta b)]$$

$$+ D_m[(f-R)(\zeta\sinh\theta b\cos\zeta b + \theta\cosh\theta b\sin\zeta b) - g(\zeta\cosh\theta b\sin\zeta b - \theta\sinh\theta b\cos\zeta b)]$$

$$= 0 \qquad \text{(VIII.2.18)}$$

From equations (VIII.2.15) and (VIII.2.16)

$$\Pi_m = \frac{F - g D_m}{f}$$

$$B_m = -C_m \frac{\theta(f - R - 2D_{22}\zeta^2)}{\zeta(f - R + 2D_{22}\theta^2)} = -C_m \cdot \frac{M}{N}$$

Substitute the above into equation (VIII.2.17) to obtain

$$C_m \sinh\theta b \cos\zeta b\left[f - \frac{M}{N} g\right] - C_m \cosh\theta b \sin\zeta b\left[g + f \cdot \frac{M}{N}\right]$$

$$+ D_m \sinh\theta b \sin\zeta b\left[f + g^2/f\right]$$

$$= F\left[1 - (1/f)(f\cosh\theta b \cos\zeta b - g \sinh\theta b \sin\zeta b)\right]$$

Hence $$C_m = \frac{F\left[1 - (1/f)(\cosh\theta b\cos\zeta b - g\sinh\theta b\sin\zeta b) - D_m \sinh\theta b \sin\zeta b\left(f + g^2/f\right)\right]}{\sinh\theta b \cos\zeta b\left(f - g\frac{M}{N}\right) - \cosh\theta b \sin\zeta b\left(g + f\frac{M}{N}\right)}$$

Now substitute into equation (VIII.2.18) C_m, B_m and Π_m

$$\therefore \frac{F - D_m \cdot g}{f}\left[(f - R)(\theta\sinh\theta b\cos\zeta b - \zeta\cosh\theta b\sin\zeta b) - g(\zeta\sinh\theta b\cos\zeta b + \theta\cosh\theta b\sin\zeta b)\right]$$

$$-\frac{M}{\partial C N} \cdot F\begin{bmatrix} 1 - (1/f)(f\cosh\theta b\cos\zeta b - g\sinh\theta b\sin\zeta b) \\ - D_m \sinh\theta b \sin\zeta b\,(f + g^2/f) \end{bmatrix}\begin{bmatrix} (f - R)(\zeta\cosh\theta b\cos\zeta b + \theta\sinh\theta b\sin\zeta b) \\ -g(\zeta\sinh\theta b\sin\zeta b - \theta\cosh\theta b\cos\zeta b) \end{bmatrix}$$

$$+ \quad \ldots .$$

$$+\frac{F}{\mathcal{H}}\begin{bmatrix} 1-(1/f)(f\cosh\theta b\cos\zeta b - g\sinh\theta b\sin\zeta b) \\ -D_m\sinh\theta b\sin\zeta b\,(f+g^2/f) \end{bmatrix}\cdot\begin{bmatrix} (f-R)(\theta\cosh\theta b\cos\zeta b - \zeta\sinh\theta b\sin\zeta b) \\ -g(\zeta\cosh\theta b\cos\zeta b + \theta\sinh\theta b\sin\zeta b) \end{bmatrix}$$

$$+D_m\left[(f-R)(\zeta\sinh\theta b\cos\zeta b+\theta\cosh\theta b\sin\zeta b) - g(\zeta\cosh\theta b\sin\zeta b - \theta\sinh\theta b\cos\zeta b)\right]$$

(VIII.2.19)

where $\mathcal{H} = \sinh\theta b\cos\zeta b\left[f - g\cdot\frac{M}{N}\right] - \cosh\theta b\sin\zeta b\left[g + f\cdot\frac{M}{N}\right]$

Separate the terms containing F from the above to obtain:

$$\frac{F}{Fg}\Big\{\tanh\theta b\left[(f-R)g\cdot\theta - g^2\zeta\right] - \tan\zeta b\left[(f-R)g\cdot\zeta + g^2\theta\right]$$

$$-\frac{M}{N}\cdot\frac{F}{H}\Big\{\frac{1}{\cosh\theta b\cos\zeta b}\Big[\tanh\theta b\tan\zeta b\{(f-R)\theta - g\zeta\} + \{(f-R)\zeta + g\theta\}\Big]$$

$$-\left[\tanh\theta b\tan\zeta b\{(f-R)\theta - g\zeta\} + \{(f-R)\zeta + g\theta\}\right]$$

$$+(1/f)\left[\tanh\theta b\tan\zeta b\{(f-R)g\zeta + g^2\theta\} + \tanh^2\theta b\tan^2\zeta b\{(f-R)g\theta - g^2\zeta\}\right]\Big\}$$

$$+\frac{F}{\mathcal{H}}\Big\{\frac{1}{\cosh\theta b\cos\zeta b}\Big[-\tanh\theta b\tan\zeta b\{(f-R)\zeta + g\theta\} + \{(f-R)\theta - g\zeta\}\Big]$$

$$-\left[-\tanh\theta b\tan\zeta b\{(f-R)\zeta + g\theta\} + \{(f-R)\theta - g\zeta\}\right]$$

$$+(\tfrac{1}{f})\left[\tanh\theta b\tan\zeta b\{(f-R)g\theta - g^2\zeta\} - \tanh^2\theta b\tan^2\zeta b\{(f-R)g\zeta + g^2\theta\}\right]\Big\}$$

(VIII.2.20)

Examine the terms:

$$\{(f-R)\theta - g\zeta\} \quad \text{and} \quad \{(f-R)\zeta + g\theta\}$$

$$(f-R)\theta - g\zeta = \theta\left\{D_{22}\theta^2 - D_{22}\zeta^2 - D_{12}\left(\frac{m\pi}{a}\right)^2 - 4D_{66}\left(\frac{m\pi}{a}\right)^2\right\} - 2D_{22}\theta\zeta^2$$

$$= \theta\left\{D_{22}\theta^2 - D_{22}\zeta^2 - D_{12}\left(\frac{m\pi}{a}\right)^2 - 4D_{66}\left(\frac{m\pi}{a}\right)^2 - 2D_{22}\zeta^2\right\}$$

$$= \theta\left\{f - R - 2D_{22}\zeta^2\right\} = \underline{\underline{M}}$$

similarly $(f-R)\zeta + g\theta = \underline{\underline{N}}$

Using these relationships and collecting appropriate terms expression (VIII.2.20) for the sum of the F terms becomes

$$\frac{F}{f}\left\{M\tanh\theta b - N\tan\zeta b\right\}$$

$$-\frac{F}{\mathcal{H}}\left(\frac{M^2+N^2}{N^2}\right)\left\{\frac{\tanh\theta b\,\tan\zeta b}{\cosh\theta b\,\cos\zeta b} - \tanh\theta b\tan\zeta b + \frac{g}{f}\tanh^2\theta b\tan^2\zeta b\right\} \quad \text{(VIII.2.21)}$$

Now separating the terms containing D_m from equation (VIII.2.19) to obtain:

$$-\frac{D_m \cdot g}{f}\left\{(f-R)(\theta\tanh\theta b - \zeta\tan\zeta b) - g(\zeta\tanh\theta b + \theta\tan\zeta b)\right\}$$

$$+\frac{D_m}{\mathcal{H}}\cdot\frac{M}{N}\tanh\theta b\tan\zeta b\left(f+\frac{g^2}{f}\right)\left\{(f-R)(\zeta + \theta\tanh\theta b\tan\zeta b) - g(\zeta\tanh\theta b\tan\zeta b - \theta)\right\}$$

$$-\frac{D_m}{\mathcal{H}}\tanh\theta b\tan\zeta b\left(f+\frac{g^2}{f}\right)\left\{(f-R)(\theta - \tanh\theta b\tan\zeta b) - g(\zeta + \theta\tanh\theta b\tan\zeta b)\right\}$$

$$+D_m\left\{(f-R)(\zeta\tanh\theta b + \theta\tan\zeta b) - g(\zeta\tan\zeta b - \theta\tanh\theta b)\right\}$$

On expansion and collection of terms using the relationships $(f-R)\theta - g\zeta = M$ and $(f-R)\zeta + g\theta = N$ the above becomes:

$$\frac{D_m}{F}\left\{ \left[\tanh\theta b\,(fN-gM) + \tan\zeta b\,(fM+gN) \right] + \frac{(M^2+N^2)}{\mathcal{H}\cdot N}(f^2+g^2)\tanh^2\theta b\,\tan^2\zeta b \right\} \qquad \text{(VIII.2.22)}$$

Equating (VIII.2.22) to − (VIII.2.21) and solving for D_m

$$D_m = F\left\{ \frac{\left[\frac{f(M^2+N^2)\tanh\theta b\,\tan\zeta b}{\cosh\theta b\cos\zeta b}\left\{ \frac{1}{\cosh\theta b\cos\zeta b} - 1 + \frac{g}{f}\tanh\theta b\,\tan\zeta b \right\} \right] - \left\{ M\tanh\theta b - N\tan\zeta b \right\}\left\{ (fN-gM)\tanh\theta b - (gN+fM)\tan\zeta b \right\}}{\left[\left\{ \tanh^2\theta b\,(fN-gM)^2 - \tan^2\zeta b\,(gN+fM)^2 \right\} + \frac{(M^2+N^2)(f^2+g^2)\tanh^2\theta b\,\tan^2\zeta b}{\cosh\theta b\cos\zeta b} \right]} \right\}$$

Hence:

$$C_m = FN\left\{ \frac{\frac{1}{\cosh\theta b\cos\zeta b} - 1 + \frac{g}{f}\tanh\theta b\,\tan\zeta b}{(fN-gM)\tanh\theta b - (gN+fM)\tan\zeta b} \right\}$$

— . . .

$$-FN\left\{\begin{array}{l}\dfrac{(M^2+N^2)(f^2+g^2)\tanh^2\theta b\tan^2\zeta b\left\{\dfrac{1}{\cosh\theta b\cos\zeta b}-1+\dfrac{g}{f}\tanh\theta b\tan\zeta b\right\}}{\cosh\theta b\cos\zeta b\left\{(fN-gM)\tanh\theta b-(gN+fM)\cdot\tan\zeta b\right\}} \\ \\ \dfrac{-\left(\dfrac{1}{f}\right)\tanh\theta b\tan\zeta b(f^2+g^2)(M\tanh\theta b-N\tan\zeta b)}{\left\{(fN-gM)^2\tanh^2\theta b-(fM+gN)^2\tan^2\zeta b\right\}} \\ \\ +\dfrac{(M^2+N^2)}{\cosh\theta b\cos\zeta b}(f^2+g^2)\tanh^2\theta b\tan^2\zeta b\end{array}\right\}$$

$$A_m = \frac{1}{f}(F - g D_m)$$

$$B_m = -C_m \cdot \frac{M}{N}$$

(VIII.2.23)

Thus the deflected form given by equation (VIII.2.14) is fully defined for the case of complex roots resulting from the relationship $D_{33}^2 < D_{11} D_{22}$

Therefore equations (VIII.2.13) and (VIII.2.23) fully characterize the solution of the orthotropic plate equation (VIII.2.1)

In the analysis for anticlastic curvature detailed in Appendix VIII.3 the cases of real and complex roots to the characteristic equation (VIII.3.11) give the groups of equations (VIII.3.14) and (VIII.3.17)/

(VIII.3.17) respectively.

The solution of these equations can be carried out in a manner identical to the above by considering appropriate terms in the equations of section VIII.2 above replaced by the corresponding terms of section VIII.3.

Thus ϕ and ψ are replaced by ζ and ξ

$\frac{4D_2}{(m\pi)^3 a^2}$ is replaced by $\nu_{21}\cdot\mu$

θ and ζ are replaced by χ and λ

The solution of the equations for the bending to an anticlastic surface of an orthotropic strip under a pure moment is therefore obtained as in the above analysis and the resultant forms are given in equations (VIII.3.15) and (VIII.3.18).

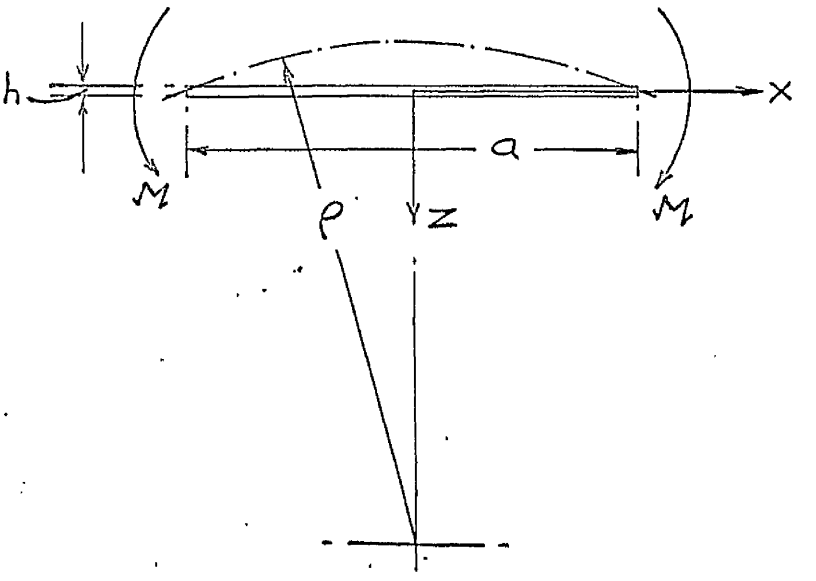

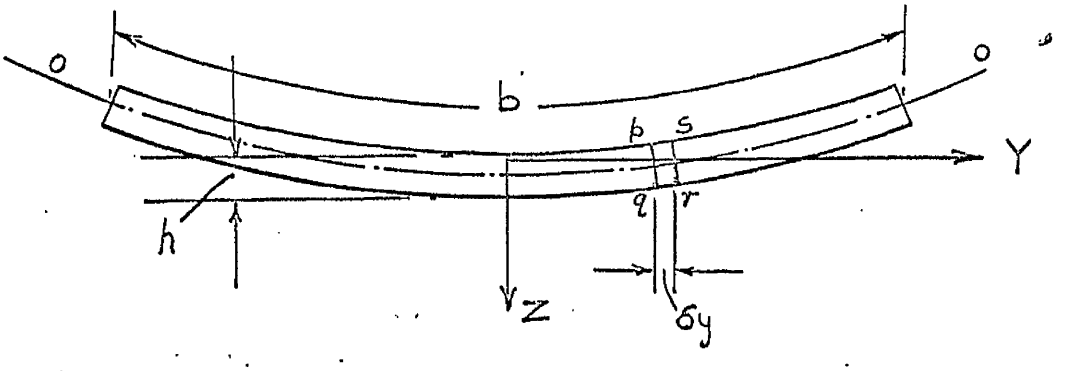

FIG.VIII.2 Distorted cross-section of an orthotropic plate under pure bending.

VIII.3. THE BENDING OF AN ORTHOTROPIC STRIP TO AN ANTICLASTIC SURFACE.

If an orthotropic strip of length a breadth b and thickness h is subjected to a uniform moment of intensity M per unit length across its ends, let it be assumed that the distorted cross-section is shown in Fig. VIII.2.

Assuming that the elastic properties of the plate material are given as:

E_{11} = Young's Modulus in the x-direction.

E_{22} = Young's Modulus in the y-direction.

ν_{12} = Poisson's Ratio relating an extensional strain in the x-direction to the corresponding strain in the y-direction.

ν_{21} = Poisson's Ratio relating an extensional strain in the y-direction to the corresponding strain in the x-direction.

In Fig. VIII.2 the neutral axis of longitudinal strain has been taken as the y-axis.

Consider the section $pqrs$ which as δy tends to zero becomes a rectangle whose centre of gravity will lie on the line O - O. Consider the stress distribution normal to the face $pqrs$ given by the/

the customary equation

$$\frac{\sigma_x}{z} = \frac{E_{11}}{\rho} \qquad \text{(VIII.3.1)}$$

As has been argued by Searle and Ashwell the longitudinal stresses over the faces of $pqrs$ are proportional to their distances from the neutral axis, therefore the average stress over the element will be the stress at the centre of gravity of the section. Thus the resultant force on $pqrs$ will be:

$$T = \frac{E_{11} \cdot z}{\rho} \cdot h \cdot \delta y \qquad \text{(VIII.3.2)}$$

where z is now the distance of the section centre line from the neutral axis.

As T will be tensile when z is positive, the longitudinal strip of which $pqrs$ is the cross-section is subjected to a nett tension if the centre of gravity is above the neutral axis and a nett compression if the centre of gravity is below the neutral axis. This strip is, however, bent to a radius ρ and by the analysis of Searle relating bending about the principal axis to circumferential tensions and compressions this bending has the effect of a nett pressure of magnitude P per unit length along the/

the plate where:

$$P = \frac{E_{11} \cdot z \cdot h \cdot \delta y}{\rho^2} \qquad \text{(VIII.3.3)}$$

This pressure tends to deflect the strip towards the neutral axis. This is the effect discussed by Searle when analysing the tendency for the anticlastic curvature to be neutralised.

Now consider cut across the plate a strip whose dimension in the direction of the x-axis is δa. This segment will be known as the "transverse strip" in contrast to the longitudinal strip whose cross-section is $pqrs$. As the plate bends under the moment M the transverse strip should develop a curvature of magnitude ν_{12}/ρ. However, as has been shown above, the development of this curvature is inhibited by the pressure developed longitudinally. This restriction of free development produces strains across the plate which in turn imply additional longitudinal strains. However, no longitudinal strains can occur other than those given by the relationship $\epsilon = z/\rho$ therefore the implied longitudinal strains must appear as changes in the longitudinal stresses. Assume that the usual bending theory for the transverse strip holds, i.e. that the transverse stress at any point is proportional/

proportional to distance from the neutral axis, which neutral axis will be the horizontal centre line of the cross-section of the transverse beam since a resultant transverse force cannot exist. This can only mean that the transverse stresses due to the change in curvature induced by the pressure variation along the transverse strip add up at any section to a pure moment or couple about this assumed neutral axis.

Therefore, along the neutral axis of the transverse strip, the strain is given by

$$E_{22}\epsilon = \sigma_y - \nu_{21}.\sigma_x = 0 \qquad \text{(VIII.3.4)}$$

but the bending moment M is given by

$$M = \int_{-h/2}^{h/2} \sigma_x . z . dz \qquad \text{(VIII.3.5)}$$

Therefore the couple acting on the transverse beam is given by

$$C = \int_{-\frac{h}{2}}^{\frac{h}{2}} \sigma_y . z . dz = \nu_{21} . M \qquad \text{(VIII.3.6)}$$

This suggests that the change in curvature of the transverse strip does not affect the magnitude of the nett force on the element $pqrs$, which force is therefore still represented by equation (VIII.3.2)./

(VIII.3.2). This means that the transverse beam is in effect a beam on an elastic foundation, the non uniformly distributed load of intensity $E_{\perp} z h \delta a / \rho^2$ per unit length transversely being proportional to z the distance of the centre line from the x-axis.

The author would at this point suggest that a solution for the anticlastic curvature of an orthotropic plate under uniform moment can be obtained as follows:

It has been shown in Section II.4 that the equations (II.4.4), (II.4.5) and (II.4.6) described the behaviour and boundary conditions of an orthotropic plate subjected to a general loading of intensity q. Thus from the above analysis the problem of the bending to an anticlastic surface of an orthotropic plate under a moment of intensity M can be approached through the solution for displacement of a transverse strip of such a plate subjected to a uniform moment of intensity $\nu_1 M$ and a non uniform pressure $E_{\perp} w h \delta a / \rho^2$ where w is the displacement of any point in the middle plane of the strip from the y-axis.

Therefore equation (II.4.4) yields the compatibility equation for such a strip of unit width to be

$$D_{11}\frac{\partial^4 w}{\partial x^4} + 2(D_{12}+2D_{66})\frac{\partial^4 w}{\partial x^2 \partial y^2} + D_{22}\frac{\partial^4 w}{\partial y^4} + \frac{E_{11} h w}{\rho^2} = 0 \qquad \text{(VIII.3.7)}$$

Considering the co-ordinate system for the strip to be as in Fig. II.4 the boundary conditions on the ends $y = 0, b$ are given by

$$D_{12}\frac{\partial^2 w}{\partial x^2} + D_{22}\frac{\partial^2 w}{\partial y^2} = \nu_{21} M$$

$$D_{22}\frac{\partial^3 w}{\partial y^3} + D_{12}\frac{\partial^3 w}{\partial x^2 \partial y} + 4D_{66}\frac{\partial^3 w}{\partial x \partial y^2} = 0 \qquad \text{(VIII.3.8)}$$

As the strip is bent into a cylindrical form of radius of curvature ρ it is suggested that the following transform in the x-direction is applicable.

$$w = \sum_{m=1,3,\ldots}^{\infty} Y_m \sin\frac{m\pi x}{a} \qquad \text{(VIII.3.9)}$$

Substitution of this form into the equation (VIII.3.7) gives the characteristic equation

$$\frac{d^4 Y_m}{dy^4} - 2\frac{D_{33}}{D_{22}}\left(\frac{m\pi}{a}\right)^2\frac{d^2 Y_m}{dy^2} + \left[\frac{D_{11}}{D_{22}}\left(\frac{m\pi}{a}\right)^4 + \frac{E_{11} h}{\rho^2 D_{22}}\right] Y_m = 0 \qquad \text{(VIII.3.10)}$$

It is important at this point to examine the ratio $E_{11} h / \rho^2 D_{22}$ and to rephrase it within the confines of the present "small deflection" analysis.

1. It can be readily shown from equations (II.1.7), (II.2.5) and (II.3.3) that $D_{11} = \frac{E_{11} h^3}{12(1-\nu_{12}.\nu_{21})}$

2. If a strip of length a and thickness h is bent by a moment M such that its central deflection is Hh its radius of curvature ρ is given by $\rho = a^2/8Hh$ where H is a constant

therefore $$\frac{E_{11} h}{\rho^2 D_{22}} = \frac{D_{11}}{D_{22}} \cdot \frac{96 H (1-\nu_{21}.\nu_{12})}{a^4}$$

Therefore equation (VIII.3.10) can be restated as :

$$\frac{d^4 Y_m}{dy^4} - 2\frac{D_{33}}{D_{22}}\left(\frac{m\pi}{a}\right)^2 \frac{d^2 Y_m}{dy^2} + \frac{D_{11}}{D_{22}}\left(\frac{m\pi}{a}\right)^4 \left[1 + \frac{96H(1-\nu_{21}.\nu_{12})}{(m\pi)^4}\right] Y_m = 0 \qquad \text{(VIII.3.11)}$$

The four roots of this equation $\pm\zeta$, $\pm\xi$ where

$$\zeta = \frac{m\pi}{a}.\frac{1}{\sqrt{D_{22}}}\left[D_{33} + \sqrt{D_{33}^2 - D_{11}D_{22}\left\{1 + \frac{96H(1-\nu_{12}.\nu_{21})}{(m\pi)^4}\right\}}\right]^{\frac{1}{2}}$$

$$\xi = \frac{m\pi}{a}.\frac{1}{\sqrt{D_{22}}}\left[D_{33} - \sqrt{D_{33}^2 - D_{11}D_{22}\left\{1 + \frac{96H(1-\nu_{21}.\nu_{12})}{(m\pi)^4}\right\}}\right]^{\frac{1}{2}} \qquad \text{(VIII.3.12)}$$

As in section II.5 it can be stated that there are three possible cases consistent with the actual values of D_{11} etc. Inspection will be made/

made of the two more important cases, namely, that of four real roots to the characteristic equation and that of four complex roots.

1. Four Real Roots.

The deflection w is given by the expression

$$w = \sum_{m=1,3,\ldots}^{\infty} \left(A_m \cosh \varsigma y + B_m \sinh \varsigma y + C_m \cosh \xi y + D_m \sinh \xi y \right) \sin \frac{m\pi x}{a} \qquad \text{(VIII.3.13)}$$

Substitution of this expression into the boundary conditions (VIII.3.8) gives the following simultaneous equations:

$$\gamma A_m + \delta C_m = \nu_{21} M$$

$$\phi B_m (\gamma - R) + \psi D_m (\delta - R) = 0$$

$$\gamma A_m \cosh \varsigma b + \gamma B_m \sinh \varsigma b + \delta C_m \cosh \xi b + \delta D_m \sinh \xi b = \nu_{21} M$$

$$\varsigma A_m (\gamma - R) \sinh \varsigma b + \varsigma B_m (\gamma - R) \cosh \varsigma b + \xi C_m (\delta - R) \sinh \xi b + \xi D_m (\delta - R) \cosh \xi b = 0$$

(VIII.3.14)

where $$\gamma = D_{22} \varsigma^2 - D_{12} \left(\frac{m\pi}{a} \right)^2$$

$$\delta = D_{22} \xi^2 - D_{12} \left(\frac{m\pi}{a} \right)^2$$

$$R = 4 D_{66} \left(\frac{m\pi}{a} \right)^2$$

The solution of the group of equations (VIII.3.14) is indicated in Appendix VIII.2. The expressions for A_m etc. are:

$$A_m = \frac{\nu_{21}.M}{\mathcal{H}}\left[\xi\gamma^2\sinh\zeta b\sinh\xi b + \zeta\delta^2(1+\cosh\zeta b-\cosh\xi b-\cosh\zeta b\cosh\xi b)\right]\xi\gamma$$

$$B_m = \frac{\nu_{21}.M}{\mathcal{H}}\left[\zeta\delta^2\sinh\zeta b(\cosh\xi b-1) - \xi\gamma^2\sinh\xi b(\cosh\zeta b-1)\right]\xi\gamma$$

$$C_m = \frac{\nu_{21}.M}{\delta\mathcal{H}}\left[\zeta^2\delta^4\sinh\zeta b\sinh\xi b + \zeta\delta^2\xi\gamma^2(1-\cosh\zeta b+\cosh\xi b-\cosh\zeta b\cosh\xi b)\right]$$

$$D_m = \frac{\nu_{21}.M}{\mathcal{H}}\left[\xi\gamma^2\sinh\xi b(\cosh\zeta b-1) - \zeta\delta^2\sinh\xi b(\cosh\zeta b\cosh\xi b-1)\right]\zeta\delta$$

(VIII.3.15)

where $\mathcal{H} = (\zeta^2\delta^4+\xi^2\gamma^4)\sinh\zeta b\sinh\xi b - 2\zeta\delta^2\xi\gamma^2(\cosh\zeta b\cosh\xi b-1)$

2. Four Complex Roots.

The deflection w is given by

$$w = \sum_{m=1,3,..}^{\infty}\left[(A_m\cos\lambda y + B_m\sin\lambda y)\cosh\chi y + (C_m\cos\lambda y + D_m\sin\lambda y)\sinh\chi y\right]\sin\frac{m\pi x}{a} \qquad \text{(VIII.3.16)}$$

where

$$\zeta = \chi \pm i\lambda \;;\quad \xi = -\chi \pm i\lambda$$

$$\chi = \frac{m\pi}{a}.\frac{D_{33}}{D_{22}} \;;\quad \lambda = \frac{m\pi}{a}.\frac{1}{D_{22}}\left[D_{33}^2 - D_{11}D_{22}\sqrt{1+\frac{96H(1-\nu_{12}.\nu_{21})}{(m\pi)^4}}\right]^{\frac{1}{2}}$$

Substitution of equation (VIII.3.16) into the boundary conditions (VIII.3.8) gives the following group of equations

$$A_m \cdot f + D_m \cdot g = \nu_{21} \cdot M_1$$

$$B_m \chi (f - R + 2D_{22}\lambda^2) + C_m \cdot \lambda (f - R - 2D_{22}\chi^2) = 0$$

$$A_m (f \cosh \lambda b \cos \chi b - g \sinh \lambda b \sin \chi b)$$

$$+ B_m (f \cosh \lambda b \sin \chi b + g \sinh \lambda b \cos \chi b)$$

$$+ C_m (f \sinh \lambda b \cos \chi b - g \cosh \lambda b \sin \chi b)$$

$$+ D_m (f \sinh \lambda b \sin \chi b + g \cosh \lambda b \cos \chi b) = \nu_{21} M_1$$

$$A_m \{(f-R)(\lambda \sinh \lambda b \cos \chi b - \chi \cosh \lambda b \sin \chi b) - g(\chi \sinh \lambda b \cos \chi b + \lambda \cosh \lambda b \sin \chi b)\}$$

$$+ B_m \{(f-R)(\chi \cosh \lambda b \cos \chi b + \lambda \sinh \lambda b \sin \chi b) - g(\chi \sinh \lambda b \sin \chi b - \lambda \cosh \lambda b \cos \chi b)\}$$

$$+ C_m \{(f-R)(\lambda \cosh \lambda b \cos \chi b - \chi \sinh \lambda b \sin \chi b) - g(\chi \cosh \lambda b \cos \chi b + \lambda \sinh \lambda b \sin \chi b)\}$$

$$+ D_m \{(f-R)(\chi \sinh \lambda b \cos \chi b + \lambda \cosh \lambda b \sin \chi b) - g(\chi \cosh \lambda b \sin \chi b - \lambda \sinh \lambda b \cos \chi b)\}$$

$$= 0 \qquad \text{(VIII.3.17)}$$

where $f = D_{22}(\lambda^2 - \chi^2) - D_{12}\left(\frac{m\pi}{a}\right)^2$

$$g = 2 \cdot \lambda \cdot \chi \cdot D_{22} \quad ; \quad R = 4D_{66}\left(\frac{m\pi}{a}\right)^2$$

The solution of the above equations is/

is indicated in Appendix VIII.2 which gives the following expressions for the constants A_m etc.

$$D_m = \frac{\sqrt{2}\,l.\,M}{K}\left\{\begin{array}{l} f(M^2+N^2)\,\dfrac{\tanh\lambda b\,\tan\chi b}{\cosh\lambda b\,\cos\chi b}\left\{\dfrac{1}{\cosh\lambda b\cos\chi b} - 1 + \left(\dfrac{g}{f}\right)\tanh\lambda b\,\tan\chi b\right\} \\ -(M\tanh\lambda b - N\tan\chi b)\left\{(fN-gM)\tanh\lambda b - (fM+gN)\tan\chi b\right\} \end{array}\right\}$$

$$C_m = \sqrt{2}\,l.\,M.\,N.\left\{\begin{array}{l} \dfrac{1}{L}\left\{\dfrac{1}{\cosh\lambda b\cos\chi b} - 1 + \left(\dfrac{g}{f}\right)\tanh\lambda b\,\tan\chi b\right\} \\ -\dfrac{1}{K}\left\{\dfrac{(M^2+N^2)(f^2+g^2)\tanh^2\lambda b\,\tan^2\chi b\left\{\dfrac{1}{\cosh\lambda b\cos\chi b} - 1 + \left(\dfrac{g}{f}\right)\tanh\lambda b\,\tan\chi b\right\}}{\cosh\lambda b\,\cos\chi b\left[(fN-gM)\tanh\lambda b - (gN+fM)\tan\chi b\right]}\right. \\ \left. -\dfrac{1}{f}\tanh\lambda b\,\tan\chi b\,(f^2+g^2)(M\tanh\lambda b - N\tan\chi b)\right\} \end{array}\right\}$$

$$A_m = \frac{\sqrt{2}\,l.\,M}{f} - \frac{g\,D_m}{f}$$

$$B_m = -C_m.\frac{M}{N}$$

(VIII.3.18)

where $M = \lambda(f - R - 2D_{22}\chi^2)$

$N = \chi(f - R + 2D_{22}\lambda^2)$

$L = (fN-gM)\tanh\lambda b - (fM+gN)\tan\chi b$

$K = (fN-gM)^2\tanh^2\lambda b - (fM+gN)^2\tan^2\chi b + (M^2+N^2)(f^2+g^2)\,\dfrac{\tanh^2\lambda b\,\tan^2\chi b}{\cosh\lambda b\,\cos\chi b}$

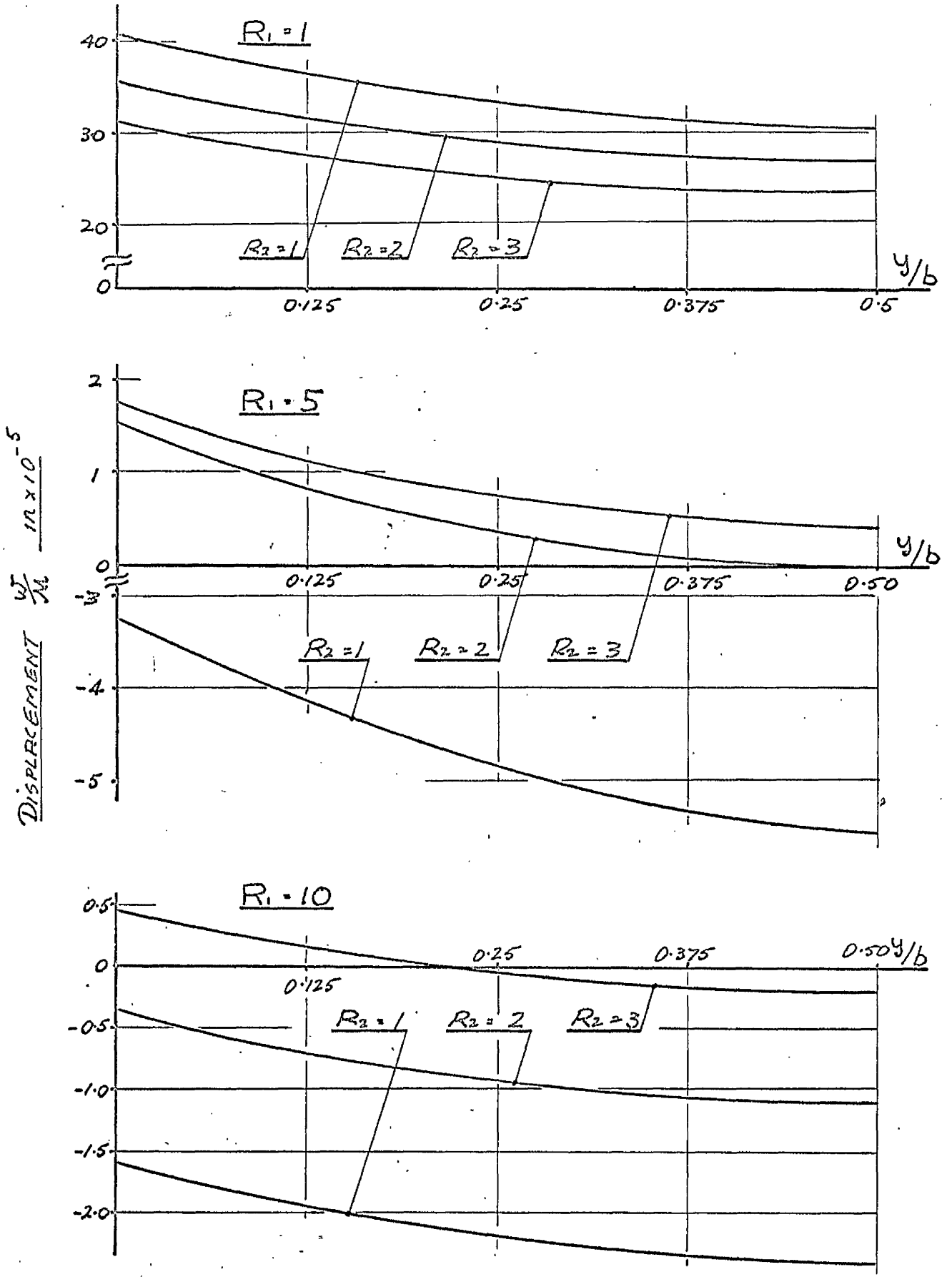

FIG.VIII.3 Cross-section deformation at x = a/2

D_{22} = 300 a/b = 4

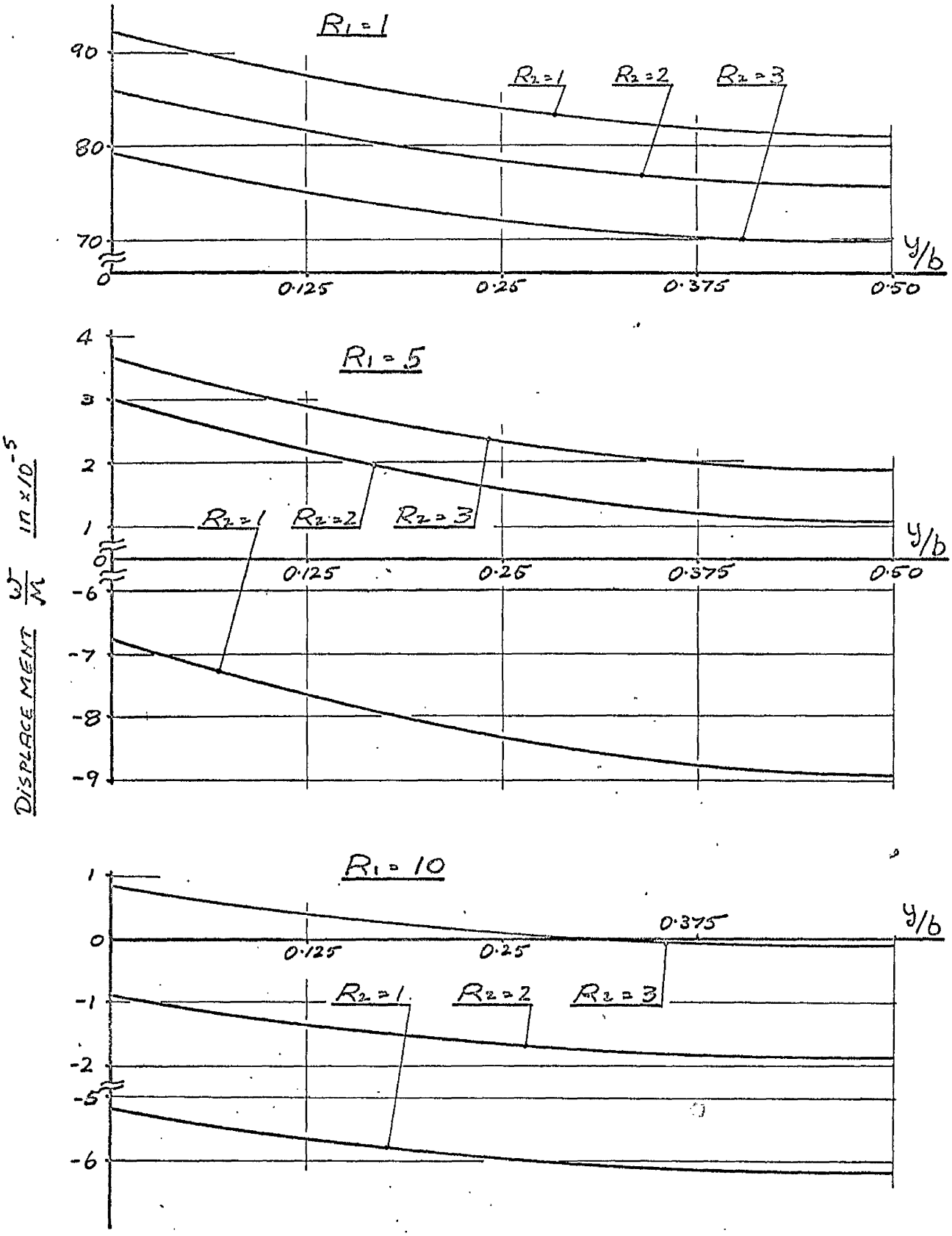

FIG.VIII.4 Cross-section Deformation at x = a/2

D_{22} = 300 a/b = 6

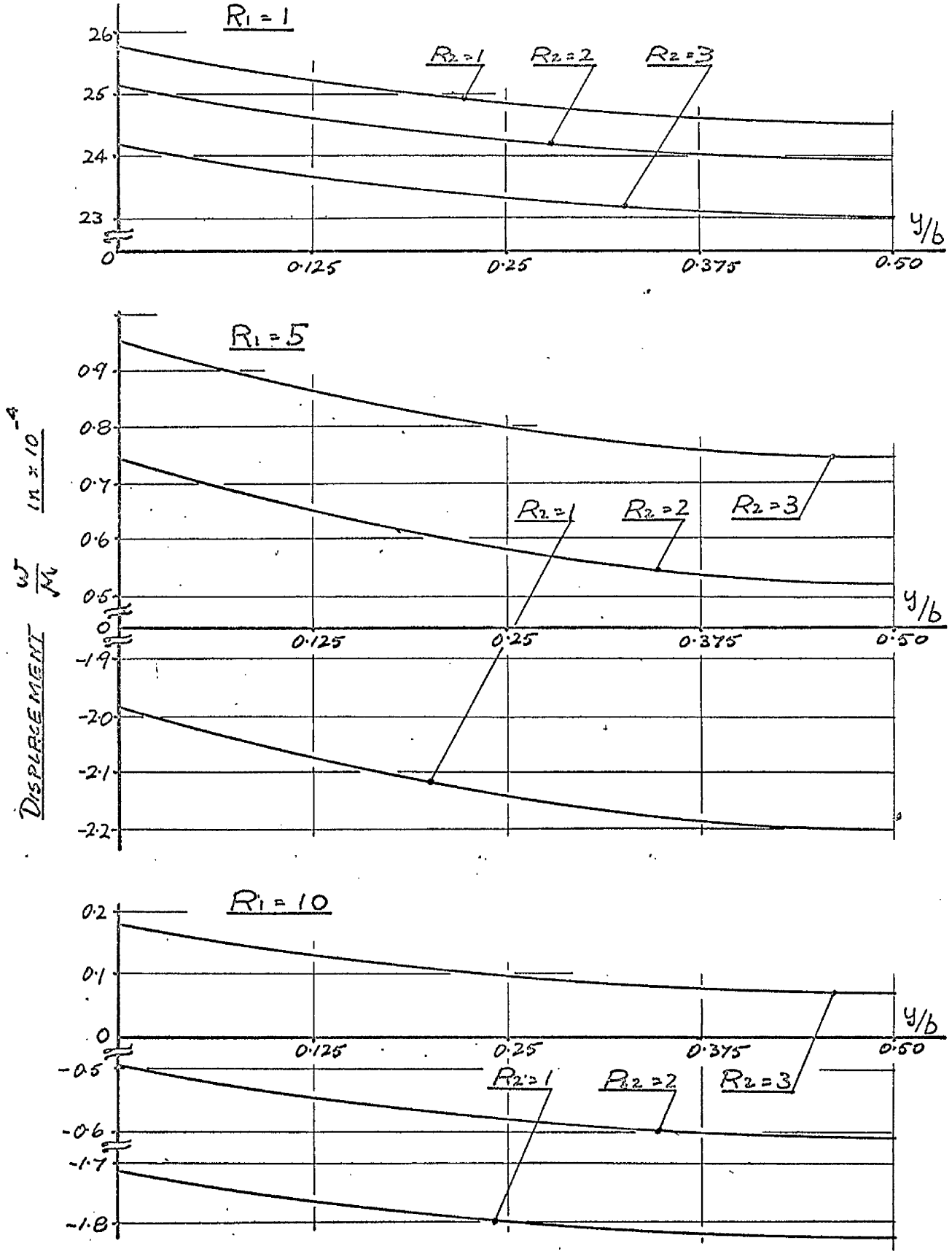

FIG.VIII.5 Cross-section deformation at x = a/2

D_{22} = 300 a/b = 10

It is seen from the above derivation and analysis that the anticlastic behaviour of an orthotropic strip under a constant moment can be obtained for a variety of central deflections defined as a constant H times the plate thickness. In the following discussion the above expressions are used to obtain for a value of H = 0.125 the deflected form for a variety of stiffnesses and aspect ratio.

Figs. VIII.3, VIII.4 and VIII.5 show the variation of the displacement w across the strip for three values of the ratios R_1, R_2 and a/b. The values shown are for the value of m equal to unity, i.e., the first term only of the infinite series for w. The convergence of the equation for w is discussed in Appendix VIII.5 and it can be stated that the utilisation of the first term only of the infinite series is adequate to describe the cross-section distortion of a strip subjected to pure moment. All the graphs were drawn considering the strip bent by a positive value of moment M giving for the principal strip a deflected form convex downwards. Thus a positive value of the displacement w indicates distortion away from the centre of principal curvature and a negative value of the displacement is indicative/

indicative of distortion towards this centre. It is convenient to examine the mode of distortion by discussing the effect on this distortion of variation of each of the parameters $R_1 = D_{11}/D_{22}$, $R_2 = D_{66}/D_{22}$ and the length to breadth ratio a/b.

For a constant value of R_1 increase of the ratio a/b causes the magnitude of the distortion at any section from the cylindrical form of radius ρ to increase. However, the variation of this distortion across the plate decreases with increasing a/b that is, the statements of LAMB and SEARLE that the cross-section of the strip becomes progressively flatter as the length to breadth ratio is increased is confirmed for an orthotropic plate. Also, for fixed values of the ratios R_1 and a/b increase of the ratio R_2 depresses the magnitude of the distortion but alters the variation across the strip by a negligible amount.

For a value of R_1 of unity the distortion of the cross-section is positive, that is, the displacement is away from the centre of principal curvature. This agrees with the experimental work carried out by ASHWELL on isotropic plates and can be stated to be/

be due to the relative dominance of the effect of the couple $\nu_{21} M$ on the distorted cross-section. However, as R_1 increases the overall effect of this couple $\nu_{21} M$ diminishes and that due to the non-uniform pressure $E_{11} h w / \rho^2$ in consequence increases. Thus the strip is distorted more towards the centre of principal curvature than hitherto and the actual magnitude of the distortion increases.

Increase in the value of R_2 for any value of R_1 other than unity has the effect of increasing the magnitude of the distortion at any section away from the centre of principal curvature. This is not readily explained without reference to the solution of equation (VIII.3.11) and careful examination of the roots. It can briefly be stated, however, that an increase in the value of D_{66} for a fixed ratio R_1 causes the value of the root ξ of equation (VIII.3.12) to decrease faster than the rate at which the root ζ increases. This in turn causes the constants A_m and B_m and thence the terms $A_m \cosh \zeta y$ and $B_m \sinh \zeta y$ to dominate the expressions for the displacement w. As the terms involving A_m and B_m are always positive, while those involving C_m and D_m alternate in sign and decrease faster than those containing/

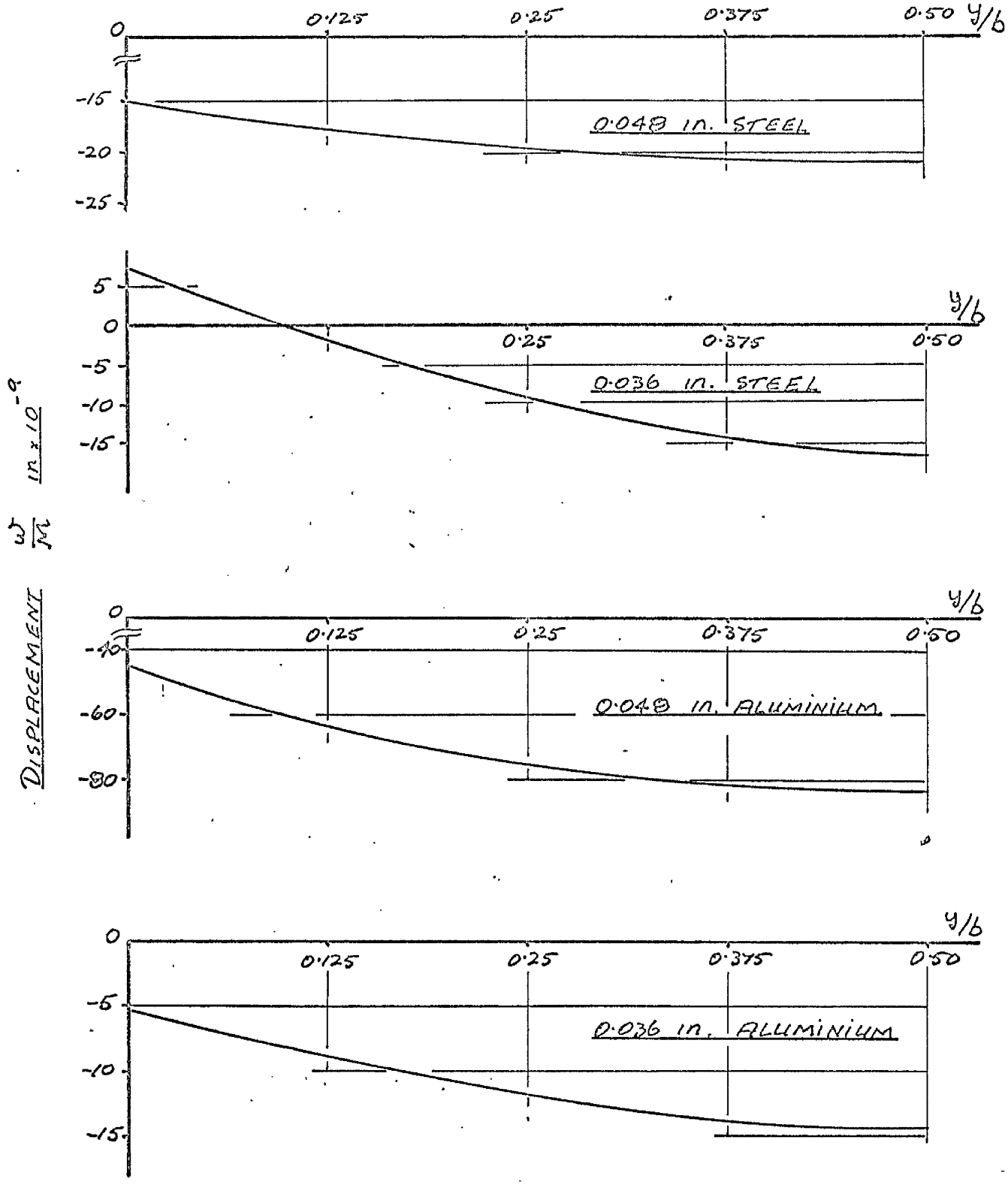

FIG.VIII.6 Cross-section deformation at x = a/2

Test beams a/b = 9.885

containing A_m and B_m the value of the displacement w becomes more positive as R_2 increases.

Thus, although the present theoretical investigation has not been as exhaustive as that carried out by LAMB and SEARLE on isotropic plates, it can readily be seen that all the salient points that they derive for isotropic plates are relevant to the behaviour of orthotropic plates under pure bending.

Fig. VIII.6 gives the curves for the actual experimental beams of Chapter III, these beams having a ratio $a/b = 9.885$. These curves are as would be expected from the above analysis, namely, those beams with the lower values of R_2 exhibit the largest negative value of deviation from the cylindrical form.

The actual beams were $2\frac{1}{2}$ in. deep and from Figs, VIII.12 and VIII.13 the end load to give a central deflection of 0.3125 in. for each beam can be found.

For 0.048 in. thick steel this load is 54.25 lbf.

Beam	Central Distortion ins. x 10^{-6}	Half Width Distortion ins. x 10^{-6}
0.048" steel	24.01	6.92
0.036" steel	13.92	20.25
0.048" alum.	27.70	11.40
0.036" alum.	360.3	225.5

TABLE VIII.1(a) $\nu_{21} = \nu_{12} (D_{22}/D_{11})$

Beam	Central Distortion inches	Half Width Distortion inches
0.048" steel	0.3877	0.1628
0.036" steel	0.2855	0.1150
0.048" alum.	0.1618	0.1650
0.036" alum.	0.4780	0.2800

TABLE VIII.1(b) $\nu_{21} = \nu_{12}$

The bending moment M is 54.25 x 1.75 x 12 = 1139.25 lbf.in.

From Fig. VIII.6 the distortion at the beam centre is 24.01 x 10^{-6} in. i.e. this is the distortion from the cylindrical form of radius ρ .

Also from Fig. VIII.6 the distortion across half the beam width is 6.92 x 10^{-6} in.

This calculation has been carried out for each beam specimen and the salient results are given in Table VIII.1(a).

It is readily seen that these distortions would not be detected by dial gauges nor indeed would they have any significant bearing on a calculation based on the assumption that the beam is bent into a cylindrical form of radius $\rho = a^2/8Hh$

As has already have mentioned in the Critical Review sections I.1 and I.3, and in the Theoretical Analysis section II.6, a point of discussion among previous writers has been the application of the Maxwell Reciprocal relationships to the study of orthotropic plates, in particular to the identity $a_{12} = a_{21}$

From equation (II.3.3) assuming these relationships to hold $a_{12} = -\frac{\nu_{12}}{E_{11}} = -\frac{\nu_{21}}{E_{22}}$

$$\text{i.e.} \quad \nu_{21} = \nu_{12} \cdot \frac{E_{22}}{E_{11}} = \nu_{12} \cdot \frac{D_{22}}{D_{11}} \qquad \text{(VIII.3.19)}$$

For the beam specimens described in Chapter III and using the above analysis for anticlastic curvature it is possible to evaluate the distortion of the cross-section assuming equation (VIII.3.19) is not true.

For each beam the value of the Poisson's Ratio ν_{12} has been taken as that for the unformed plate material, i.e. 0.28 and 0.33 for steel and aluminium respectively. As shown in Appendix VIII.4 this gives values of ν_{21} of 21.42×10^{-6}, 9.802×10^{-6}, 35.86×10^{-6}, and 17.26×10^{-6} for 0.048 in. and 0.036 in. thick steel and aluminium respectively.

However, if equation (VIII.3.19) does not hold, the rational alternative for the light gauge beams considered would be that $\nu_{21} = \nu_{12} = 0.28$ or 0.33 the Poisson's Ratios for the unformed beam materials.

It is therefore relevant to compute the/

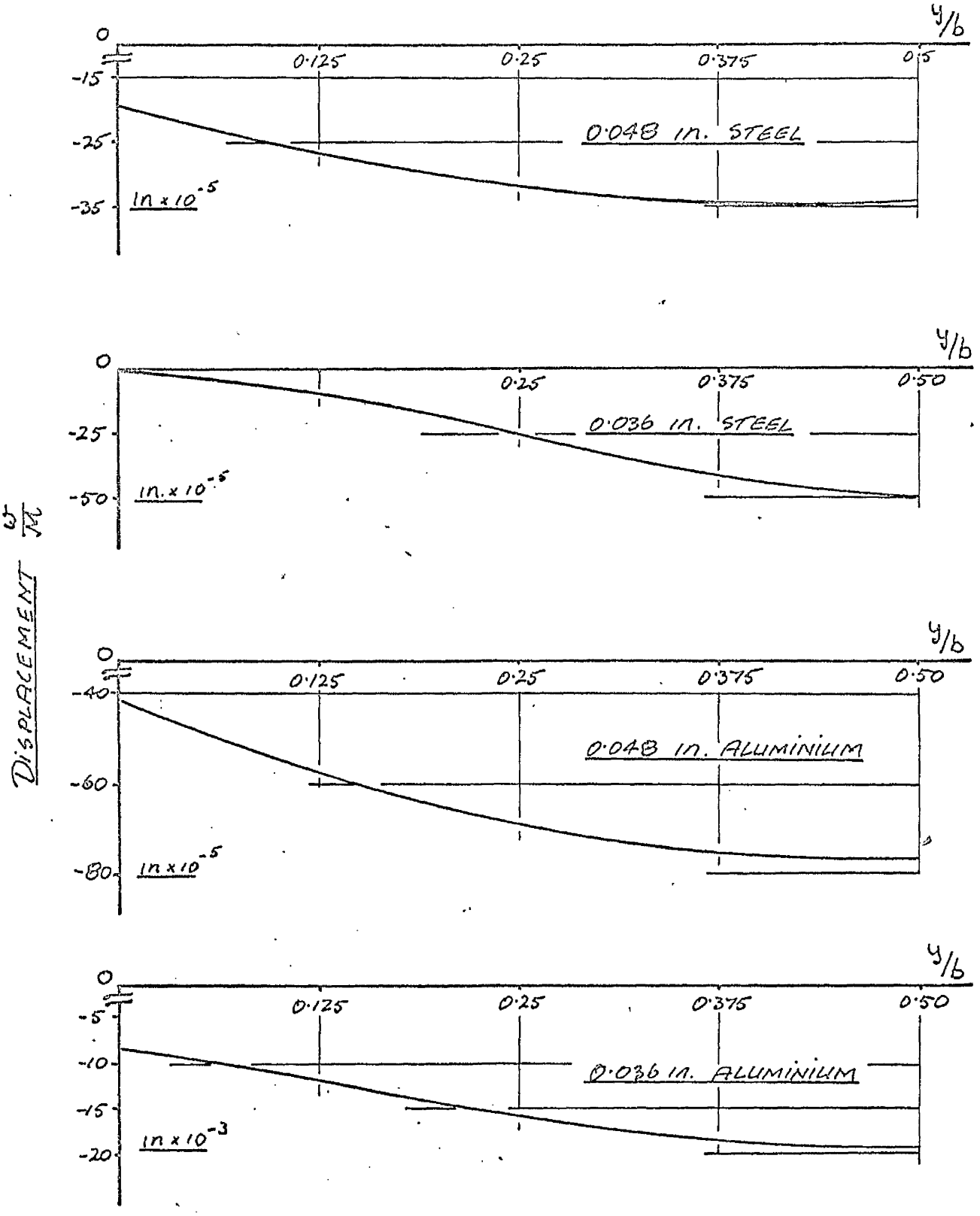

FIG.VIII.7 Cross-section deformation at x = a/2

Assumes $\nu_{21} = \nu_{12}$

the constants given by (VIII.3.18) for this case and subsequently from (VIII.3.16) obtain the distortion across the beam cross-section.

Fig. VIII.7 gives the results for this computation of the distorted cross-section of the beams.

For the 0.048 in. steel the distortion at the beam centre is therefore $1139.25 \times 34 \times 10^{-5} =$ 0.3877 inches.

Also the distortion across half the beam width is 0.1628 in.

Values for the other specimens are shown in Table VIII.1(b).

The implications of the magnitudes of these distortions across the cross-section are that there would be considerable rotation and displacement of the beam edges. For a beam characterized by the stiffness values obtained for 0.048 in. thick steel, the analysis indicates that a rotation across the beam from edge to edge of some $12\frac{1}{2}^{o}$ of arc would be evident.

This is at variance with the experimental work reported in Chapter III and commented upon in Chapter IV where it was stated that no such effect transpired during the bending tests to determine a_{11} even at high values of applied moment.

The author therefore concludes that for the plates considered in this thesis, the assumption $a_{12} = a_{21}$ which implies the relationship (VIII.3.19) between the two Poisson's Ratios, is correct.

VIII.4. THE CALCULATION OF THE ELASTIC MODULI AND STIFFNESSES.

In the following sections, full details are given for the calculation of the moduli and stiffnesses for plates formed from 0.048 in. thick steel sheet, the moduli and stiffnesses for the other types of plates considered being presented in Table VIII.2.

The Calculation of the modulus a_{22}: for the co-ordinate system used for this test - shown in Fig. III.2, the points (1) and (5) have the co-ordinates $(-y, 0)$ and $(y, 0)$ respectively. Thus, from equation (II.3.2) the deflection w of these points relative to that of the central point (9) is given by:

$$w = -\frac{\sigma_y}{h} \cdot a_{22} \cdot y^2 \text{ in.}$$

since, for an orthotropic plate $a_{16} = a_{26} = 0$

For the bending configuration described

$$\sigma_y = -6 \cdot \frac{M_y}{h^2} \text{ lbf/in}^2$$

where M_y is the moment intensity acting on a plane parallel to the x-axis.

From Fig. III.2 $M_y = \frac{6}{7} \cdot P \ \frac{in\ lbf}{in}$

$$\therefore a_{22} = \frac{7 \cdot w \cdot h^3}{36 \cdot P \cdot y^2} \cdot in^2/lbf$$

For the plates and points considered $y = 6$ in. and the values of the average deflection $w = \frac{1}{2}(w_1 + w_5)$ for increasing values of P are graphed in Figs. VIII.8 and VIII.9.

For 0.048 in. steel the computed equations to the three sets of experimental values are

$$P = 12.046\,w + 0.06707$$
$$P = 11.655\,w - 0.06318$$
$$P = 11.865\,w + 0.00655$$

Taking from these an average of the three gradients P/w, a_{22} can be calculated as:

$$a_{22} = \frac{7h^3}{36^2 \cdot 11.865} = \frac{455.61 \times 10^{-6} h^3}{} \ in^2/lbf$$

The Calculation of the modulus a_{66}: the co-ordinate system used in this test is given in Fig. III.9, the points (2), (4), (6) and (8) respectively having the co-ordinates $(-x, y)$, (x, y) $(x, -y)$ and $(-x, -y)$

Therefore, for the points (4) and (8) and (2) and (6) respectively with a twisting moment M_{xy} only acting, equation (II.3.2) reduces to

$$w - \tfrac{1}{2}(w_4 + w_8) = -\frac{z_{xy}}{h} \cdot a_{66} \cdot xy \text{ in.}$$

$$w = \tfrac{1}{2}(w_2 + w_6) = \frac{z_{xy}}{h} \cdot a_{66} \cdot xy \text{ in}$$

$$\text{where } z_{xy} = -6\frac{M_{xy}}{h^2} \text{ lbf/in}^2$$

From Fig. III.6 $M_{xy} = (3/7)P$

$$\therefore a_{66} = \frac{7 \cdot w \cdot h^3}{36 \cdot P \cdot xy}$$

where for the plates considered x = y = 6 in. and the values of the deflection $w = \tfrac{1}{2}(w_4 + w_8) - \tfrac{1}{2}(w_2 + w_6)$ for increasing values of P are graphed in Figs. VIII.10 and VIII.11.

For 0.048 in. steel the computed equations to the three sets of experimental values are

$$P = 16.181\,w - 0.17867$$

$$P = 15.741\,w + 0.00083$$

$$P = 16.126\,w - 0.07164$$

Averaging the three gradients (P/w), a_{66} can be calculated as:

$$a_{66} = \frac{7h^3}{36^2 . 16.016} = \underline{337.24 \times 10^{-6} h^3 \text{ in}^2/\text{lbf.}}$$

The Calculation of the modulus a_{11}: Figs. VIII.12 and VIII.13 indicate the experimental values obtained from the bending tests performed to obtain the modulus a_{11}

From equations (II.3.3) $a_{11} = \frac{1}{E_{11}}$

For a beam bending a pure moment M

$$E_{11} I_{11} = \frac{M d^2}{2w}$$

where w is the lateral deflection between two points on the beam a distance $2d$ apart, E_{11} and I_{11} being the Young's Modulus and second moment of area for the principal direction x.

For the beams described in Section III.1 the dial gauges labelled (2) and graphed in Figs. VIII.12 and VIII.13 were positioned 2 feet from the centre of the beam, the deflection of centre being read on the dial gauge (1).

The computed equation from the three sets of experimental values relating load P and deflection/

deflection w are for gauge (1) of the 0.048 in. steel beams.

$$P = 1.6916\, w \times 10^3 + 1.9996$$
$$P = 1.6304\, w \times 10^3 + 2.1425$$
$$P = 1.6385\, w \times 10^3 + 2.2664$$

and for the experimental values of the gauges (2) the computed equations are:

$$P = 5.6685\, w \times 10^3 + 6.6292$$
$$P = 5.3008\, w \times 10^3 + 6.8677$$
$$P = 5.4098\, w \times 10^3 + 6.6825$$

Taking an average of each of the gradients (P/w) the rate of change of deflection $w_{①}$ and $w_{②}$ over the half length d for a given value of P can be determined as:

$$w_{①} = (P/1.6535) \times 10^{-3} = 0.60478\, P \times 10^{-3} \text{ ins.}$$
$$w_{②} = (P/5.4597) \times 10^{-3} = 0.18316\, P \times 10^{-3} \text{ ins.}$$
$$\therefore a_{11} = \frac{1}{E_{11}} = \frac{2(w_{①} - w_{②})I_{11}}{P x . d^2}$$

where x is the moment arm of the load P carried by a 6 in. wide beam.

In the tests described in Chapter III/

Chapter III

$$x = 21 \text{ in} \quad , \quad d = 24 \text{ in.}$$

$$\therefore a_{11} = \frac{2.I_{11}.6.0.42162 \times 10^{-3}}{21.24^2}$$

$$= \underline{0.41827 \times 10^{-7} I_{11}} \text{ in}^2/\text{lbf.}$$

The Calculation of the Stiffnesses: considering as above the 0.048 in. steel specimen.

From equation (II.3.3)

$$E_{22} = \frac{1}{a_{22}} = 2194.9\, h^{-3} \text{ lbf/in}^2$$

$$E_{11} = \frac{1}{a_{11}} = 2.3908 \times 10^6 / I_{11} \text{ lbf/in}^2$$

Observing the normal relationships for orthotropic plates

$$D_{12} = D_{21} = \frac{\nu_{21}.E_{11}.h^3}{12(1-\nu_{21}.\nu_{12})} = \frac{\nu_{12}.E_{22}.h^3}{12(1-\nu_{21}.\nu_{12})}$$

$$\therefore \nu_{21}.E_{11}.I_{11} = \nu_{12}.E_{22}.\frac{h^3}{12}$$

For the specimens considered in this thesis ν_{12} is taken as the Poisson's Ratio for the beam/

Constant	0.048" steel	0.036" steel	0.048" alum.	0.036" alum.
a_{11} in^2/lbf	$0.41827 \times 10^{-6} I_{\parallel}$	$0.54136 \times 10^{-6} I_{\parallel}$	$1.4055 \times 10^{-6} I_{\parallel}$	$1.8854 \times 10^{-6} I_{\parallel}$
a_{22} in^2/lbf	$455.61 \times 10^{-6} h^3$	$1292.0 \times 10^{-6} h^3$	$1077.0 \times 10^{-6} h^3$	$3003.1 \times 10^{-6} h^3$
a_{66} in^2/lbf	$337.24 \times 10^{-6} h^3$	$635.24 \times 10^{-6} h^3$	$1182.7 \times 10^{-6} h^3$	$2233.5 \times 10^{-6} h^3$
E_{11} lbf/in^2	$2.3908 \times 10^{6} / I_{\parallel}$	$1.8472 \times 10^{6} / I_{\parallel}$	$0.71486 \times 10^{6} / I_{\parallel}$	$0.53039 \times 10^{6} / I_{\parallel}$
E_{22} lbf/in^2	$2194.9\ h^{-3}$	$776.03\ h^{-3}$	$932.26\ h^{-3}$	$333.02\ h^{-3}$
G_{66} lbf/in^2	$2975.6\ h^{-3}$	$1576.1\ h^{-3}$	$845.60\ h^{-3}$	$447.14\ h^{-3}$
D_{11} $lbf.in$	2.3908×10^{6}	1.8472×10^{6}	0.71486×10^{6}	0.53039×10^{6}
D_{22} $lbf.in$	182.91	64.669	77.689	27.752
D_{12} $lbf.in$	51.215	18.107	25.637	9.1581
D_{66} $lbf.in$	247.13	132.17	70.467	37.262
D_{33} $lbf.in$	545.475	282.447	166.571	83.682
ν_{12}	0.28	0.28	0.33	0.33
ν_{21}	21.42×10^{-6}	9.802×10^{-6}	35.86×10^{-6}	17.26×10^{-6}

TABLE VIII.2 - Constants for actual plates.

beam material, i.e. ν_{12} = 0.28 and 0.33 for steel and aluminium respectively.

$$\therefore \nu_{21} = \frac{0.28 \cdot 2194.9}{12 \cdot 2.3908 \times 10^6} = 21.42 \times 10^{-6}$$

$$\therefore 1 - \nu_{12} \cdot \nu_{21} = 0.999994$$

$$\therefore D_{11} = \frac{h^3 \cdot E_{22}}{12\,(1 - \nu_{12} \cdot \nu_{21})} = \underline{182.91}\ \text{lbf.in}$$

$$D_{12} = \nu_{12} \cdot D_{22} = \nu_{21} \cdot D_{11} = \underline{51.215}\ \text{lbf.in}$$

$$D_{66} = \frac{h^3}{12} \cdot G_{66} = \frac{h^3}{12} \cdot \frac{1}{q_{66}} = \underline{247.13}\ \text{lbf.in}$$

$$D_{33} = D_{12} + 2D_{66} = \underline{545.475}\ \text{lbf.in}$$

Table VIII.2 gives the complete range of values of the derived moduli and stiffnesses.

VIII.5. DETAILS OF THE NUMERICAL WORK.

The numerical work carried out in the thesis will be represented here by reference to 0.048 in. thick steel.

For this material the Poisson's Ratio $\nu_{12} = 0.28$.

The ratio $D_{33}^2 / D_{11} D_{22}$ defines the mode of solution of the behaviour equation.

$$\frac{d^4 Y_m}{dy^4} - 2\frac{D_{33}}{D_{22}}\left(\frac{m\pi}{a}\right)^2 \frac{d^2 Y_m}{dy^2} + \frac{D_{11}}{D_{22}}\left(\frac{m\pi}{a}\right)^4 Y_m = 0 \qquad \text{(VIII.5.1)}$$

where the roots of the equation are $\pm\phi$, $\pm\psi$

$$\phi = \frac{m\pi}{a}\frac{1}{\sqrt{D_{22}}}\left\{D_{33} + \sqrt{D_{33}^2 - D_{11}D_{22}}\right\}^{\frac{1}{2}}$$

$$\psi = \frac{m\pi}{a}\frac{1}{\sqrt{D_{22}}}\left\{D_{33} - \sqrt{D_{33}^2 - D_{11}D_{22}}\right\}^{\frac{1}{2}} \qquad \text{(VIII.5.2)}$$

For real roots $D_{33}^2 < D_{11} D_{22}$ this implies that:

for $\frac{D_{66}}{D_{22}} = 1$; $\frac{D_{11}}{D_{22}} < 5.1984$ for real roots

for $\frac{D_{66}}{D_{22}} = 2$; $\frac{D_{11}}{D_{22}} < 18.3186$ for real roots

for $\frac{D_{66}}{D_{22}} = 3$; $\frac{D_{11}}{D_{22}} < 39.4384$ for real roots

since $D_{33} = D_{12} + 2D_{66} = \nu_{12} \cdot D_{22} + 2D_{66}$

From section II.5 the moments etc. throughout an orthotropic plate are:

$$M_x = -\left(D_{11} \frac{\partial^2 w}{\partial x^2} + D_{12} \frac{\partial^2 w}{\partial y^2} \right)$$

$$M_y = -\left(D_{12} \frac{\partial^2 w}{\partial x^2} + D_{22} \frac{\partial^2 w}{\partial y^2} \right)$$

$$R_x = -\left[D_{11} \frac{\partial^3 w}{\partial x^3} + (D_{12} + 4D_{66}) \frac{\partial^3 w}{\partial x \partial y^2} \right]$$

$$Q_y = -\left[D_{22} \frac{\partial^3 w}{\partial y^3} + (D_{12} + 2D_{66}) \frac{\partial^3 w}{\partial x^2 \partial y} \right]$$

$$Q_x = -\left[D_{11} \frac{\partial^3 w}{\partial x^3} + (D_{12} + 2D_{66}) \frac{\partial^3 w}{\partial x \partial y^2} \right]$$

$$M_{xy} = -2 D_{66} \left(\frac{\partial^2 w}{\partial x \partial y} \right) \qquad \text{(VIII.5.3)}$$

Any discussion of the convergence of the assumed series for deflection w and the above quantities can be resolved into that of an examination of the terms. w, $\frac{\partial^2 w}{\partial y^2}$, $\frac{\partial^3 w}{\partial y^3}$, $\frac{\partial^3 w}{\partial x^2 \partial y}$. This being due to the assumed sinusoidal form for deflection in the direction x .

For ease of computation the dimensions were/

were considered to be:

the plate length, defined by $x = 0, a/b$

the plate breadth, defined by $y = 0, 1$

1. Real Roots.

Thus from section II.5 for real roots the plate deflection is given by

$$w = \frac{q(a/b)}{D_{11}} \sum_{m=1,3,..}^{\infty} \left[\frac{4}{(m\pi)^5} + A_m \cosh \phi y + B_m \sinh \phi y + C_m \cosh \psi y + D_m \sinh \psi y \right] \sin \frac{m\pi x}{(a/b)}$$

$$\frac{\partial^2 w}{\partial y^2} = \frac{q(a/b)}{D_{11}} \sum_{m=1,3,..}^{\infty} \left[\phi^2 A_m \cosh \phi y + \phi^2 B_m \sinh \phi y + \psi^2 C_m \cosh \psi y + \psi^2 D_m \sinh \psi y \right] \sin \frac{m\pi x}{(a/b)}$$

$$\frac{\partial^3 w}{\partial y^3} = \frac{q(a/b)}{D_{11}} \sum_{m=1,3,..}^{\infty} \left[\phi^3 A_m \sinh \phi y + \phi^3 B_m \cosh \phi y + \psi^3 C_m \sinh \psi y + \psi^3 D_m \cosh \psi y \right] \sin \frac{m\pi x}{(a/b)}$$

$$\frac{\partial^3 w}{\partial x^2 \partial y} = -\frac{q(a/b)(m\pi)}{D_{11}(a/b)^2} \sum_{m=1,3,..}^{\infty} \left[\phi A_m \sinh \phi y + \phi B_m \cosh \phi y + \psi C_m \sinh \psi y + \psi D_m \cosh \psi y \right] \sin \frac{m\pi x}{(a/b)}$$

(VIII.5.4)

For the above expressions, the constants A_m etc. are those obtained by substitution of the quantities D_{11} etc. and the plate dimensional ratio/

$D_{11}/D_{22} = 1$; $D_{66}/D_{22} = 1$

Constant	m = 1	m = 3	m = 5
$4/(m\pi)^5$	$0.13071053 \times 10^{-1}$	$0.53790350 \times 10^{-4}$	$0.41827367 \times 10^{-5}$
A_m	$0.90560120 \times 10^{-3}$	$0.37266974 \times 10^{-5}$	$0.28979771 \times 10^{-6}$
B_m	$-0.89165650 \times 10^{-3}$	$-0.37222782 \times 10^{-5}$	$-0.28943303 \times 10^{-6}$
C_m	$0.14049000 \times 10^{-3}$	$0.57347000 \times 10^{-6}$	$0.45402000 \times 10^{-7}$
D_m	$-0.46712209 \times 10^{-4}$	$-0.19500316 \times 10^{-6}$	$-0.15162866 \times 10^{-7}$

$D_{11}/D_{22} = 10$; $D_{66}/D_{22} = 2$

Constant	m = 1	m = 3	m = 5
A_m	$0.63340250 \times 10^{-3}$	$0.26206551 \times 10^{-5}$	$0.20378747 \times 10^{-6}$
B_m	$-0.56781360 \times 10^{-3}$	$-0.23263478 \times 10^{-5}$	$-0.18089136 \times 10^{-6}$
C_m	$-0.62782650 \times 10^{-3}$	$-0.26703960 \times 10^{-5}$	$-0.20768290 \times 10^{-6}$
D_m	$0.20850698 \times 10^{-3}$	$0.85425870 \times 10^{-6}$	$0.66425170 \times 10^{-7}$

TABLE VIII.3. Constants

Real Roots.

ratio (a/b) into equations (II.5.11). Table VIII.3 gives the values computed for two cases of real roots, namely,

(1) $D_{11}/D_{22} = 1$, $D_{66}/D_{22} = 1$

(2) $D_{11}/D_{22} = 10$, $D_{66}/D_{22} = 2$

where for 0.048 in. thick steel $D_{22} = Eh^3/12(1-\nu^2)$

$= 300$ lbf.in.

Thus from equations (VIII.5.2), for (1) above

$$\phi = 1.595\, m\pi \qquad \psi = 0.3595\, m\pi$$

At the plate centre, y = 0.5. Thus considering the successive values of ϕy for increasing m

m = 1 $\phi y = 0.7975\pi$ $= 0.80\pi$ say, for convenience in reading values from tables

$\therefore \cosh \phi y = 6.21314$, $\sinh \phi y = 6.13214$

m = 3 $\cosh \phi y = 911.65311$, $\sinh \phi y = 911.65256$

m = 5 $\cosh \phi y = 138941.39538$ 55129

$\sinh \phi y = 138941.39538$ 19142

$D_{11}/D_{22} = 1$; $D_{66}/D_{22} = 1$; $\bar{D} = D_{22}/q\,(a/b)^4$

Quantity	$\sum m = 1$	$\sum m = 1,3$	$\sum m = 1,3,5$	Position
$w \times \bar{D} \times 10^3$	13.39	13.36	13.37	$x = a/2$
$M_x \times \bar{D}$	23.53	22.05	21.93	$x = a/2$
$M_y \times \bar{D} \times 10$	51.39	50.43	50.22	$x = a/2$
$R_x \times \bar{D}$	28.78	39.70	40.41	$x = 0$
$Q_y \times \bar{D}$	0.005640	0.005400	0.005340	$x = a/2$
$M_{xy} \times \bar{D}$	-0.0710	-0.0741	-0.0750	$x = 0$
$Q_x \times \bar{D}$	41.81	44.24	46.03	$x = 0$

$D_{11}/D_{22} = 10$; $D_{66}/D_{22} = 2$; $\bar{D} = D_{22}/q\,(a/b)^4$

Quantity	$\sum m = 1$	$\sum m = 1,3$	$\sum m = 1,3,5$	Position
$w \times \bar{D} \times 10^3$	1.292	1.281	1.281	$x = a/2$
$M_x \times \bar{D}$	22.07	21.16	21.31	$x = a/2$
$M_y \times \bar{D} \times 10$	2.881	2.265	2.064	$x = a/2$
$R_x \times \bar{D}$	9.437	34.25	36.52	$x = 0$
$Q_y \times \bar{D}$	-3.968	-3.542	-3.237	$x = a/2$
$M_{xy} \times \bar{D}$	-0.7002	-0.7315	-.7414	$x = 0$
$Q_x \times \bar{D}$	36.54	41.85	43.36	$x = 0$

TABLE VIII.4 - Calculated quantities

Real Roots

Using a computer operating to the eighth digit means that accuracy can be preserved for $m = 1$.

For $m = 3$ accuracy is dependent on the values of A_m etc. In fact as can be seen from Table VIII.3 the pairs A_m/B_m and C_m/D_m always constitute a pair of constants each of which is of opposite sign. Thus the values can be inaccurate for a case where A_m and B_m are similar in magnitude and accuracy is dependent on the fifth digit of the values of $\cosh \phi y$ and $\sinh \phi y$.

However, for $m = 5$ there is no difference between $\cosh \phi y$ and $\sinh \phi y$ to the eighth digit, and for cases where the values of A_m and B_m are similar the problem of lost accuracy can assume serious proportions particularly as the ratio D_{33}/D_{22} rises.

This effect is known as "front end cancellation" and could not be readily circumvented on the Ferranti Sirius computer. This meant that to preserve accuracy prolonged arithmetical computations had to be carried out by hand calculator.

Table VIII.4 gives the significant values of/

of the forces and moments etc. at certain positions in an orthotropic plate whose aspect ratio $a/b = 4/3$ These values correspond to the values of the constants A_m etc. in Table VIII.3.

2. Complex Roots.

For this case $D_{33}^2 < D_{11} D_{22}$ and the roots of equation (VIII.5.1) are

$$\phi = \theta \pm i\zeta \quad ; \quad \psi = -\theta \pm i\zeta$$

where

$$\theta = \frac{m\pi}{(a/b)}\sqrt{\frac{D_{33}}{D_{22}}} \quad ; \quad \zeta = \frac{m\pi}{(a/b)} \cdot \sqrt[4]{\frac{D_{11} D_{22} - D_{33}^2}{\sqrt{D_{22}}}}$$

and the relevant expressions are:

$$w = \frac{q(a/b)^4}{D_{11}} \sum_{m=1,3,..}^{\infty} \left[\frac{4}{(m\pi)^5} + (A_m \cos\zeta y + B_m \sin\zeta y)\cosh\theta y + (C_m \cos\zeta y + D_m \sin\zeta y)\sinh\theta y \right] \sin\frac{m\pi x}{(a/b)}$$

$$\frac{\partial^2 w}{\partial y^2} = \frac{q(a/b)^4}{D_{11}} \sum_{m=1,3..}^{\infty} \left\{ (\theta^2 - \zeta^2) \left\{ (A_m \cos\zeta y + B_m \sin\zeta y)\cosh\theta y + (C_m \cos\zeta y + D_m \sin\zeta y)\sinh\theta y \right\} + 2\theta\zeta \left\{ (B_m \cos\zeta y - A_m \sin\zeta y)\sinh\theta y + (D_m \cos\zeta y - C_m \sin\zeta y)\cosh\theta y \right\} \right\} \sin\frac{m\pi x}{(a/b)}$$

$D_{11}/D_{22} = 10$; $D_{66}/D_{22} = 1$

Constant	m = 1	m = 3	m = 5
$4/(m\pi)^5$	$0.13071053 \times 10^{-1}$	$0.53790350 \times 10^{-4}$	$0.41827367 \times 10^{-5}$
A_m	$-0.27502799 \times 10^{-3}$	$-0.48871326 \times 10^{-5}$	$0.34417298 \times 10^{-5}$
B_m	$0.98858660 \times 10^{-3}$	$-0.13400014 \times 10^{-4}$	$-0.14203707 \times 10^{-4}$
C_m	$-0.41681885 \times 10^{-4}$	$-0.56498860 \times 10^{-6}$	$-0.59887410 \times 10^{-6}$
D_m	$0.80693330 \times 10^{-3}$	$0.31600500 \times 10^{-5}$	$0.40923091 \times 10^{-6}$

$D_{11}/D_{22} = 1.314 \times 10^{4}$ $D_{66}/D_{22} = 1.358$

Constant	m = 1	m = 3	m =5
A_m	$-0.29007006 \times 10^{-4}$	$-0.12653302 \times 10^{-6}$	$-0.10409890 \times 10^{-7}$
B_m	$-0.13805251 \times 10^{-4}$	$-0.62607850 \times 10^{-7}$	$-0.55428840 \times 10^{-8}$
C_m	$0.27429337 \times 10^{-4}$	$0.12439408 \times 10^{-6}$	$0.11013024 \times 10^{-7}$
D_m	$0.11658069 \times 10^{-4}$	$0.26351496 \times 10^{-7}$	$0.32617019 \times 10^{-9}$

TABLE VIII.5. Constants

Complex Roots.

$$\frac{\partial^3 w}{\partial y^3} = q\frac{(a/b)^4}{D_{11}}\sum_{m=1,3,\ldots}^{\infty}\left[(\theta^2-\zeta^2)\left\{\begin{array}{l} A_m(\theta\sinh\theta y\cos\zeta y - \zeta\cosh\theta y\sin\zeta y)\\ +B_m(\zeta\cosh\theta y\cos\zeta y + \theta\sinh\theta y\sin\zeta y)\\ +C_m(\theta\cosh\theta y\cos\zeta y - \zeta\sinh\theta y\sin\zeta y)\\ +D_m(\zeta\sinh\theta y\cos\zeta y + \theta\cosh\theta y\sin\zeta y)\end{array}\right\}\right.$$
$$\left.+2\theta\zeta\left\{\begin{array}{l} A_m(-\zeta\sinh\theta y\cos\zeta y - \theta\cosh\theta y\sin\zeta y)\\ +B_m(\theta\cosh\theta y\cos\zeta y - \zeta\sinh\theta y\sin\zeta y)\\ +C_m(-\zeta\cosh\theta y\cos\zeta y - \theta\sinh\theta y\sin\zeta y)\\ +D_m(\theta\sinh\theta y\cos\zeta y - \zeta\sinh\theta y\sin\zeta y)\end{array}\right\}\right]\sin\frac{m\pi x}{(a/b)}$$

$$\frac{\partial^3 w}{\partial x^2\partial y} = -q\frac{(a/b)^4}{D_{11}}\frac{(m\pi)^2}{(a/b)^2}\sum_{m=1,3,\ldots}^{\infty}\left\{\begin{array}{l} A_m(\theta\sinh\theta y\cos\zeta y - \zeta\cosh\theta y\sin\zeta y)\\ +B_m(\theta\sinh\theta y\sin\zeta y + \zeta\cosh\theta y\cos\zeta y)\\ +C_m(\theta\cosh\theta y\cos\zeta y - \zeta\sinh\theta y\sin\zeta y)\\ +D_m(\theta\cosh\theta y\sin\zeta y + \zeta\sinh\theta y\cos\zeta y)\end{array}\right\}\sin\frac{m\pi x}{(a/b)}$$

(VIII.5.5)

The values of the constants A_m etc. in the above equations appear in Table VIII.5 for the following two cases:

(1) $D_{11}/D_{22} = 10$, $D_{66}/D_{22} = 1$

(2) $D_{11}/D_{22} = 1.314 \times 10^4$, $D_{66}/D_{22} = 1.358$

Case (2) is the actual 0.048 in. thick steel decking for which the actual values of D_{11} etc. appear in Table VIII.2.

For case (1), $y = 0.5$

$$\theta = \frac{m\pi b}{a}\sqrt{\frac{D_{33}}{D_{22}}} = 1.134\, m\pi$$

$$\zeta = \frac{m\pi b}{a}\sqrt[4]{\frac{D_{11}D_{22} - D_{33}^2}{D_{22}}} = 1.648\, m\pi$$

$m = 1$ $\quad \theta y = 0.567\pi = 0.57\pi$ say.

$\cosh \theta y = 3.08026 \qquad \sinh \theta y = 2.91342$

$m = 3$ $\quad \cosh \theta y = 104.33254 \; ; \; \sinh \theta y = 104.32774.$

$m = 5$ $\quad \cosh \theta y = 3747.99374$

$\sinh \theta y = 3747.99360$

As can be seen from the above, the same difficulties arise as for the case of real roots, with however the additional complication that for complex roots the values of A_m etc. do not remain consistent in sign. Further, the equations/

$D_{11}/D_{22} = 10$; $D_{66}/D_{22} = 1$ $\quad \bar{D}_1 = D_{22}/q\,(a/b)^4$

Quantity	$\Sigma m = 1$	$\Sigma m = 1,3$	$\Sigma m = 1,3,5$	Position
$w \times \bar{D}_1 \times 10^3$	1.237	1.232	1.233	$x = a/2$
$M_x \times \bar{D}_1$	20.75	20.42	20.73	$x = a/2$
$M_y \times \bar{D}_1 \times 10$	-2.044	-2.481	-2.663	$x = a/2$
$R_x \times \bar{D}_1$	35.34	40.21	42.02	$x = 0$
$Q_y \times \bar{D}_1$	-2.118	-1.903	-1.962	$x = a/2$
$M_{xy} \times \bar{D}_1$	-4.118	-6.544	-7.981	$x = 0$
$Q_x \times \bar{D}_1$	36.08	40.95	45.43	$x = 0$

$D_{11}/D_{22} = 1.314 \times 10^4$; $D_{66}/D_{22} = 1.358$; $\bar{D}_2 = D_{11}/q\,(a/b)^4$

Quantity	$\Sigma m = 1$	$\Sigma m = 1,3$	$\Sigma m = 1,3,5$	Position
$w \times \bar{D}_2 \times 10^3$	13.22	13.09	13.07	$x = a/2$
$M_x \times \bar{D}_2 \times 10^{-3}$	173.4	167.2	166.2	$x = a/2$
$M_y \times \bar{D}_2 \times 10^2$	2.811	3.526	4.670	$x = a/2$
$R_x \times \bar{D}_2 \times 10^{-4}$	40.89	45.43	47.07	$x = 0$
$Q_y \times \bar{D}_2 \times 10^{39}$	-51.05	-44.80	-47.36	$x = a/2$
$M_{xy} \times \bar{D}_2 \times 10^{43}$	37.90	39.42	39.80	$x = 0$
$Q_x \times \bar{D}_2 \times 10^{-4}$	40.89	45.43	47.07	$x = 0$

TABLE VIII.6 - Calculated quantities

Complex Roots.

equations (VIII.5.5) show that no simplifying assumptions can be made as the hyperbolic terms are qualified by simple trigonometric expressions.

This implies that for all values of m , the computations need to be checked by hand calculation for possible numerical instability.

It was therefore to obviate the above difficulties that the method indicated in Section IV.2 was used to determine the lateral strain $\epsilon_y = z \frac{\partial^2 w}{\partial y^2}$

For the deflection forces and moments, the convergence of the assumed series is indicated in Table VIII.6.

From the above results for both real and complex roots to the characteristic equation the author considers that qualitatively the Lévy method gives satisfactory results for m = 1. Increasing accuracy can be obtained with further terms or by altering the plate aspect ratio a/b , an increase in which - from the considered value of $4/3$ - will depress the value of ϕ for real roots, and θ for complex roots. This will lead to increased accuracy/

accuracy in computation and a possible avoidance of numerical instability, particularly in the expressions for deflection w .

The author therefore considers that if an orthotropic plate, either by virtue of its stiffness ratios or its physical form, can be approximated to by a series of linked beams, the slight loss of accuracy in computation of deflections etc. inherent in this approximation is more than offset by the resulting simplification in the necessary computational work.

VIII.6. RESULTS OF THE EXPERIMENTAL INVESTIGATIONS.

Material Properties: throughout the decking tests specimens were cut from the failed component to obtain experimental values of Young's Modulus E and Poisson's Ratio ν . These were carried out on specimens 0.95 in. wide using a small testing machine and $\frac{1}{2}$ in, foil electrical strain gauges.

For the theoretical work utilising orthotropic plate theory, only the value of Poisson's Ratio for each specimen was required and two typical tests are illustrated in Figs. VIII.36 and VIII.37 for 0.048 in. thick steel and 0.036 in. thick aluminium respectively. For these two specimens the material properties can be calculated to be:

Steel: Young's Modulus $E = 13,600$ Tonf/in^2.

Poisson's Ratio $\nu = 0.275$

Aluminium Alloy:

Young's Modulus $E = 4,700$ Tonf/in^2 .

Poisson's Ratio $\nu = 0.317$

For all the specimens tested, some seventy in all, the average values were:

Steel/

Specimen	Poisson's Ratio	Mean
0.048 in. steel	0.282, 0.275, 0.281, 0.292, 0.278, 0.250, 0.264, 0.300, 0.255, 0.255, 0.288, 0.244, 0.268, 0.271, 0.276, 0.286, 0.295.	0.28
0.036 in. steel	0.285, 0.302, 0.278, 0.279, 0.282, 0.260, 0.268, 0.296, 0.305, 0.259, 0.289, 0.292, 0.272, 0.766, 0.265, 0.307, 0.284, 0.274.	
0.048 in. alum.	0.344, 0.332, 0.326, 0.314, 0.328, 0.351, 0.345, 0.318, 0.322, 0.325, 0.344, 0.338, 0.350, 0.306, 0.341, 0.346, 0.315, 0.309.	0.33
0.036 in. alum.	0.332, 0.350, 0.341, 0.328, 0.326, 0.319, 0.320, 0.325, 0.339, 0.335, 0.346, 0.315, 0.316, 0.310, 0.309, 0.352, 0.347, 0.334.	

TABLE VIII.7 Poisson's Ratios for Decking Specimens.

Steel: Young's Modulus $E = 13,400$ Tonf/in^2

Poisson's Ratio $\nu = 0.28$

Aluminium Alloy:

Young's Modulus $E = 4,460$ Tonf/in^2

Poisson's Ratio $\nu = 0.33$

For both materials there was some scatter of results, the largest variation being of the order of 10% from the mean. The full range of results for Poisson's Ratio is given in Table VIII.7.

The Critical Load: for the calculation of the critical stress and the "local plate stress factor" individual values of the material constants and the yield stress σ_y were used. These were determined as above, σ_y for the aluminium being the 0.1% proof stress.

For the 0.048 in. thick steel strut whose compression test is shown in Fig. VIII.28(a) the values of the material properties were:

$E = 13,600$ Tonf/in^2.

$\nu = 0.28$

$\sigma_y = 16.5$ Tonf/in^2.

From equation (V.1.1)

$$\sigma_c = \frac{K\pi^2 E}{12(1-\nu^2)}\left(\frac{t}{b}\right)^2$$

For 0.048 in. thick steel the profile is as shown in Fig. VIII.38. Using the above values the stress initiating local elastic buckling is given as:

$$\sigma_c = 6.44 \text{ Tonf/in}^2$$

This compares with the experimental value of:

$$\sigma_c = \frac{3.55}{0.512} = \underline{6.95 \text{ Tonf/in}^2}.$$

On the basis of simple beam theory and assuming a fully effective compression flange

$\sigma_c = 6.44$ Tonf/in^2 gives a value of moment

$M = 3.40$ Tonf.in .

∴ The loading to initiate elastic buckling

$$= \frac{3.40 \times 2240}{8 \times 6} = \underline{1.11 \text{ lbf/in}}.$$

The Collapse Load of Decking: for the calculation of the theoretical collapse load of 0.048 in. thick steel decking made up of a series of troughs of the profile shown in Fig. VIII.38 the procedure is as follows:

$$\frac{b}{t} = \frac{4.2}{0.048} = 87.5$$

$\therefore$ From Fig. V.1 for mild steel

$$C_L = 0.4727$$

The effective width b_e = 1.98 in.

The position of the neutral axis N-N is determined from the condition that the area above and below it shall be equal. This gives

e = 1.48 in. c = 1.47 in.

f = 1.04 in. d = 1.03 in.

At collapse it is assumed that the yield stress is reached across the complete effective section.

Therefore the collapse moment M_c is given by:

$$M_c = \sum R.y.\sigma_y$$

$$= [(0.99 \times 1.03) + (1.04 \times 0.515) + (1.48 \times 0.735) + (0.55 \times 1.47)].2.0.048.\sigma_y$$

For this material the average value of yield stress was found to be 16.5 Tonf/in .

$\therefore$ $\underline{M_c = 5.47 \text{ Tonf.in}}$.

Collapse loading

$$= \frac{5.47 \times 2240}{8 \times 6} = 256 \text{ lbf/ft}^2.$$

$$= \underline{1.78 \text{ lbf/in}^2}.$$

The above procedures for critical and collapse loading can be carried out for all the types of decking considered and the results are given in Table V.1.

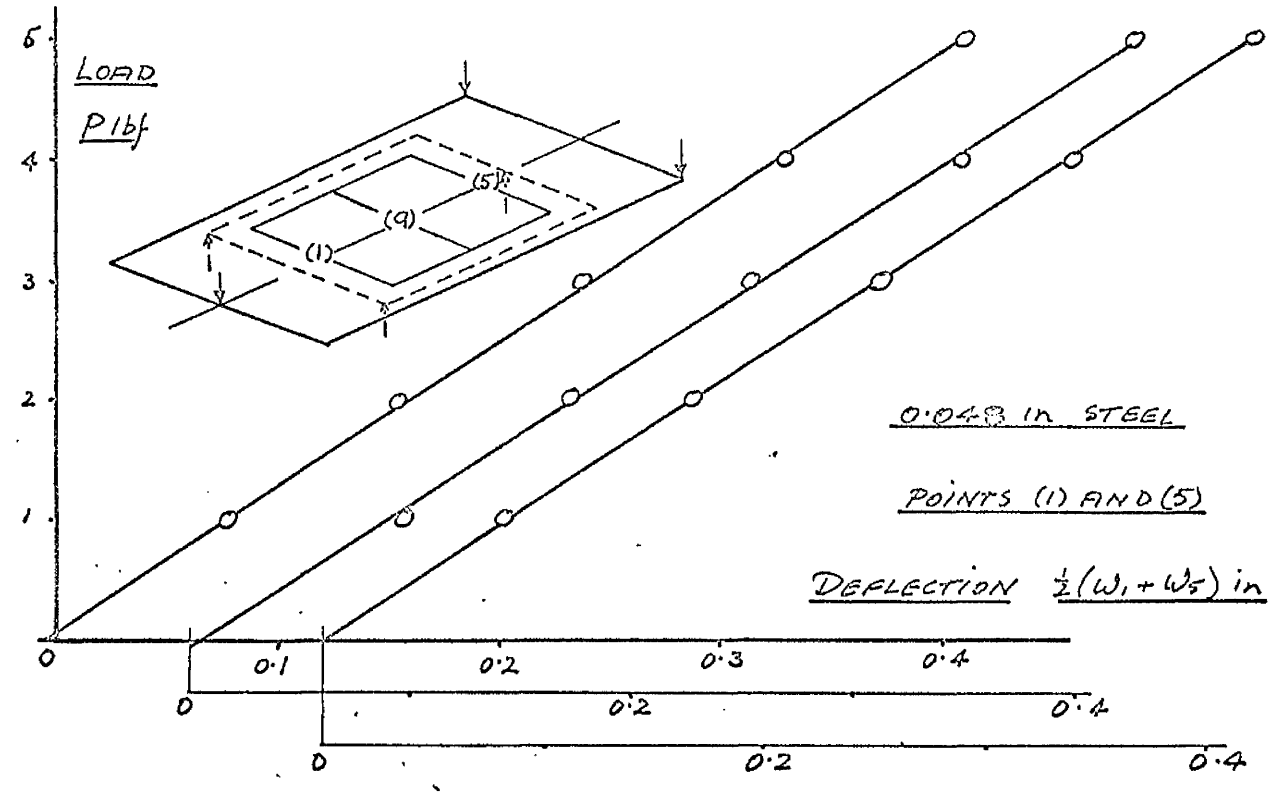

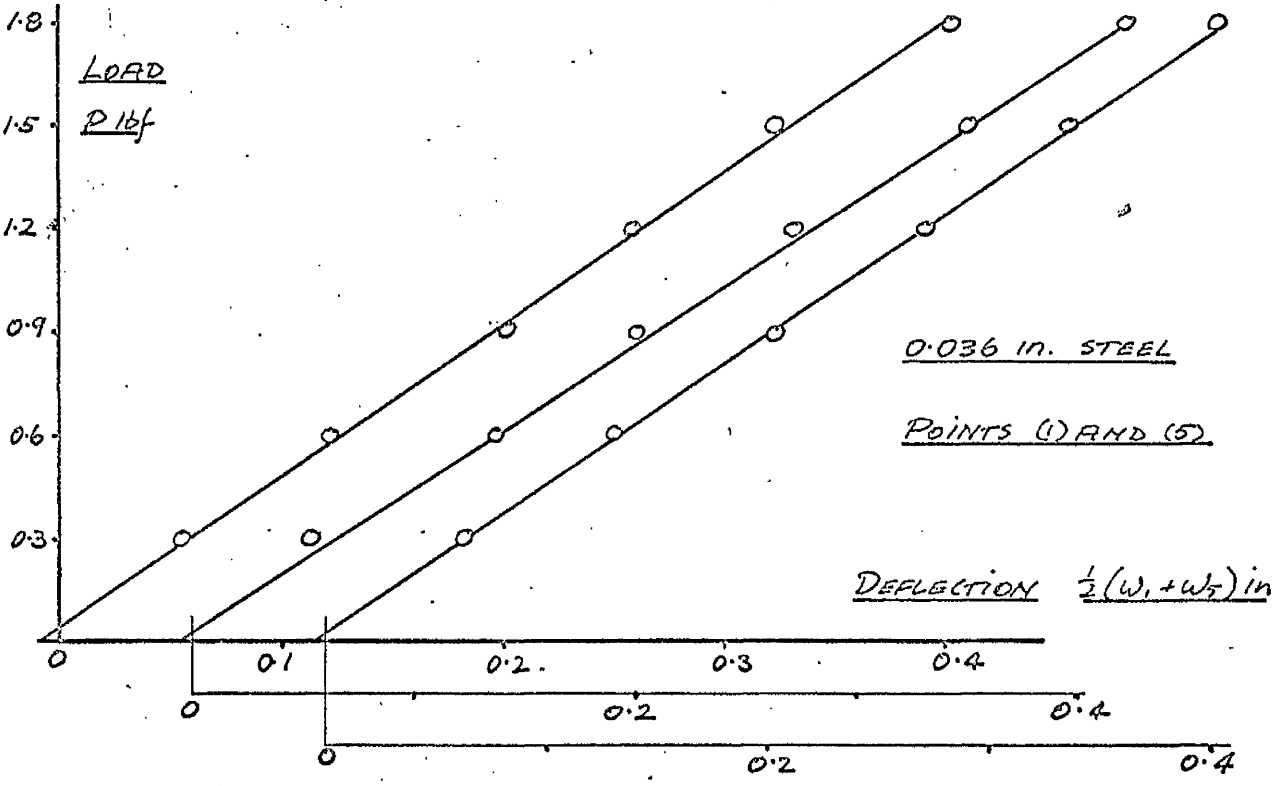

FIG.VIII.8 Bending tests for a_{22}

Deflections relative to (9)

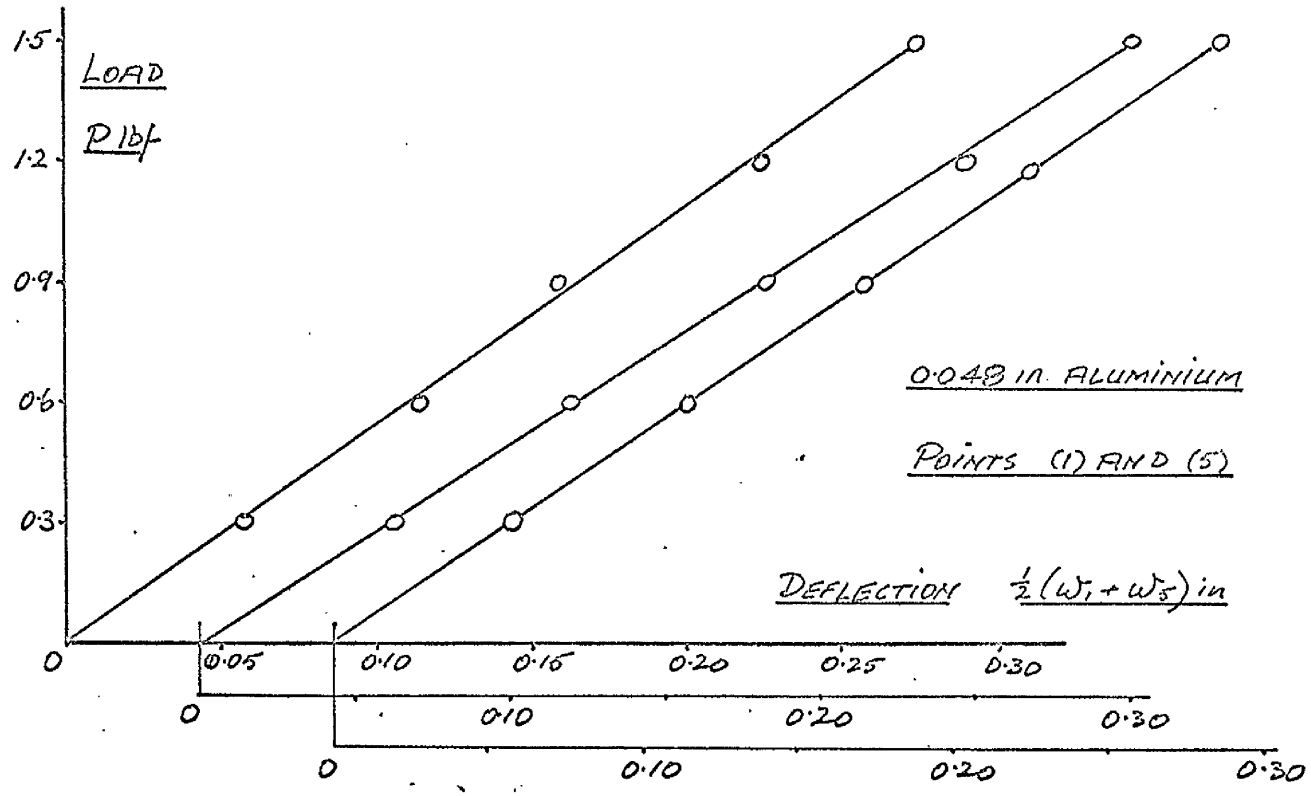

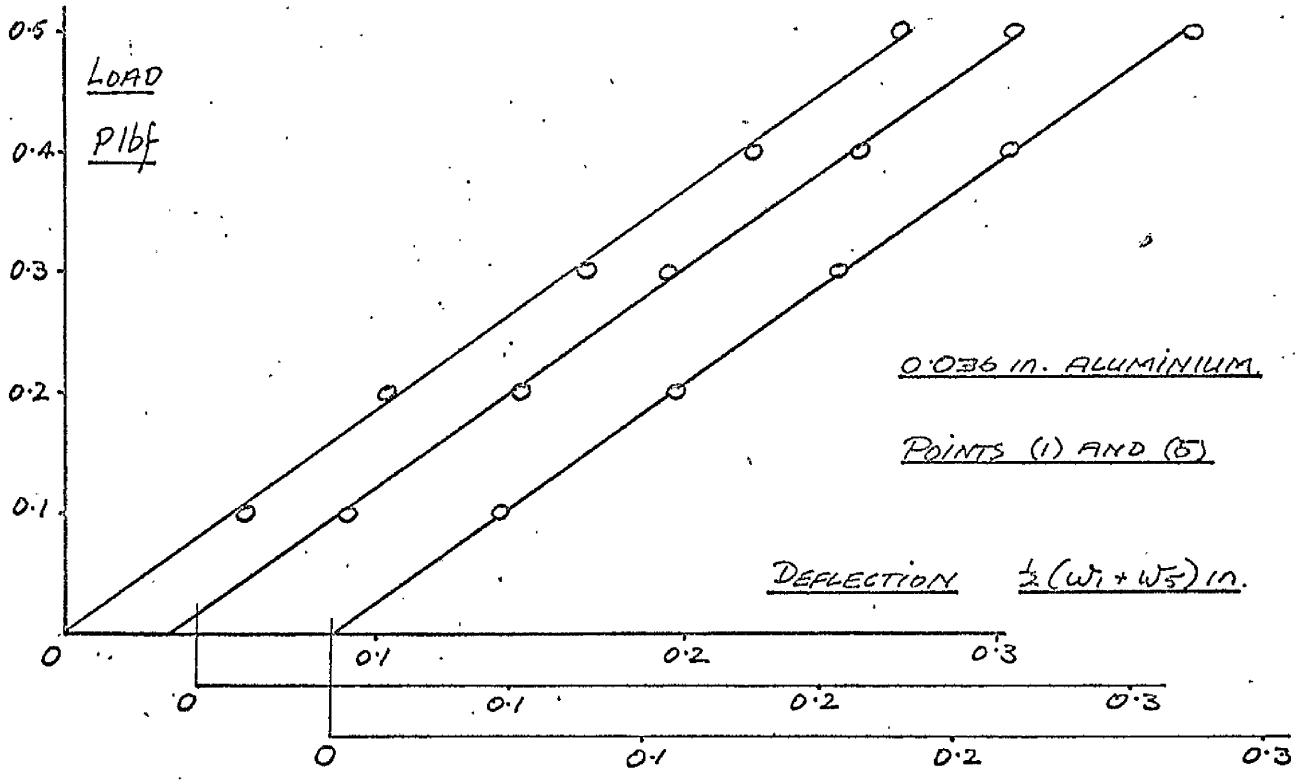

FIG.VIII.9 Bending tests for a_{22}

Deflections relative to (9)

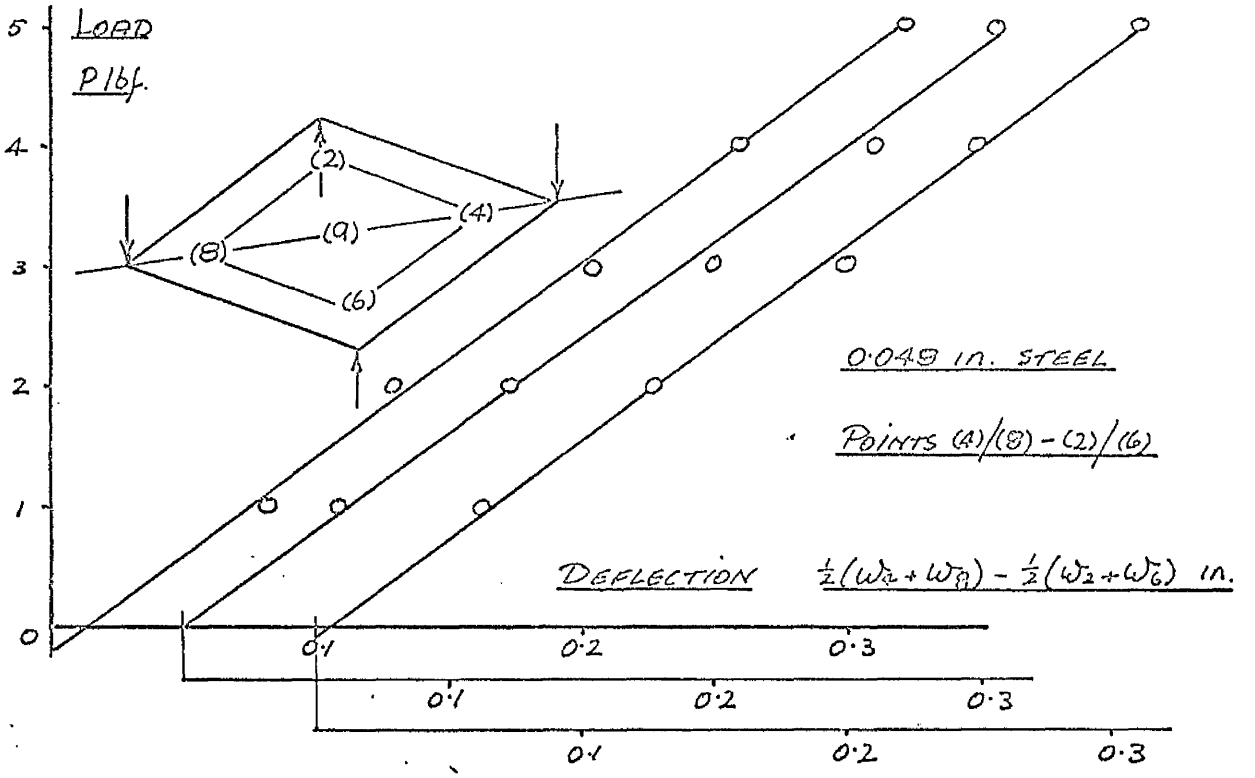

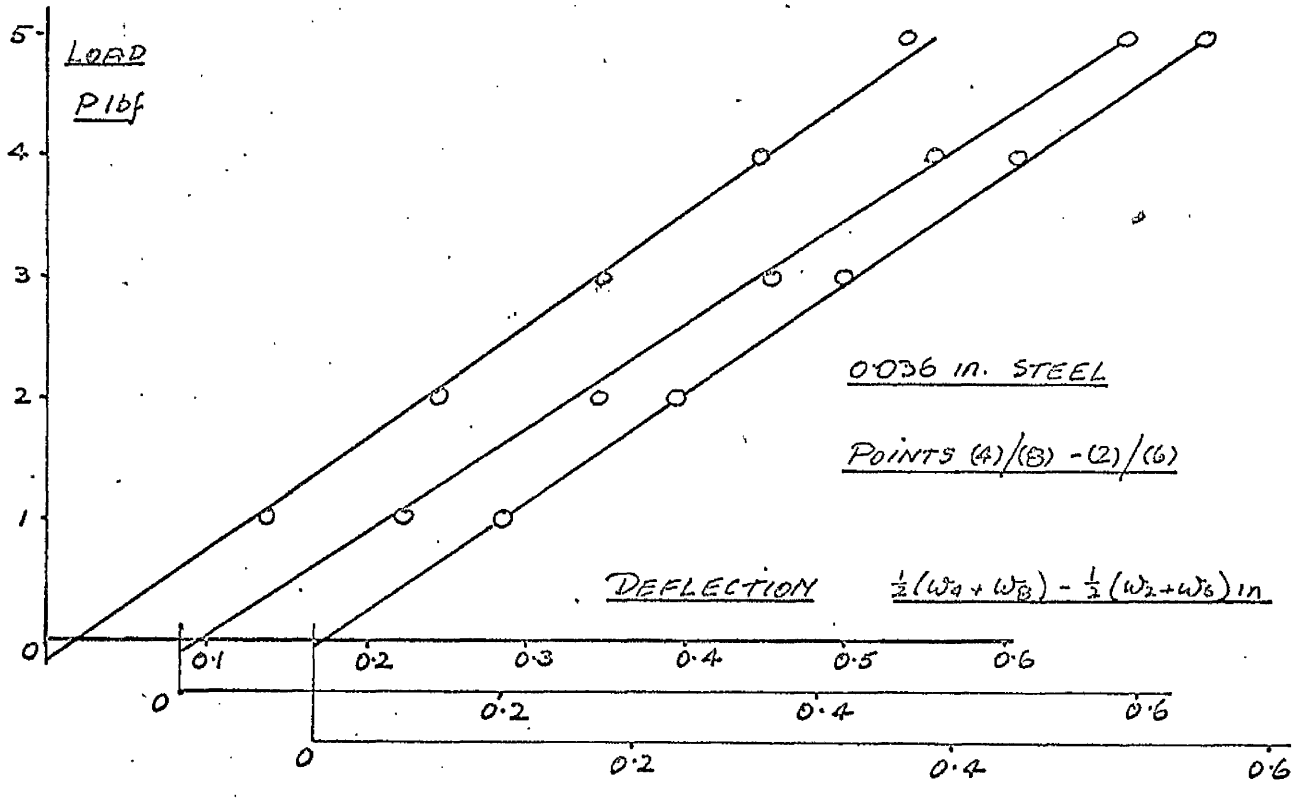

FIG.VIII.10 Twisting tests for a_{66}

Deflections relative to (9)

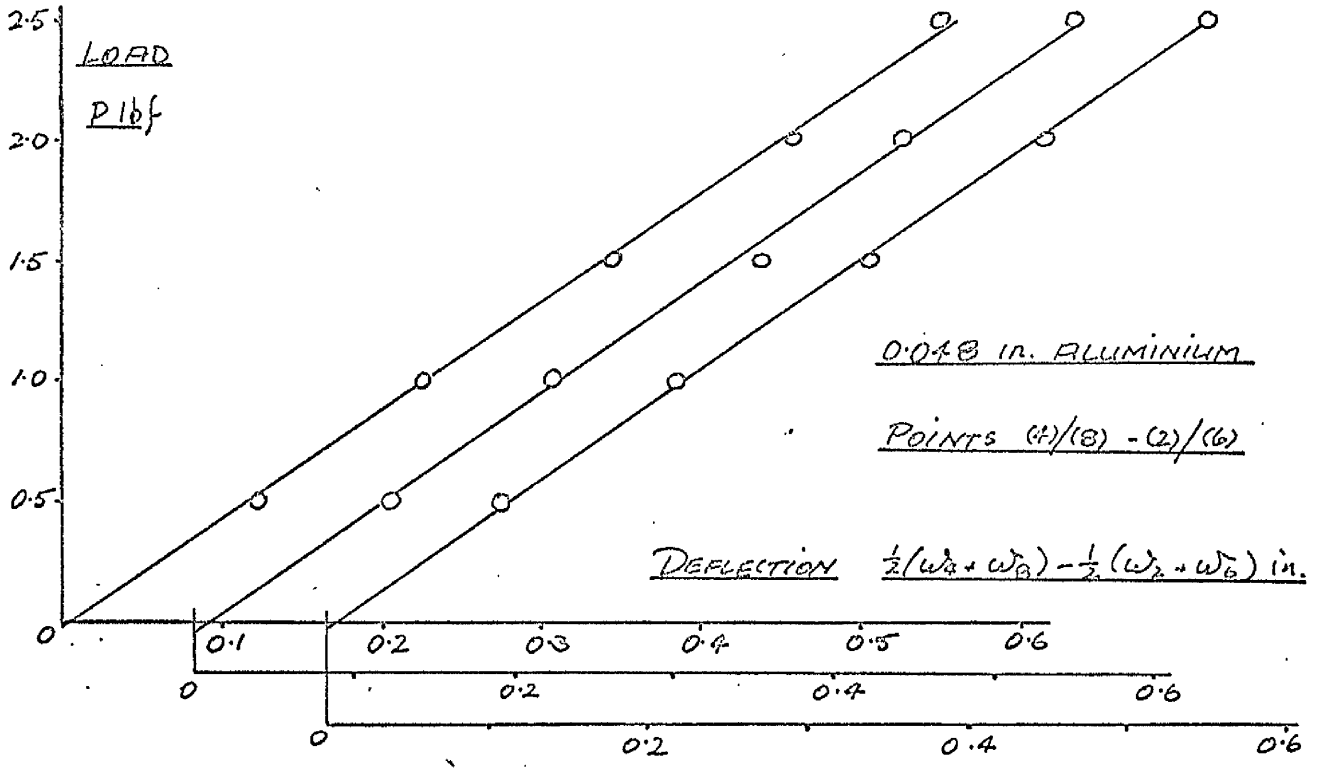

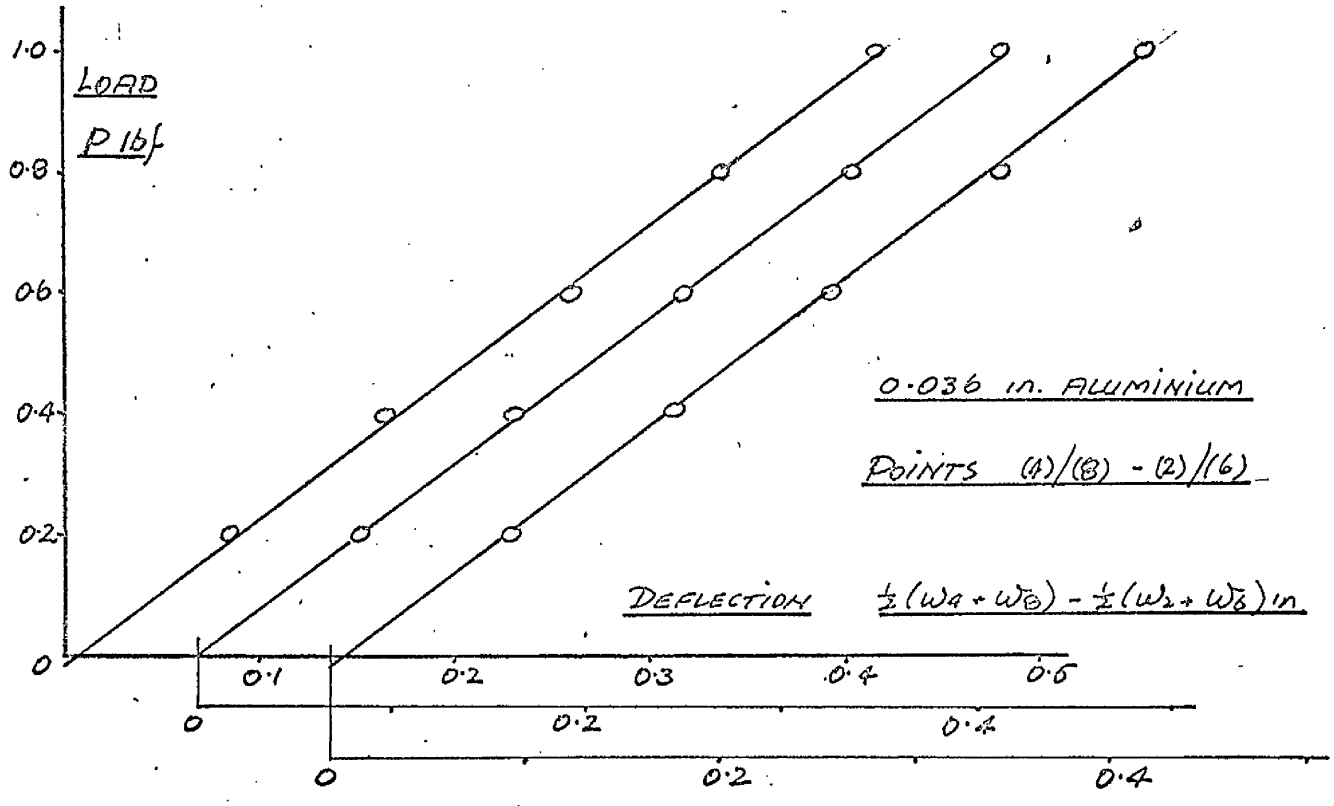

FIG.VIII.11 Twisting tests for a_{66}

Deflections relative to (9)

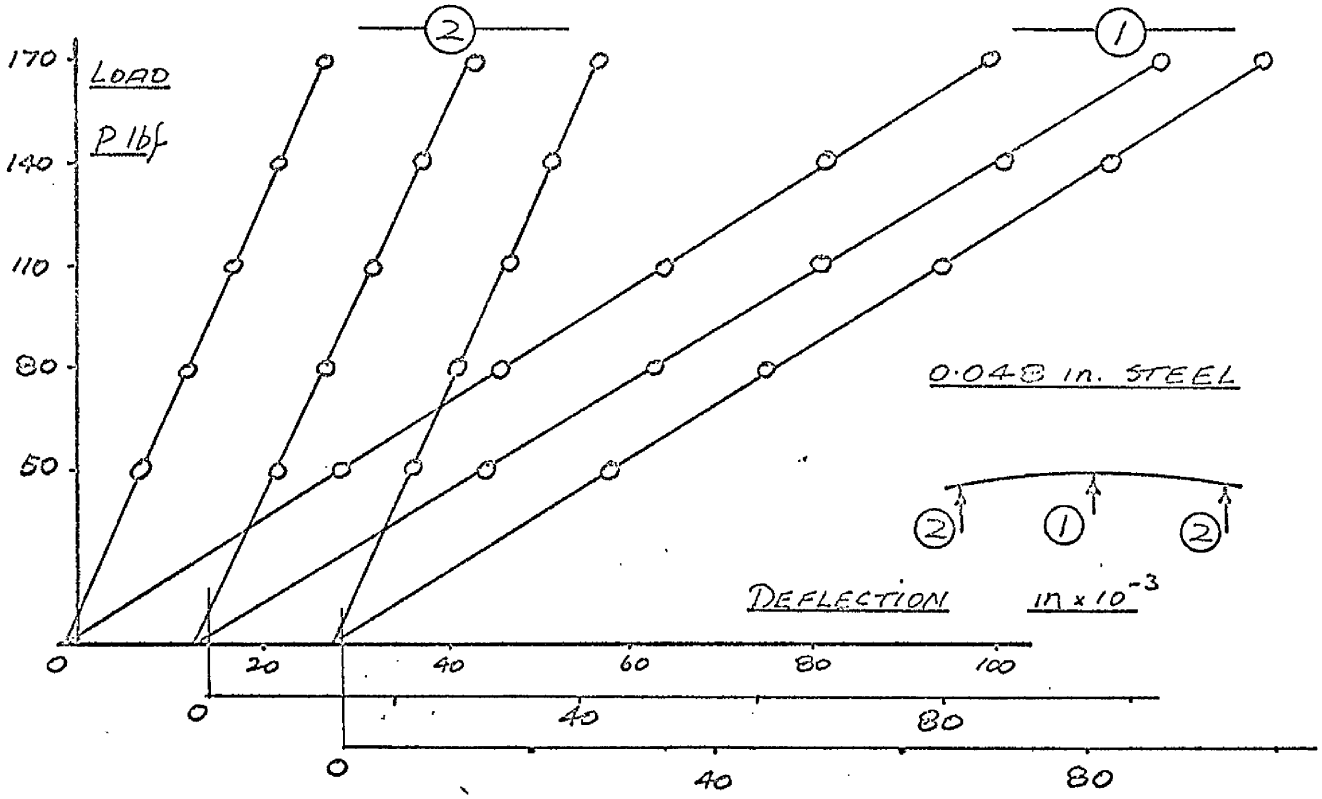

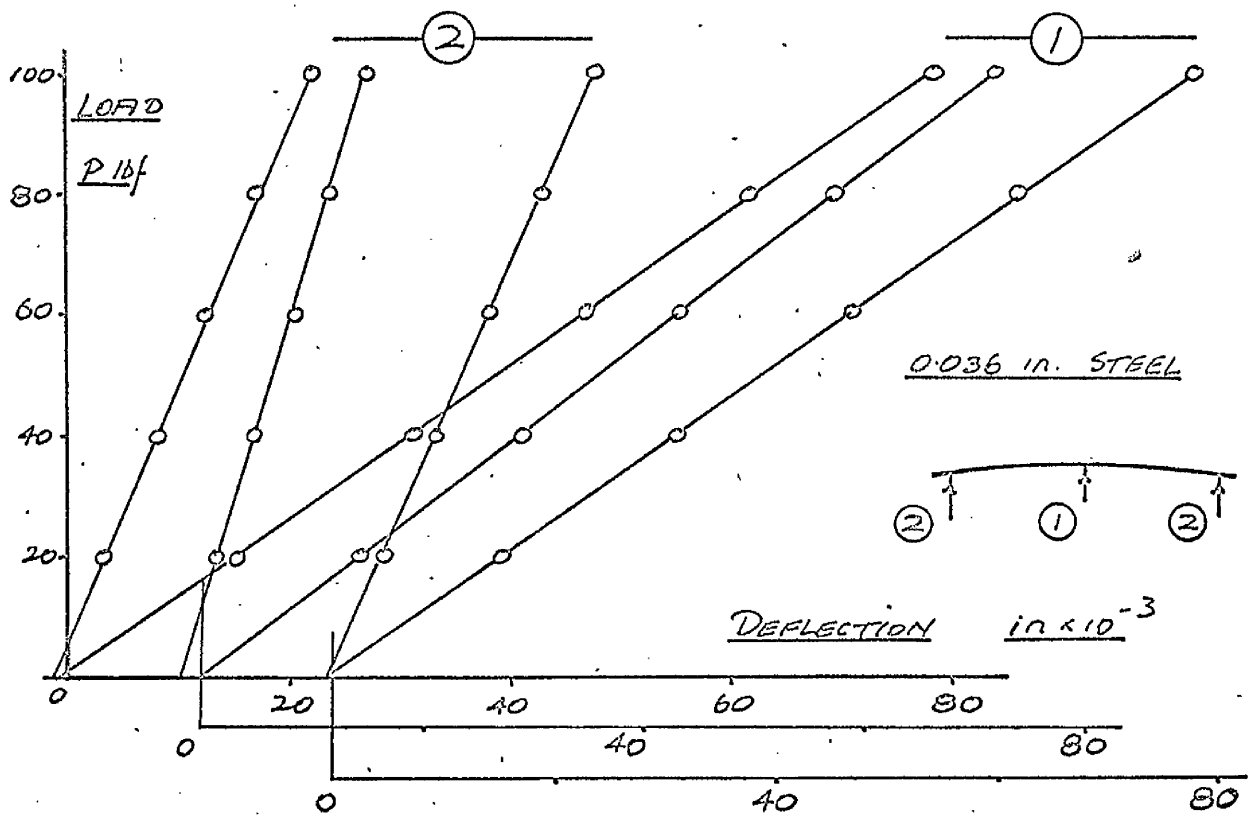

FIG.VIII.12 Bending tests for a_{11}

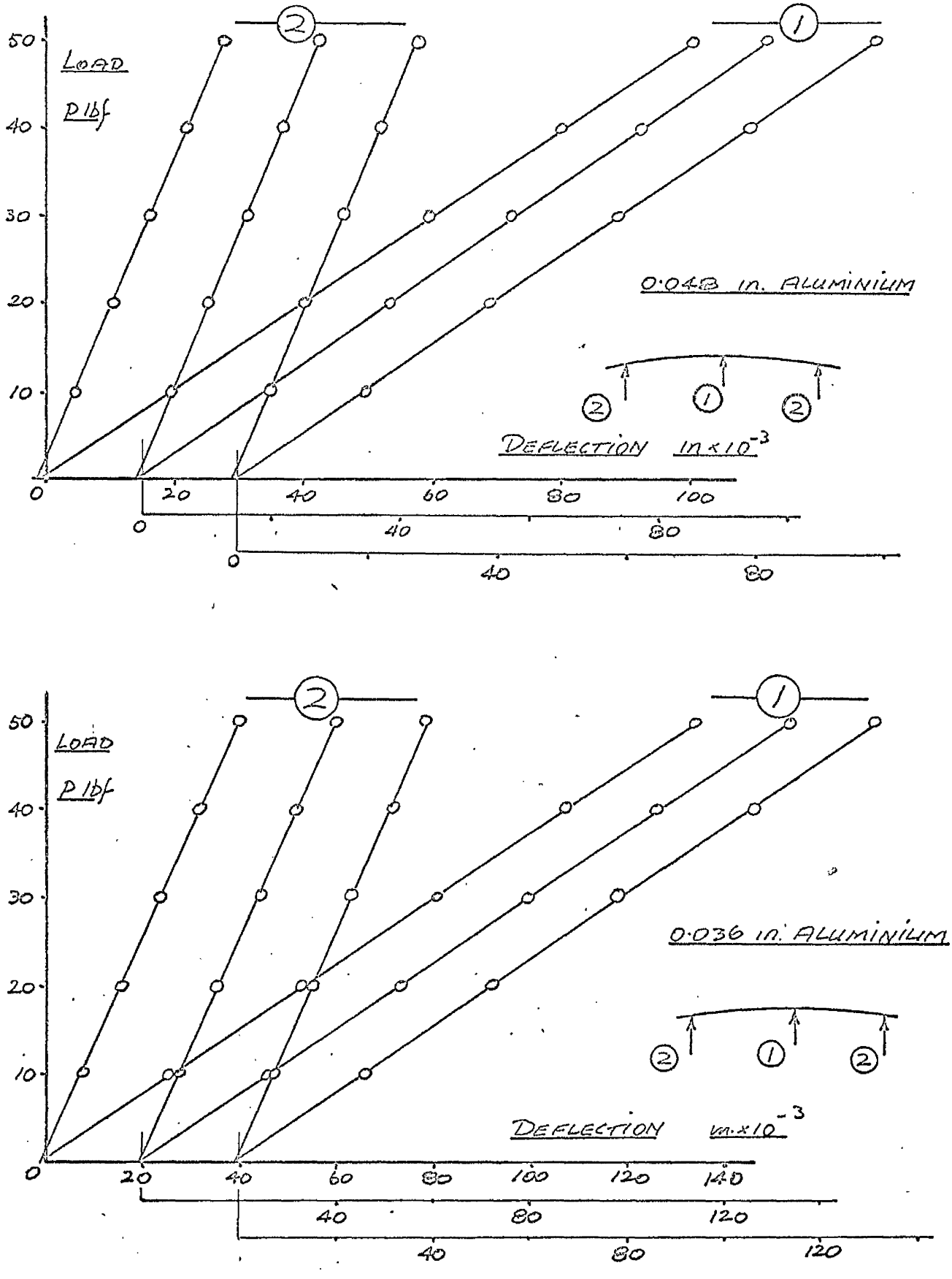

FIG.VIII.13 Bending tests for a_{11}

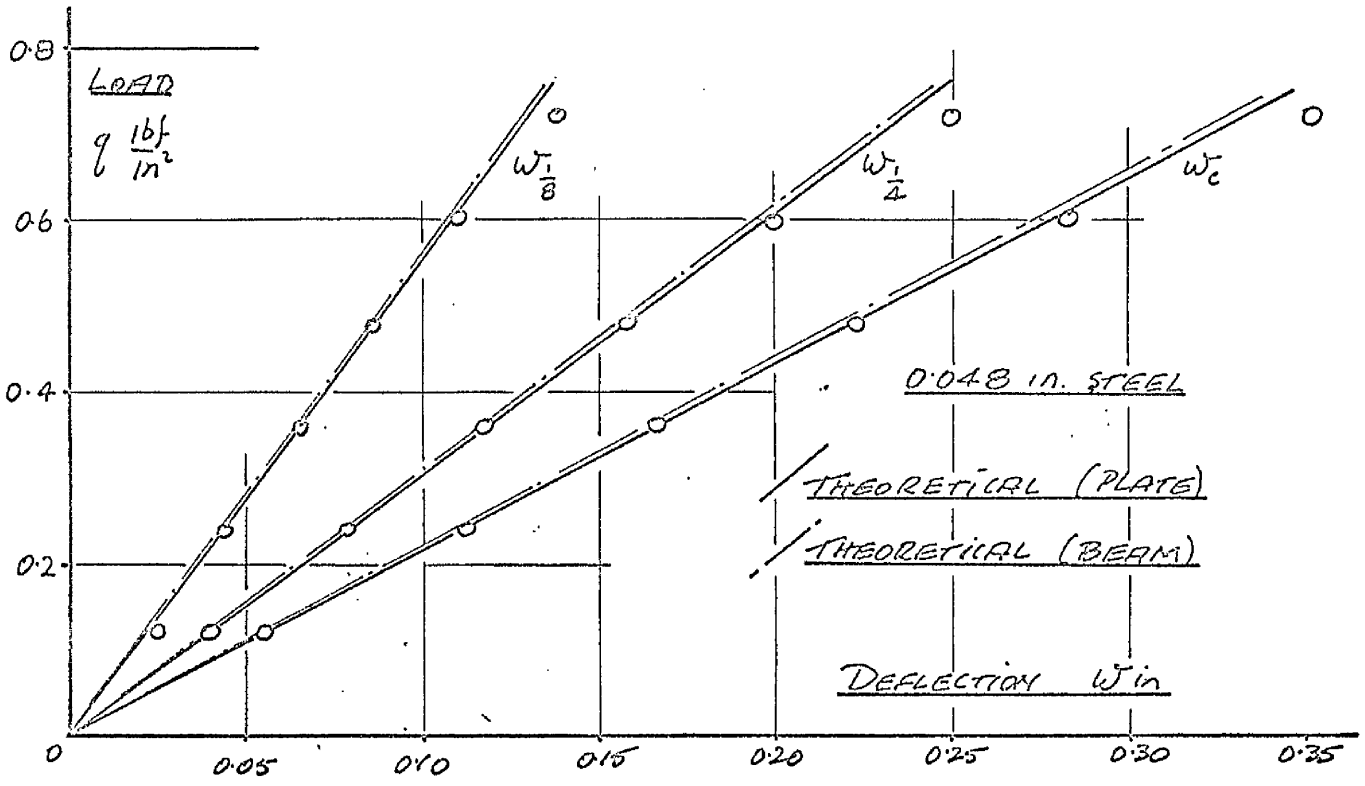

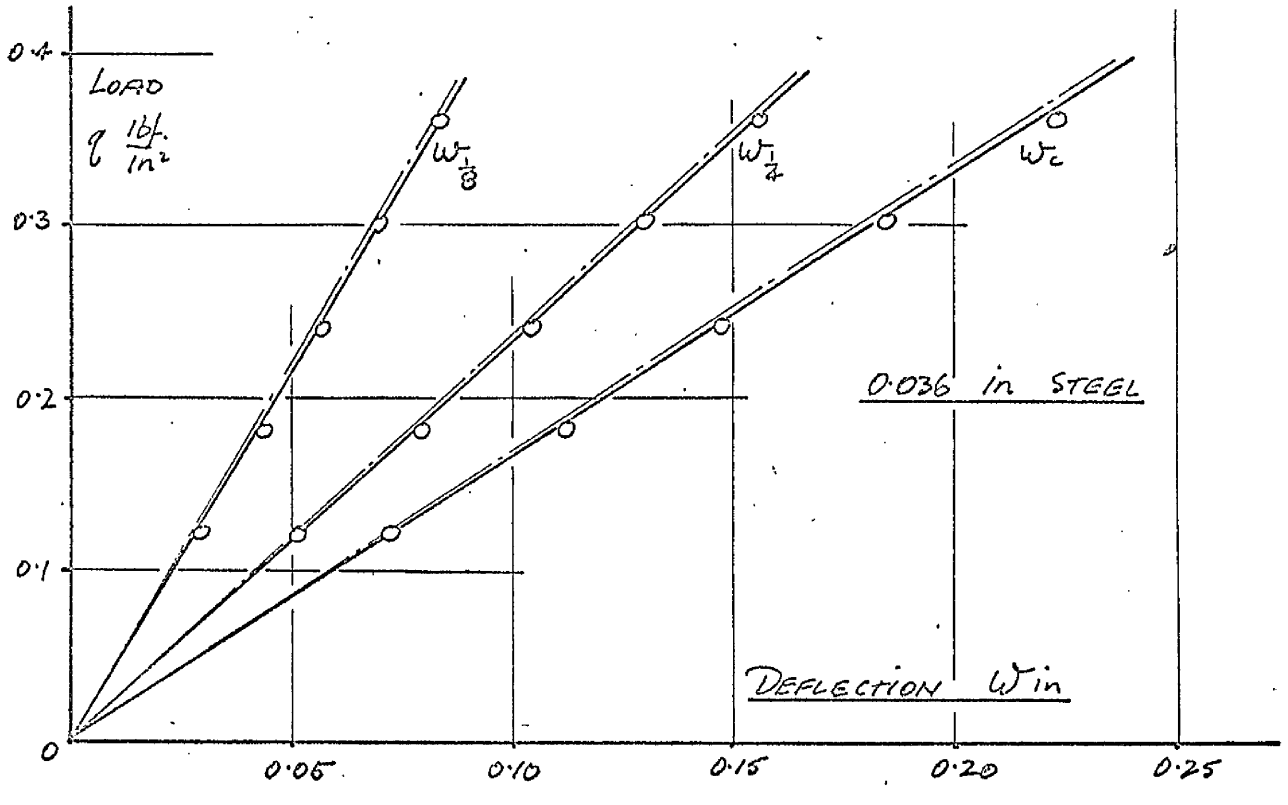

FIG.VIII.14 $\frac{1}{8}$, $\frac{1}{2}$ and centre line deflections of full scale decking tests.

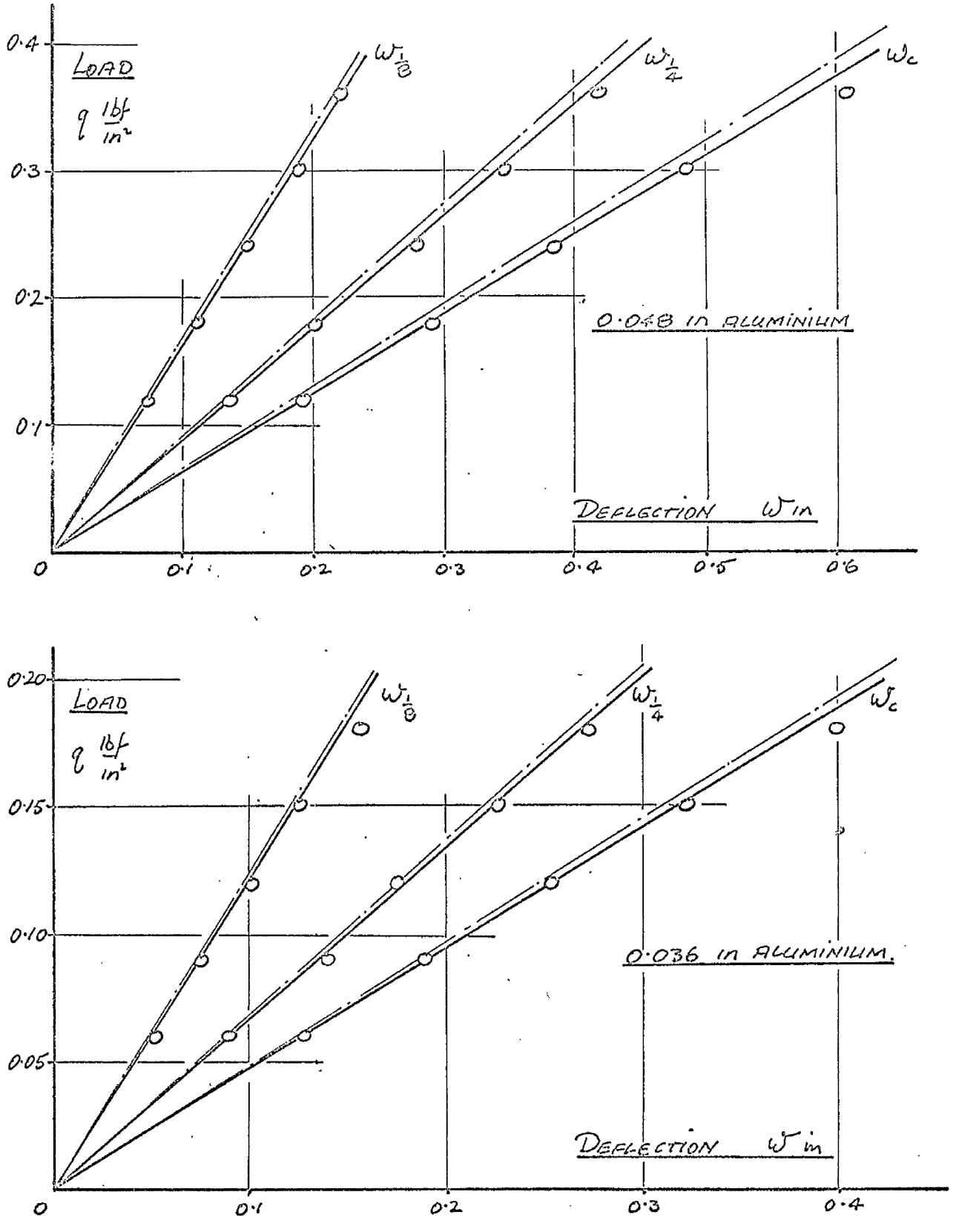

FIG.VIII.15 $\frac{1}{8}$, $\frac{1}{4}$ and centre line deflections of full scale decking tests.

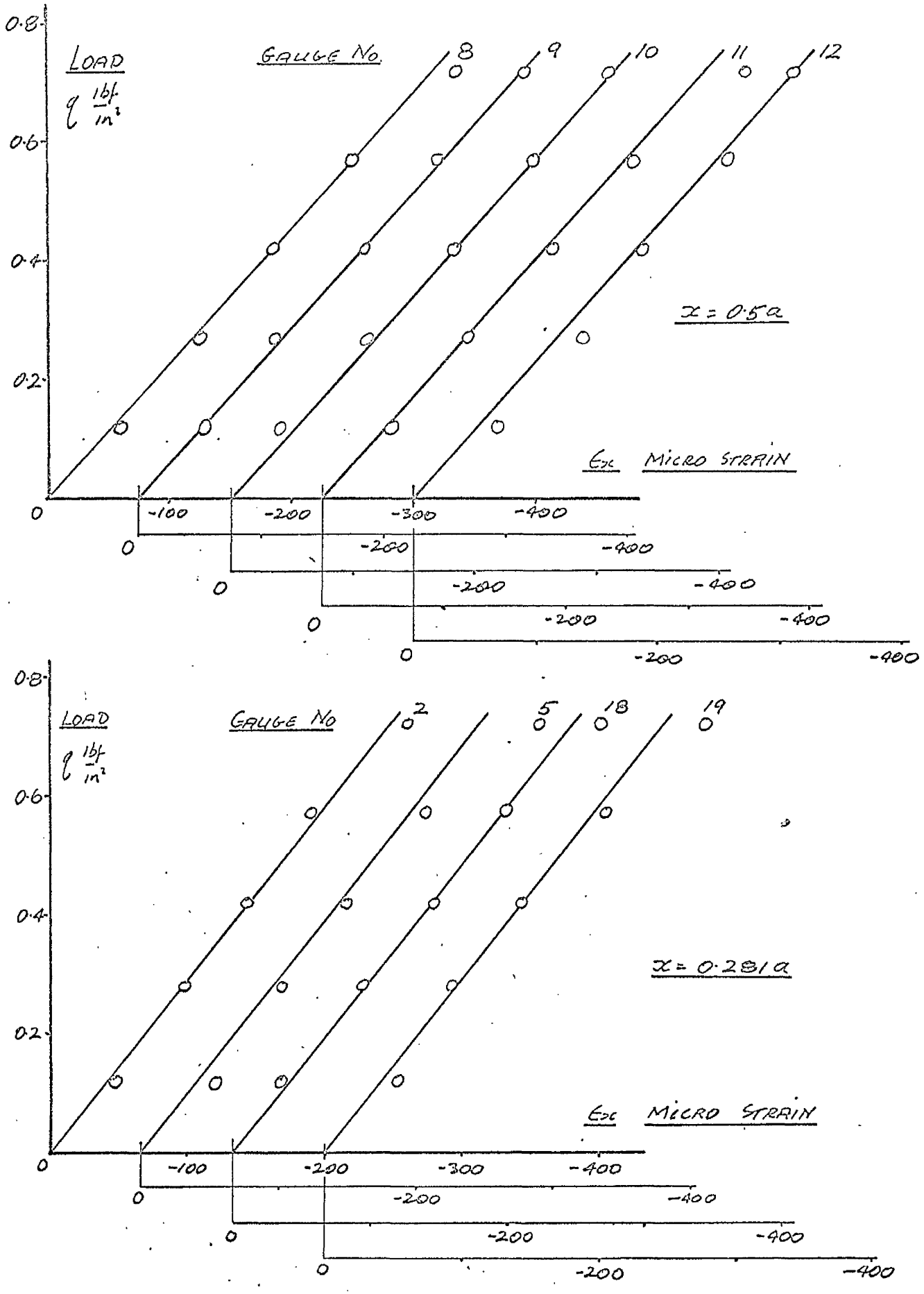

FIG.VIII.16 Longitudinal strains ϵ_x for 0.048 in. steel deck.

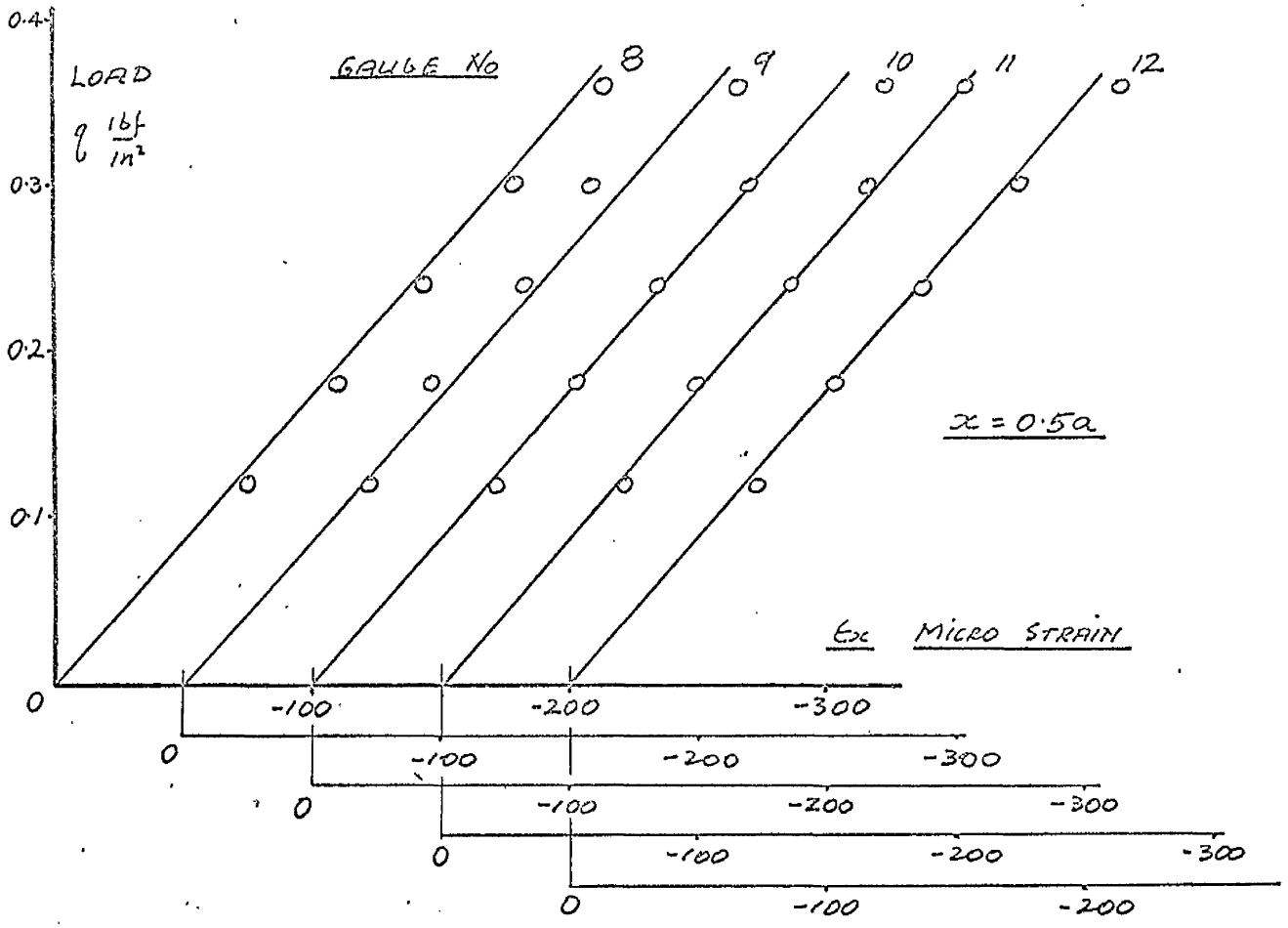

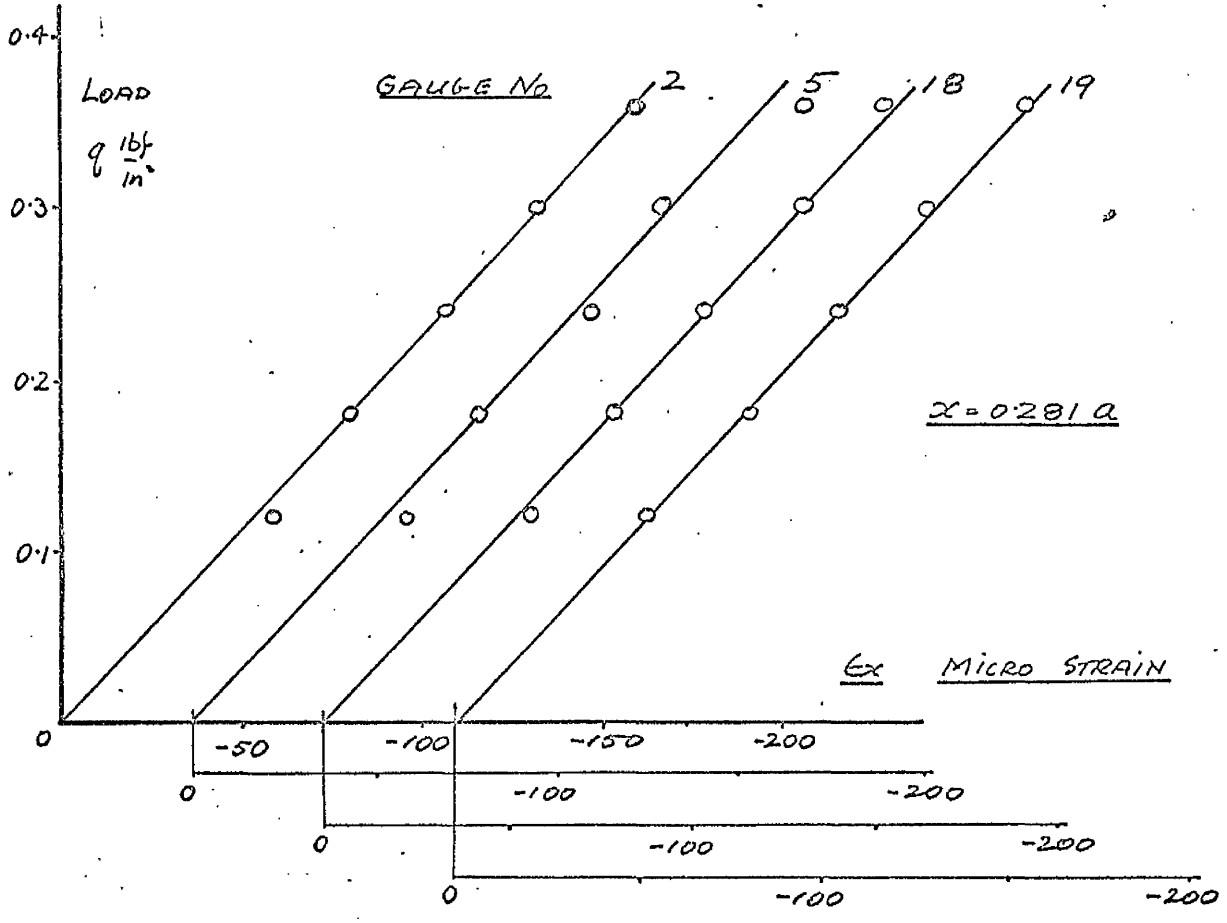

FIG.VIII.17 Longitudinal strains ϵ_x for 0.036 in. steel deck.

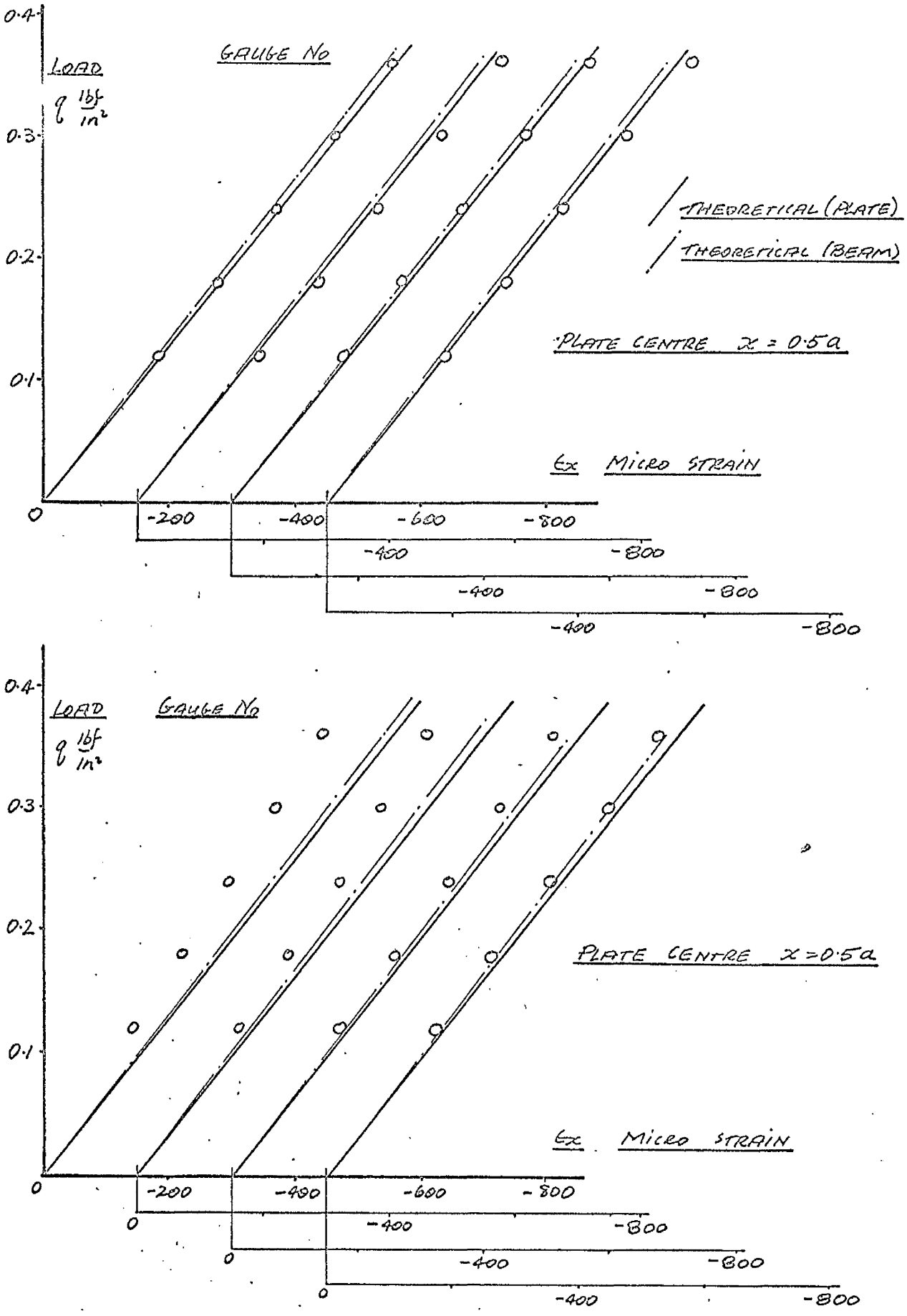

FIG.VIII.18 Longitudinal strains ϵ_x for 0.048 in. aluminium deck.

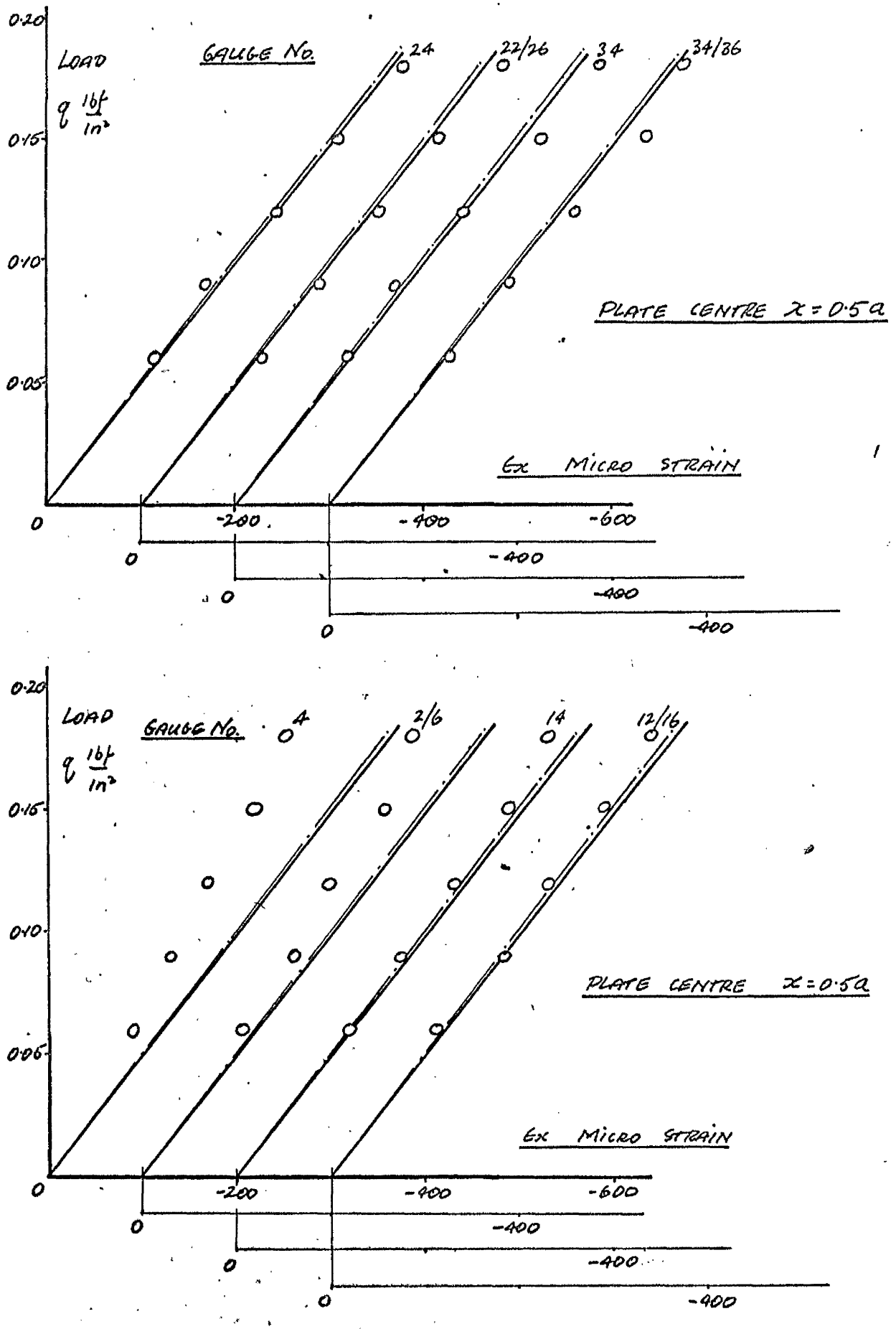

FIG.VIII.19 Longitudinal strains ϵ_x for 0.036 in. aluminium deck.

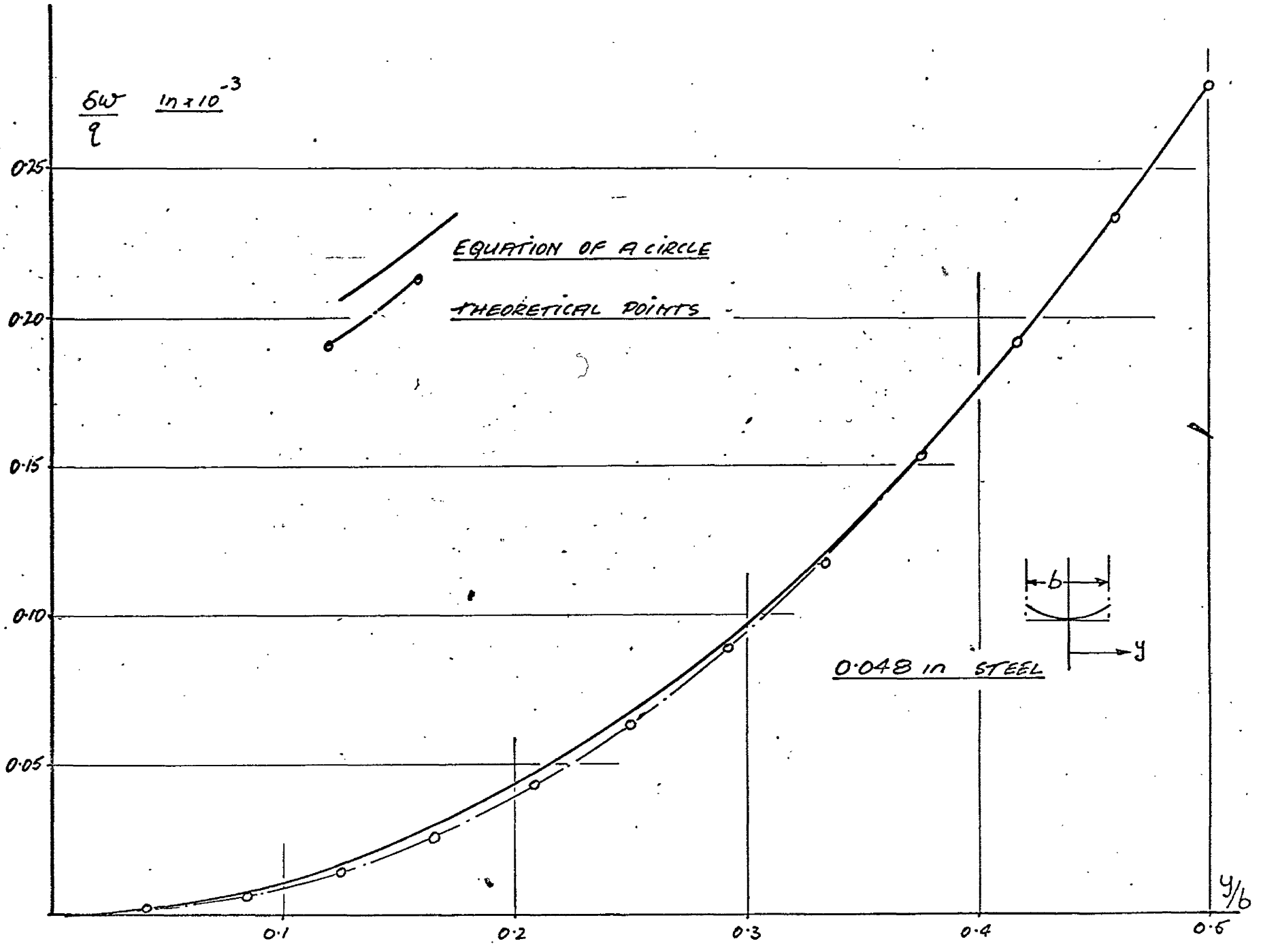

FIG.VIII.20 Theoretical transverse deflected form for a single trough of 0.048 in. steel deck compared with the equation of a circle.

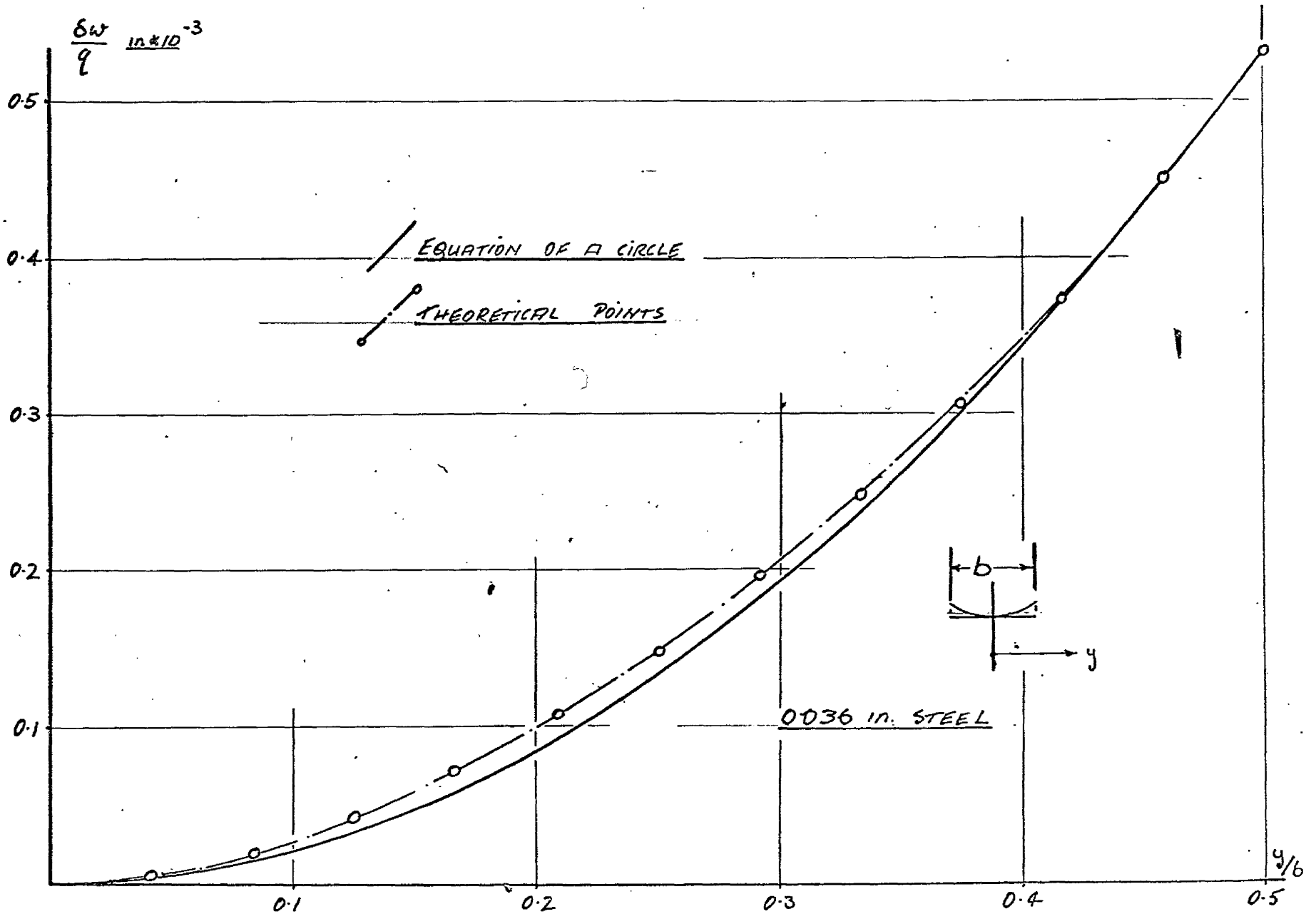

FIG.VIII.21 Theoretical transverse deflected form for a single trough of 0.048 in. aluminium deck compared with the equation of a circle.

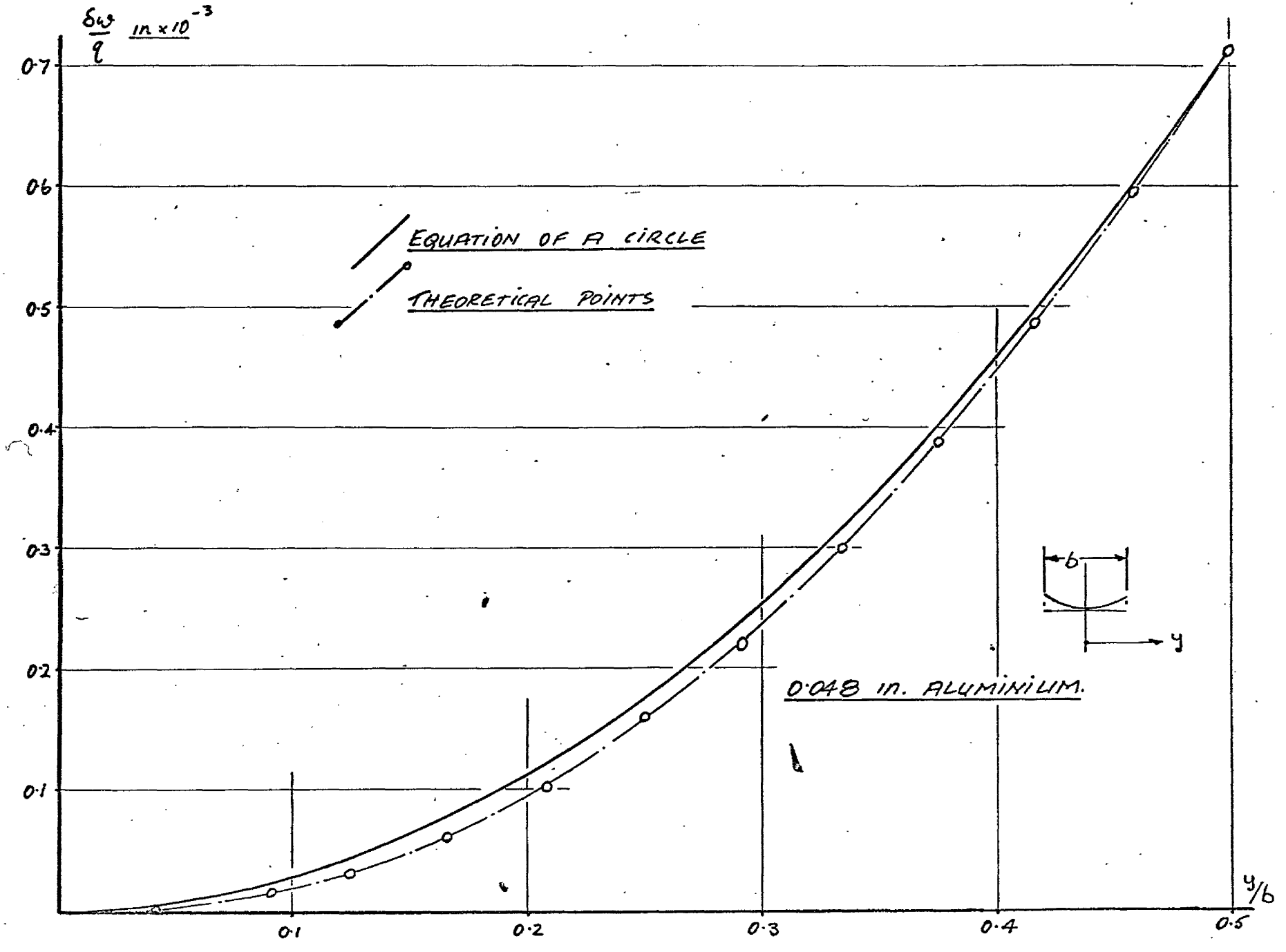

FIG.VIII.22 Theoretical transverse deflected form for a single trough of 0.036 in. aluminium deck compared with the equation of a circle.

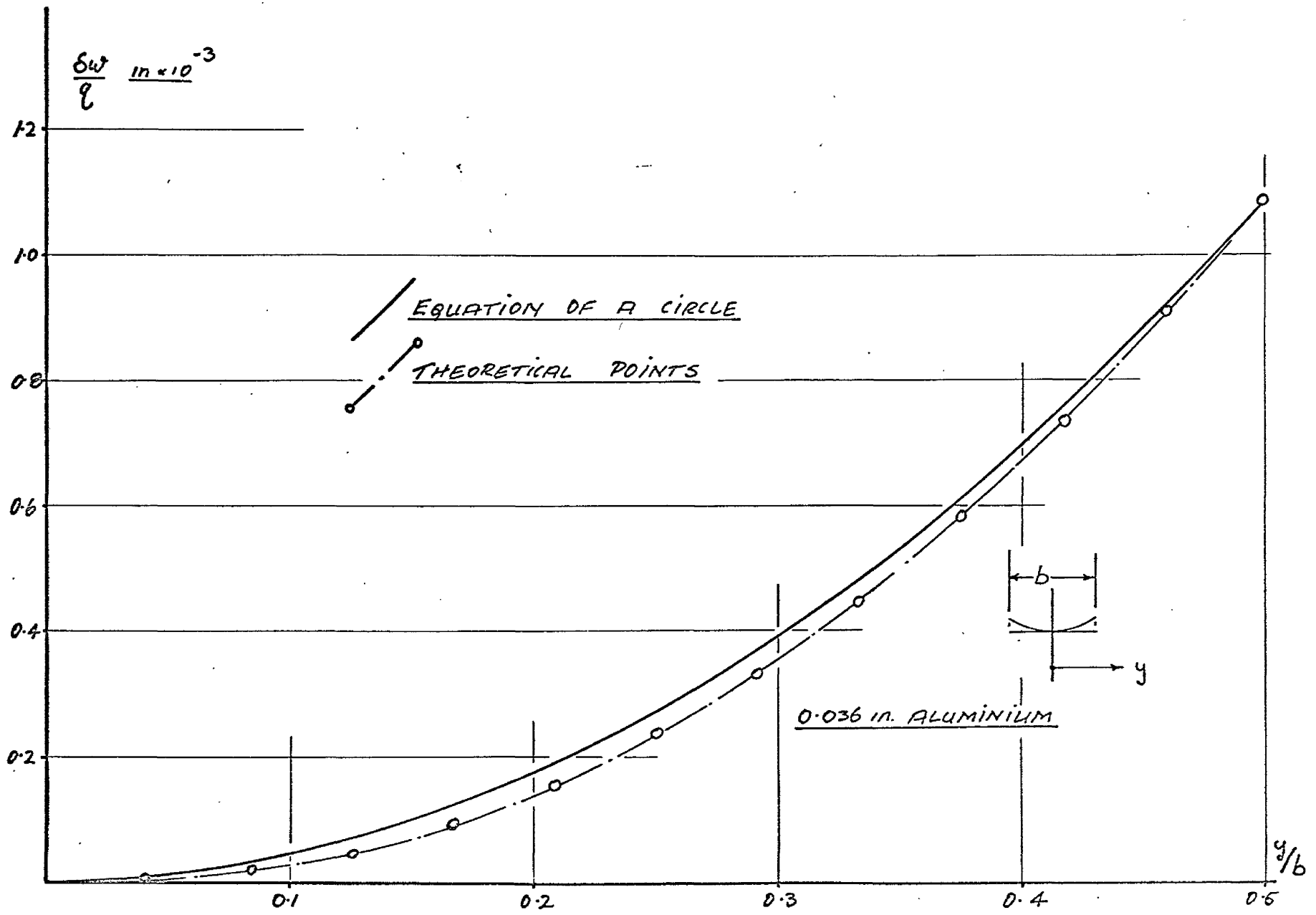

FIG.VIII.23 Theoretical transverse deflected form for a single trough of 0.036 in. steel deck compared with the equation of a circle.

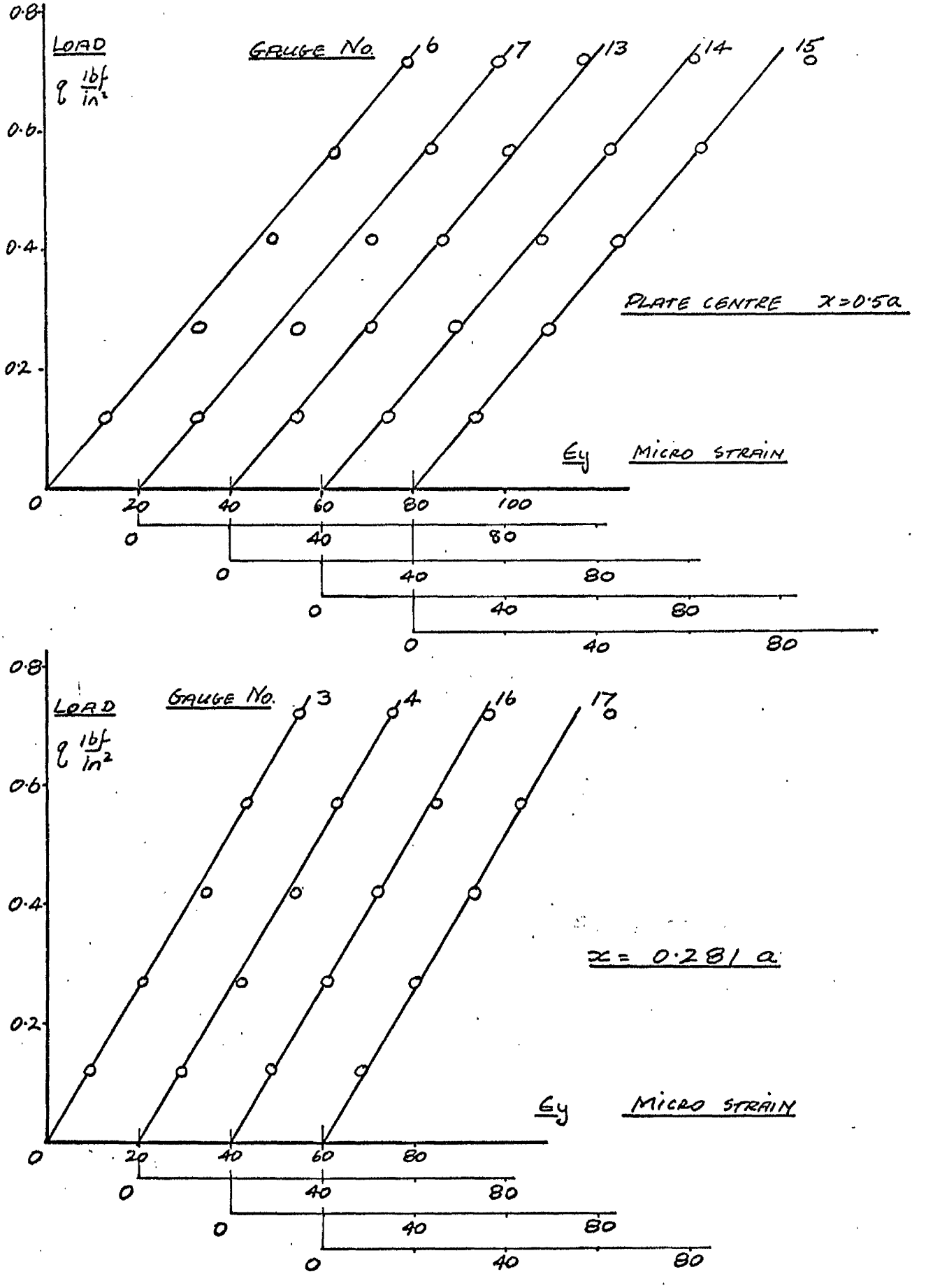

FIG.VIII.24 Lateral strains ε_y for 0.048 in. steel deck.

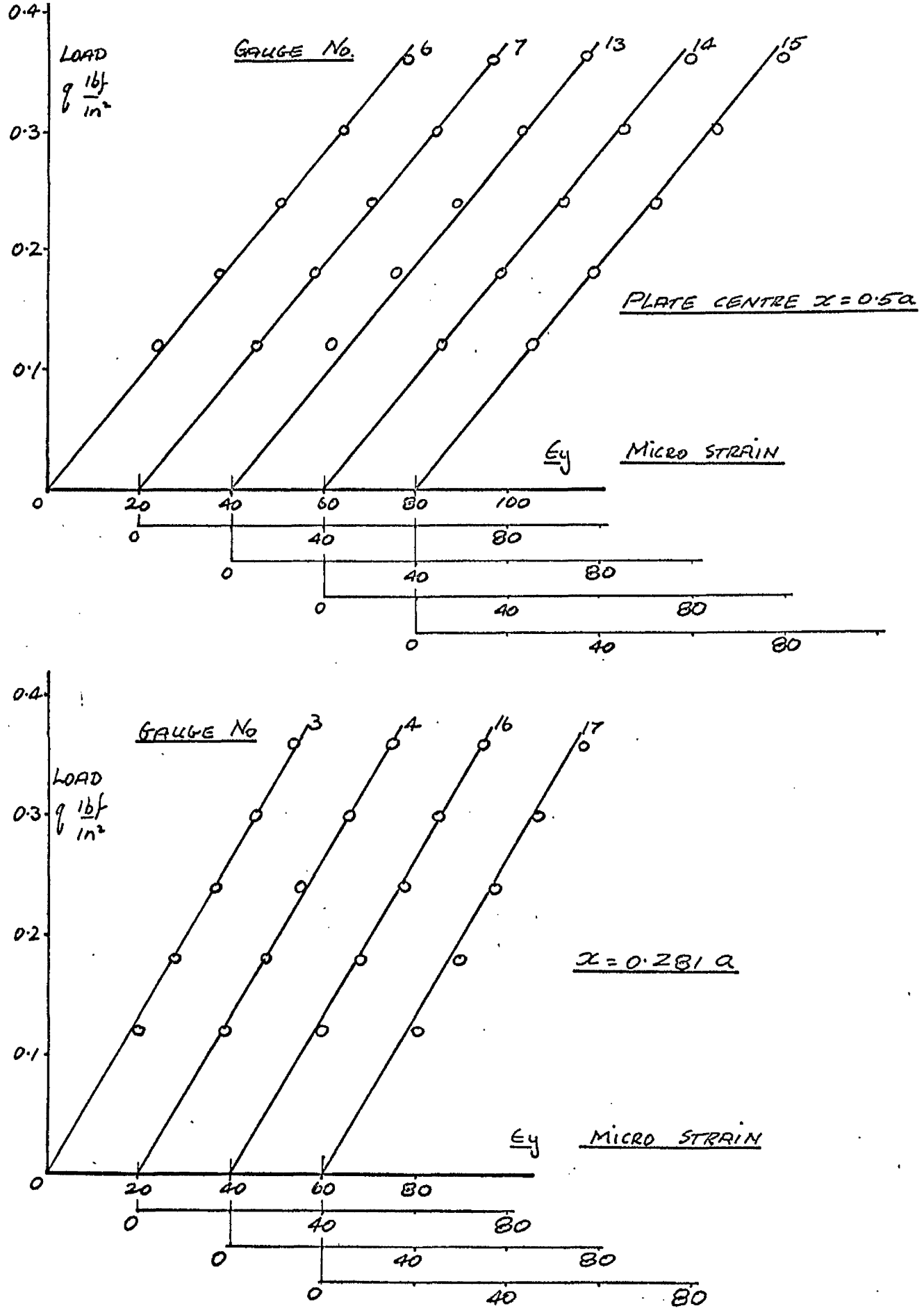

FIG.VIII.25 Lateral strains ϵ_y for 0.036 in. steel deck.

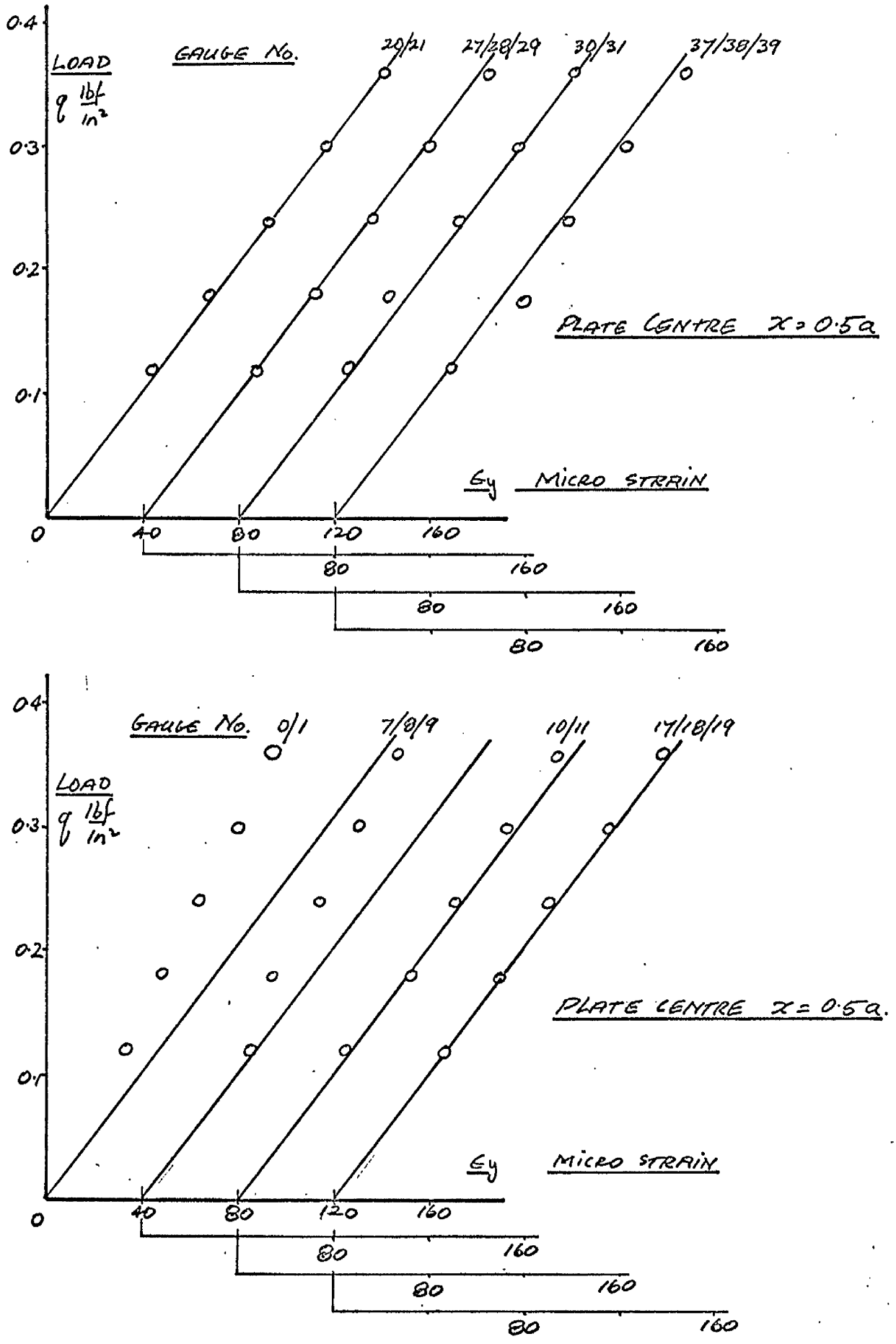

FIG.VIII.26 Lateral strains ϵ_y for 0.048 in. aluminium deck.

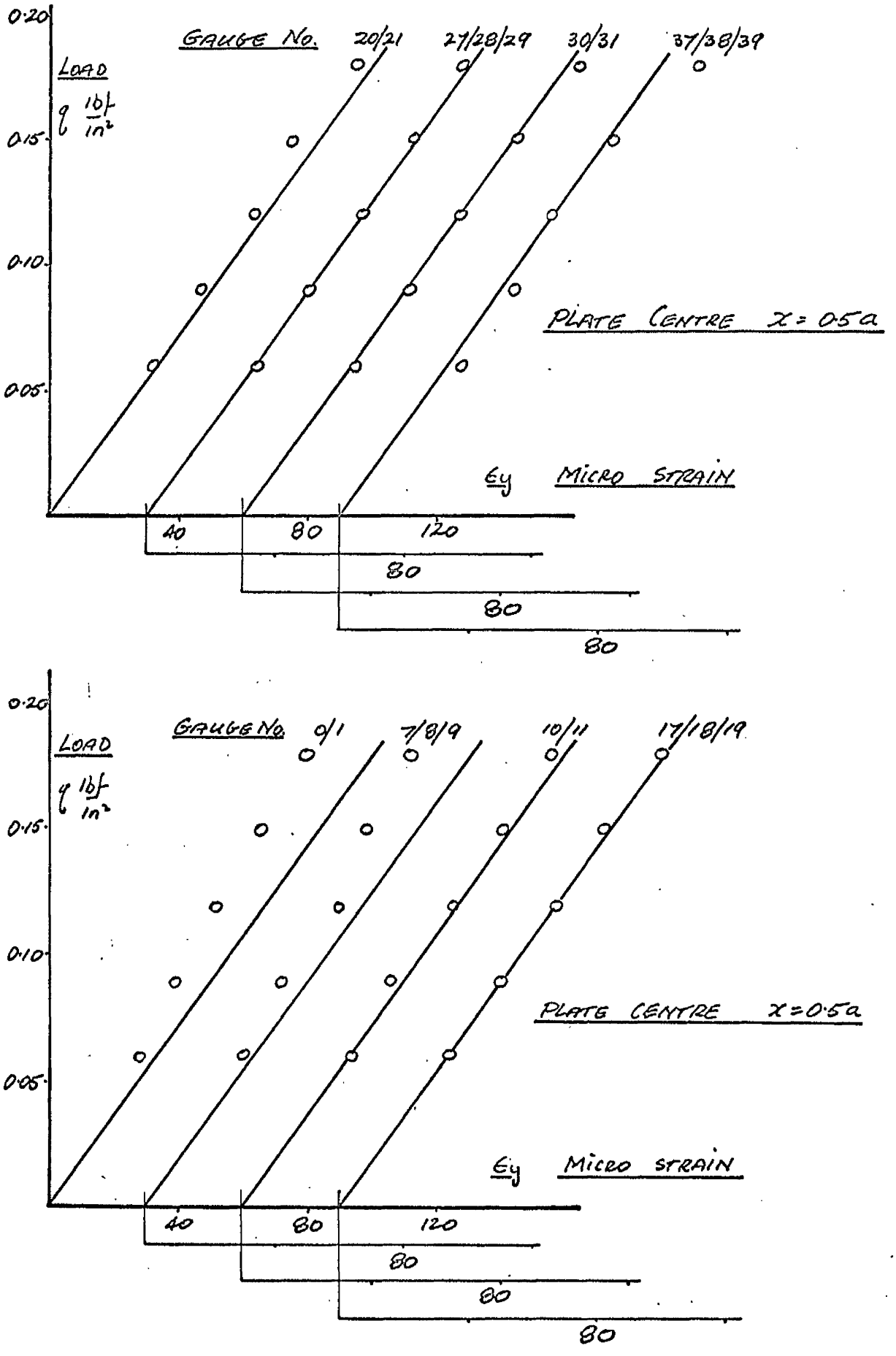

FIG.VIII.27 Lateral strains ε_y for 0.036 in. aluminium deck.

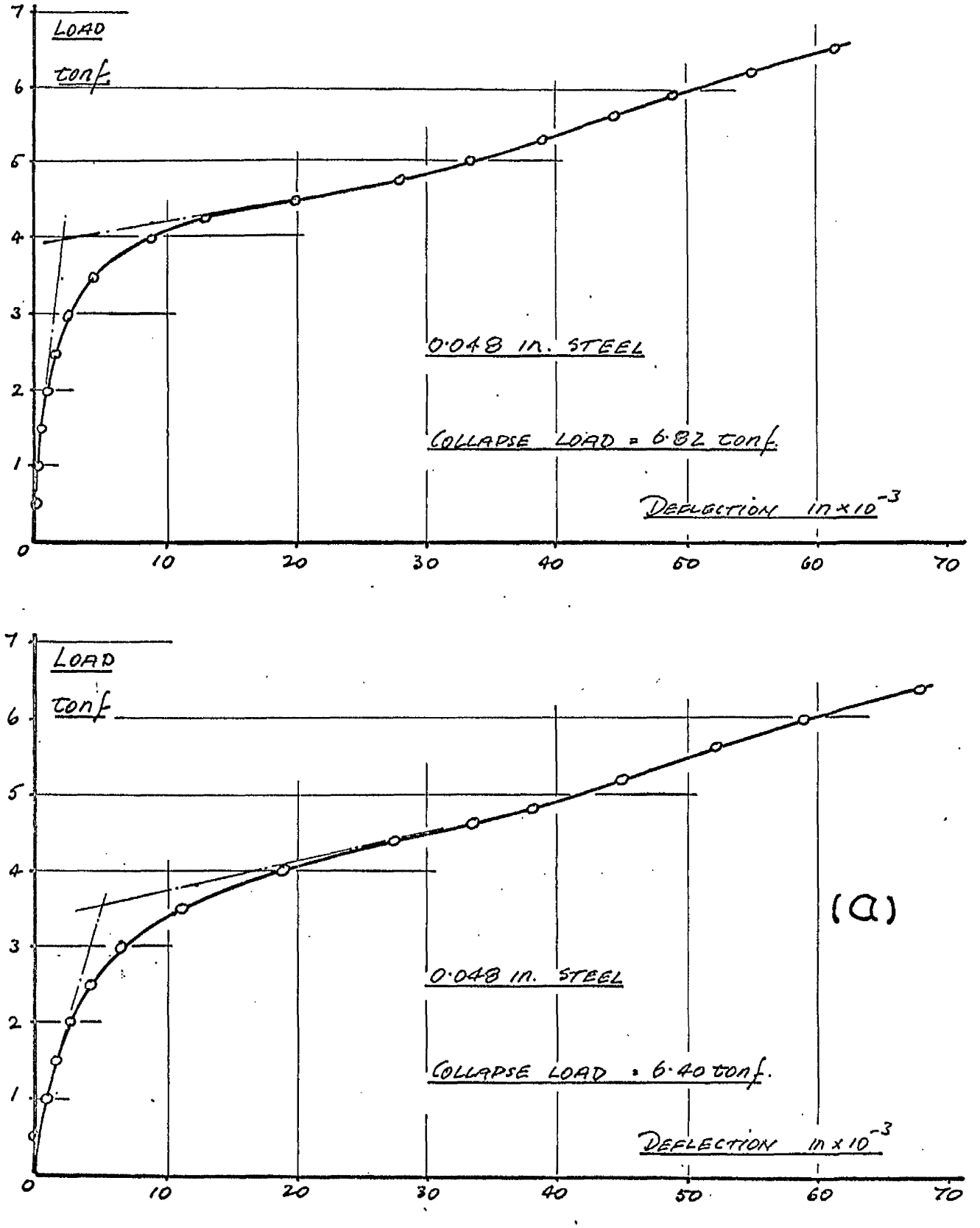

FIG.VIII.28 Strut tests - load v. flange deflection
0.048 in. steel

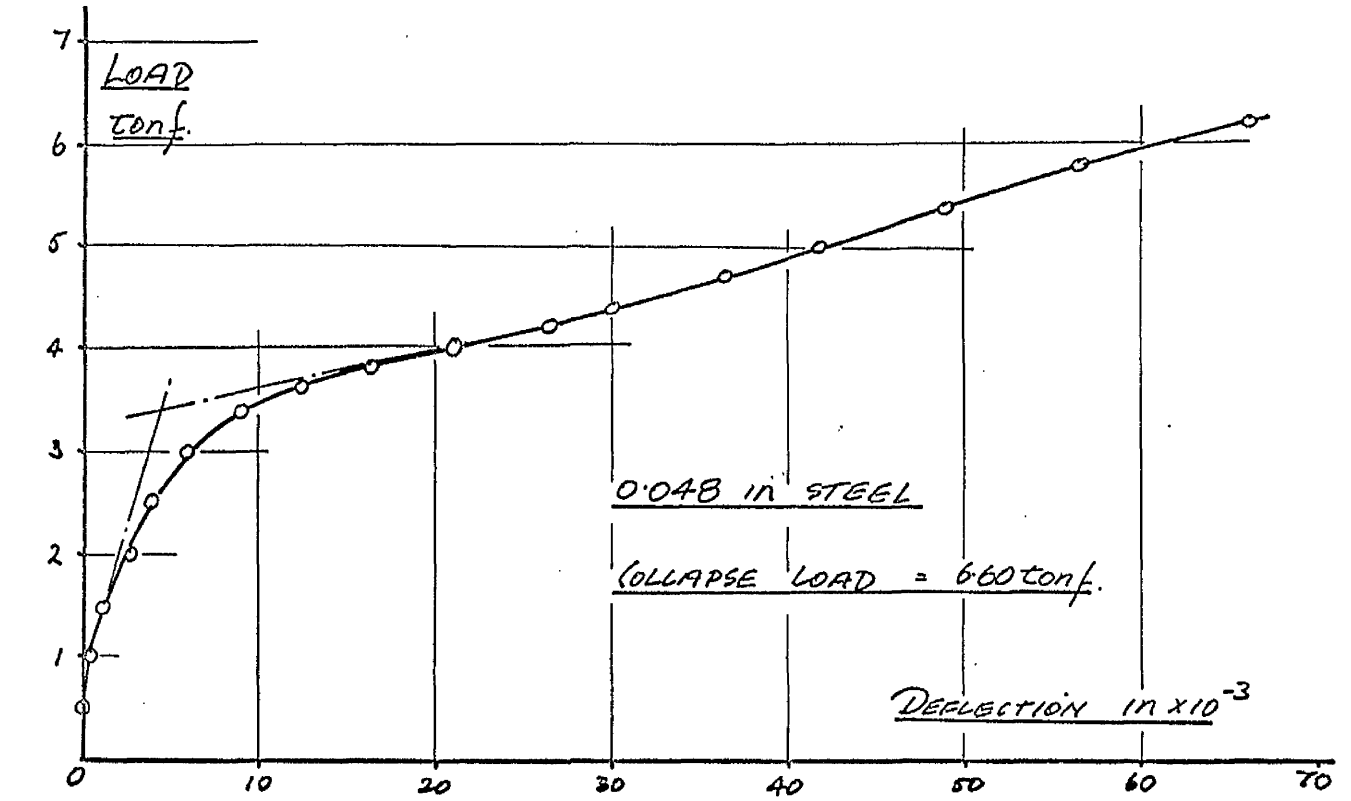

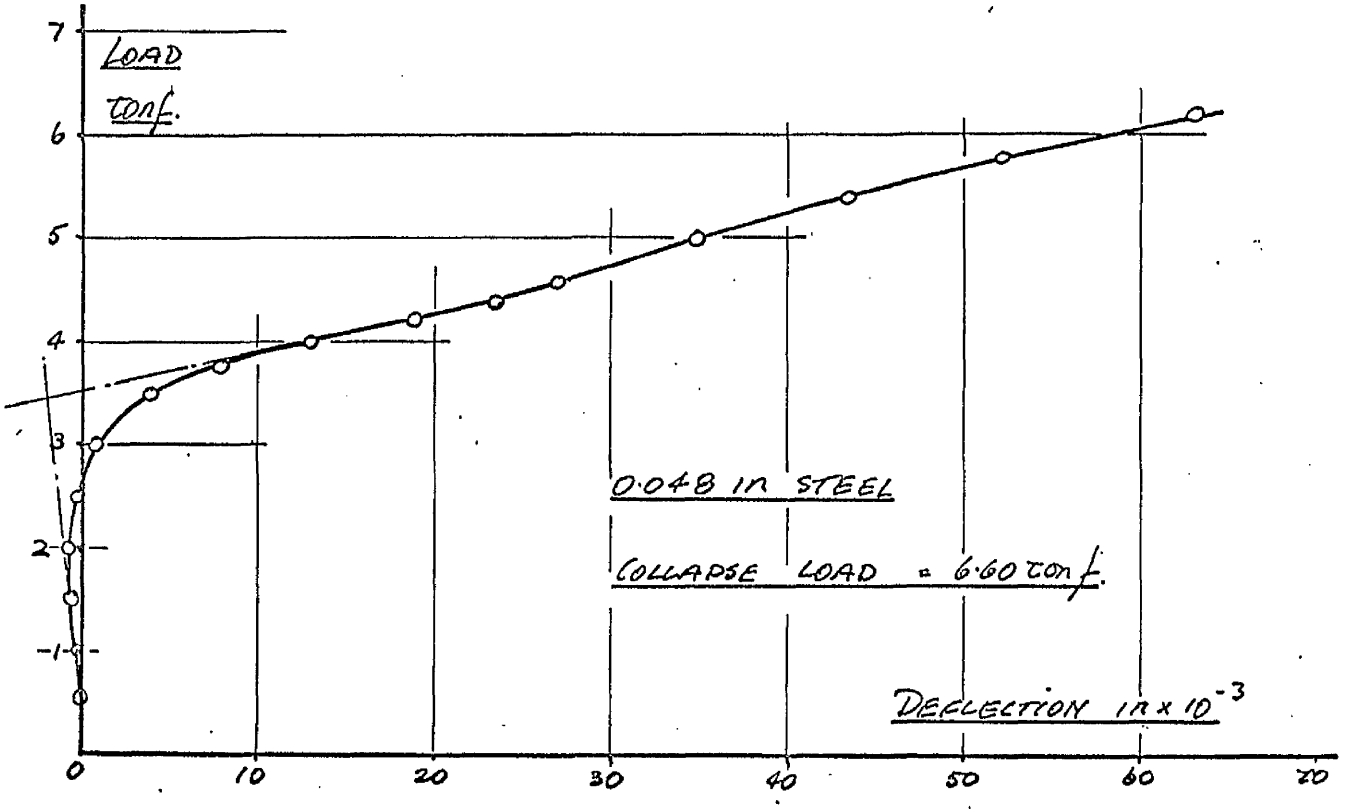

FIG.VIII.29 Strut tests - load v. flange deflection
0.048 in. steel

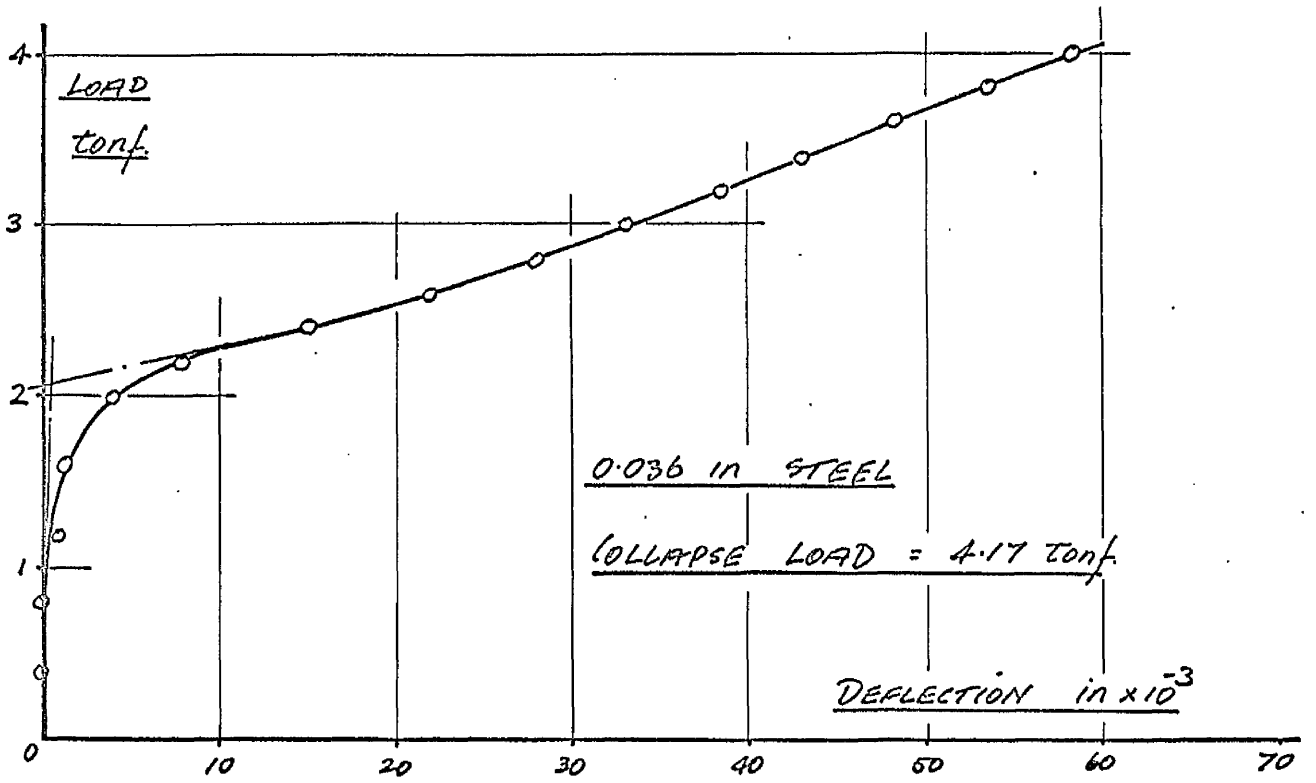

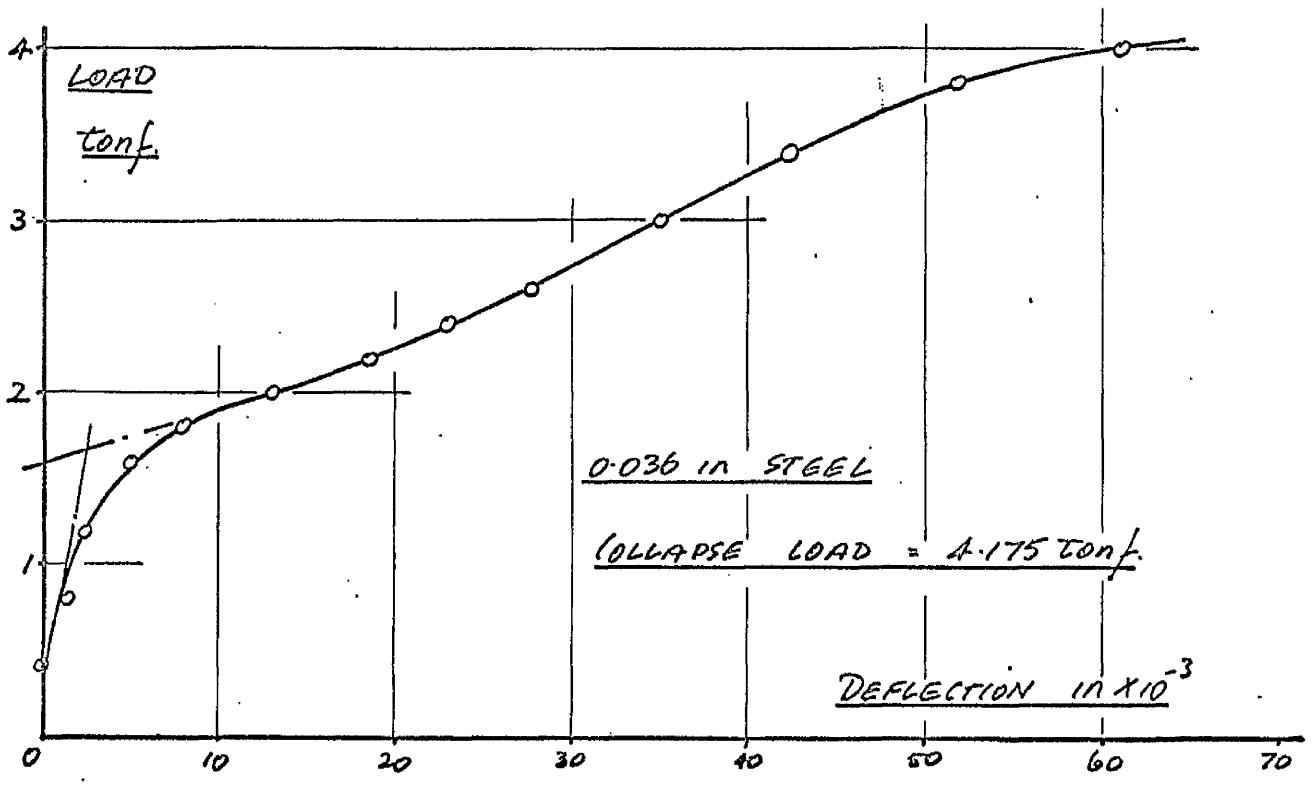

FIG.VIII.30 Strut tests - load v. flange deflection
0.036 in. steel

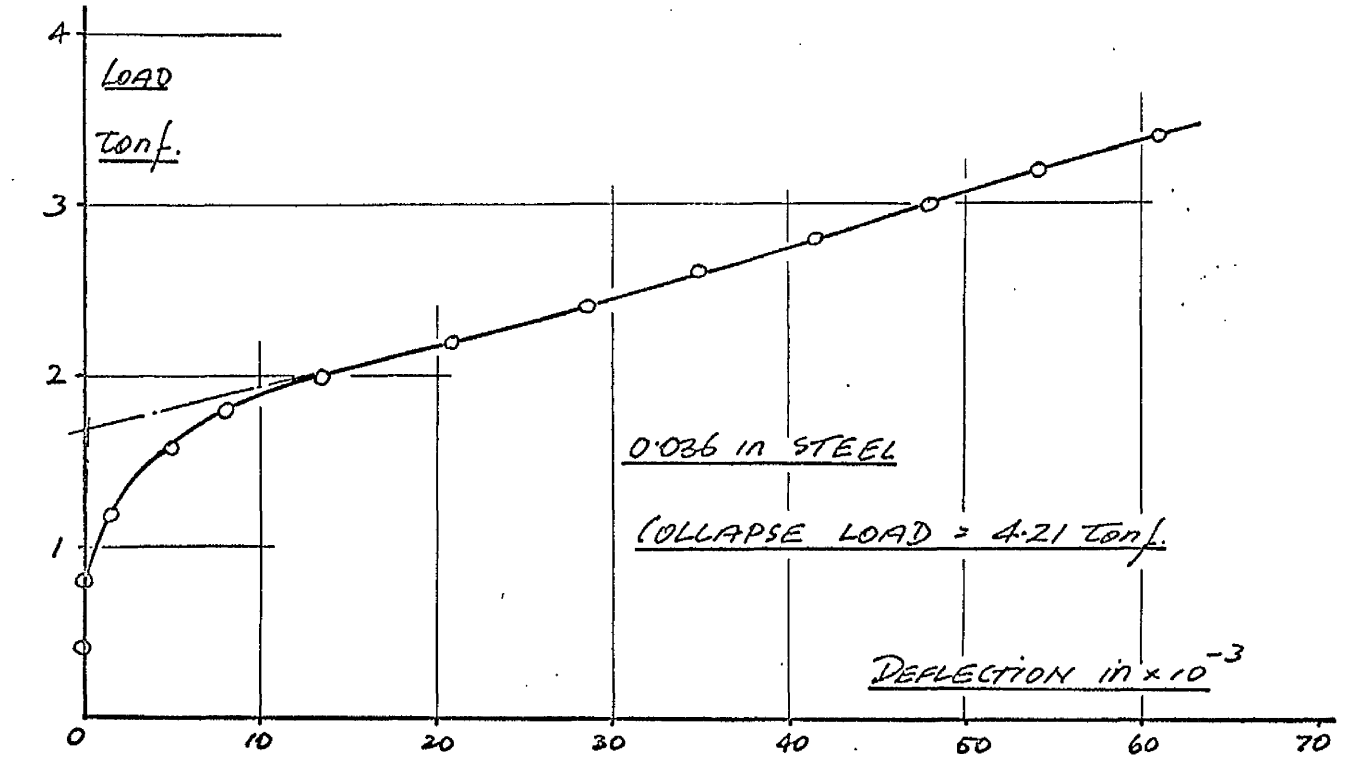

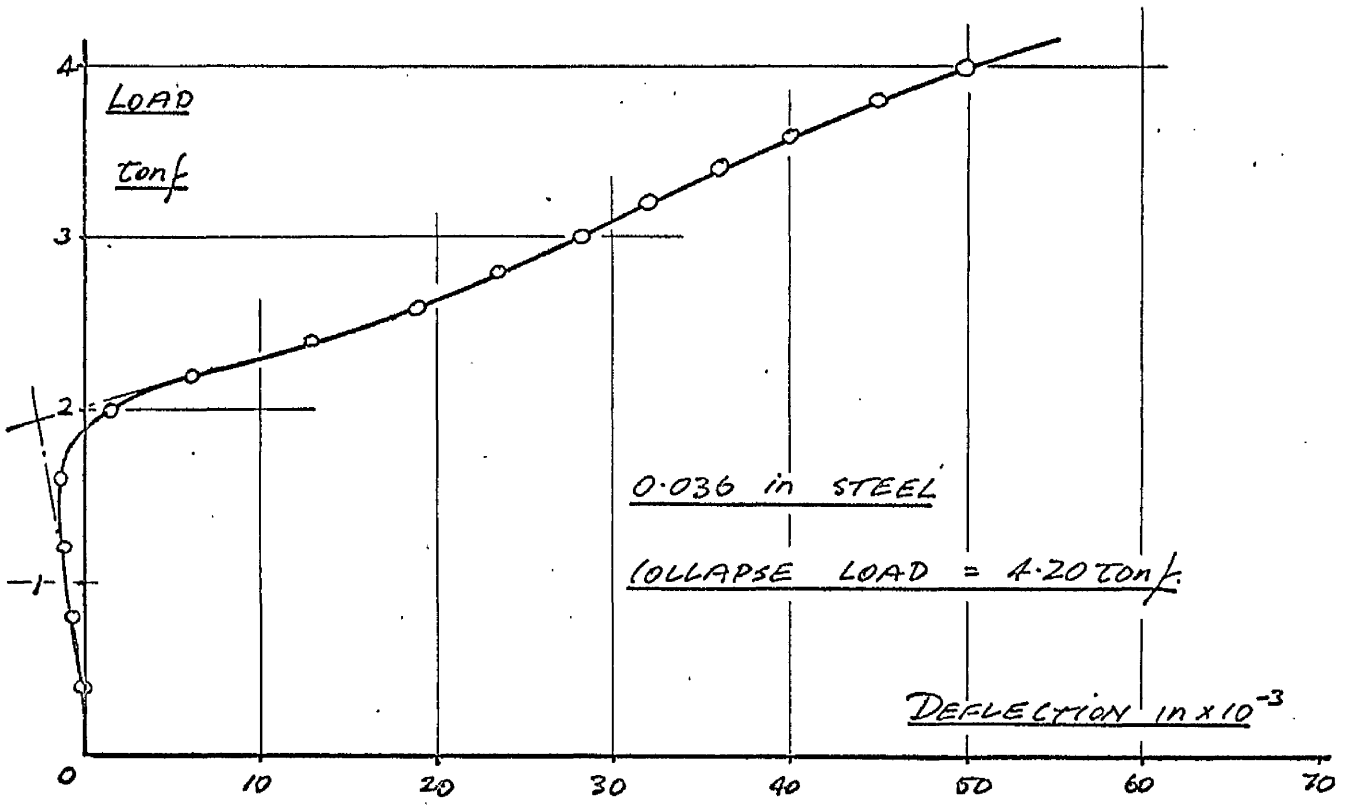

FIG.VIII.31 Strut tests - load v. flange deflection
0,036 in. steel

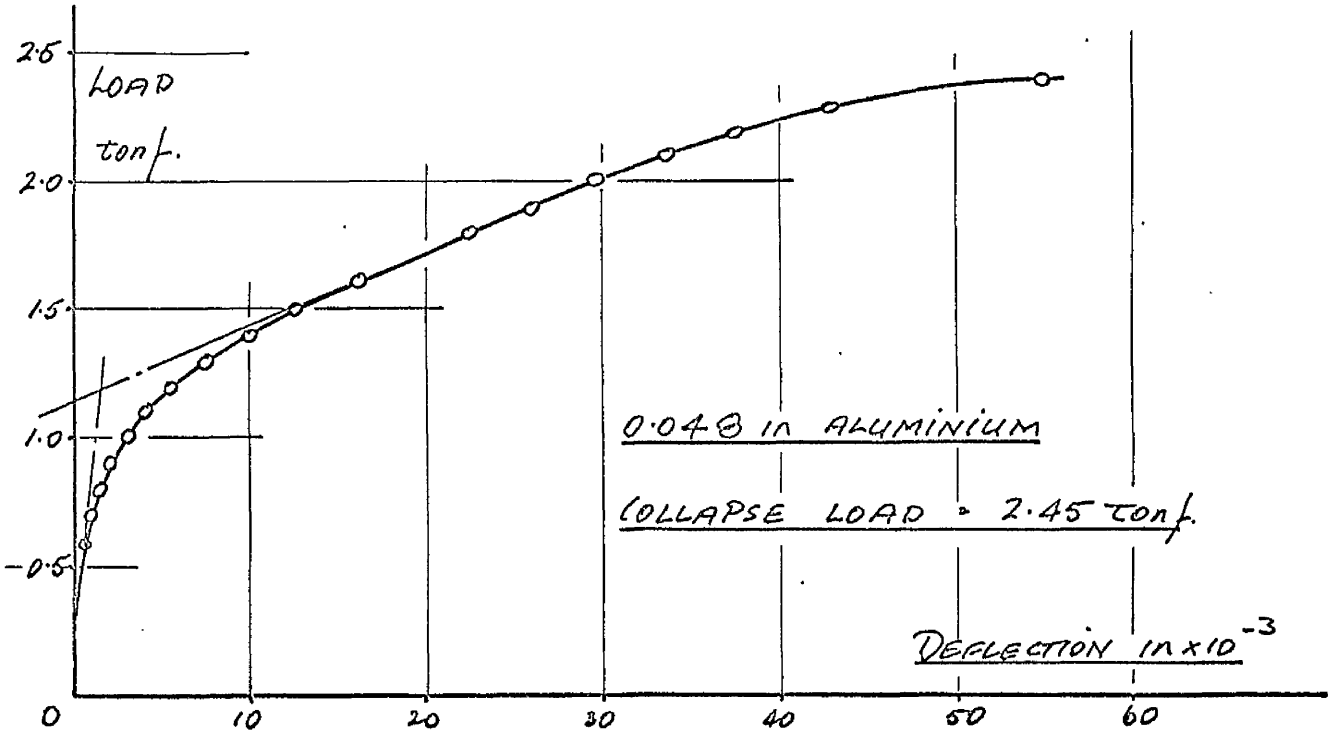

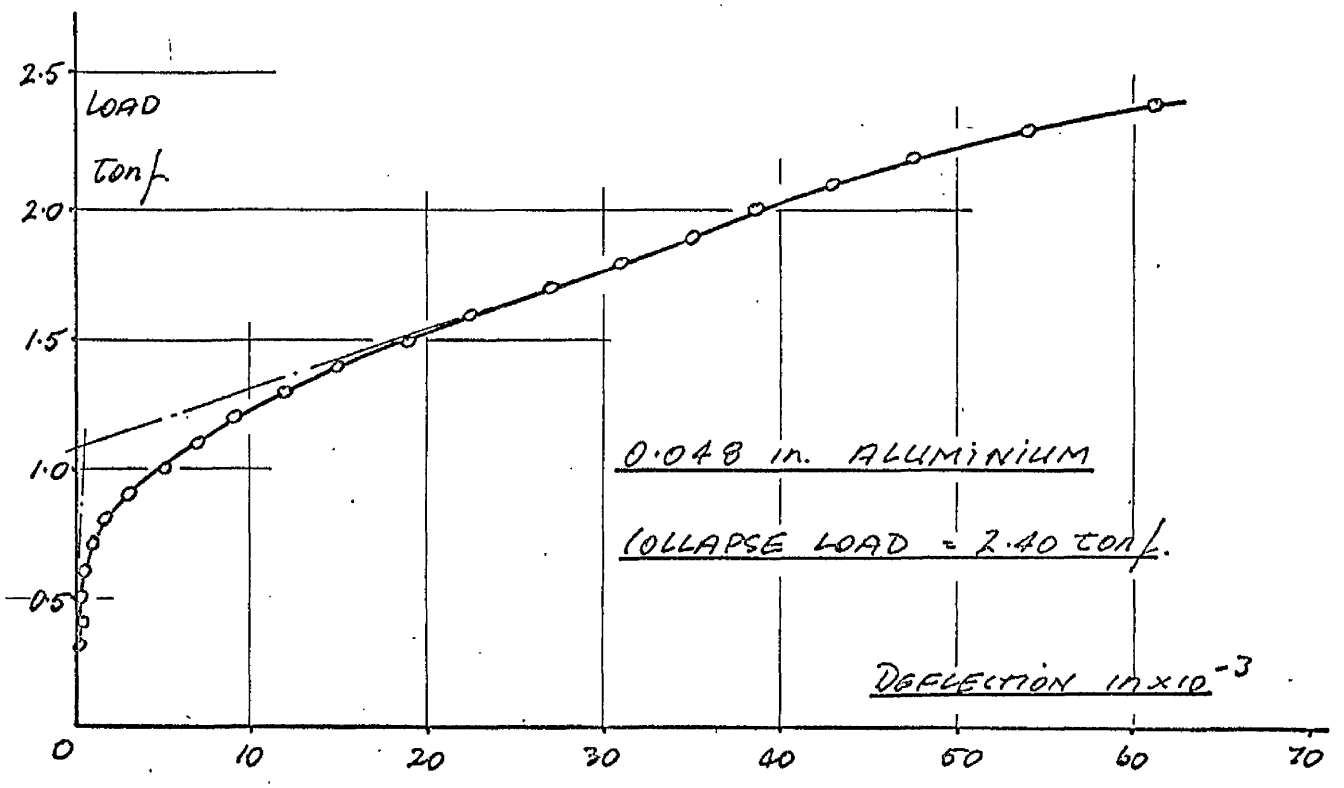

FIG.VIII.32 Strut tests - load v. flange deflection
0.048 in. aluminium

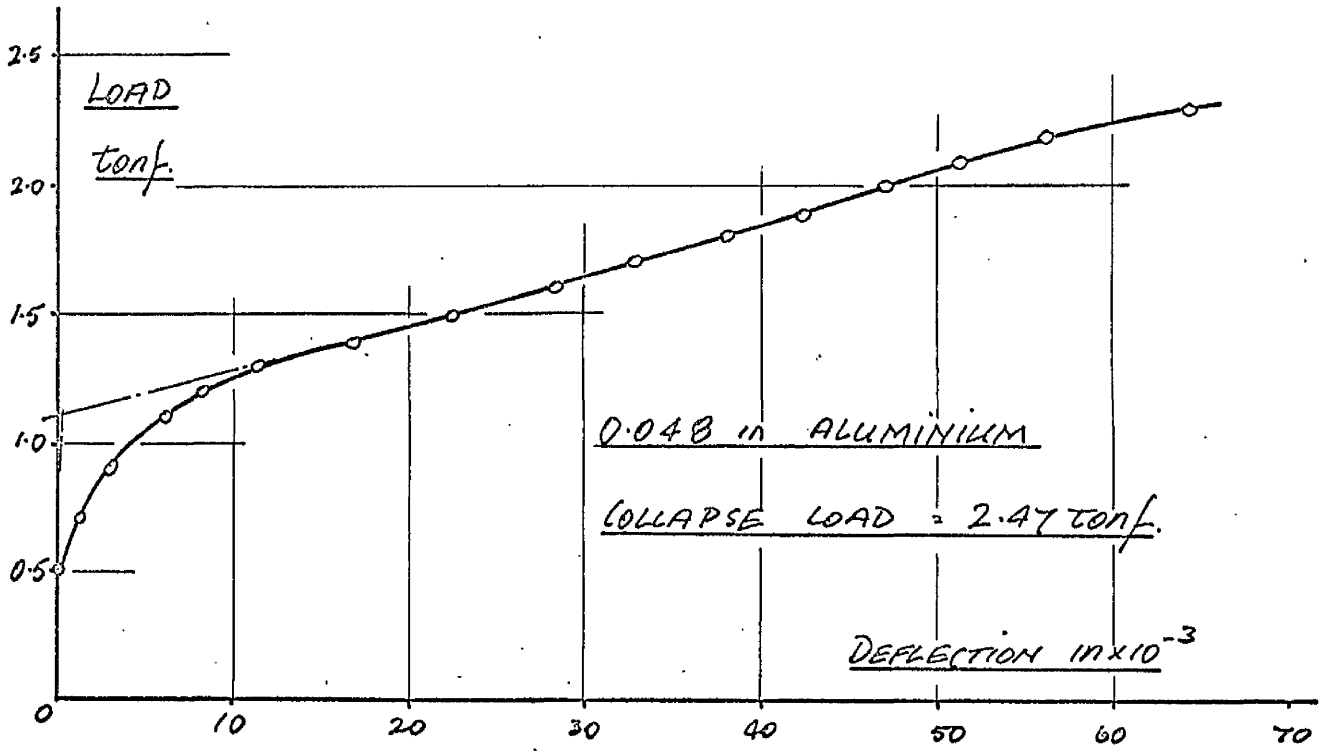

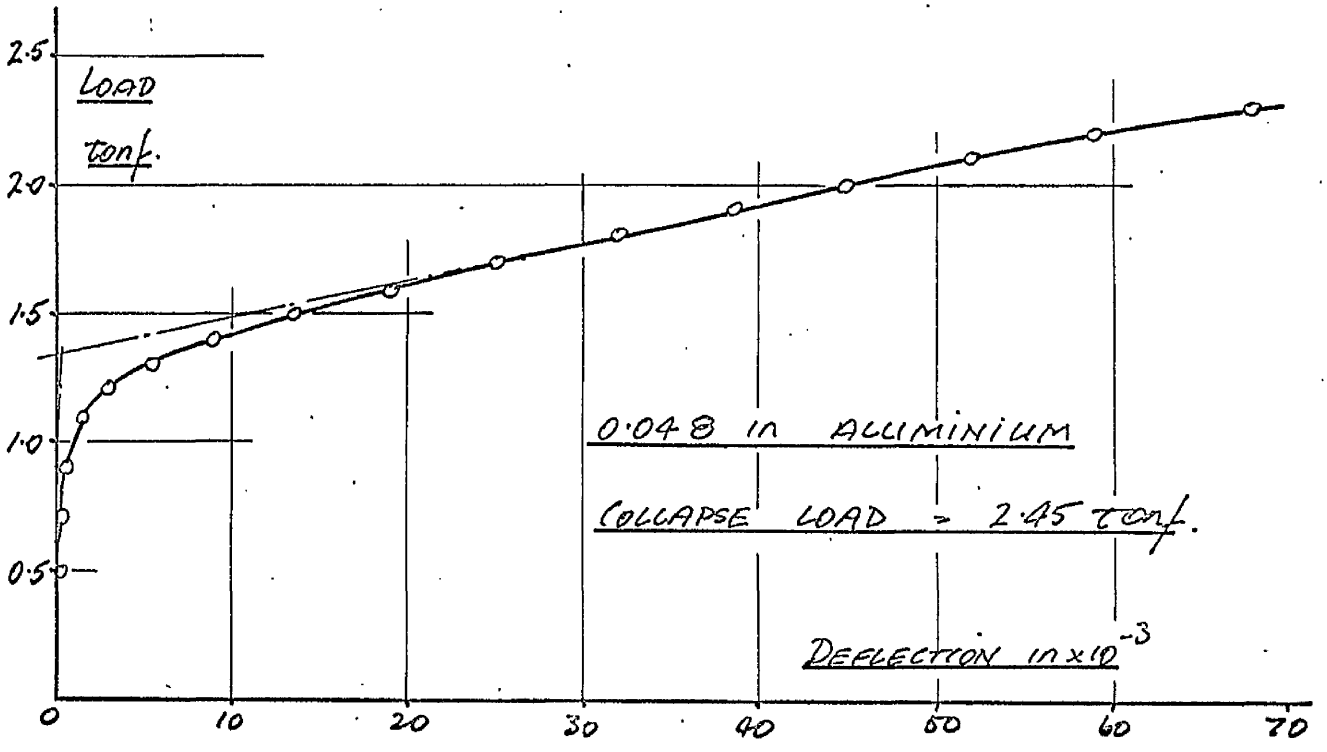

FIG.VIII.33 Strut tests - load v. flange deflection
0.048 in. aluminium

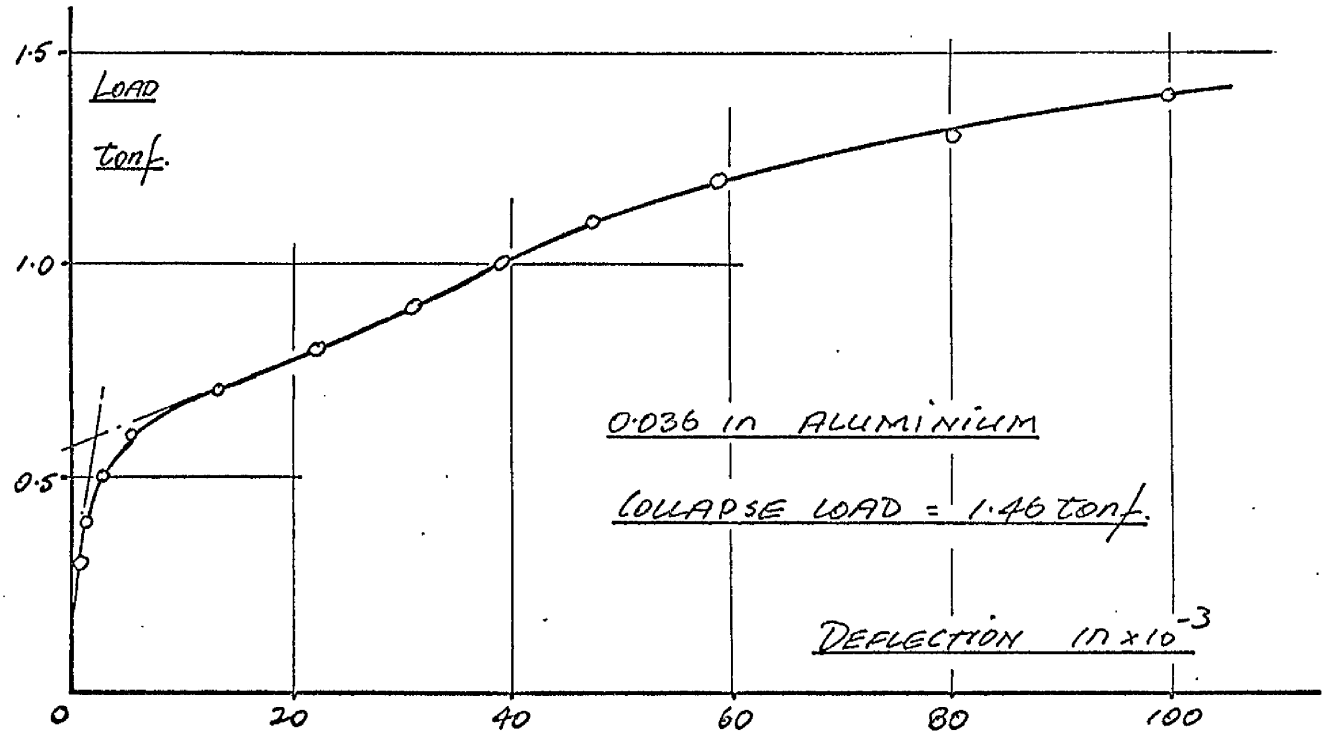

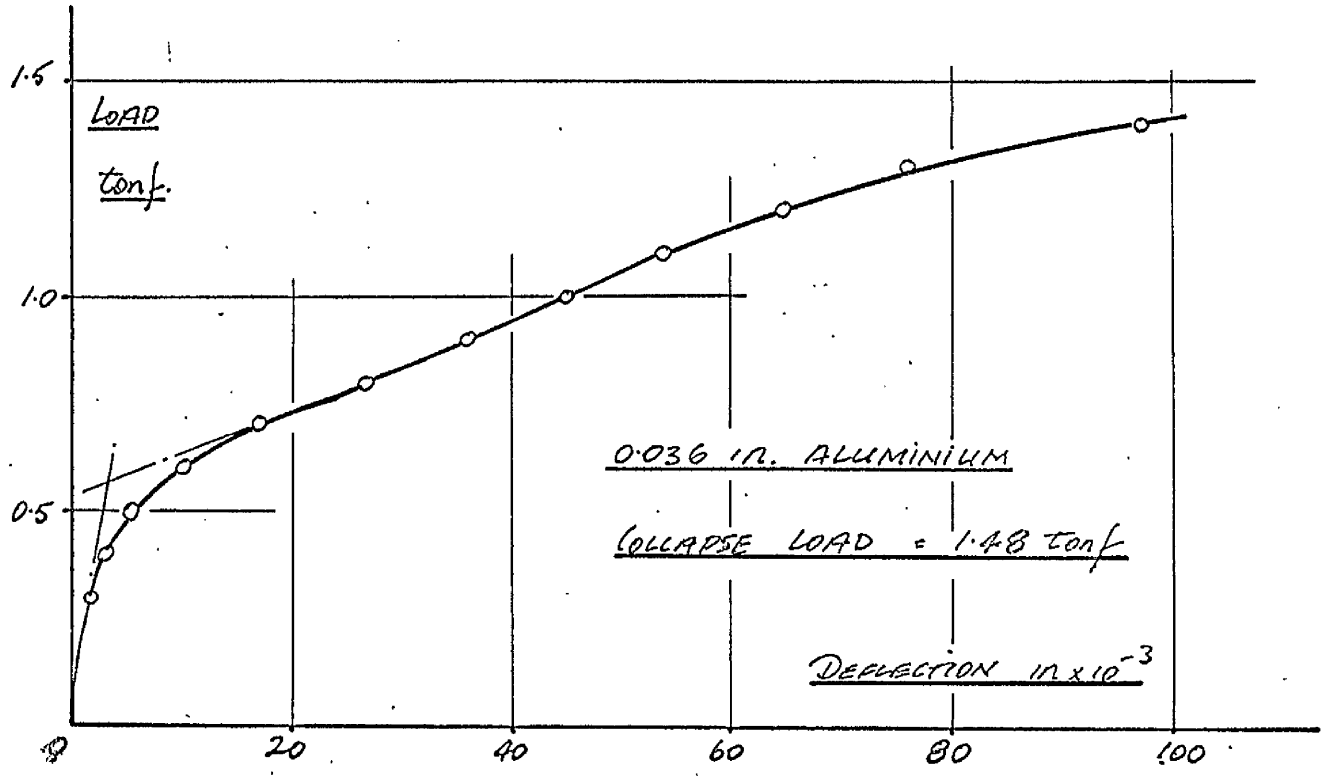

FIG.VIII.34 Strut tests - load v. flange deflection
0.036 in. aluminium

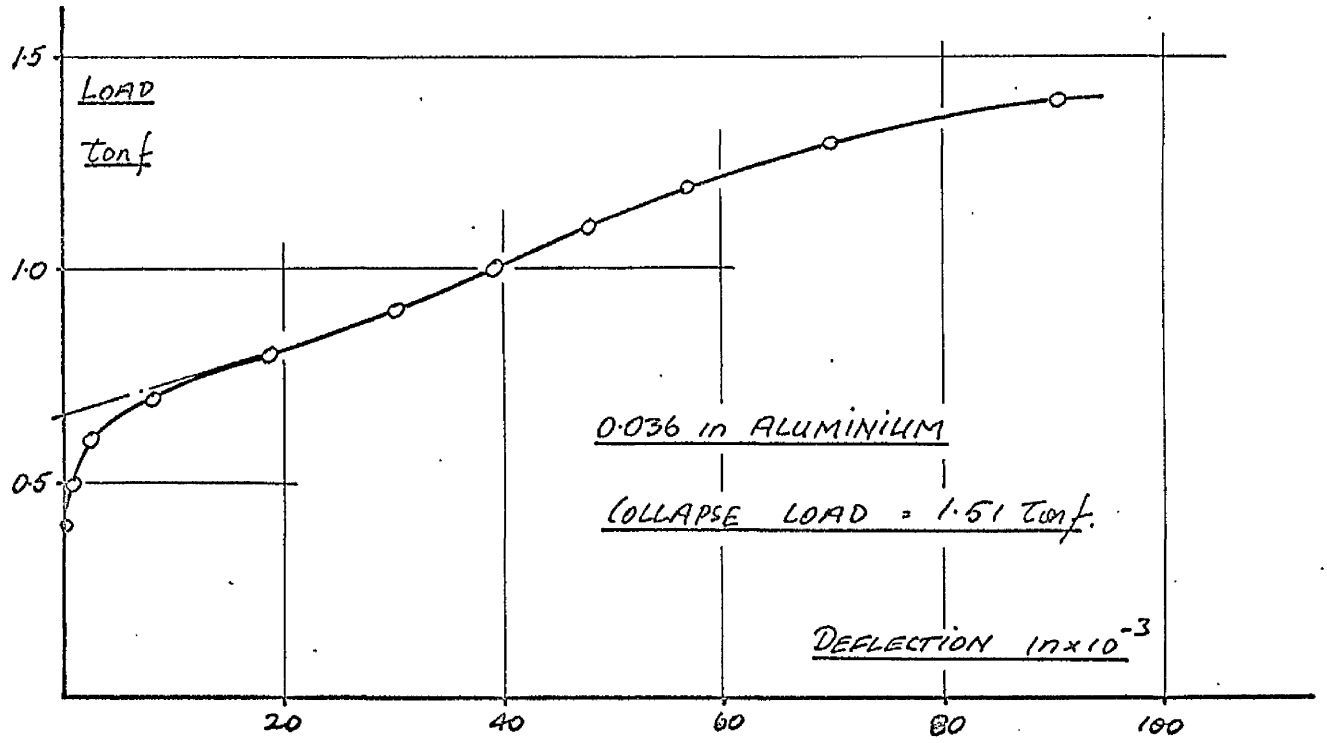

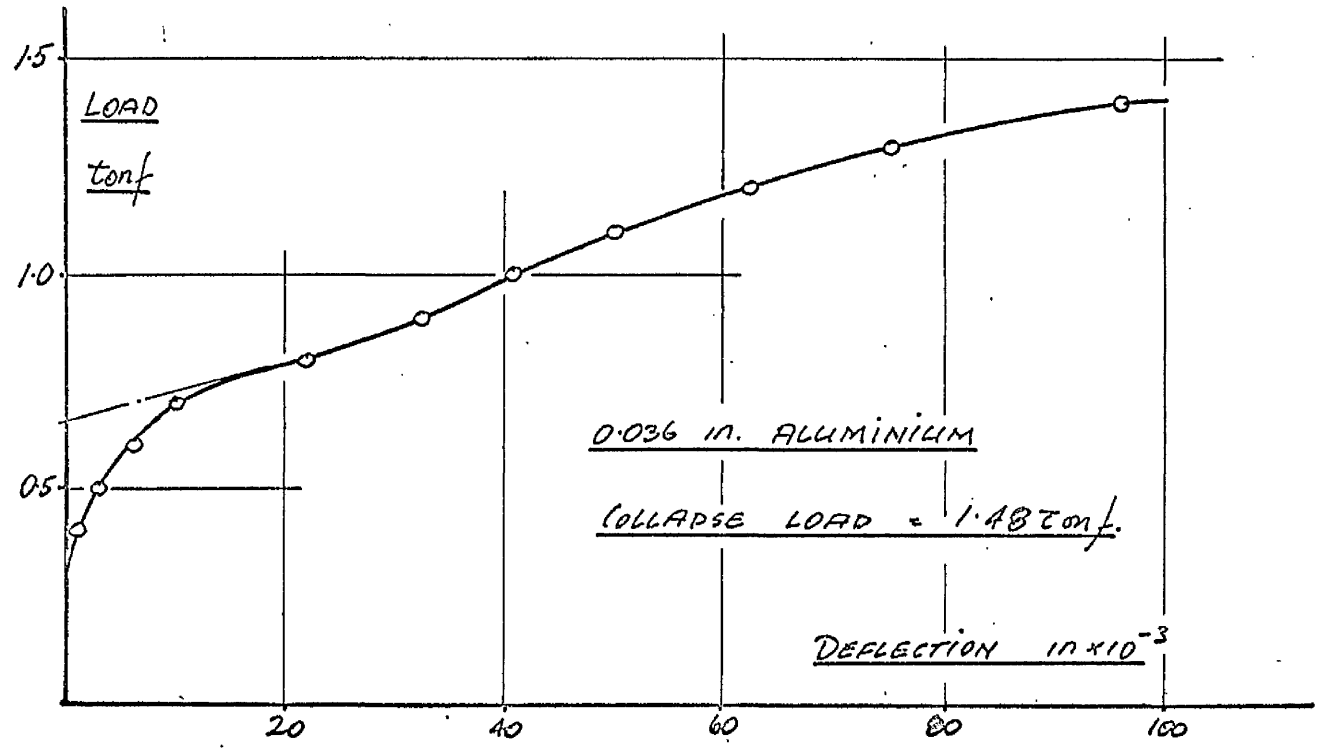

FIG.VIII.35 Strut tests - load v. flange deflection
0.036 in. aluminium

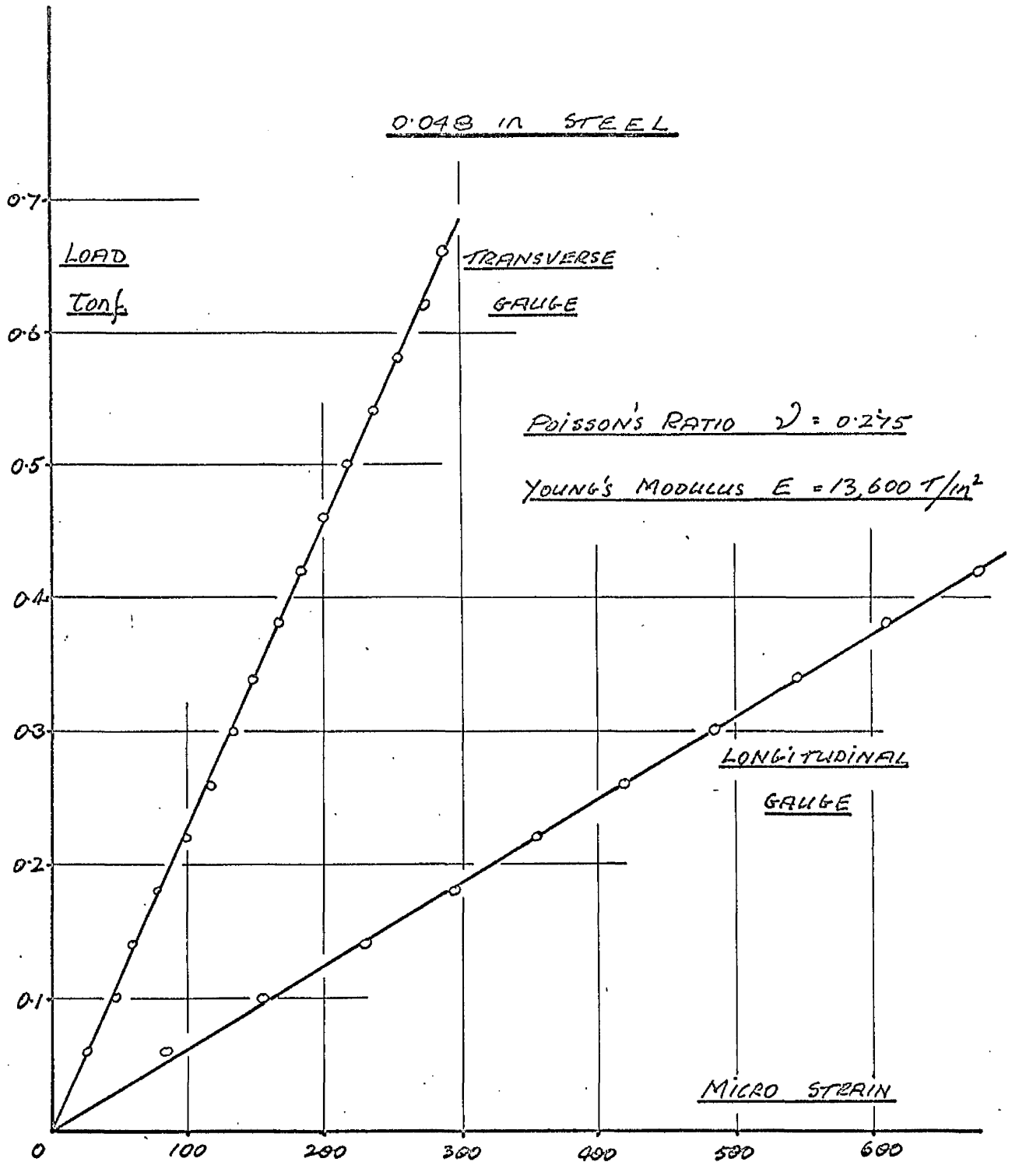

FIG.VIII.36 Test for Poisson's Ratio

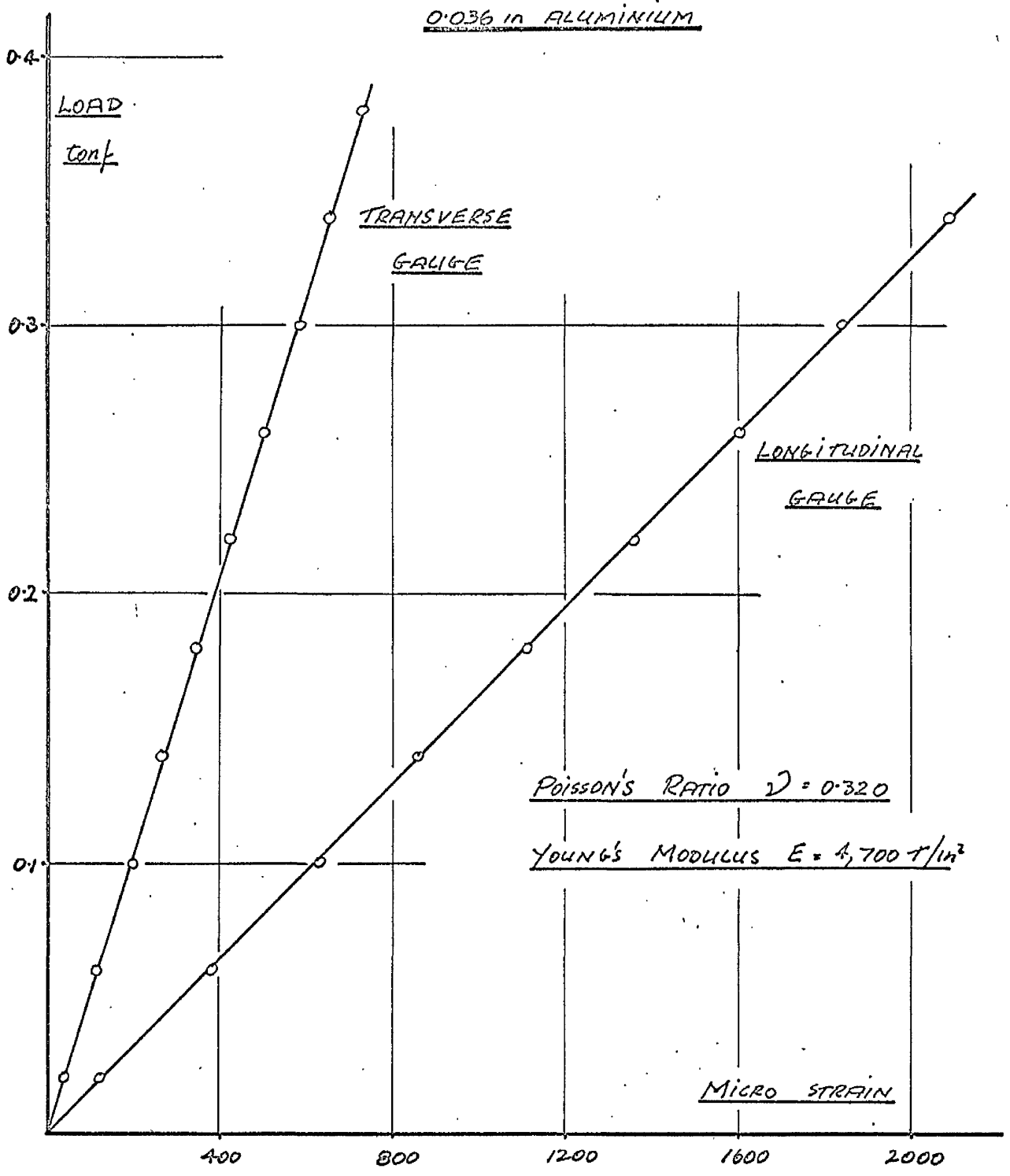

FIG.VIII.37 Test for Poisson's Ratio

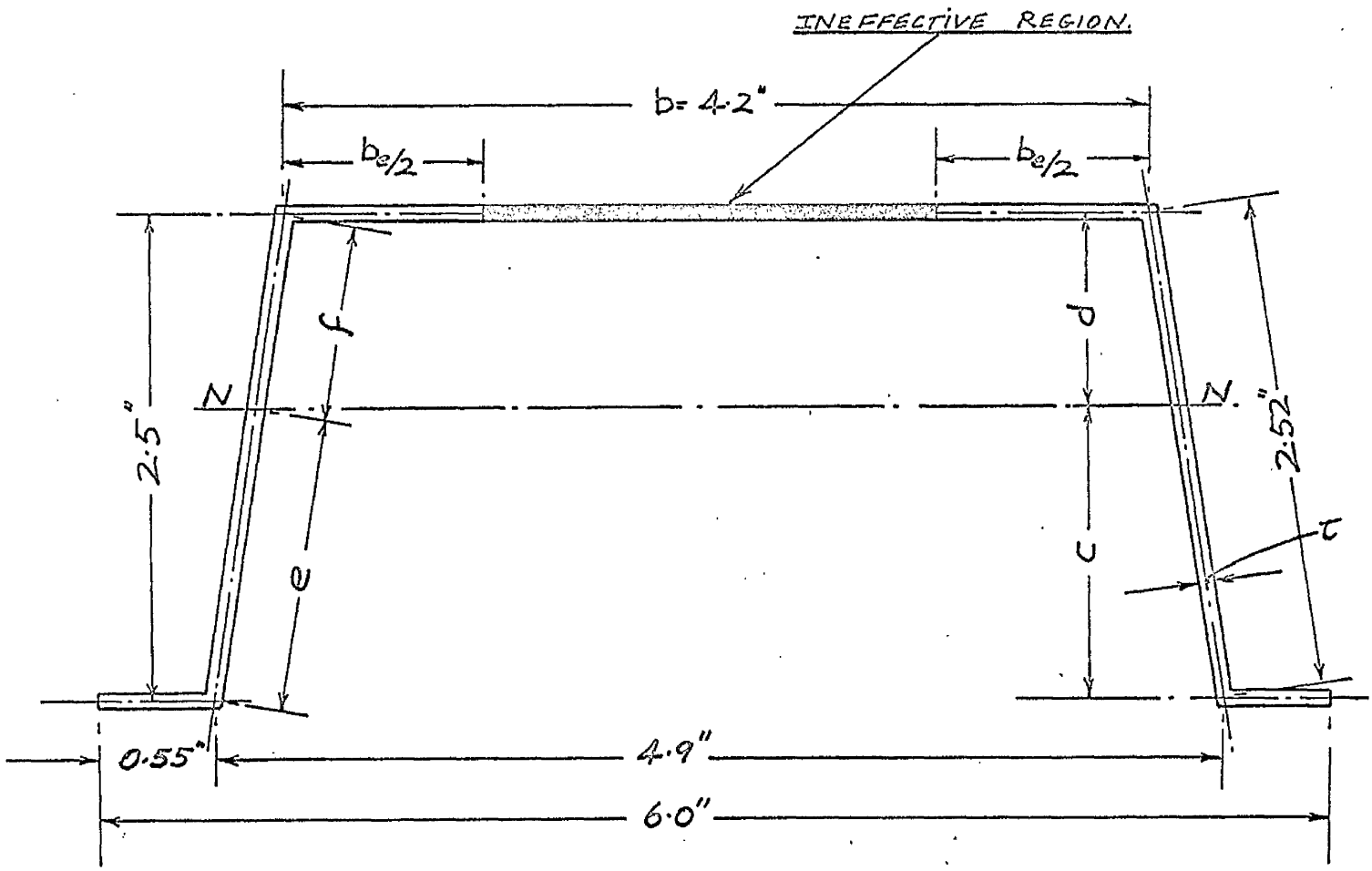

FIG.VIII.38 Steel Profile.

A C K N O W L E D G E M E N T S

The author wishes to express his thanks to Professor A.S.T. Thomson, Head of the Department of Mechanical Engineering at the University of Strathclyde, Glasgow, for the use of the facilities of the Department.

A debt of gratitude to Professor R.M. Kenedi, Research Professor of Bio-Engineering at the University for his continued interest and guidance is warmly acknowledged, as is the advice and encouragement offered by Dr. J.M. Harvey during the period of research.

Henry Kinloch.